

Robustness in Structural Steel Framing Systems

Final Report Submitted to

American Institute of Steel Construction, Inc.
Chicago, IL

By
Christopher M. Foley, Ph.D, P.E.
Kristine Martin, MS
Carl Schneeman, MS



Marquette University
Department of Civil and Environmental Engineering
Report MU-CEEN-SE-07-01

January 19, 2007

Copyright © 2007

By

American Institute of Steel Construction, Inc.

Acknowledgements

The authors would like to thank Thomas Schlafly of the American Institute of Steel Construction for his support and understanding in completing this work. The authors would also like to thank the AISC Committee on Research members for their input and comments as well as Kurt Gustafson of AISC for his very helpful recommendations.

Special thanks are due to Brian Crowder of Naval Facilities Engineering Command – Atlantic and David Stevens of Protection Engineering Consultants. Their extraordinarily diligent review of the entire manuscript with subsequent detailed and insightful comments is greatly appreciated. It is without question that the report has been significantly improved as a result of their review. The authors would also like to thank Professor Sherif El-Tawil of the University of Michigan for his review of the report and recommended corrections in the literature review.

This page is intentionally left blank.

Executive Summary

A structural engineering design that has resistance to disproportionate (or progressive) collapse can be thought of as having a level of robustness such that an event that compromises (renders ineffective) a relatively small portion of the structural system cannot grow to encompass a portion of the structure much greater than the area involved in the initial event. There are many design methodologies and philosophies in the structural engineering profession for generating structural system designs that have resistance to progressive collapse resulting from threat-specific component-compromising scenarios. However, there is precious little information available that quantifies the sources and levels of inherent robustness present in structural steel building systems. Furthermore, there are no specifications available to demonstrate that a steel structural system has a quantifiable minimum level of general structural integrity. The present study seeks to begin the process by which the structural steel industry can generate specification provisions that will result in all structural steel systems having a consistent and quantifiable minimal level of general structural integrity or robustness. These recommendations can then be used to justify a more competitive playing field for structural steel in the built environment and demonstrate the economy and safety of structural steel framing systems in the event of component-compromising events.

To meet the stated goals, a literature survey was conducted to gain insights from past experience in both the United States, the United Kingdom and elsewhere. The development of modern progressive collapse resistant design methodologies and code provisions was reviewed as well as current state-of-the-art thinking related to analytically modeling structure response to compromising events. Experimental efforts related to quantifying robustness in structural systems and connections were also reviewed. This literature survey and synthesis resulted in a sound research direction for the present effort that extends the current body of knowledge and is able to set the table for achieving the stated goals of the research effort.

Three structural steel building frames were considered to evaluate moment-resisting frame robustness after exterior columns are rendered ineffective. The three-, ten-, and twenty-story SAC pre-Northridge Boston buildings were modeled and analyzed using elastic and inelastic time history analysis (when appropriate). Recommendations regarding the inherent robustness seen in these framing systems are made. Axial, shear, and bending moment demands seen in the members and connections during the compromising events considered were quantified in the anticipation that these demands can be used to formulate detailed finite element models and experimental studies to further evaluate detailed connection behavior and track the robustness concept from the framing system down to the connections. Minimum connection design forces for these structural systems as well as the importance of Vierendeel action in determining these forces is demonstrated and discussed.

The lack of Vierendeel action developing to span compromised regions of a structural system as one rises upward through multistory steel frames lead to a study of two-way membrane and catenary action within the structural steel system and the typical concrete-steel composite floor slab likely to be present. These load transfer mechanisms were evaluated through consideration of a variety of compromised structural component scenarios including loss of: single in-fill beams; multiple in-fill beams; spandrel beam and adjacent in-fill beam; a spandrel girder; and an interior column. These scenarios were intended to generate a variety of additional measures of inherent structural integrity or robustness in the structural steel framing system and point to economical approaches and specification-type recommendations to enhance the robustness inherently present in the steel floor framing system.

The research effort reveals that there are many sources of inherent robustness and general structural integrity present in the typical structural steel building framing system. Its completion furthers the process of identifying and quantifying these sources in the hope that the research effort can grow into further systematic analytical and experimental procedures to define levels of reliability for this integrity and development of specification provisions to aid structural steel designers in creating systems with identifiable sources of robustness so that owners can see that the structural steel system is indeed competitive with, and in many cases surpasses the expected performance of, other building systems.

Table of Contents

Chapter 1 – Introduction

1.1	Research Motivation	1
1.2	Report Overview	2

Chapter 2 – Literature Review and Synthesis

2.1	Introduction.....	5
2.2	U.K. Experience and Philosophy	5
2.3	ACI 318 Philosophy.....	12
2.4	Current Design Philosophies and Design Guidelines	21
2.5	General Reviews of Design and Studies in Structural Performance.....	47
2.6	Experimental Work.....	56
2.7	Analytical Methods for Assessing Performance	60
2.8	Literature Synthesis and Research Objectives	65

Chapter 3 – Three-Story SAC Frame

3.1	Introduction and Building Description	69
3.2	Critical Load Analysis and Diaphragm Modeling	72
3.3	Elastic Analysis of Compromised Frame.....	79
3.4	Inelastic Time History Analysis of Framework.....	100
3.5	Concluding Remarks and Recommendations	115

Chapter 4 – Ten-Story SAC Frame

4.1	Introduction and Building Description	119
4.2	Critical Load Analysis and Diaphragm Modeling	122
4.3	Elastic Analysis of Compromised Frame.....	126
4.4	Concluding Remarks.....	140

Chapter 5 – Twenty-Story SAC Frame

5.1	Building Description.....	143
5.2	Column Removal (Ineffectiveness) Rates.....	149
5.3	Time History Analysis Results for 20-Story Frame.....	153
5.4	Concluding Remarks	166

Chapter 6 – Membrane and Catenary Action

6.1 Introduction 169
6.2 Tension Action in Concrete Floor Systems 169
6.3 Membrane Action in Composite Deck Structural Steel Systems 176
6.4 Ineffective Element Scenarios 177
6.5 Concluding Remarks 210
Appendices 215

Chapter 7 – Summary, Conclusions and Recommendations

7.1 Summary 235
7.2 Conclusions 235
7.3 Recommendations for Further Research 243

Cited References 247

List of Figures

Chapter 2 – Literature Review and Synthesis

Figure 2.1	Flowchart Indicating Sequence of Events During Collapse Event (adapted from Leyendecker and Ellingwood 1977).....	22
Figure 2.2	Flowchart Indicating Design Procedure that Includes Consideration of Progressive Collapse (adapted from Leyendecker and Ellingwood 1977)	24
Figure 2.3	Flowchart 1 of Exemption Process (GSA 2003).....	30
Figure 2.4	Flowchart 2 of Exemption Process (GSA 2003).....	31
Figure 2.5	Flowchart 3 of Exemption Process (GSA 2003).....	32
Figure 2.6	Flowchart 4 of Exemption Process (GSA 2003).....	33
Figure 2.7	Flowchart 6 of Exemption Process (GSA 2003).....	34

Chapter 3 – Three Story SAC Frame

Figure 3.1	Framing Plan Used for SAC 3-Story Modified Boston Building Frame	69
Figure 3.2	Column Schedule for SAC 3-Story Boston Modified Boston Building Frame	70
Figure 3.3	Framework Elevation Along Column Lines 1 and 5 Looking North.....	71
Figure 3.4	Framework Elevation Along Column Lines A and G Looking West.....	71
Figure 3.5	Extruded View Illustrating Basic SAP2000 Model of Uncompromised SAC 3-Story Modified Boston Framework Without Diaphragm X- Bracing.....	72
Figure 3.6	SAP2000 Displaced Shape Plot Illustrating Buckling Mode Shape Corresponding to the First Buckling Mode: $(\gamma_{cr})_1 = 0.200$	73
Figure 3.7	SAP2000 Displaced Shape Plot Illustrating Buckling Mode Shape Corresponding to the First Buckling Mode: $(\gamma_{cr})_2 = 0.364$	73
Figure 3.8	Conceptualization of Diaphragm Behavior with a Compromised Building	74
Figure 3.9	Typical Steel Floor Framing System Used as Basis for Diaphragm Model	75
Figure 3.10	Floor Panel Shear Deformations Assumed to be Present in Diaphragm Model.....	75
Figure 3.11	Diagonal Bracing Members Used to Model Diaphragm Shear Deformations	76
Figure 3.12	Schematic Illustrating Locations for Diaphragm X-Bracing within Framework.....	77

Figure 3.13	Extruded View Illustrating Basic SAP2000 Model of Uncompromised SAC 3-Story Modified Boston Framework With Diaphragm X-Bracing In Place	78
Figure 3.14	SAP2000 Displaced Shape Plot Illustrating Buckling Mode Shape Corresponding to the First Buckling Mode: $(\gamma_{cr})_1 = 1.226$	78
Figure 3.15	SAP2000 Displaced Shape Plot Illustrating Buckling Mode Shape Corresponding to the Second Buckling Mode: $(\gamma_{cr})_2 = 1.367$	81
Figure 3.16	Ineffective Columns (on column at a time) Considered with the Analysis Conducted.....	81
Figure 3.17	Extruded View Illustrating Basic SAP2000 Model of Compromised SAC 3-Story Modified Boston Framework With Diaphragm X-Bracing In Place and Column D-5 Removed	82
Figure 3.18	SAP2000 Displaced Shape Plot Illustrating Buckling Mode Shape Corresponding to the First Buckling Mode with Column D5 at First Floor Level Removed: $(\gamma_{cr})_1 = 2.064$	82
Figure 3.19	SAP2000 Displaced Shape Plot Illustrating Buckling Mode Shape Corresponding to the Second Buckling Mode with Column D5 at First Floor Level Removed: $(\gamma_{cr})_2 = 2.469$	83
Figure 3.20	SAP2000 Displaced Shape Plot Illustrating Buckling Mode Shape Corresponding to the Third Buckling Mode with Column D5 at First Floor Level Removed: $(\gamma_{cr})_3 = 4.857$	83
Figure 3.21	SAP2000 Displaced Shape Plot Illustrating Buckling Mode Shape Corresponding to the Fourth Buckling Mode with Column D5 at First Floor Level Removed: $(\gamma_{cr})_4 = 6.061$	84
Figure 3.22	Conceptualization of Column Death Loading Scenario Implemented in the SAP2000 Time History Analysis of the Compromised Framework	84
Figure 3.23	Impact of Column Death Rates on Elastic Linear and Nonlinear Geometric Response of the Modified SAC 3-Story Framework Used (displacement is immediately above lost column)	86
Figure 3.24	Axial Load Strain Rates (micro-strain per second) for Columns Along Line C in the Moment-Resisting Frame	87
Figure 3.25	Shear Strain Rates (micro-strain per second) for Columns Along Line C in the Moment-Resisting Frame	88

Figure 3.26	Bending Moment Strain Rates (micro-strain per second) for Columns Along Line C in the Moment-Resisting Frame.....	88
Figure 3.27	Axial Load Strain Rates (micro-strain per second) for Columns Along Line E in the Moment-Resisting Frame.....	89
Figure 3.28	Shear Strain Rates (micro-strain per second) for Columns Along Line E in the Moment-Resisting Frame.....	89
Figure 3.29	Moment Strain Rates (micro-strain per second) for Columns Along Line E in the Moment-Resisting Frame	90
Figure 3.30	Axial Load Strain Rates (micro-strain per second) in the Beams of the Moment-Resisting Frame with Ineffective Column	90
Figure 3.31	Shear Strain Rates (micro-strain per second) in the Beams of the Moment-Resisting Frame with Ineffective Column	91
Figure 3.32	Bending Moment Strain Rates (micro-strain per second) in the Beams of the Moment-Resisting Frame with Ineffective Column	91
Figure 3.33	Demand to Capacity Ratios for Beams in Frame Affected by Ineffective Column at D-5	95
Figure 3.34	Demand-to-Capacity Ratios (DCR's) Assuming Elastic Response for Columns Along Line C in Frame.....	96
Figure 3.35	Demand-to-Capacity Ratios (DCR's) Assuming Elastic Response for Columns Along Line E in the Frame	96
Figure 3.36	Axial Load Demand for Members in Moment-Resisting Frame Containing Ineffective Column.....	98
Figure 3.37	Transverse Shear Demand for Members in Moment-Resisting Frame Containing Ineffective Column.....	98
Figure 3.38	Bending Moment Demand for Members in Moment-Resisting Frame Containing Ineffective Column.....	99
Figure 3.39	Moment Hinge Insertions to Frame Model Using Results of Elastic Time History Analysis	99
Figure 3.40	Moment Hinge Parameters Used for SAP2000 Frame Hinge Properties	100
Figure 3.41	Frame Elevation Illustrating Key to Output Information for Nonlinear Material Analysis of the SAC 3-Story Framework.....	101
Figure 3.42	Elastic Versus Inelastic Response Comparison for Frame with Ineffective Column at First Floor and Location D-5.....	102

Figure 3.43	Bending Moment Time-History Response for Members Framing Together at the Second Floor Beam-to-Column Connection at Column Line C.....	103
Figure 3.44	Bending Moment Time-History Response for Members Framing Together at the Third Floor Beam-to-Column Connection at Column Line C.....	104
Figure 3.45	Bending Moment Time-History Response for Members Framing Together at the Roof Beam-to-Column Connection at Column Line C.....	105
Figure 3.46	Bending Moment Time-History Response for Second Floor Beam (Element 268) Spanning from Column Line C to D	106
Figure 3.47	Bending Moment Time-History Response for Roof Beam (Element 270) Spanning from Column Line C to D	106
Figure 3.48	Bending Moment Time-History Response for Third Floor Beam (Element 272) Spanning from Column Line D to E.....	107
Figure 3.49	Moment Hinge Formation Computed During Response of Frame to Ineffective Column at the First Floor at Location D-5.....	108
Figure 3.50	Non-Dimensional Force Demands and Demand-to-Capacity Ratio Time Histories for Element 268 at the Left End (Column Line C)	109
Figure 3.51	Non-Dimensional Force Demands and Demand-to-Capacity Ratio Time Histories for Element 1143 at the Top (Roof Level).....	109
Figure 3.52	Non-Dimensional Force Demands and Demand-to-Capacity Ratio Time Histories for Element 271 at the Right End (Column Line E)	110
Figure 3.53	Non-Dimensional Force Demands and Demand-to-Capacity Ratio Time Histories for Element 272 at the Right End (Column Line E)	110
Figure 3.54	Non-Dimensional Force Demands and Demand-to-Capacity Ratio Time Histories for Element 273 at the Right End (Column Line E)	111
Figure 3.55	Illustration of Beam Member Angle Generated During Time History Response.....	114
 Chapter 4 – Ten-Story SAC Frame		
Figure 4.1	Framing Plan Used for SAC 10-Story Modified Boston Building Frame.....	119
Figure 4.2	Column Schedule for SAC 10-Story Boston Modified Boston Building Frame.....	120
Figure 4.3	Framework Elevation Along Column Lines 1 and 5 or A and F Looking North.....	121

Figure 4.4	Extruded View Illustrating Basic SAP2000 Model of Uncompromised SAC 10-Story Modified Boston Framework Without Diaphragm X-Bracing.....	122
Figure 4.5	SAP2000 Displaced Shape Plot Illustrating Buckling Mode Shape Corresponding to the First Buckling Mode: $(\gamma_{cr})_1 = 0.413$	123
Figure 4.6:	SAP2000 Displaced Shape Plot Illustrating Buckling Mode Shape Corresponding to the Second Buckling Mode: $(\gamma_{cr})_1 = 0.582$	123
Figure 4.7	Schematic Illustrating Locations for Diaphragm X-Bracing within Framework	124
Figure 4.8	Extruded View Illustrating Basic SAP2000 Model of Uncompromised SAC 3-Story Modified Boston Framework With Diaphragm X-Bracing In Place	125
Figure 4.9	SAP2000 Displaced Shape Plot Illustrating Buckling Mode Shape Corresponding to the First Buckling Mode: $(\gamma_{cr})_1 = 3.712$	125
Figure 4.10	SAP2000 Displaced Shape Plot Illustrating Buckling Mode Shape Corresponding to the Second Buckling Mode: $(\gamma_{cr})_2 = 3.878$	126
Figure 4.11	Ineffective Columns (one column at a time) Considered with the Analysis Conducted	127
Figure 4.12	Extruded View Illustrating Compromised SAC 10-Story Modified Boston Framework With Diaphragm X-Bracing In Place and Column A-3 Removed	128
Figure 4.13	SAP2000 Displaced Shape Plot Illustrating Buckling Mode Shape Corresponding to the First Buckling Mode with Column A-3 at First Floor Level Removed: $(\gamma_{cr})_1 = 6.128$	128
Figure 4.14	Conceptualization of Column Death Loading Scenario Implemented in the SAP2000 Time History Analysis of the Compromised Framework.....	129
Figure 4.15	Elastic Linear and Nonlinear Geometric Response of The Modified SAC 10- Story Framework Used (displacement is immediately above lost column)	130
Figure 4.16	Axial Load Strain Rates (micro-strain per second) for Columns Along Line D in the Moment-Resisting Frame	131
Figure 4.17	Shear Strain Rates (micro-strain per second) for Columns Along Line in the Moment- Resisting Frame.....	132

Figure 4.18	Bending Moment Strain Rates (micro-strain per second) for Columns Along Line D in the Moment-Resisting Frame	132
Figure 4.19	Axial Load Strain Rates (micro-strain per second) for Columns Along Line B in the Moment- Resisting Frame	133
Figure 4.20	Shear Strain Rates (micro-strain per second) for Columns Along Line B in the Moment-Resisting Frame	133
Figure 4.21	Moment Strain Rates (micro-strain per second) for Columns Along Line B in the Moment-Resisting Frame	134
Figure 4.22	Axial Load Strain Rates (micro-strain per second) in the Beams of the Moment-Resisting Frame with Ineffective Column.....	134
Figure 4.23	Shear Strain Rates (micro-strain per second) in the Beams of the Moment-Resisting Frame with Ineffective Column.....	135
Figure 4.24	Bending Moment Strain Rates (micro-strain per second) in the Beams of the Moment-Resisting Frame with Ineffective Column.....	135
Figure 4.25	Demand to Capacity Ratios for Beams in Frame Affected by Ineffective Column at A-3	137
Figure 4.26	Demand-to-Capacity Ratios (DCR's) Assuming Elastic Response for Columns Along Line B in Frame	137
Figure 4.27	Demand-to-Capacity Ratios (DCR's) Assuming Elastic Response for Columns Along Line D in the Frame	138
Figure 4.28	Axial Load Demand for Members in Moment-Resisting Frame Containing Ineffective Column	139
Figure 4.29	Transverse Shear Demand for Members in Moment-Resisting Frame Containing Ineffective Column	140
Figure 4.30	Bending Moment Demand for Members in Moment-Resisting Frame Containing Ineffective Column	140

Chapter 5 – Twenty-Story SAC Frame

Figure 5.1	Typical Floor Plan With Orientation Of Columns	143
Figure 5.2	Column Schedule for Modified SAC 20-Story Building Used in the Present Study	144
Figure 5.3	Typical Floor Plan With Diagonal Members	145
Figure 5.4	Elevations Of The 20-Story Building With Fixities And Member Releases	146

Figure 5.5	First Critical Buckling Mode. Note The Minor-Axis Buckling Of Lower, Next-To-Corner Columns	147
Figure 5.6	Detail Of First Critical Buckling Mode	147
Figure 5.7	Axial Load, Shear and Moment Diagrams for Elevations along Column Lines A and F.....	148
Figure 5.8	Axial Load, Shear and Moment Diagrams for Elevations along Column Lines 1 and 7.....	148
Figure 5.9	Highest Realistic Vibration Mode Of Model Structure ($T = 0.495$ sec.).....	150
Figure 5.10	Time-History Functions Used In Analysis Of The Twenty-Story Building	151
Figure 5.11	Flex (Column) Loads Used to Simulate Ineffective Column	151
Figure 5.12	Comparison Of Turn-Off Intervals	152
Figure 5.13	Comparison Of Linear And Non-Linear Behavior For Column A3 Removal at Ground Floor with Ineffectiveness Rate Of 0.01 Seconds	153
Figure 5.14	Typical floor plan with column removals. Columns A3 and C1 were found to produce maximum results.....	154
Figure 5.15	Central-Difference Numerical Approximation Used to Compute Strain Rates	155
Figure 5.16	Axial Load Strain Rates For Column Stack at Line B when Column C1 Is Compromised.....	156
Figure 5.17	Shear Strain Rates For Column Stack at Line B When Column C1 Is Compromised.....	157
Figure 5.18	Bending Moment Strain Rates For Column Stack At Line B When Column C1 Is Compromised	157
Figure 5.19	Axial Load Strain Rates For Column Stack At Line C When Column C1 Is Compromised.....	158
Figure 5.20	Shear Strain Rates For Column Stack At Line C When Column C1 Is Compromised.....	158
Figure 5.21	Bending Moment Strain Rates For Column Stack At Line C When Column C1 Is Compromised	159
Figure 5.22	Axial Load Strain Rates For Beams When Column C1 Is Compromised	159
Figure 5.23	Shear Strain Rates For Beams When Column C1 Is Compromised.....	160
Figure 5.24	Bending Moment Strain Rates For Beams When Column C1 Is Compromised.....	160
Figure 5.25	Locations Of Largest Strain Rates When Column C1 Compromised.....	161
Figure 5.26	Member Numbers When Column C1 Is Rendered Ineffective.....	163

Figure 5.27	Member Numbers When Column A3 Is Rendered Ineffective	163
Figure 5.28	Demand-To-Capacity Ratios Along Column Line B When Column C1 Is Rendered Ineffective	164
Figure 5.29	Demand-To-Capacity Ratios Along Column Line D When Column C1 Is Rendered Ineffective	164
Figure 5.30	Demand-To-Capacity Ratios In Exterior Beams When Column C1 Is Rendered Ineffective	165
Figure 5.31	Demand-To-Capacity Ratios Along Column Line A2 When Column A3 Is Rendered Ineffective	165
Figure 5.32	Demand-To-Capacity Ratios Along Column Line A4 When Column A3 Is Rendered Ineffective	166
Figure 5.33	Demand-To-Capacity Ratios In Beams When Column A3 Is Rendered Ineffective.....	166

Chapter 6 – Membrane and Catenary Action

Figure 6.1	Two-Way Membrane Action in Reinforced Concrete Slab	171
Figure 6.2	Fundamental Representation of Catenary Action.....	172
Figure 6.3	Schematic of Two-Way Membrane Action in Composite Steel-Concrete Floor System when One In-Fill Beam is Rendered Ineffective.....	178
Figure 6.4	Schematic of Two-Way Membrane Action in Composite Steel-Concrete Floor System When Two In-Fill Beams are Rendered Ineffective	181
Figure 6.5	Schematic Illustrating Ineffective Spandrel Beam Scenario.	182
Figure 6.6	Schematic Illustrating Ineffective Spandrel and Immediately Adjacent Beam Scenario.....	185
Figure 6.7	Schematic Illustrating Ineffective Spandrel Girder Scenario	185
Figure 6.8	Two-Way Membrane Action Resulting from Ineffective Interior Column.....	188
Figure 6.9	Two-Way Catenary/Flexure Action Resulting from Ineffective Interior Column.....	188
Figure 6.10	Web-Cleat to Bolt Element Transformation.....	189
Figure 6.11	Double Angle Bolt Element Tension-Deformation Response	190
Figure 6.12	Double Angle Bolt Element Compression-Deformation Response	191
Figure 6.13	Bolt Element Tension and Compression Response for L4x3.5 Double Angles and W18x35	194
Figure 6.14	Bolt Element Tension and Compression Response for L4x3.5 Double Angles and W21x68	194

Figure 6.15	Double-Angle Pure-Moment Strength Condition.....	195
Figure 6.16	Bolt Element Tension Response with Secant Stiffness Representation.....	197
Figure 6.17	Schematic Illustrating Procedure Used to Compute Web-Cleat Connection Flexural Stiffness.....	198
Figure 6.18	Steel Grillage Model Schematic (System 1) Illustrating Axial and Moment Connection Modeling for MASTAN2 Nonlinear Analysis.....	200
Figure 6.19	Member and Connection Interaction Surfaces for Connected Member and Three Grillage Systems (connection characteristics vary).....	202
Figure 6.20	Peak Displacement Variation in SAC 3-Story Building for Various Analysis Types and Column Ineffectiveness Rates	203
Figure 6.21	Load Deformation Response of System 1 (see Figure 6.18)	204
Figure 6.22	Steel Grillage Model Schematic (System 2) Illustrating Axial and Moment Connection Modeling for MASTAN2 Nonlinear Analysis.....	206
Figure 6.23	Load Deformation Response of Grillage Systems 1 and 2 (see Figures 6.18 and 6.22)	207
Figure 6.24	Steel Grillage Model Schematic (System 3) Illustrating Axial and Moment Connection Modeling for MASTAN2 Nonlinear Analysis.....	208
Figure 6.25	Load Deformation Response of Three Grillage Systems Considered	209

This page is intentionally left blank.

List of Tables

Chapter 2 – Literature Review and Synthesis

Table 2.1	Acceptance Criteria for Nonlinear Analysis (GSA 2003)	37
Table 2.2	Multiplication Factors to Translate Lower-Bound Strengths to Expected Strengths (GSA 2003).....	40
Table 2.3	Lower-Bound Material Strengths (GSA 2003).....	41
Table 2.4	Acceptance Criteria for Linear Procedures (GSA 2003)	42

Chapter 3 – Three-Story SAC Frame

Table 3.1	Uniformly Distributed Superimposed Dead Loading and Live Loading Magnitudes (kips per linear foot) Applied to Members in the Structural Analysis	72
Table 3.2	Peak Non-Dimensional Member Demands and Demand-to-Capacity Ratios for Elastic Response to Ineffective Column at Location D-5	97
Table 3.3	Peak Non-Dimensional Member Demands and Demand-to-Capacity Ratios for Inelastic Response to Ineffective Column at Location D-5	112
Table 3.4	Peak Axial Tie Forces Computed in Beams Using Inelastic Analysis (T – Tension; C – Compression).....	117

Chapter 4 – Ten-Story SAC Frame

Table 4.1	Peak Non-Dimensional Member Demands and Demand-to-Capacity Ratios for Elastic Response to Ineffective Column at Location A-3	139
------------------	--	-----

Chapter 5 – Twenty-Story SAC Frame

Table 5.1	Maximum Vertical Displacements (Downward) After Column Indicated Is Rendered Ineffective	155
Table 5.2	Peak Strain Rates When Column C1 Is Compromised.....	161

Chapter 6 – Membrane and Catenary Action

Table 6.1	One-Way Catenary Reinforcement Capacities with Variation in Distributed Slab Reinforcement.....	184
Table 6.2	One-Way Membrane Reinforcement Capacities with Variation in Distributed Slab Reinforcement (2VLI22 steel deck).....	186

Table 6.3	Bolt-Element Tension and Compression Response Parameters for Varying Angle Thickness (all units in table are kips and inches)	193
Table 6.4	Pure Tensile, Pure Shear and Pure Moment Capacities for Double Angle Connections (all forces are in kips and kip-feet)	196
Table 6.5	Stiffness Characteristics of Web Cleat Connections	199

Chapter 1

Introduction

1.1 Research Motivation

In late fall 2004 the American Institute of Steel Construction commissioned a research study to investigate sources of robustness present in structural steel systems. There were several objectives of the research effort and the request for proposals problem statement is likely the best descriptor of its motivation. This section of the chapter outlines the RFP description so that the reader may gain a feel for the need for the research effort.

Experience with natural disasters such as earthquakes have indicated that structural steel systems such as moment resisting frames can suffer local failures at connections and still retain their ability to resist loads but some repairs will be needed. Connections retain their integrity without failure, localized plasticity may develop but subsequent repairs may not be necessary. When unusual loads such as fire or blast occur, connections remain the primary components that permit redistributions and the means of mitigated progressive collapse. For some loadings, it may be desirable to provide a “break away” segment to limit the propagation of the failure so that the entire structure is not destroyed.

This study is intended to examine the benefits of various types of structural steel systems, their connections, robustness and capability to resist unusual loads. The focus should be on the various types of connections used in moment frames and braced frames with partially restrained connections and composite structural steel or concrete members. The vision of this project is to select the most prevalent connection types in use in buildings today and perform an engineering analysis on those connection configurations under unanticipated loads. Unanticipated loads include loads in unanticipated directions, loads that are applied in an uneven fashion and rare or short loads significantly above design loads. Connections include gravity loaded shear connections, columns splices, brace connections and common moment connections.

The resulting report will include estimates of what unanticipated loads such connection will withstand, what connections are subject to notable weaknesses and it will recommend the most robust configurations, denote configurations subject to weaknesses and adjustments to configurations that can be made to make them more robust. Analytical reviews should include significant issues such as static load capacity, ductility, fracture mechanics issues, connector properties related to high-speed loadings.

As the research effort got underway, it was readily apparent that there was very limited understanding of the force and ductility demands placed on connections within steel structural systems when subjected to abnormal loading events. As a result, the objectives of the present research effort took one step backward in a more fundamental direction and sought not only to evaluate certain connection types, but to also generate

estimates for the inherent robustness in structural steel systems and the force and displacement/rotation demands that would likely be placed on the connections within structural steel systems. This information is tailor made for the next step in evaluating connections for robustness and resiliency.

1.2 Report Overview

The research report contains a literature review and synthesis that draws insights from previous work, experience, and discussion in the United States and the United Kingdom. The literature survey culminates in a synthesis that serves to provide a sound foundation for the present research direction seeking to extend the current body of knowledge in the area of robustness in structural steel systems.

Three structural steel building systems were analyzed for GSA-type scenarios in which columns within the perimeter of the framework were compromised (rendered ineffective). Three-, ten-, and twenty-story SAC pre-Northridge Boston buildings were analyzed using elastic time history analysis and inelastic time history analysis (when appropriate). The structural analyses conducted outlines member and system response characteristics typical of structural steel framing systems with low, moderate, and high redundancy. Furthermore, these analyses give insight into the demands placed on connections and members within typical structural steel framing systems during abnormal loading events.

Membrane and catenary action within the structural steel system (with 30-ft by 30-ft regular framing grid) and concrete-steel composite floor slab were also evaluated using theory previously established for two-way reinforced concrete slab systems and nonlinear structural analysis. The inherent robustness contributed by composite steel-concrete slab systems typically found in steel buildings is quantified as well as the synergistic effects of the floor slab and structural steel framing in contributing to overall general structural integrity in the steel building. Recommendations are made regarding concrete floor slab reinforcement and connection characteristics designed to enhance inherent structural integrity and robustness in the structural steel framing system.

Observations regarding the analysis results were synthesized and conclusions were drawn with respect to the demands placed on the connections within perimeter moment-resisting frame systems, the likelihood of catenary action in multistory framing systems, and the demands placed on column splices and moment resisting connections during abnormal loading events of the type considered. The membrane and catenary study yielded recommendations for connection characteristics, slab reinforcement scenarios, and anchorage forces that lead to enhanced robustness in the steel system.

The report concludes with a summary of the research effort undertaken and conclusions that can be drawn. Recommendations regarding future research that may be conducted to enhance or support the findings of the present research effort are made as well.

This page is intentionally left blank.

Chapter 2

Literature Review and Synthesis

2.1 Introduction

This chapter contains a review of the literature pertaining to robustness, progressive collapse, connection behavior, design philosophies, and the evolution of state-of-the-art design and analysis procedures for progressive collapse mitigation. The literature review is broken down in to several main sections: the ACI 318 philosophy, the U.K. experience, current design philosophies and design guidelines, general reviews of design and studies in structural performance, experimental work, and analytical methods for assessing performance.

Within each section of the chapter, the review attempts to present the literature contributions in chronological order and simply reviews research efforts and presents conclusions that could be confidently drawn. Synthesizing the literature and providing justification for the direction of the present research effort is left to the final section of the chapter.

2.2 U.K. Experience and Philosophy

One can most certainly consider the United Kingdom structural engineering profession as the first group to consider progressive collapse in a systematic manner after the accident at Ronan Point on May 16, 1968. While certainly widely reviewed, the collapse is only one of the very interesting aspects of the experience in the United Kingdom. As is sometimes the case, code provisions tend to evolve very rapidly in response to unfortunate events in the building industry. As with the WTC investigations that have been recently completed (NIST 2005), the structural engineering community in the United Kingdom assembled a group of individuals to review the current state of practice of design and construction of modular reinforced concrete buildings who then issued a report (Griffiths *et al.* 1968) with recommended changes to the state of engineering practice in relation to progressive collapse mitigation in these structures.

Some of the recommendations contained in this report were quite controversial and the Institute of Structural Engineers conducted a series of public hearings designed to address the profession's concerns. As there is a significant level of research currently underway examining the blast and progressive collapse resistance of steel structures, it is prudent to review the past experience of our colleagues across the Atlantic to glean insight into how we should be undertaking and reviewing this research and the recommendations that result. The present section in this chapter will review the discussions that arose following the publication of the inquiry into the collapse at Ronan Point and will also review the current building regulations in the United Kingdom related to progressive collapse mitigation.

ISE (1969)

An open discussion was held at The City University in London on February 27, 1969. This document is a transcript of the discussion of the meeting and it holds insight into how the structural engineering profession viewed the regulation recommendations proposed following the collapse at Ronan Point. Sir Alfred Pugsley relayed some of his observations regarding the state of the profession at the time and these were really quite interesting and likely still valid today. He quite correctly observed that the history of structural engineering prior to the collapse at Ronan Point saw tremendous refinement in design calculations, but a "...gradual decline in really independent checking" (ISE 1969). This observation is likely true today and one certainly wonders if independent checking of structural system layouts would send up warning flags regarding tendencies for progressive collapse sensitivity in structural systems and would recommend improvements in load path without the need for additional design provisions.

The Report (Griffiths *et al.* 1968) recommended a 5-psi (720-psf) pressure loading intended to simulate the loading magnitude generated by a gas or other explosion. The magnitude of this loading is enormous and the profession at the time had significant concern that the probability of a loading magnitude such as this was statistically low enough to be considered unreasonable for design. At the time it was felt that if one type of building was required to consider loading such as this, it would render this structural system uneconomical and therefore, unusable.

Some structural engineers in the audience expressed concerns that the Report (Griffiths *et al.* 1968) assumed structural engineers considered removal of critical structural members in the design phase of a structural system. The concern was then and still is today to make sure that the building stands up using the most economical structural system and configuration. A speaker at the meeting went on to say that "...you do not ensure this ... by duplication of all critical parts or inclusion of redundant members"(ISE 1969). This speaker then went on to make the observation that any regulations or codes should not "...constrain or hinder the chartered engineer in the execution of his professional skill and judgment." (ISE 1969). One can argue that this concern is present today in some members of the structural engineering community, but one can also argue that others rely on code provisions to constrain and frame their designs.

There was discussion related to a tiered system of design where specifications or codes of practice would apply to traditional systems that lie within the realm of the current state of the art and state of practice. In other words, the specifications and codes would apply to those systems that have stood the test of time. It was then recommended that systems that stretch the boundary of standard practice should be reviewed by an external body prior to construction. This is much like the current peer-review process that some owners utilize and it also implies that there would be some provisions present in standards and codes of practice to ensure minimal levels of structural integrity for the traditional systems. One can argue, however, that the

general structural integrity of today's bread-and-butter systems is not fully understood and therefore, drawing this line is very difficult, if not impossible, at the moment.

Some researchers in the audience expressed the opinion that provisions which involve evaluating structural response after removal of key load-resisting elements would likely lead to the most economical solutions to structural engineering problems involving abnormal loading events. The design provision of 5-psi pressure loading on walls was also criticized. It was correctly observed that this magnitude of pressure was impossible to economically design for and removal of gas service (the event at Ronan Point was initiated by a gas explosion) from housing was likely a more economical solution to the problem of gas explosion in residential housing. It was suggested that the gas equipment be placed in "...expendable compartments..." or blast-relief panels replicating what is often done in industrial facilities (ISE 1969).

One architect/engineer in the audience pointed out the timeless concern that "...interpretation of a set of regulations from which the design of a building evolves and is deemed adequate because it meets the requirements laid down in a Code of Practice, is not satisfactory and should never be the basis of the approach of an engineer" (ISE 1969). Even in 1969 structural engineers recognized the danger of code and specification provisions being a dogmatic validation of structural integrity.

A university professor present at the meeting echoed concerns of the senior writer of this report in stating that "...it is not my experience that it is the common aim of structural engineers to design structures so that they are fail safe" (ISE 1969). The educational process certainly advocates the benefits of redundant structural systems, but unilaterally designing structures with *a-priori* load paths to allow ineffective or redundant members was eloquently stated as being "...extremely wasteful and is quite unnecessary in all the usual framed buildings" (ISE 1969). The tendency for structural engineers to be "harassed" to increase the economy of the structural system thereby reducing the initial construction cost was mentioned in the comments made as well. We can see the reduction in redundancy in the structural system when one simply examines perimeter moment frame buildings studied later on in this report. Reduction of initial construction cost, pressures the engineer to limit moment-resisting connections to relatively few bays along the perimeter of the structure whereas better distribution of moment resisting connections throughout the framing system is likely to create more load paths without explicit *a-priori* consideration of progressive collapse resistance in the typical framing system.

One very interesting point related to how the law will interpret failure and how limit state design interprets failure was made by one of the participants. In LRFD, there is a defined probability of failure. The law on the other hand often assigns failure to negligent design. Extending this further, the participant went on to say that the probability for progressive collapse to occur in the structural framing system is finite and

therefore, the courts and public should be made aware that there is a finite probability of failure in all structural systems.

The final statements of interest that bring a dose of reality to the table is the restatement of a line in the report (Griffiths *et al.* 1968) that mentioned "...the common aim is to provide alternate load paths of support..." in structural systems (ISE 1969). One of the participants mentions that this was the furthest from the mind of the designer in many, many cases. It is expected this is true today just as it was then. It was then mentioned that: "Cinema balcony main beams, bridge piers, single suspension cables are examples of the many cases where failure of a vital member would mean disaster" (ISE 1969). These statements serve to point out that structural engineers design non-redundant systems all the time without evaluating loss of critical load-carrying elements in the design phase. In fact, many structural systems would not be possible or economical if this were routinely considered.

The difficulty in assessing the loading magnitudes and damage to the structural system was also discussed. The interaction among the slab, the framing system, partitions, facades, etc..., is a significant source of redundancy and alternate load paths inherent in the structural system. Many are not counted on in design. The arching, catenary, and cantilever action in the structural system arising as elements become ineffective were described as structural phenomena that should be considered when quantifying robustness.

One very important statement was made during the discussion of the intent of the provisions recommended in the report (Griffiths *et al.* 1968). It appeared that the recommendation that structures be evaluated after removal of critical elements was not initially intended as being applied as a design provision, but was a mechanism to force the engineer "...to make a calm and conscious assessment of this aspect so that appropriate action can be taken" (ISE 1969). It is interesting to note that this activity is now a part of state-of-the-art design guidelines, but not as a thought exercise. It is a design procedure and requirement.

One very sobering statement was made by a participant at this gathering nearly 4 decades ago. "There has been talk in the newspapers, and alas also among engineers, about designing to take the impact of aircraft flying into buildings. If such a large aircraft hits a building in a vulnerable area, causing stresses well in excess of the normal and it nevertheless does not fall down, should the engineering profession feel proud or should we feel deeply ashamed that we permitted this waste of society's resources" (ISE 1969). This statement brings the double-edged sword to life. Any design procedure that is developed must be cognizant of the wasting of resources through recognition that some loading events are truly abnormal and tragic.

ISE (1971)

The U.K. building regulations published in 1970 contained a fifth amendment for which the Institution of Structural Engineers formulated a series of provisions that could be used to design structural steel and reinforced concrete buildings over 4 stories in height. These provisions as put forth by the Institute are contained in this reference. The first concern expressed in the statement was that the Amendment would lead to unwarranted strength and cost in structural systems. The Institute wanted to go on record stating that the multistory building configurations to which the amendment would apply were “fully-framed structures in concrete and steel” designed using rigidly connected beams or continuous columns with pinned beam-to-column connections where the frame is able to “accommodate unpredictable loads” provided the building is designed according to the Building Regulations and the British Standards.

Several minimal structural integrity provisions were written into this statement and these provisions are not that far removed from those found in the current ACI Code (ACI 2005). The framing system should have “...uninterrupted horizontal tensile elements capable of supporting ... 1,700 pounds per linear foot width of building measured at right angles to the tensile elements” (ISE 1971). These tension ties are to be placed at each floor and roof level at angles that are close to 90 degrees. The floor and roof slabs should “... in every case be effectively anchored in the direction of their span either to each other or their supports in such a manner as to be capable of resisting a horizontal tensile force at 1,700 pounds per foot width” (ISE 1971). There was a clause in these provisions that recommended a floor span maximum of approximately 17 feet and total floor loading of 150 psf. It was mentioned that the tying forces and anchoring forces should be proportionally increased for longer spans and larger loading magnitudes.

ISE (1972b); ISE (1972a)

The Institute of Structural Engineers in the U.K. issued a report entitled “Stability of Modern Buildings” and the tradition of the Institute providing an open forum for discussion by its members was maintained. This report was intended to emphasize to the structural engineer that he/she should orient their approach to structural design towards “...the development of his project so that, above all, he concentrates on the need to *identify* clearly the basic anatomy of stability of the building” (ISE 1972b).

The stability report described in these references also coined the term “partial stability” of the structural system in which the building structure “... suffers local damage..., but without involving complete collapse of the structure” (ISE 1972b). One very interesting recommendation in the stability report is the notion that all building designs contain a brief designer’s statement outlining the “...anatomy of stability of his structure” (ISE 1972b). This statement can then be used by independent reviewers of the structural system to examine details to confirm that this intent is met. This goes beyond shop drawings.

An appendix in ISE (1972b) contains a design procedure whereby the partial stability of the structural system can be preserved. The design procedure recommended is based upon the philosophy that when a structural element is rendered ineffective, the adjacent structural components can effectively bridge the compromised member using catenary action. It was recommended that the sag in the catenary should be limited to "...about 20% of an adjacent single span"(ISE 1972b). There was a caveat to this statement mentioning that this limit should be evaluated for particular cases.

The discussion of the report in the transcript (ISE 1972a) is very useful as it once again points out professional and academic interpretations of the report and these provide insights into developing appropriate and widely acceptable provisions for structural integrity in steel systems. The importance of the structural components above compromised or ineffective members in multistory systems was stressed. It was correctly pointed out that catenary sag in situations with a significant number of floors above the affected area is small. Furthermore, the presence of exterior cladding and its ability to aide in cantilevering over the affected area as a beam element was discussed.

The eminent Professor K.I. Majid astutely pointed out that "...it is not sufficient to reduce the stability of a complete building to that of two-dimensional plane frames" (ISE 1972a). He went on to quote Prof. George Winter as saying: "I myself have never seen a two-dimensional building". The 3D versus 2D issue is then discussed via a wind loading example where a yielding framework gives up loading to a lesser loaded framework within a 3D structural system demonstrating the fundamentals of redundancy.

The loss of column supports at the corner of the building structure was discussed in great detail. It was recommended that the most critical condition at the corner is loss of the column supports adjacent to the corner column along orthogonal building edges. It was recommended that a stiffened edge or strut be provided at the slab edge. In the structural steel system, this is a built-in condition because the structural steel spandrel members will provide this strut to the column. Furthermore, these components are located throughout the height of the structure and therefore only the floor and roof levels near the top can be considered critical.

One participant made a very interesting comment during the discussion. The individual said that: "Structural stability should be self-evident; the stability of the structure should be obvious. If it is not, there is something wrong with the viewer, or there is something wrong with the structure, or there is something wrong with both. In any case, whatever is wrong, it will not be righted by calculation. Calculations are primarily required to substantiate the correctness of the conception – not to create it" (ISE 1972a). This is a very important point. When one examines a framing plan containing pin-connected interior framing does the structural stability of the system ever come into question? Analysis of the SAC structures later on in this

report demonstrate the need for diaphragm modeling to ensure analytically stable structures under gravity loading. Application of this participant’s “view” to the SAC structures would call their stability into question. This comment also implies that if a structural engineer can see load paths and stability in a framing system, explicit provisions for structural integrity may not be required.

The designers in the U.K. have had the unenviable opportunity to see their structures attacked on a regular basis. Some participants relayed post-attack performance observations of structures they designed when no consideration of these attacks was considered in the initial design. The three-dimensional composite behavior of all components in the structural system was found to be the reason for these building’s satisfactory performance and resistance to progressive collapse after the initial damage. One structural engineer stressed that “...we need consciously to build this concept into the structure. Otherwise it may or may not come fortuitously to our aid when disaster occurs” (ISE 1972a). This comment makes the very important point that when structural systems are conceived, they should contain the ability to form three-dimensional synergistic behavior between all components in the structural system: beams, columns, slab, cladding, etc. It also suggests that these beneficial aspects may be inherent in all systems.

Another very important point made in the stability report and the subsequent discussion of its contents is that from a design provision point of view, it was felt that design provisions that outlined extent of damage due to abnormal events were likely a better approach than threat-specific evaluations.

ODPM (2005)

The Building Regulations Part A in the United Kingdom is the document that contains provisions for prevention of disproportionate collapse in Section A3. The provision is deceptively simple:

Disproportionate Collapse

A3. The building shall be constructed so that in the event of an accident the building will not suffer collapse to an extent that is disproportionate to the cause.

A sub-section of Section A3 is titled “Reducing the sensitivity of the building to disproportionate collapse in the event of an accident”. Requirement A3 can be considered to be satisfied if a systematic approach outlined in the guidance section is followed. It should be noted that a very nice outline discussing this requirement and the guidance provisions is available (Khabbazan 2005). The following discussion will outline the procedure used to satisfy Requirement A3 specific to office occupancy buildings of structural steel, which will be considered later in this report. It should be noted that the U.K. literature reviewed in the immediately preceding sections can be seen in the A3 provision and the guidance section established to provide the engineer with a roadmap for satisfying the requirement.

The first step is to classify the building being designed. Offices not exceeding 4 stories are classified as Class 2A and offices exceeding 4 stories are classified as 2B. In the low-rise or Class 2A buildings, effective horizontal ties are required as are effective anchorage of suspended floors and walls. The structural requirements become a little more complicated when mid- to high-rise structures are considered. In this situation, horizontal and vertical tying forces are required. As an alternative approach to providing the minimum horizontal and vertical ties, the following analysis can be performed (ODPM 2005):

- Check that upon the notional removal of each supporting column and each beam supporting one or more columns that the building remains stable;
- Demonstrate that the floor at any story at risk of collapse does not exceed the smaller of 15% of the floor area of that story or 750 square feet;
- Ensure that damage does not extend further than the immediate adjacent stories.

If the notional removal of columns results in damage that exceeds the limits above, then this column is considered a “key element” (ODPM 2005). The key elements are then designed for an accidental loading pressure of 5 psi (720 psf) applied in the horizontal and vertical directions (one direction at a time) to the member and any attached components. This accidental loading should be assumed to act simultaneously with 1/3 of all normal characteristic loading.

It should be noted that the 4-story division in classification appears arbitrary. One could argue that when an 8-story building is considered, there is significant opportunity for the stories above the effected area to span across or bridge compromised columns. As the height decreases, this ability is limited. Aside from the increased occupancy in the taller structure, there may be a greater danger for the low-rise building to suffer disproportionate collapse. In fact this breakdown was a concern expressed in a subsequent guidance document (BRE 2005a).

There are procedures available (much like the commentaries in U.S. codes and specifications) for buildings that warrant particular examination outside the simple procedure outlined previously. These provisions are contained in BRE (2005a) and newer recommended modifications (BRE 2005b).

2.3 ACI 318 Philosophy

The methodology used to enhance the structural integrity of cast-in-place and precast reinforced concrete building structures (ACI 2005) was developed through research efforts undertaken in the aftermath of the Ronan Point collapse in 1968. The fact that this structure was precast and had wall components that relied solely on bond, friction, and gravity (Popoff 1975) for structural integrity naturally forced a serious look at precast concrete structural systems. However, the structural integrity provisions were not limited to precast

systems, but are interspersed throughout the provisions for cast-in-place concrete structures as well. This section of the literature review will schematically address the evolution of the ACI provisions for structural integrity (ACI 2005) designed to enhance the inherent robustness in the concrete system.

Popoff (1975)

This contribution to the archival literature outlines the code provisions at time of publication related to progressive collapse and also provides discussion of those code provisions. It is interesting in that the design philosophy proposed was based upon seismic design principles and its major thrust is very simple calculations for connection details and minimum reinforcement levels to enhance the structural integrity of the system.

The methodology seeks to exploit the inherent ductile features present in the cast-in-place (c.i.p.) concrete building. For example, temperature and shrinkage steel present in slabs creates an inherently ductile structural failure in a situation where the area of steel provided is not needed for strength. Secondly, columns in c.i.p. concrete buildings are required to maintain at least 1% longitudinal reinforcement. As a result, these concrete columns have inherent strength and ductility not counted on in the original design. Another source of inherent robustness is the requirement of minimum reinforcement in walls that runs in orthogonal directions and many times at both faces of the wall. While these criteria are rather arbitrary and unsubstantiated in their effectiveness, one cannot deny that there is ductility and strength present in a c.i.p. reinforced concrete structure that goes above and beyond that needed in the design.

It is interesting that the author of this former work recognized "...time honored and arbitrary criteria..." encountered in the design of structural steel building systems that lead to added strength and ductility not counted on in the originating design. For example, slenderness limits, semi-empirical design of stiffeners, minimum connection design forces, minimum connection configurations for truss members, and minimum size and length of welds present in earlier additions of the AISC specifications are listed as these criteria. Modern specifications (AISC 2005a) have removed explicit slenderness limits and minimum connection strengths. However, the author's points are well taken and it is very likely that if the ductility and strength that results from these types of provisions could be elucidated, the inherent robustness in structural steel building systems could be better understood and methods to enhance this inherent robustness could be proposed and evaluated.

In lieu of progressive collapse computations as recommended in present-day guidelines (GSA 2003; DOD 2005), the author proposed a "structural review". This was mentioned in ISE (1969) as well. The author coins these as "checks against reasonableness and an exercise of engineering judgment" (Popoff 1975). This is a rather interesting approach because it leads to very simple procedures that (in the senior writer's opinion) have become the foundation for the ACI 318 philosophies.

The first recommendation made is that each building should be designed for a minimum lateral load. In reality, this is not unlike the notional loads that are utilized in the direct analysis method (ACI 2005). The author proposed that a minimum lateral load with magnitude equal to 1.5% of the building's self-weight (unfactored) be defined. The notional base shear should then be distributed equally over the height of the building. If one assumes that each story in the multi-story building has the same self-weight, then this would equate to a notional load coefficient of 0.015. This is significantly greater than the notional load coefficient of 0.002 currently recommended in the specifications (AISC 2005a). Although arbitrary, this magnitude of minimum lateral load will result in added strength in the structure. However, it is not clear if this will enhance resistance to progressive collapse. The concept of designing for a minimum lateral loading magnitude is analogous to sway limitation recommendations (NIST 2005) intended to enhance structural integrity. These types of recommendations are questionable with regard to enhancing resistance to progressive collapse.

A very simple approach to quantifying a minimum force magnitude needed to tie floor slabs to supporting walls was proposed. The minimum temperature and shrinkage reinforcement required in the slab on a per-foot basis ($0.0018 \cdot 12'' \cdot h$) is used to generate tension and shear capacity requirements for slab to wall connections. This simply ensures that any strength that results from the minimum reinforcement present in the slab is transferred in its entirety to the supporting wall. While this does not guarantee the effectiveness of catenary action in the slab, it does effectively preserve a small level of robustness in the system rather than simply the component. It was also recommended that two continuously lap spliced #5 re-bars be present at all exterior walls and around all openings. Finally, it was recommended that "nominal" connections be made between flanges of double tee members and supporting walls.

There were other recommendations regarding vertical wall reinforcement and horizontal joint detailing provided in the manuscript, but these will not be reviewed here as they appeared to have minimal application in steel skeleton structures such as those considered in the present research.

The proposed methodology emphasized precast construction and therefore, the fact that precast beams are simply supported and have negligible negative moment capacity at the supports was taken to be an opportunity to enhance structural integrity through frame action. For example, consider a situation where minimum tie reinforcement from double tee topping to the supporting member is provided. This will likely generate some frame action and negative bending moment at the supports. The methodology proposed sought to exploit this frame action and provide some negative moment capacity. The proposal included minimum areas of steel computed using,

$$(A_s)_{\min,1} = \frac{200}{f_y} \cdot bd$$

and

$(A_s)_{\min,2}$ based upon a nominal live load moment of $w_L L^2/10$.

The levels of steel reinforcement computed using these recommendations were really quite nominal when the procedure was demonstrated. It should be noted that factored live loading was recommended for computation of minimum area, which is very conservative. The philosophy of generating frame action was sound, but the magnitude of the loading considered was too conservative. It should be noted that the area of steel computed also included incorporation of $\phi = 0.90$ (again, conservative).

The ACI 318 provisions (then and now) require that there be tensile continuity through column joints. Precast concrete systems have difficulty meeting this requirement. The solution to this problem is to minimize the number of column splices in the structure. In other words, it was recommended to consider precasting the columns in 3 or more story stacks. This protocol would result in a minimization of column joints in the system. This is a recommendation that most certainly could be adopted by the steel industry provided handling, fabrication and erection requirements are met.

Speyer (1976)

The PCI Committee on Precast Concrete Bearing Wall Buildings assembled guidelines for precast bearing wall buildings subjected to abnormal loading. These guidelines place emphasis on creating horizontal, vertical and peripheral tying mechanisms to preserve interaction between all building components. These are much the same as the modern guidelines (GSA 2003; DOD 2005). While no calculation of forces specific to a compromised structure are recommended, there are very simple calculations for generating numerical values for these tying forces. Many of the requirements contained in this document were also mentioned in Popoff (1975).

First of all, the guidelines recommend use of service-level loads and resistance factors of unity. This is more rational than the factored-load magnitudes and reduction factors originally recommended in (Popoff 1975). A minimum lateral load equal to 2% of the structure's service dead load magnitude (self-weight and superimposed dead load) was recommended. It was further recommended that the "...strength and stability of the structure be investigated for this combination of loading" (Speyer 1976).

The committee also recommended that vertical and horizontal tension ties be provided in the walls, the floors, and the roof systems for structures over two stories in height. The strength of these ties could be assessed using the yield stress for the material. A continuous peripheral tie should be present at each floor and roof level. The force capacity of this tie must be sufficient to create diaphragm action (Popoff 1975), but should be at least 16,000 lbs. The basis of the 16,000 lb capacity requirement was unclear. The committee

also suggested that a precast floor or roof slab can be utilized as an edge beam if the continuous tie reinforcement lies within 4 feet of the exterior wall.

It was further suggested that each floor and roof level include continuous longitudinal and transverse internal ties oriented orthogonally to one another across the building. The ties in the direction of the floor span (termed longitudinal) were recommended to have design strength equal to 2.5% of the service load on the wall (not be less than 1,500 plf). The spacing of these ties was recommended to be 8 feet on center or less. When exterior walls are encountered, the committee recommended that mechanical anchors be used to develop the tie force. It should be noted that it appears that the 2.5% of the wall force is very similar to the tried-and-true magnitude of bracing force needed to force an inflection point in an Euler column. The origination of the 1,500 plf force magnitude appears to be influenced by the 1,700 plf magnitude discussed previously (ISE 1971) and the force required to develop the minimum slab reinforcement (Popoff 1975). It was recommended that the ties transverse to the direction of the floor span be designed for a force of 1,500 lb/ft measured in the direction of the floor or roof span. If ties were spaced at 8 feet on center, then each tie should be capable of supporting 12,000 lbs. Finally, the committee recommended that flexural and temperature reinforcement usually provided within the floor systems could be used to provide part or all of the required tie forces provided this reinforcement was properly detailed.

In cases where the structure considered exceeds two stories, the committee recommended that continuous vertical ties be provided from the foundation to roof in all load bearing components (*e.g.* bearing walls, shear walls). The capacity of these ties was recommended to be sufficient to resist any net uplift or tension force calculated and should have design strength of at least 3,000 lbs per linear foot of wall.

Breen and Siess (1979)

A symposium was held in 1975 at the ACI annual convention to provide explanation of the problem of progressive collapse and to make the ACI membership and code writers aware of the problem. The synopsis of the symposium provides indication that the discussion was very much like that at the Institution of Structural Engineers 6 years earlier (ISE 1969). It is noteworthy that the authors felt at the time that "...it seems obvious that the profession has not yet made up its mind as to whether something specific should be done about the problem of progressive collapse" (Breen and Siess 1979). The authors stressed the importance of determining the answer to the question of "how safe is safe enough?". It was further surmised that the profession needed society, a regulatory agency, or code-writing body to define the problem associated with progressive collapse. One can argue that 30 years after the symposium, the definition has not yet arrived.

Fintel and Schultz (1979)

One might argue that this manuscript is the fundamental basis for the ACI 318 philosophy on structural integrity and progressive collapse resistance. The focus of the manuscript is on precast bearing wall structures that are similar to that found at Ronan Point. The authors point out that the progressive collapse that occurred in this famous accident resulted from the structure's inability to bridge over a local failure (loss of a bearing wall). It was argued that the abnormal loading hazard was an inevitable consequence and that the "...susceptibility of a structure to progressive collapse..." poses the "...real risk..." to structures (Fintel and Schultz 1979).

The authors outlined three approaches to mitigate the risk of progressive collapse in buildings. The first was eliminating the hazards present at or in building structures. Examples of this is eliminating gas installations in multistory buildings as discussed in the public hearings immediately following the issuance of the Ronan Point report (Griffiths *et al.* 1968; ISE 1969), or ensuring stand off distances (DOD 2002; GSA 2003). The second was to design the structure so that a hazard cannot compromise the entire structure through preventing local failure. The final approach recommended is to allow local failures to occur, but to allow alternate load paths to activate once a local failure has taken place.

Fintel and Schultz (1979) successfully argue (in the senior writer's opinion) that a realistic solution to the progressive collapse problem can only come from considering *all* abnormal loading conditions and that this cannot be done. Therefore, considering abnormal loading events and designing for those events cannot be a realistic design solution. The authors subscribe to the philosophy that abnormal loading events are going to happen. The type of abnormal loading event and its magnitude are unpredictable and therefore, cannot be realistically posed in design scenarios and/or loading combinations. As a result, they recommend allowing the inevitable local failures to occur, but "...provide alternate load paths within the structure to avoid an overall collapse" (Fintel and Schultz 1979). The authors define the structure's ability to bridge over local failures as "General Structural Integrity (GSI)".

It was suggested that the GSI approach can be implemented in several ways. First, design specifications can recommend and provide a systematic methodology to create structural integrity in building systems. Examples of this approach are the GSA (2003) and DOD (2005) guidelines. An alternative approach is to have specification or code-writing bodies develop minimum detailing provisions such that minimum levels of continuity and ductility are present in all structures designed using the written specifications. Several advantages to the minimum continuity requirements are discussed by the authors (Fintel and Schultz 1979):

- specification writers and researchers have a general responsibility to evaluate details to assure structure safety.

- design engineers should not be required to directly consider the effects of abnormal loads for one form of construction and not another.
- minimum detailing requirements based upon sound engineering judgment can establish adequate levels of structural integrity.

The goal of these minimum requirements would be to design structures with indirect (or built in) alternate load paths when local failures occur.

Discussions of the work of Fintel and Schultz (1979) was published in the *ACI Journal* soon after its publication. It is interesting to note that the discussion that followed publication of this manuscript followed very much the same lines as the discussion following issuance of the Ronan Point Report (Griffiths *et al.* 1968; ISE 1969; ISE 1971; ISE 1972b; ISE 1972a). Several very important points were raised in the discussion provided by (Buettner 1979). It was argued that several sources of abnormal loading are “absolutely avoidable” including gas explosions and vehicle collisions. It was also argued that a second group of abnormal loadings are incalculable (*e.g.* bombings). The basis for this second argument is found in the following statements: “If I design for two sticks of dynamite, will the saboteur not use three? If I design for collision by a Cessna, will fate not direct impact from a 747? At what point is the line drawn?” (Buettner 1979). Furthermore, it is argued that providing additional tying mechanisms in a structure to address loading scenarios with very low probabilities of occurrence is wasteful of resources. These are felt to be very important points and must be considered when developing specification provisions for structural integrity. It suggests that an understanding of the inherent robustness of traditionally constructed structural systems in response to some well-defined accident type (*e.g.* removal of a column, loss of a beam member) be considered before demanding that unjustified tie force magnitudes be used in building design.

Hawkins and Mitchell (1979)

This manuscript outlines a systematic approach to developing progressive collapse resistance in flat plate structures. The main initiator of progressive collapse in these structures was felt to be punching shear failure at columns. Four defenses for resisting progressive collapse were outlined (Hawkins and Mitchell 1979):

- design the structure for higher live loadings;
- require that integral beam stirrup reinforcement be placed in the slab;
- require bottom reinforcement be continuous through columns or properly anchored within the column;
- design the bottom reinforcement for tensile membrane action.

Providing slab reinforcement capable of facilitating tensile membrane action in the slab system in the event that a punching shear failure occurs was felt to be the best solution to the problem of eliminating

disproportionate collapse. The basic premise of the design philosophy is to provide continuous reinforcement in orthogonal directions within the slab system whereby a two-way tensile membrane can form if a column punching shear failure occurs. This membrane action will serve to bridge the lost support and inhibit the start of a progressive collapse sequence. Comparison of membrane strength prediction equations and experimental results was made. The reinforcement detailing recommendations made appear to be the basis for ACI 318 recommendations. It was recommended that the ACI 318-77 slab reinforcement provisions be changed to require bottom steel to be effectively continuous throughout the slab system. Splices within the slab reinforcement must be capable of developing the bar's tensile strength. It was recommended that additional spandrel beams be added to flat plate structures to provide a mechanism for development of membrane compression rings at the edge of the slab panels. These spandrel elements also were thought to provide a means of anchoring slab reinforcement at the panel edge.

The procedures outlined in this manuscript will be used later on in this report to quantify the membrane strength of composite steel-concrete slab systems found in structural steel buildings. As a result, its discussion will be limited in this literature review as more details will be provided later.

Mitchell and Cook (1984)

An often-referenced description for progressive collapse is a collapse scenario in a structure that is disproportionate to the instigating event. This research effort sought to develop and evaluate procedures for preventing progressive collapse where the instigating event would be punching shear failure in slab systems at interior and exterior columns in c.i.p. concrete systems. The slab system focused on in the research was typical two-way edge supported and column supported slab systems.

Assuming that a punching shear failure occurs in the slab at an interior column, the philosophical basis for the methodology proposed was to provide continuous steel reinforcement through the column and attempt to “hang” the slab from this column using this reinforcement. In the event that this through-column reinforcement becomes ineffective, membrane action of the reinforced slab would also be counted on to help distribute loading to the surrounding un-compromised columns. The basis for the methodology proposed is summarized by: “The key in preventing progressive collapse may be to design and detail slabs such that they are able to develop secondary load carrying mechanisms after initial failures have occurred” (Mitchell and Cook 1984).

There were both experimental and analytical efforts included in this research. One set of experiments clearly demonstrated the ability of continuous reinforcement through an edge column to “hang” a failed slab from that column. If bottom bars were not continuous through the column along with continuous negative moment reinforcement, this “hanging action” would not develop. The manuscript also provides a very nice

discussion related to the development of principal compression stress trajectories (*i.e.* compression rings) in edge-supported slab panels. When the slab is vertically supported around its four edges on very stiff supports, the compression ring is able to form in the slab and the tensile membrane action is able to form. However, if the slab panel is allowed to deflect vertically at its edges as in the case of column-supported panels, the internal horizontal edge restraint is not present and the compression rings cannot form. As a result, the authors recommended providing well-anchored continuous bottom reinforcement around the perimeter of the slab panels.

The effort also examined a scenario that has some similarities to situations present in structural steel systems: the two-way slabs supported on extremely stiff (relative to slab) beams. It was shown that this scenario allows very effective formation of membrane action in the slab panel and therefore, the methods for quantifying the two-way membrane action in the composite steel-concrete slabs present in steel buildings are good candidates for the present study. Furthermore, the philosophy of ensuring that secondary load-carrying mechanisms can develop in the structural system is a good one to carry forward in the present effort.

ACI (2005)

The evolution of the current ACI 318 recommendations is apparent when one reflects back on the previous contributions to the literature outlined in this section. ACI 318-05 has explicit provisions related to structural integrity. It is felt that these provisions are relatively simple and will enhance the inherent robustness of a concrete structural system and it was thought that these types of provisions could be easily incorporated into the steel specifications if proper justification could be provided.

The structural integrity requirements are interspersed throughout the code and the first appearance of provisions occurs in the reinforcement detailing chapter (Chapter 7). Section 7.13 requires that the detailing of reinforcement in the reinforced concrete system effectively tie together the members within the structure. There are minimum requirements related to mild-steel reinforcement continuity in cast-in-place systems. Specifically, at least one-sixth the negative moment reinforcement must be continuous through or anchored into the support; and at least one-quarter of the mid-span positive moment reinforcement must be continuous through or anchored into the support. At least two bars (top and bottom) must be continuous in these beams.

Requirements for structural integrity of slab systems are contained in Chapter 13 of ACI 318. These provisions are very similar to the perimeter beam provisions described previously (at least in concept). Section 13.3.8 outlines the requirements for bottom bar continuity. All bottom reinforcement bars within the column strip in two-way slab panels are required to be continuous or spliced such that the yield strength of the bars can be developed in each direction. There are specific locations where splices can be made and at least two of the bottom bars shall pass through the column cores and must be anchored at exterior supports. This

provision is directly taken (more or less) from the work of Hawkins and Mitchell (1979) and Mitchell and Cook (1984).

The Ronan Point effect is seen in the provisions found in Chapter 16 (precast concrete). Section 16.5 outlines the structural integrity provisions. Longitudinal and transverse tension ties are required to be placed throughout the structural system. The tensile strength of the connection between a floor system diaphragm and the members being supported laterally shall be 300 pounds per linear foot. Vertical tension ties in the structural system are also required. These ties can be provided in one of the following ways (ACI 2005):

- The precast concrete column must have a minimum tensile strength of $200A_g$, where A_g is the required cross-sectional area of the column for strength considerations.
- Precast wall panels should have a minimum of two ties per panel with a minimum strength of 10,000 pounds per tie. A tie can consist of properly anchored groups of reinforcing bars sufficient to provide the required tie force.
- If the design forces result in no net uplift (or tension) at the base, the 10,000 pound ties may be anchored into an appropriately reinforced concrete slab on grade.

When a precast structure exceeds three stories in height, provisions similar to those found in the U.K. building regulations (ODPM 2005) and those discussed earlier (ISE 1971) are recommended. Longitudinal and transverse ties must be provided within the floor system. These ties should have a minimum strength of 1,500 pounds per linear foot of width or length. These ties cannot be spread out too far apart within the system (10-foot maximum spacing or the bearing wall spacing – whichever is smaller). Perimeter ties in the system must have a tensile capacity that exceeds 16,000 pounds. Continuous vertical tension ties over the height of the building must also be present in the structural system. These ties must have a minimum tensile strength of 3,000 pounds per horizontal foot of wall. A minimum of two ties per precast wall panel are required.

2.4 Current Design Philosophies and Design Guidelines

The present section of the literature review provides a look into current design guidelines for mitigating progressive collapse or enhancing robustness in structural systems. Those efforts thought to be most influential in leading up to the state of practice related to mitigating progressive collapse in structural systems are also briefly reviewed. The documents reviewed are those that most directly affect the state of practice in the United States although the very brief provisions contained in the Canadian steel design manual and the National Building Code of Canada are reviewed.

Leyendecker and Ellingwood (1977)

This is one of the earliest government-sponsored efforts related to developing design methodologies for resisting progressive collapse in structural systems in response to the accident at Ronan Point. A review of the Ronan Point investigation is provided in the manuscript and an extensive bibliography is included. The philosophy proposed in this document serves as the basis for the progressive collapse mitigative design guidelines used in current practice.

The manuscript contains a nice description of the sequence of events that occur during structural collapse. These events may or may not lead to progressive collapse as there are cases where the initial damage is indeed proportionate to the initiating event. Figure 2.1 contains a reproduction of a flowchart illustrating the sequence of events that can occur during structural collapse. This flowchart is very useful in helping to identify the role of inherent robustness in the structural system.

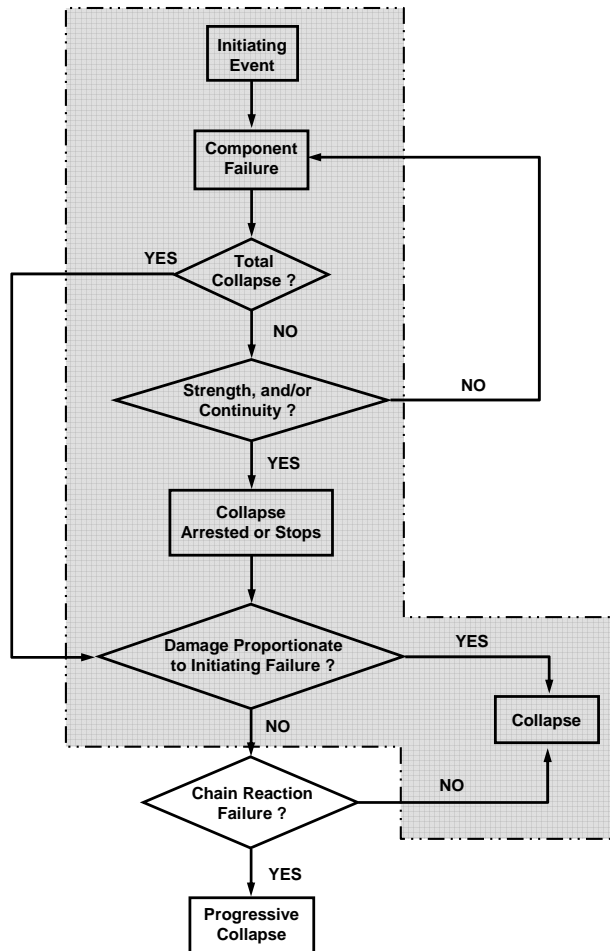


Figure 2.1 Flowchart Indicating Sequence of Events During Collapse Event - adapted from Leyendecker and Ellingwood (1977).

As long as the collapse event remains within the shaded flowchart area in Figure 2.1, the initiating event will not lead to progressive collapse. The structural system that is able to remain within this shaded area can be considered robust. It should be noted that if there is not sufficient strength or continuity in the structure to prevent cyclic component failure, the collapse scenario can still be classified as simple collapse if the damage is proportionate to the initiating event.

Three methods were recommended for keeping the structural system within the bounds of the shaded region of the flowchart in Figure 2.1. These design philosophies were: event control; direct design; and indirect design (Leyendecker and Ellingwood 1977). Event control attacks the problem of progressive collapse by starting at step one in the flowchart. Direct design can take two approaches. The first is ensuring that alternate load paths exist in the structural system to arrest a collapse and the second was termed the specific local resistance method in which sufficient strength to resist component failure (refer to the flowchart in Figure 2.1) is provided. The indirect design philosophy seeks to create sufficient strength and continuity in the structural system through specification of minimum levels of each. In effect, specifications of this type are what ACI 318 does in their structural integrity provisions.

It was argued that event control is not always a practical design approach and indirect and direct design methods are most appropriate for consideration by the design professional and specification- or code-writing bodies. Direct design was felt to be most appropriate for unusual buildings and those likely to face a defined threat, while indirect design was thought to be adequate for regular buildings. A second flowchart adapted from this work is given in Figure 2.2. In order for the shaded area to be utilized and the indirect design procedure to be accepted for the typical steel building structure, the minimum levels of strength and continuity need to be defined so that building officials and structural engineers can have confidence that following the design specifications will provide minimum levels of progressive collapse resistance (*i.e.* robustness and structural integrity). Leyendecker and Ellingwood (1977) recommend that this be done using laboratory investigations. However, any laboratory investigations undertaken must be designed to represent reality and include experimental protocols that are capable of simulating the demands expected on structural components during abnormal events.

The present effort will focus on the shaded region of the flowchart shown in Figure 2.2, which is the indirect design path whereby general provisions for structural integrity could be proposed. In order to make these recommendations and provide insights into experimental testing that is required to ensure these recommendations will be reliable, the inherent robustness or inherent structural integrity (ISI) must be identified for the usual structural steel building system. “By virtue of the normal design process, a certain amount of strength and continuity is provided which is also available to resist abnormal load” (Leyendecker and Ellingwood 1977). There have been many, many cases stretching back many years where a normally

executed design provides protection against abnormal events. Examples of these are many of the buildings in and around the World Trade Center (NIST 2005), structures bombed during World War II (ISE 1969), and behavior seen after bombings in Northern Ireland (ISE 1969). Therefore, it is imperative to quantify these sources of inherent resistance to disproportionate collapse as they will provide insight into the form minimum ductility, tying force, strength, and stiffness provisions will take.

Leyendecker and Ellingwood (1977) insightfully argue that the materials, configuration, height, etc..., of the “normal” building will likely change with time. Construction materials are always under development and new structural systems are continually being proposed to meet the economic challenges of the changing fiscal environment. As a result, any provisions that are recommended must clearly identify what constitutes the “normal” structural system (*e.g.* typical framing layout, materials strengths, connection configurations, story heights, initial loading conditions, etc...) as these conditions may change with future construction.

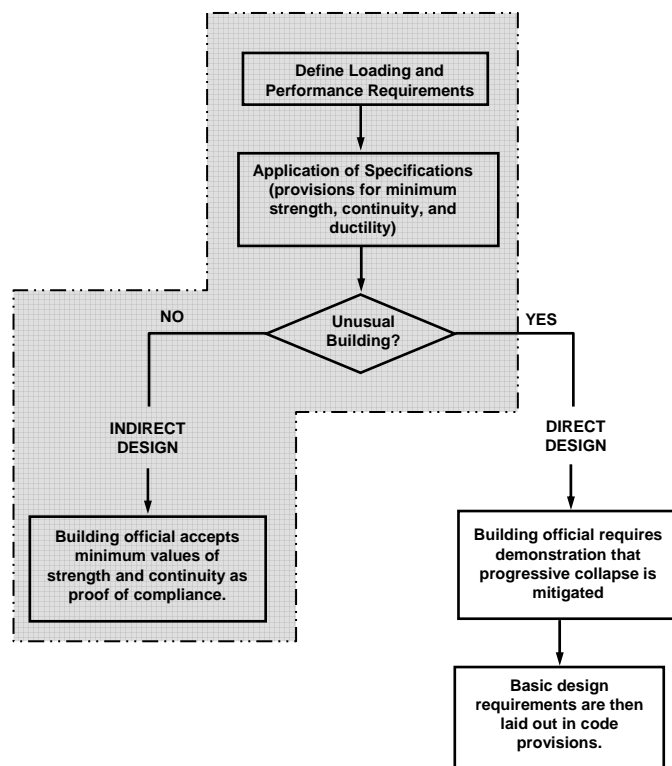


Figure 2.2 Flowchart Indicating Design Procedure that Includes Consideration of Progressive Collapse - adapted from Leyendecker and Ellingwood (1977).

Direct design and alternate load path design strategies, including probabilistically based load factors and resistance factors are discussed as well. As the present research effort will consider alternate load path methods by first establishing the likely inherent robustness present in the framing system, the recommendations regarding the alternate path method will be briefly discussed. Assuming that alternate load paths will form within the structure implies that some damage to the structural system is expected. This damage may or may not cause fatalities and many design provisions (ODPM 2005) have been developed under assumptions that the damaged region will be limited (ISE 1971). Leyendecker and Ellingwood (1977) recommend that damage in any given story be limited to 750 square feet or 15% of the floor area. This is essentially a 27-ft by 27-ft region within the floor plan (*i.e.* a typical framing bay in steel systems). This floor area was felt to limit deaths due to collapse events to one per event on average (Leyendecker and Ellingwood 1977). This damaged zone may also be used as a sacrificial area within the structural system through use of isolation joints or expansion joints. Unintended sacrificial regions within the structure worked very well during the 9-11 attacks on the Pentagon as collapse was limited to those portions of the structural system between expansion joints. Use of sacrificial structural regions was felt to be most appropriate for low-rise structural systems (Leyendecker and Ellingwood 1977).

With regard to development of minimum structural integrity provisions, there are some very good points made in the manuscript. First of all, the alternate load path method conducted with removal of key structural elements (*e.g.* major load carrying beams, floor slabs between supports, columns) can be considered “... a feasible means of determining minimum requirements for strength and continuity which can result in buildings said to possess structural integrity” (Leyendecker and Ellingwood 1977). The authors emphasize that the reasons for the minimums should be clearly illustrated in any code provisions and that these provisions would likely need to be developed for different construction types. Precast concrete panelized systems have been addressed (Fintel and Schultz 1979) and reinforced concrete slab systems also received consideration (Hawkins and Mitchell 1979; Mitchell and Cook 1984). Structural steel systems are notably absent at present and the WTC research effort (NIST 2005) did not address structural integrity in steel systems. The present research effort therefore, should seek to fill the void and propose structural integrity provisions for typical structural steel framing systems. These provisions should be developed using the alternate load path philosophy and this in turn will address one-half of the design flowchart proposed in Figure 2.2.

Factored loading combinations for use in an alternate load path design methodology were also proposed. Key element removal scenarios should include evaluation of remaining member strengths under the following loading combinations (Leyendecker and Ellingwood 1977),

$$D + 0.5L_{ANSI} + 0.2W_{ANSI} \quad (2.1)$$

$$D - 0.3W_{ANSI} \quad (2.2)$$

Equation (2.1) is intended to be used when wind effects have the same “sense” as gravity loading effects and equation (2.2) is intended to be used when opposite senses occur. The wind loading was considered in these equations because it was felt that rescue operations and assessment of the stability of the damaged structure would likely take place in the days following the event, which may result in the need to consider wind loading over this time period.

DOD (2002)

The Department of Defense publishes a series of Unified Facilities Criteria (UFC) intended to be applied in the design of building facilities for the departments of the military, the defense agencies, and Department of Defense field activities. The minimum antiterrorism standards that are published by the DoD are intended to ensure that there is some level of protection against all threats that a U.S. governmental building may be exposed to and to reduce injuries and fatalities that may result from successfully executing threats. The primary means with which to achieve these goals is to maximize standoff distances and ensure that terrorist threats are kept well away from possible target facilities. Other means are preventing building collapse, minimizing hazardous flying debris, effectively laying out a facility to inhibit terrorist activity, limiting airborne contamination, and creating mechanisms for mass notification of threats to occupants of a facility. The present review will focus on those methods for preventing building collapse present in the UFC 4-010-01 document. This document is intended to be a starting point for addressing progressive collapse scenarios instigated by terrorist threat with subsequent UFC documents (one to be reviewed shortly) being used to finish design activities.

The UFC (DOD 2002) consider the risk of progressive collapse to be higher in buildings with 3 or more stories. This is consistent with the definitions of progressive collapse discussed earlier in this review as the number of stories present in the facility can limit the possibility for the “chain reaction” (Leyendecker and Ellingwood 1977) of events required in the classic definition of progressive collapse. Furthermore, when less than three stories are present, there is opportunity for only one adjacent floor to collapse given the loss of a ground-level supporting element and therefore, one could argue that all collapse scenarios for these low-rise structures would be proportionate to the initiating event (Leyendecker and Ellingwood 1977). The overall statement used to instruct designers to consider progressive collapse prevention measures is “...design the superstructure to sustain local damage with the structural system as a whole remaining stable and not being damaged to an extent disproportionate to the original local damage” (DOD 2002). The criteria then go on to mention that this can be accomplished by providing sufficient levels of continuity in the framing system, redundancy in the load paths present in the system or components, or providing energy dissipating capacity.

While the levels of redundancy, continuity, etc..., are not quantified in the criteria, a few indirect means of achieving these favorable structural characteristics are outlined.

The UFC require all exterior load carrying columns and walls to sustain a loss of lateral support at any floor level. This is accomplished very simply by demanding that all columns have unbraced lengths equal to two stories with appropriate effective length factors then applied to that unbraced length. If there is parking at the interior of the structure, internal vertical load carrying columns should also have their unbraced lengths (in effect) doubled. The structure should also be analyzed to demonstrate that one primary external or horizontal load carrying element can be removed without progressive collapse. Finally, all floors should be designed to resist net uplift (resulting from explosion) from the following loading combination;

$$D + 0.5L \quad (2.3)$$

Therefore, it is assumed that the pressure waves resulting from explosion are sufficient to lift any floor framing components with a defined measure of point-in-time live loading.

There are also several additional measures recommended to enhance favorable structural response in the event of terrorist attack (DOD 2002). It is recommended that highly redundant moment-resisting frames be used and that connections be detailed to provide continuity across joints equal to the full factored structural capacity of connected members. The detailing of members and connections should also be done in a manner that accommodates large displacements without total strength loss. It is interesting to note that the UFC do not quantify any of these targets and designers are really left to their own devices.

ASCE (2006)

The ASCE/SEI design standard also has a rather broad-reaching statement regarding general structural integrity. In essence, the Standard requires that buildings be designed to withstand local damage without damage to the structural system being out of proportion to the event that initiated the damage. Furthermore, the structural system should remain stable after the local damage occurs (*i.e.* the structure should not collapse).

Although no specific guidance is given (none should be expected from a minimum design load standard), there is some guidance given into the methods that can be used to achieve the resistance to progressive collapse demanded as well as recommendations regarding how probabilities of failure should be defined. The alternate load path concept (Leyendecker and Ellingwood 1977) is recommended whereby the structural system is arranged in a manner that allows the portions of the damaged structure to be bridged by those undamaged components thereby transferring the gravity loading to the foundation around the compromised portion of the structure. It is recommended that these alternate load paths be built into the

structure by providing “...sufficient continuity, redundancy, or energy-dissipating capacity (ductility), or a combination thereof, in the members of the structure” (ASCE 2006).

GSA (2003)

One of the most comprehensive guidelines available for designing to mitigate progressive collapse in structural systems is published by the General Services Administration. The procedure contained in these guidelines is essentially a direct design procedure (Leyendecker and Ellingwood 1977). The Guidelines implement a flowchart methodology whereby the structural engineer walks through a series of questions. These questions culminate in a decision that a given structure under design is exempt from consideration of progressive collapse, or it requires further consideration of progressive collapse and application of the Guidelines for detailed analysis and design for progressive collapse resistance.

The questions to be considered start with determination if the structure in question may be *exempt* from further consideration of progressive collapse. In general, the answers to each question issued in the exemption process should have a detailed written component as well as a graphical component sufficient to support the answers provided. The questions address *local attributes* and *global attributes* pertaining to the structural system and its components that lead to a resilient and robust design. Global attributes are simply column spacing, the number of stories, and significant structural irregularities (if present). Local attributes are essential connection elements and their ability to preserve structural continuity across a removed vertical element, and achieve a robust and resilient design. The structural engineer must document the methodology to achieve connection redundancy, connection resilience and distributed beam-to-beam continuity. These terms are defined as follows (GSA 2003);

Connection Redundancy: A beam-to-column connection that provides direct, multiple load paths through the connection.

Connection Resilience: A beam-to-column connection exhibiting the ability to withstand the rigorous and destructive loading conditions that accompany column removal without rupture.

Robustness: Ability of a structure or structural components to resist damage without premature and/or brittle fracture due to events like explosions, impacts, fires or consequences of human error, due to its vigorous strength and toughness.

Discrete Beam-to-Beam Continuity: A distinct, clearly defined beam-to-beam continuity link across a column, for beam-to-column framing applications, that is capable of independently transferring gravity loads for a removed column condition, regardless of the actual or potential damage state of the column.

The questions that arise during the exemption process are posed in the Guidelines (GSA 2003) in the form of a flowchart for ease of use. The series of flowcharts are given in Figures 2.3 through 2.7. The most economical design for a structural steel building system is a system that inherently provides progressive collapse resistance and maintains the public's safety in the absence of spending additional resources (*e.g.* structural engineering time, structural steel material cost, labor cost) specifically targeted to generate the resistance to progressive collapse in a structural system. In order to achieve this economy, one must move their way through this flow chart and seek all avenues possible whereby the “exempt box” is reached. These paths are within the shaded regions in the flowcharts.

We can start detailed examination of the exemption process and assemble the structural characteristics that are needed to achieve the most economical steel structure (*i.e.* the structure exempt from detailed consideration of progressive collapse) by walking through each flowchart. Flowchart 1 in Figure 2.3 really leaves little opportunity to find the exempt path. Most typical structural steel buildings will result in a “NO” answer for the first six questions. Assuming one would like to avoid considering designing and constructing to the progressive collapse criteria (GSA 2003), connection redundancy, connection resilience, system robustness, and discrete beam-to-beam continuity will have to be demonstrated. It will be assumed at this point that this will be confirmed through detailed analysis of several typical structural steel framing systems and therefore, we must move onto Flowchart 2 in Figure 2.4.

Flowchart 2 begins with a question that is really an “event control” question (Leyendecker and Ellingwood 1977). It will be assumed that the typical structural steel building will not have minimum stand-off distances and therefore, there is no path for exemption and we must move to Figure 2.5 (Flowchart 3). Hiring a blast engineer to design primary and secondary structural members (*e.g.* frame, roof, wall, foundation) for blast loads will most certainly lead to a more expensive structure and this should be avoided if at all possible. Therefore, in order to continue the process Flowchart 4 (Figure 2.6) must be consulted.

Most typical structural steel framing systems will not have pre- or post-tensioned elements. It will be further assumed that the facility does not have uncontrolled public areas (*e.g.* a security guard or surveillance activity will be present), or uncontrolled parking. Adherence to the seismic design requirements in severe seismic zones will generate significant levels of inherent ductility and toughness in the structural connections. At this point, we will assume that the connections that will be present are sufficiently ductile (to be verified through analysis) and the final flowchart for structural steel systems can be consulted (Flowchart 6 in Figure 2.7).

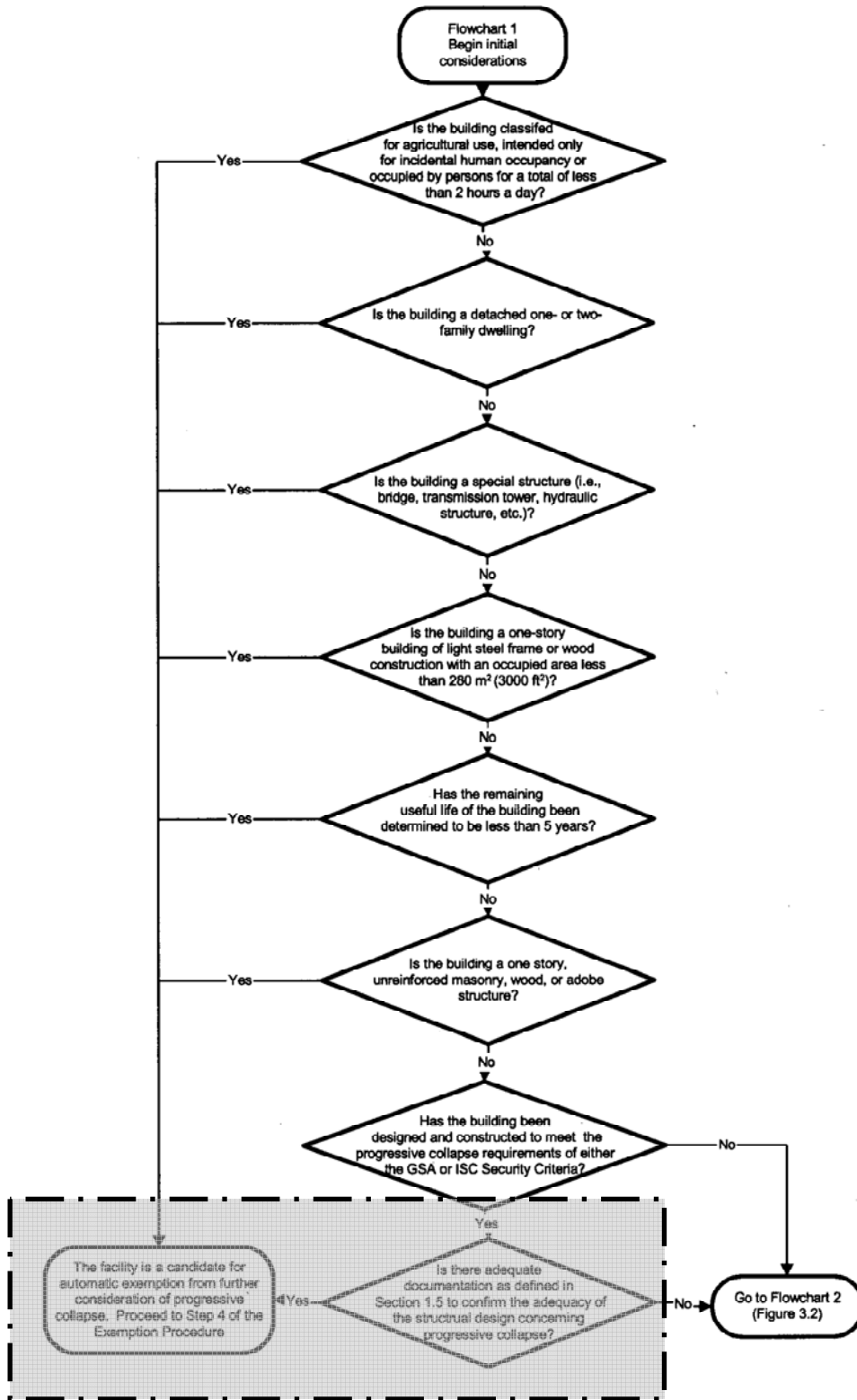


Figure 2.3 Flowchart 1 of Exemption Process (GSA 2003).

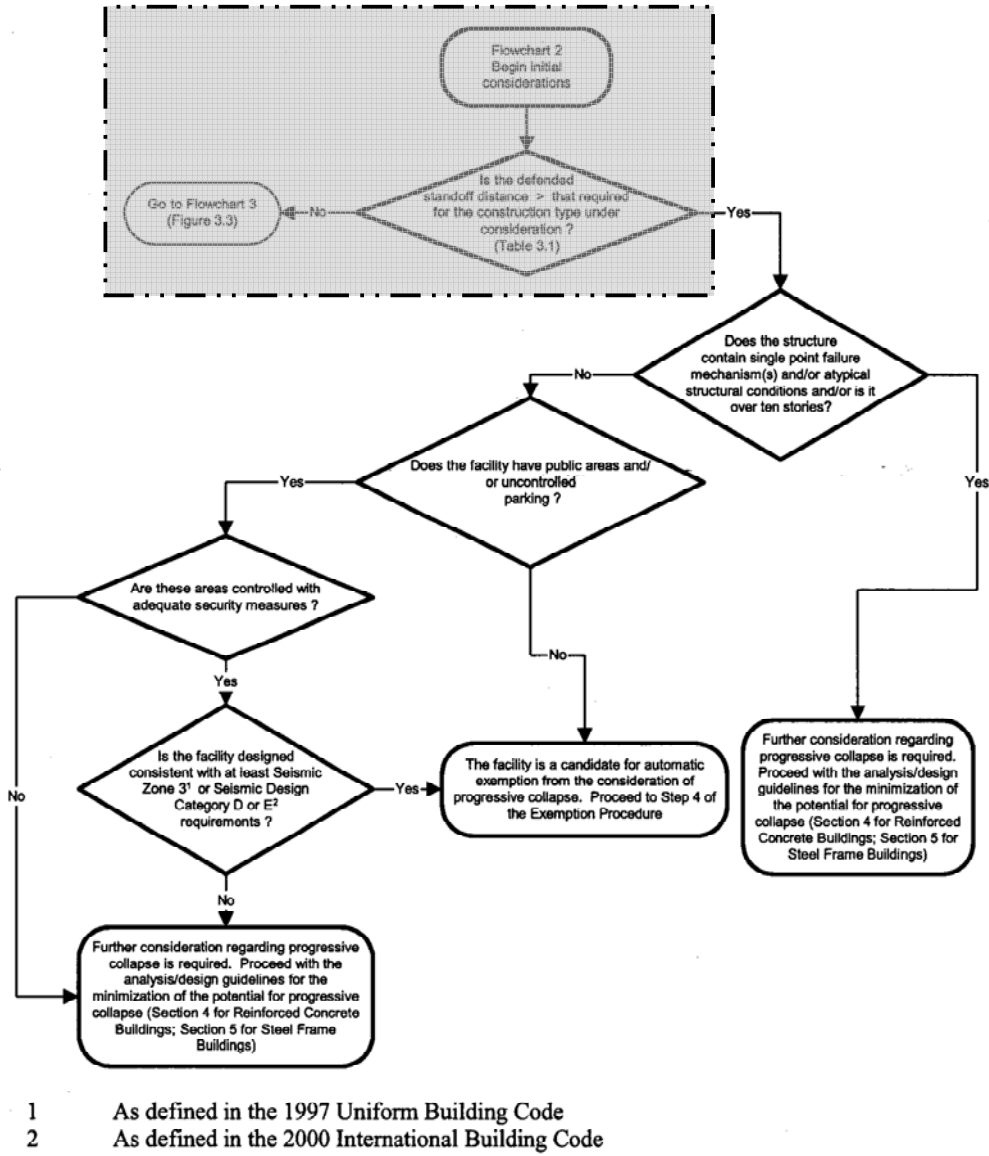
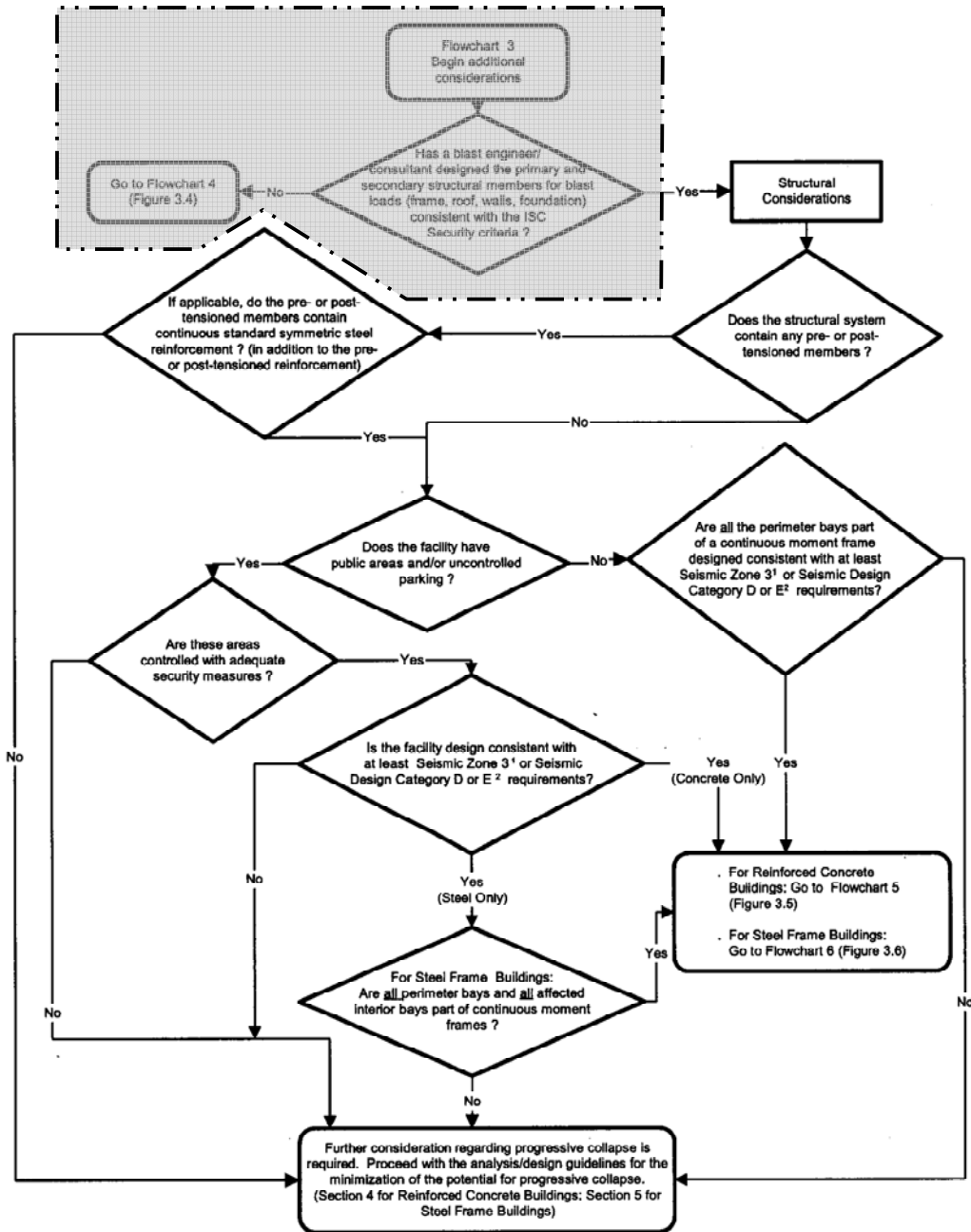
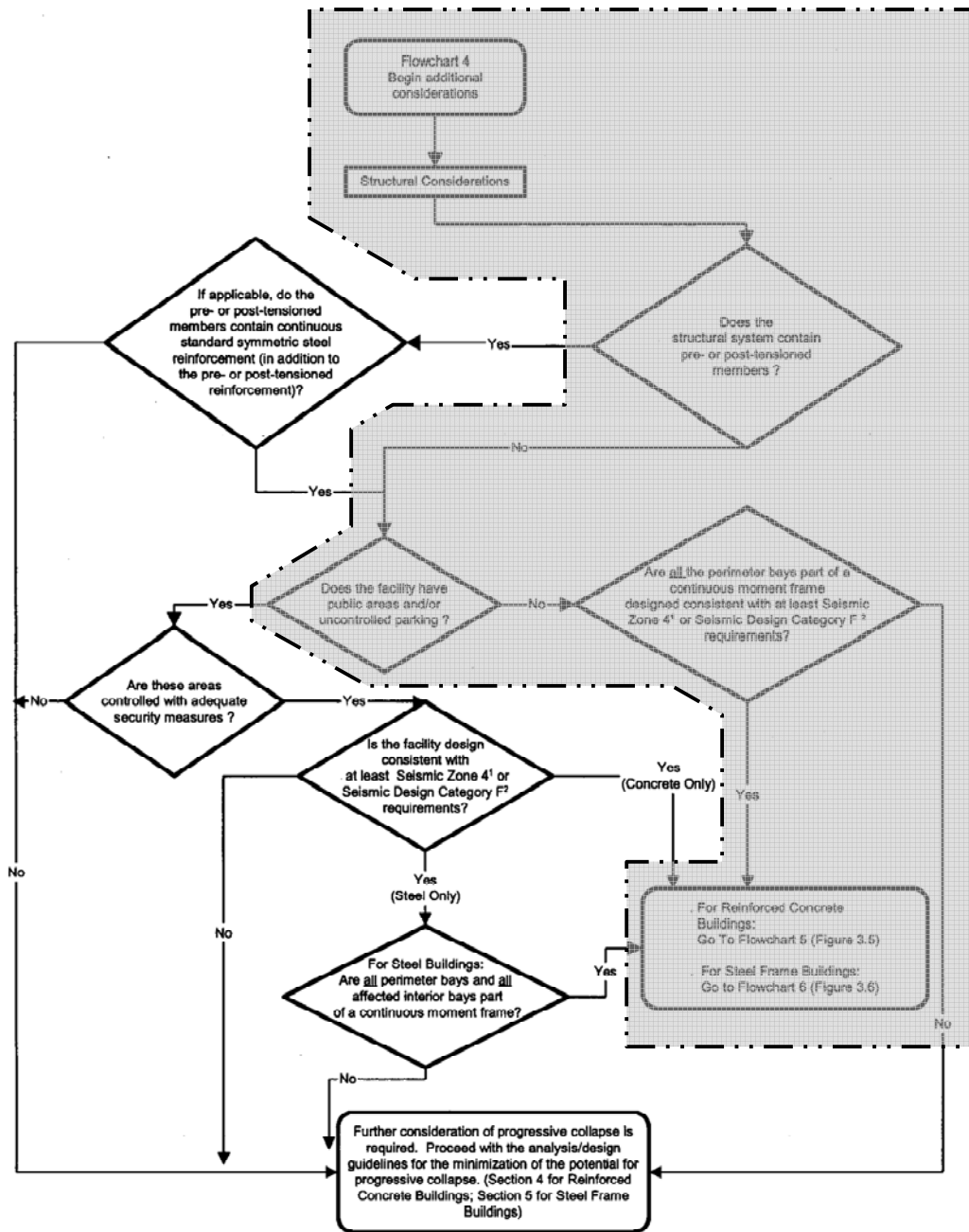


Figure 2.4 Flowchart 2 of Exemption Process (GSA 2003).



- 1 As defined in the 1997 Uniform Building Code
- 2 As defined in the 2000 International Building Code

Figure 2.5 Flowchart 3 of Exemption Process (GSA 2003).



- 1 As defined in the 1997 Uniform Building Code
- 2 As defined in the 2000 International Building Code

Figure 2.6 Flowchart 4 of Exemption Process (GSA 2003).

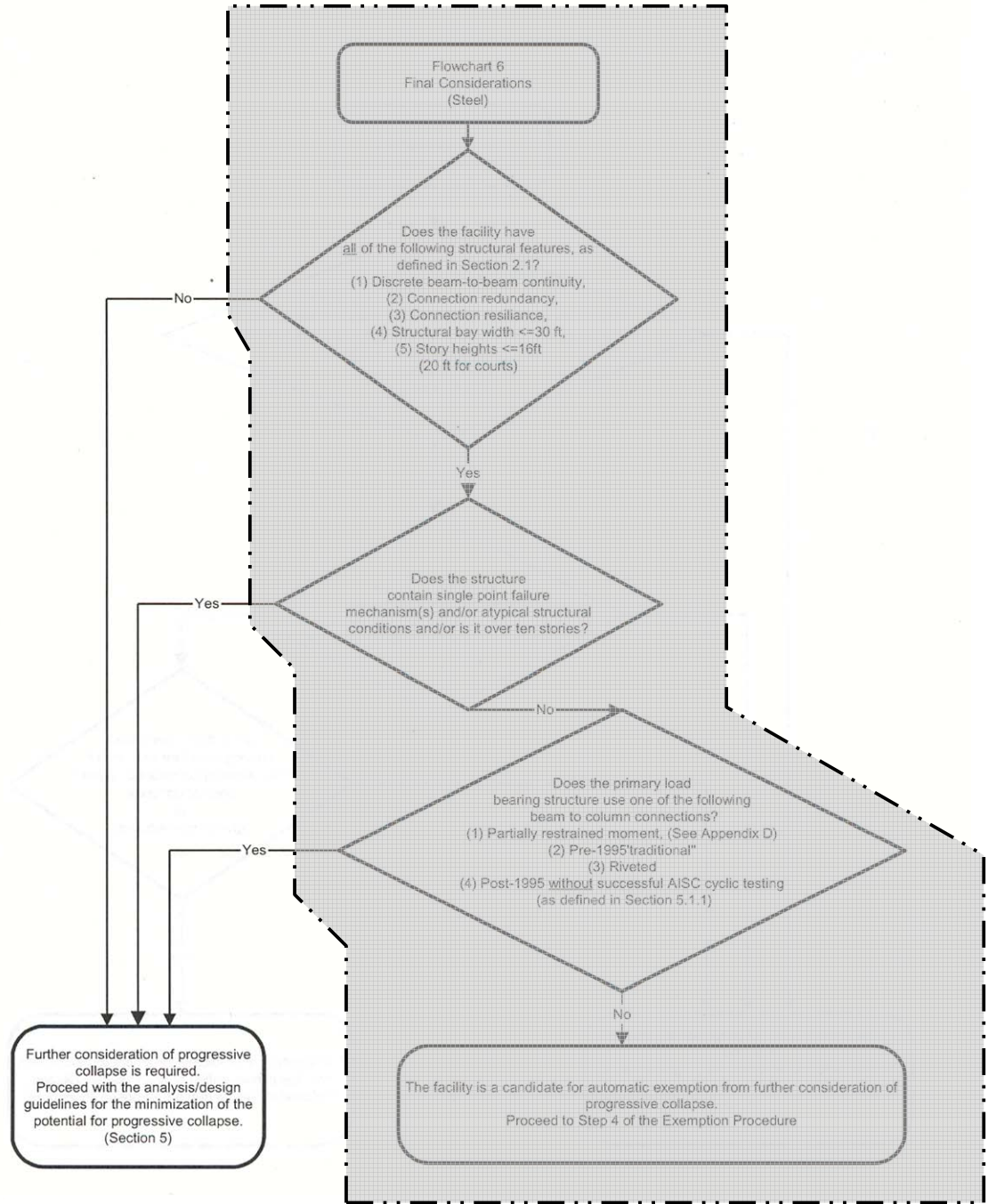


Figure 2.7 Flowchart 6 of Exemption Process (GSA 2003).

The questions in Flowchart 6 in Figure 2.7 can be answered via structural analysis. The GSA Guidelines (GSA 2003) recommend analysis procedures designed to assess the tendency for a structural steel system to exhibit tendencies for progressive collapse. These analysis procedures will be discussed shortly and they can also be used to determine minimum levels of demand placed throughout the structural steel system's members and connections as outlined in Leyendecker and Ellingwood (1977). The present research effort can use these questions to formulate a systematic analytical effort for a set of steel building frames, whereby the results may be used as the basis for supporting an exemption route for structural steel buildings that is consistent with that of cast in place reinforced concrete systems. The questions posed in Flowchart 6 used to guide the formulation of the analysis effort conducted in this research effort are as follows.

Does the facility have discrete beam-to-beam continuity? Does the facility have connection redundancy? Does the facility have connection resilience?

Answers to these questions can come from detailed structural analysis of the typical steel framing systems. The structural analysis conducted in the present effort will use GSA Guideline recommended loading combinations (to be discussed later in this section) and a variety of scenarios involving ineffective key load resisting elements to determine axial load, shear and bending moment demands that are placed on the beam-to-column connections when various ineffective member scenarios are introduced into the structural system. These demands will: (a) reveal force and ductility demands that need to be met to ensure beam-to-beam continuity; (b) indicate likely connection configurations that will be able to meet the loading and ductility demands placed on the connections during abnormal loading events, thus allowing their redundancy to be evaluated and allowing these configurations to be used as a basis for recommended connection types; and (c) allow connection resilience to be evaluated through consideration of force demand, ductility demand and loading rates.

Does the facility have bay widths less than or equal to 30 feet? Does the facility have story heights less than or equal to 16 feet?

For steel buildings these questions will contain affirmative answers because the buildings chosen for detailed analysis will contain story heights less than or equal to 16 feet and will have bays that are 30 feet or less. One building chosen will likely push the 30-foot bay dimension slightly so that this limit can be evaluated directly in the research effort. Thus, the answers to these questions will result in a "YES" answer in the flowchart.

Does the structure contain a single point failure mechanism(s) and/or atypical structural conditions and/or is it over ten stories?

The presence of failure mechanisms during the lost key element scenarios will reveal the tendency for the frameworks considered to form single point failure mechanisms. The structural systems

considered will be regular and under 10 stories, equal to ten stories and over ten stories. Therefore, the answers to these questions will be “NO” in the flowchart.

Does the primary load bearing structure use one of the following beam-to-column connections: partially restrained moment; pre-1995 traditional; riveted; or post-1995 without AISC cyclic testing?

The analysis conducted will utilize partially restrained and fully restrained moment connections. The results of the analysis will recommend the connection types that are most likely to satisfy the behavior and demands seen in the structural analysis conducted. The answers to these questions in the flowchart will therefore, be “NO”.

If one follows these questions and answers down through the flowchart, the path taken will lead to the conclusion that the facility is a candidate for exemption from further consideration of progressive collapse. As a result, the present study has the opportunity to establish minimum structural criteria for typical structural steel systems that will result in the exemption criteria in the GSA Guidelines being satisfied.

Nonlinear structural analysis appears to be the preferred technique for application of the Guidelines (GSA 2003). In fact, there is a plethora of information related to ductility demand, demand-to-capacity ratios, etc..., geared toward aiding the engineer in evaluating the structural system’s tendency for disproportionate collapse. Table 2.1 contains acceptance criteria (rotation limits) for nonlinear analysis procedures. The values in Table 2.1 allow the engineer to evaluate the resiliency and robustness of connections within the steel system in the absence of experimental data.

Two types of loading are permitted in the application of the Guidelines (GSA 2003): static; and dynamic. Linear geometric/material and nonlinear geometric/material analyses are permitted. Static analysis is conducted with the following loading combination (GSA 2003);

$$Load = \beta_{dynamic} \cdot (D + 0.25L) = 2.0 \cdot (D + 0.25L) \quad (2.4)$$

where; D is the dead loading (including self-weight); and L is the live loading (ASCE 2002). The dynamic multiplier is set to be 2.0. If transient (dynamic) loading is utilized, the loading combination that can be used for the structural analysis is (GSA 2003);

$$Load = D + 0.25L \quad (2.5)$$

The Guidelines (GSA 2003) contain sections devoted to both reinforced concrete building systems as well as structural steel. There is limited test data generated for structural steel connections that are subjected to axial, shear, and bending moment demands and deformation demands that are likely to occur during events where key load carrying elements are rendered ineffective. “As a result, the exemption process criteria have

been designed to be conservative and therefore, there will be very few exemptions for steel frame structures” (GSA 2003). Thus, the present research effort can serve to level the playing field in this regard.

Table 2.1 Acceptance Criteria for Nonlinear Analysis (GSA 2003).

Component (1)	Rotation (radians) (2)
<i>Reinforced Concrete Slabs</i>	
▪ One-way without tension membrane	0.105
▪ One-way with tension membrane	0.21
▪ Two-way without tension membrane	0.105
▪ Two-way with tension membrane	0.21
<i>Fully-Restrained (FR) Connections</i>	
▪ Welded beam flange or cover-plated	0.025
▪ Reduced beam section	0.035
<i>Partially-Restrained (PR) Connections</i>	
▪ Limit state governed by flexural yielding of plate, angle, or T-section	0.025
▪ Limit state governed by high-strength bolt shear, tension failure of bolt, or tension failure of plate, angle or T-section	0.015

It is surmised that the GSA acceptance criteria allow greater plastic hinge rotations at the reduced beam section (RBS) connections when compared to welded beam flange or cover plated connections as a result of the reduced demands placed on the beam flange to column flange welds. When limit states are given for PR connections, the Guidelines intend that the governing limit states for the connection be utilized when assigning allowable rotation capacities at PR connections. For example, when high-strength bolt shear is the governing limit state, the connection will be able to undergo less rotation prior to fracture of the bolt (and therefore failure of the connection) when compared to tensile yielding in a connected plate.

The structural design guidance pertaining to structural steel buildings given in the Guidelines (GSA 2003) is intended to address the mitigation of progressive collapse. In general, it is very important that all girders and beams at least be able to successfully accommodate a double-span condition without fracture or excessive deformations resulting in floors below a lost column being loaded with the deflected floor above. It is very important that any structural analysis undertaken evaluate the following local connection characteristics (GSA 2003):

Discrete beam-to-beam continuity: The structural analysis should be able to determine connection demands arising during abnormal loading events such that the connections can be clearly evaluated for their ability to create continuity links (through redundancy in load paths through the connection) across a column (and elsewhere) so that gravity loading can be redistributed.

Connection resilience: The force and ductility (rotational) demands obtained from the structural analysis should be able to guide the structural engineer to connections that have been demonstrated through testing to be capable of meeting these demands without premature fracture.

When structural systems are regular, two basic “lost column” analysis scenarios must be considered: loss of a series of exterior columns (one at a time); and loss of an interior column (one at a time - if underground parking or uncontrolled public areas exist). Removal of vertical load carrying elements (columns) is required to be “instantaneous”. As far as the Guidelines (GSA 2003) are considered, instantaneous is removal of a column element over a period of time equal to $1/10^{\text{th}}$ the natural period of first vibration mode that includes vertical vibrations characteristic of the response when the column is lost. In the case of exterior columns, the structural engineer conducts a series of analyses whereby single exterior columns are removed from the model with a loading combination given by equation (2.4) when static analysis is used, or the applied loading combination given by equation (2.5) when transient analysis is used. At a minimum, the following columns at the lower-level should be considered to be lost:

- column located at the middle of the short side of the building;
- column located at the middle of the long side of the building;
- column located at the corner of the building.

When an interior column is considered, it should be located at the first column line interior to the perimeter column lines.

When linear-elastic analysis is conducted for each one of these compromised element scenarios, demand-to-capacity ratios (DCR’s) for members and connections (dependent upon limit states) give the structural engineer insight into where nonlinear response and potential failure is likely. This insight can then be used to determine the extent to which the initiating event propagates failure throughout the structure. When an exterior column condition is considered, the maximum allowable spread in the collapsed portion of the structure is taken to be the smaller of the following two areas (GSA 2003):

- the bays associated directly with the instantaneously removed vertical member in the floor level directly above the instantaneously removed member;
- 1,800 square feet at the floor level directly above the compromised member.

When interior column scenarios are considered, the maximum allowable spread in the collapsed portion of the structure is taken to be the smaller of the following two areas (GSA 2003):

- the bays associated directly with the instantaneously removed vertical member in the floor level directly above the instantaneously removed member;
- 3,600 square feet at the floor level directly above the compromised member.

Acceptance criteria used to determine if a member or component (*e.g.* a connection) has failed are evaluated using the demand-to-capacity ratio,

$$DCR = \frac{Q_{UD}}{Q_{CE}} \quad (2.6)$$

where: Q_{UD} is the loading (force demand); and Q_{CE} is the expected un-reduced capacity. The loading demand placed on a connection or member within the system is computed using equations (2.4) or (2.5) depending upon whether or not static or transient analysis is utilized. The expected capacity is defined using lower-bound magnitudes of yield or tensile strength and modifiers that move the lower-bound value upwards to an expected value. This process can be simply illustrated as,

$$F_{u,e} = \eta_u \cdot F_{u,LB} \quad \text{and} \quad F_{y,e} = \eta_y \cdot F_{y,LB}$$

where the multiplication factors to translate lower-bound to expected values are given in Table 2.2 and the lower bound tensile and yield strengths are given in Table 2.3. Demand to capacity ratios generated during loading events can then be compared to limits found in the Guidelines (GSA 2003).

These acceptance criteria for members and connection components are given in Table 2.4. After structural analysis, if any component has a DCR that exceeds these limits, that component is said to have *failed*. When nonlinear material and nonlinear geometric analysis is utilized, interaction equations defining plastic hinge formation are used in lieu of demand-to-capacity ratios. A procedure is recommended (GSA 2003) whereby failed members are removed from the analytical model and re-analysis is undertaken until all failed members have been removed, or collapse has been determined.

There is one very real danger with provisions posed in this manner. It arises when mechanisms form in the structural system and if the engineer is not careful, a DCR for a member may be less than values stipulated in Table 2.4 and this may lead one to think that collapse has not occurred. However, if a DCR is greater than one (but less than the value in Table 2.4) at both ends of two adjacent beams within a structural system, this can indicate the tendency for a beam-type collapse mechanism to form within a two-span condition. In applications of progressive collapse analysis, this indicates collapse even though the DCR's are

less than the GSA limit. The structural engineer MUST be cognizant of *system behavior* as well as component behavior.

Table 2.2 Multiplication Factors to Translate Lower-Bound Strengths to Expected Strengths (GSA 2003).

Property	Year	Specification	Factor
Tensile Strength	Prior to 1961		1.10
Yield Strength	Prior to 1961		1.10
Tensile Strength	1961 - 1990	ASTM A36/A36M-001	1.10
		ASTM A572/A572M-89, Group 1	1.10
	1961 - present	ASTM A572/A572M-89, Group 2	1.10
		ASTM A572/A572M-89, Group 3	1.05
		ASTM A572/A572M-89, Group 4	1.05
		ASTM A572/A572M-89, Group 5	1.05
		1990 - present	ASTM A36/A36M-001 & Dual Grade Group 1
	ASTM A36/A36M-001 & Dual Grade Group 2		1.05
	ASTM A36/A36M-001 & Dual Grade Group 3		1.05
	ASTM A36/A36M-001 & Dual Grade Group 4		1.05
Yield Strength	1961 - 1990	ASTM A36/A36M-001	1.10
		1961 - present	ASTM A572/A572M-89, Group 1
	ASTM A572/A572M-89, Group 2		1.10
	ASTM A572/A572M-89, Group 3		1.05
	ASTM A572/A572M-89, Group 4		1.10
	ASTM A572/A572M-89, Group 5		1.05
	1990 - present	ASTM A36/A36M-001 Plates	1.10
		ASTM A36/A36M-001 Dual Grade, Group 1	1.05
		ASTM A36/A36M-001 Dual Grade, Group 2	1.10
		ASTM A36/A36M-001 Dual Grade, Group 3	1.05
		ASTM A36/A36M-001 Dual Grade, Group 4	1.05
	Tensile Strength	All	Not Listed ¹
Yield Strength	All	Not Listed ¹	1.10

1. For materials not conforming to one of the listed specifications.

Table 2.3 Lower-Bound Material Strengths (GSA 2003).

Properties based on ASTM and AISC Structural Steel Specification Stresses				
Date	Specification	Remarks	Tensile Strength ² , ksi	Yield Strength ² , ksi
1900	ASTM, A9	Rivet Steel	50	30
	Buildings	Medium Steel	60	20
1901-1908	ASTM, A9	Rivet Steel	50	25
	Buildings	Medium Steel	60	30
1909-1923	ASTM, A9	Structural Steel	55	28
	Buildings	Rivet Steel	46	23
1924-1931	ASTM, A7	Structural Steel	55	30
	Buildings	Rivet Steel	46	25
	ASTM, A9	Structural Steel	55	30
1932	ASTM, A140-32T issued as a tentative revision to ASTM, A9 (Buildings)	Plates, Shapes, Bars	60	33
		Eyebar flats unannealed	67	36
1933	ASTM, A140-32T discontinued and ASTM, A9 (Buildings) revised Oct.30, 1933	Structural Steel	55	30
	ASTM, A9 tentatively revised to ASTM, A9-33T (Buildings) revised Oct.30, 1933	Structural Steel	52	28
	ASTM, A140-32T adopted as a standard	Rivet Steel	52	28
1934 on	ASTM, A9	Structural Steel	60	33
	ASTM, A141	Rivet Steel	52	28
1961 - 1990	ASTM, A36/A36M-00 Group 1 Group 2 Group 3 Group 4 Group 5	Structural Steel	62	44
			59	41
			60	39
			62	37
			70	41
1961 on	ASTM, A572, Grade 50 Group 1 Group 2 Group 3 Group 4 Group 5	Structural Steel	65	50
			66	50
			68	51
			72	50
			77	50
1990 on	A36/36M-00 & Dual Grade Group 1 Group 2 Group 3 Group 4	Structural Steel	66	49
			67	50
			70	52
			70	49

1. Lower-bound values for material prior to 1960 are based on minimum specified values. Lower-bound values for material after 1960 are near minus one standard deviation values from statistical data.

2. The indicated values are representative of material extracted from the flanges of wide flange shapes.

Table 2.4 Acceptance Criteria for Linear Procedures (GSA 2003).

Component/Action	Values for Linear Procedures
	DCR
Beams – flexure	
a. $\frac{b_f}{2t_f} \leq \frac{52}{\sqrt{F_{ye}}}$ and $\frac{h}{t_w} \leq \frac{418}{\sqrt{F_{ye}}}$	3
b. $\frac{b_f}{2t_f} \geq \frac{65}{\sqrt{F_{ye}}}$ or $\frac{h}{t_w} \geq \frac{640}{\sqrt{F_{ye}}}$	2
c. Other	Linear interpolation between the values on lines a and b for both flange slenderness (first term) and web slenderness (second term) shall be performed, and the lowest resulting value shall be used.
Columns – flexure	
For $0 < P/P_{CL} < 0.5$	
a. $\frac{b_f}{2t_f} \leq \frac{52}{\sqrt{F_{ye}}}$ and $\frac{h}{t_w} \leq \frac{300}{\sqrt{F_{ye}}}$	2
b. $\frac{b_f}{2t_f} \geq \frac{65}{\sqrt{F_{ye}}}$ or $\frac{h}{t_w} \geq \frac{460}{\sqrt{F_{ye}}}$	1.25
c. Other	Linear interpolation between the values on lines a and b for both flange slenderness (first term) and web slenderness (second term) shall be performed, and the lowest resulting value shall be used.

Table 2.4 Acceptance Criteria for Linear Procedures (GSA 2003) – continued.

Component/Action	Values for Linear Procedures
Columns – flexure	
For $P/P_{CL} > 0.5$	
a. $\frac{b_f}{2t_f} \leq \frac{52}{\sqrt{F_{ye}}}$ and $\frac{h}{t_w} \leq \frac{260}{\sqrt{F_{ye}}}$	1
b. $\frac{b_f}{t_w} \geq \frac{65}{\sqrt{F_{ye}}}$ or $\frac{h}{t_w} \geq \frac{400}{\sqrt{F_{ye}}}$	1
Columns Panel Zone – Shear	2
Column Core – Concentrated Forces²	1.5
Fully Restrained Moment Connections	
Pre-Northridge (Pre 1995)	
Welded unreinforced flange (WUF)	2
Welded flange plate (WFP)	2
Welded cover plated flanges	2
Bolted flange plate (BFP)	2
Post-Northridge (FEMA 350) Public Domain	
Improved WUF-bolted web	2
Improved WUF-welded web	2
Free flange	2
Welded top and bottom haunches	2
Reduced beam section	2
Post-Northridge (FEMA 350) Proprietary³	
Proprietary System	≤ 3 (See Footnote 3)

Table 2.4 Acceptance Criteria for Linear Procedures (GSA 2003) – continued.

Component/Action	Values for Linear Procedures
	DCR
Partially Restrained Moment Connection	
<i>Top and bottom clip angle</i>	
a. Shear failure of rivets or bolts	3 (rivets); 1.5 (high strength bolts)
b. Tension failure of horizontal leg of angle	1.5
c. Tension failure of rivets or bolts	1.5
d. Flexural Failure of angle	3
<i>Double split tee</i>	
a. Shear failure of rivets or bolts	3 (rivets); 1.5 (high strength bolts)
b. Tension failure of rivets or bolts	1.5
c. Tension failure of split tee stem	1.5
d. Flexural Failure of split tee	3
<i>Bolted flange plate</i>	
a. Failure in net section of flange plate or shear failure of rivets or bolts	3 (rivets); 1.5 (high strength bolts)
b. Weld failure or tension failure on gross section of plate	1.5
<i>Bolted end plate</i>	
a. Yield of end plate	3
b. Yield of rivets or bolts	2 (rivets); 1.5 (high strength bolts)
c. Failure of weld	1.5
<i>Composite top and clip angle bottom</i>	
a. Failure of deck reinforcement	2
b. Local flange yielding and web crippling of column	3
c. Yield of bottom flange angle	3
d. Tensile yield of rivets or bolts at column flange	1.5 (rivets); 1 (high strength bolts)
e. Shear yield of beam flange connections	2
Shear connection with or without slab	2

1. Notation for Table 5.1:

- bf = Width of the compression flange
 F_{ye} = Expected yield strength
 h = Distance from inside of compression flange to inside of tension flange
 t_w = Web thickness
 P_{CL} = Lower bound compression strength of the column
 P = Axial force in member taken as Q_{uf}
 t_f = Flange thickness
 d = Beam depth
 d_{bg} = Depth of the bolt group

2. Column core concentrated force capacity shall be determined from AISC (1993) LRFD Specifications equations K1-1, K1-2, K1-4 and K1-8.
3. A DCR of 2 will be used for all untested proprietary fully restrained moment connections. A DCR of 1 will be used for all other untested proprietary connections. Tested proprietary connections must have documented test results that justify using DCR values greater than these. Under no circumstances should a DCR value exceeding 3 be used for any proprietary connection.
4. DCR values are for connection to strong axis of column. For connections to weak axis of column (Figure D 3 Appendix D) treat as atypical (DCR*0.75).
5. No DCR values less than 1.0 are required, even for atypical conditions.

CISC (2004)

The Canadian specifications for steel construction have notably kept their requirements for structural integrity very, very brief and have heeded the recommendations echoed throughout the discussions in the U.K. after Ronan Point (ISE 1969). Most notably, allow the structural engineer to apply his/her knowledge to solve the problem of creating structural integrity in a building system. The CISC specifications contain a relatively simple statement that has broad-reaching impacts in design.

The specifications (CISC 2004) dictate that the "...general arrangement of the structural system and the connection of its members shall be designed to provide resistance to widespread collapse as a consequence of local failure." A rather bold statement is made next: "The requirements of this Standard generally provide a satisfactory level of structural integrity for steel structures". It would be very desirable to have statement like this in all steel building design specifications, but one wonders about the body of research knowledge to date regarding steel systems and its ability to support such a statement. Reference is given to additional guidance in the National Building Code of Canada.

DOD (2005)

A second document in the UFC series is the *Design of Buildings to Resist Progressive Collapse*. These criteria are intended to be applied to new construction, major renovations and leased buildings and their use is dictated by the UFC-4-010-01 document (DOD 2002). This document contains specific design procedures for addressing progressive collapse in building systems of timber, structural steel, and reinforced concrete. The contents of these guidelines are very similar in format to the guidelines (GSA 2003) reviewed earlier.

The Criteria outline four levels of protection against progressive collapse: very low level (VLL); low level (LL); medium level (ML); and high level (HL). A structure designed for VLL must contain sufficient horizontal tie force capacity with magnitude defined with consideration of construction type. The alternate load path methodology (*i.e.* designing components to bridge compromised elements) is not done for VLL structures. Instead, components are re-designed until minimum horizontal tie forces are met. An LL structure must contain sufficient horizontal and vertical tie force capacity. If vertical tie force capacities can not be met, then re-design of components must occur to meet these capacities, or the alternate load path methodology can be used to demonstrate adequacy of the design. Medium and high levels are essentially combined. When HL and ML design is desired; horizontal tie force capacity, vertical tie force capacity, alternate load paths, and ductility requirements are all required. ML and HL structure designs are also required to have peer review that is in keeping with much of the Institute of Structural Engineers discussion of alternate load paths and review of designs for stability.

All protection levels require that load carrying elements be capable of supporting vertical loads after loss of lateral support at any floor level. This demands that an unsupported length of two stories be used in the design of columns. The loading combination to be used in the component evaluation is,

$$(0.9 \text{ or } 1.2) \cdot D + (0.5 \cdot L \text{ or } 0.2 \cdot S) + 0.2 \cdot W \quad (2.7)$$

Each bay in the structural system must also be capable of resisting a net uplift loading of,

$$1.0 \cdot D + 0.5 \cdot L \quad (2.8)$$

The assumed locations of ties within the structural system and the alternate load path methodology for design are very similar to the GSA guidelines outlined earlier in the report (GSA 2003). Alternate load paths are identified and ensured by removing load bearing elements and examining structural response using a variety of analysis complexities ranging from linear static to nonlinear dynamic. The locations of load bearing elements to be removed are identified and procedures required when failed components are defined (*e.g.* debris loading procedures). Damage limits and acceptability criteria are also discussed. The damage limits are similar to GSA recommendations and acceptability criteria (at least for steel structures) follows load and resistance factor design specifications and rotational capacities (deformation limits) that are consistent with current seismic design provisions (FEMA 2000b; AISC 2005b).

There are specific requirements for structural steel contained in the Criteria. Ultimate tensile overstrength and tensile yield overstrength for various steel materials (*e.g.* ASTM A992/A992M) are provided in tabular form so that better simulation of material properties can be implemented in the analysis. Column ties, peripheral ties, and ties at re-entrant corners are defined in regular steel framing systems. General tie arrangements involve all beams in the framing system acting as ties.

The horizontal tie force magnitudes required for steel systems depend upon whether or not the tie is considered interior or peripheral. For an internal tie, the required strength is,

$$0.5 \cdot [1.2D + 1.6L] \cdot (s_t \cdot L_s) \geq 16.9 \text{ kips} \quad (2.9)$$

When a peripheral tie is considered, the strength required is,

$$0.25 \cdot [1.2D + 1.6L] \cdot (s_t \cdot L_s) \geq 8.4 \text{ kips} \quad (2.10)$$

The span length for the tie force is defined as L_s , and s_t is the mean transverse spacing of ties adjacent to that considered.

Vertical tie forces are accomplished through continuity of column sections through the floor levels (standard construction practice) and maintaining a minimum tensile capacity of column splices. The strength of column splices required to generate vertical tie forces is (DOD 2005);

the largest factored vertical dead load and live load reaction (from all load combinations used in design) applied to the column at any single floor level located between that column splice and the next column splice down or the base of the column.

Rotational limits for steel beam-to-column connections, beams, and beam columns are also provided. For LL protection, the rotation limits for FR are 0.035 radians for welded beam flange or coverplated moment resisting connections; and 0.045 radians for connections with RBS. Depending upon the governing limit state, PR connections have rotational limits ranging from 0.023 radians to 0.035 radians. When ML and HL protection is desired, FR connection rotation limits range from 0.026 radians for welded beam-to-column and coverplated connections to 0.035 radians for connections with RBS. PR connections have rotation limits that range from 0.016 to 0.026 radians. It should be noted that testing protocols defined in state-of-the-art seismic design provisions (AISC 2005b) are allowed to be used to demonstrate rotational capacities of connections not contained or described in the Criteria.

The commentary related to tie forces in the Criteria (DOD 2005) contains very little additional information or direction related to structural steel when compared to details regarding reinforced concrete systems. A derivation for the upper-bound on basic strength for internal ties in reinforced concrete systems is provided. This derivation is based upon assumed sag equal to 10% of the catenary span length. This derivation ignores the potential Vierendeel action in the framing system above compromised elements and also includes the assumption that the 1/3 the live load is present. One would assume that the lower limit tie strengths for reinforced concrete and structural steel should be similar, but the Commentary admits to a slight difference in lower limits in favor of the concrete structural system (13.5 kips for concrete and 16.9 kips for structural steel).

2.5 General Reviews of Design and Studies in Structural Performance

Since the WTC tragedy of 9-11, the term progressive collapse has re-entered the lexicon of the structural engineer. A fairly strong body of literature providing overviews of design methodologies and the phenomenon of progressive collapse has been generated since 9-11. Furthermore, recently there has also been a steady stream of contributions in the area of reviewing structural system performance and making recommendations for improvement. The present section of the report will highlight these contributions.

Leyendecker et al. (1976)

After the Ronan Point collapse, the United States began a great many studies reviewing structural performance and documenting the body of knowledge concerning itself with the progressive collapse phenomenon. The work of Leyendecker *et al.* (1976) is an outstanding source of over 375 references related

to conditions of abnormal loading on buildings and progressive collapse covering the years 1948 through 1973. The authors of this work have provided the engineering community with a terrific resource for future efforts.

Ellingwood and Leyendecker (1978)

This manuscript provides a nicely condensed version of the NIST report (Leyendecker and Ellingwood 1977) reviewed earlier. Application of second-moment reliability analysis in the derivation of load and resistance factors for abnormal loading conditions is briefly discussed and the main thrust of the manuscript is discussion of event control, direct design, and indirect design methodologies for design of structural systems considering abnormal loading.

Girhammar (1980c)

There was a series of research efforts undertaken by the Swedish Council for Building Research related to the behavior of steel structures subjected to compromising events (*e.g.* removal of supports in continuous beams). The present manuscript considered two-span continuous beams in which the central support was instantaneously removed. Rigid body analytical models were utilized and attention was given to partial axial constraints and the role of catenary action in the response.

The role of catenary action in the two-span system with instantaneously removed central support was found (not surprisingly) to be a major influence in the response. It was concluded that very small axial constraint (*e.g.* 10% of the full – rigid support – axial constraint) was required to develop catenary action in the two-span compromised system. It was further concluded that the ultimate catenary capacity is on the order of 2-3 times the static plastic bending capacity of the two-span compromised beam (Girhammar 1980c). The dynamic multiplier for statically applied loading on the two-span beam intended to simulate dynamic loss of support was recommended to be 2.

This study suggests that catenary action in the structural steel system should be given serious consideration. More importantly, the present research effort will seek to exploit catenary action in as many components within the structural system as possible. The fact that the research effort suggests a very small percentage of the axial constraint present at the ends of the two-span beams studied was required to develop catenary action suggests that web cleat connections may be sufficient to establish 3D catenary behavior in the steel structural systems. Finally, this study recommends that the force demands arising in compromised structures must be evaluated before final recommendations or conclusions can be made. This will be a major focus of the present study.

Christiansson (1982)

This document outlines a second study undertaken as part of the research effort conducted by the Swedish Council for Building Research. This study focused on the time interval where the steel structure moves from the uncompromised to the compromised state as a result of some abnormal event. Relatively simple analytical models were utilized to consider dynamic buckling of steel column members considering nonlinear material response.

The research effort revealed that when loading is applied to a column member in a dynamic manner (*e.g.* time period equal to a small percentage of the natural period of free lateral translation of the column), the steel column has a strength that exceeds the critical buckling load. The research also suggested that when the duration of transiently increased loading on a column is of the same magnitude as the lateral vibration mode of the column, the increase in column strength is not present.

McNamara (2003)

This is a very brief review of GSA Guidelines (GSA 2003) and DoD Criteria (DOD 2002) for creating structures with resistance to progressive collapse. Although very brief, there is some very good general information that can be gleaned from the analysis of the 39-story steel building analyzed using nonlinear “push down” analysis.

The analysis conducted included removal of a column at the exterior of the building near the ground level. Typical moment resisting connections and construction types were considered (*e.g.* steel deck, concrete in-fill). When a static push-down procedure was implemented until a collapse mechanism formed in beams in the floor-levels immediately above the compromised column member it was found that yielding did not occur in these members until well above the original design load levels (McNamara 2003). The membrane action in the slab system was not considered in the analysis and it was felt that this behavior would have provided additional resistance to the system.

Corley (2002)

There is a large contingency in the structural engineering profession that feels seismic design detailing practice can help to resist progressive collapse in building systems of all material types. This manuscript outlines improvements in performance that the Alfred Murrah Federal Building may have experienced had seismic detailing been implemented in its original design and construction.

The manuscript focuses on reinforced concrete design and detailing and aside from the recommendations that seismic detailing would have been beneficial in reducing loss of life from this terrorist

attack its applicability to the present study is limited. Furthermore, the suggestion that seismic detailing alone can prevent progressive collapse has not been rigorously investigated nor demonstrated.

Ellingwood (2002)

This manuscript provides additional thoughts regarding the development of LRFD methodologies for considering abnormal loading in design. The work is essentially an updated and more concise version of Leyendecker and Ellingwood (1977). There is a significant amount of very good information in this manuscript and other contributions (Ellingwood and Leyendecker 1978) similar in nature.

Nair (2004)

This manuscript presents a very nice overview of progressive collapse and the design guidance that is available to the structural engineer when considering progressive collapse mitigation. One very important conclusion postulated in the manuscript is that a host of designer resources outlined; GSA Guidelines, ASCE 7-02, and ACI 318-02, would have had moderate impact in improving performance of the structures at Ronan Point, Oklahoma City and New York. This certainly lends support to the notion that design codes can be capable of ensuring structures have a reasonable level of general structural integrity, but in many cases, avoiding non-redundant systems (*e.g.* transfer girder structures) is likely the best approach for mitigating progressive collapse rather than creation of additional design provisions.

Magnusson (2004)

This contribution to the body of literature has a very interesting initial premise. It is: there are many building structures that have been loaded well beyond magnitudes specified in their design criteria and in manners that most certainly could be classified as abnormal without suffering collapse. It is postulated that we should study what made these structures perform in the favorable manner and replicate these situations in new construction.

The evaluation methodology of notionally removing individual columns from the structural framing system is a very common approach to progressive collapse mitigative design. In fact, this methodology was reviewed earlier in this chapter (GSA 2003; DOD 2005). It is pointed out that many structures have not been designed using these procedures and have shown the ability to lose a column without global collapse (Magnusson 2004). Concern is expressed that if "... strong horizontal construction..." is used in framing systems, that the collapsing portions of the structural system will pull down adjacent portions of the structure leading to collapse disproportionate to the initial event. It was then recommended that designers also consider adverse effects of tying the structure together excessively when the column removal technique is applied (Magnusson 2004).

Shipe and Carter (2004)

This presentation outlines a variety of recommendations for the design of steel structural systems for blast loading and progressive collapse resistance. The recommendations most applicable to the present study are those that are made in regard to design approaches that can be used for the typical steel structural system. No quantitative data was given to support the recommendations, but the recommendations are founded upon sound structural engineering principles and the guidance provided in this presentation is very important in guiding the present study's objectives.

The authors recommended that lateral load resisting systems be distributed throughout the entire building. By doing this, the structural engineer is generating redundancy in the structural framing system. Tying the structural system together through effective floor and roof diaphragms was also recommended. This affords the framing system the ability to form catenary and membrane action in the floor framing system if it is called upon. The present study will seek to provide quantitative data and recommendations with respect to what effective tying means in the typical steel framing system and how one might enhance membrane and catenary action in floor framing. It was recommended that using repetitive shapes in beam/girder floor framing and column stacks would increase inherent strength in the structural system. These are economic framing principles and they do likely result in reserve strength within the structural system.

In a majority of cases, the governing constraint in structural engineering design optimization problems is serviceability – be it interstory drift, vibration, or vertical deflection. From the point of view of strength limit states, these serviceability constraints add robustness to the system indirectly by demanding larger members sizes.

It is also recommended that connection details "...be kept clean" (Shipe and Carter 2004). When connection details are "clean", the load paths through the connection are well defined. When these load paths are clearly illustrated, the level of connection redundancy is evident as well as the presence of discrete beam-to-beam continuity (GSA 2003). Furthermore, it was recommended that filling the web of the girder with bolts (*e.g.* providing 6 rows in a W21 section rather than 4 rows) is an economical method of attaining additional shear strength as well as axial loading strength for catenary action and bending moment strength at what are traditionally assumed to be pin connections. These sources of redundancy and robustness in the steel framing system are felt to be very important in the senior writer's opinion.

The SAC-FEMA effort (FEMA 2000c; FEMA 2000d; FEMA 2000a) pointed out the difference between lower-bound material strengths and expected material strengths for steels used in building systems. As a result, the members and connecting elements are likely to have significant additional strength present

that is not counted on in the initial design. The present effort will seek to address enhanced material strengths not counted on in design and quantify their benefit in generating increased robustness in the framing system.

The membrane action that can form within the concrete slab system commonly found in the structural steel framing system is likely a very important source of robustness often not counted on. Non-structural components were also identified as contributors to system robustness. It is very easy to visualize exterior cladding panels helping to bridge a lost exterior column through cantilever action. This aspect is relatively difficult to quantify because precious little experimental evidence is present to help quantify the strength and stiffness of these systems.

Hamburger and Whittaker (2004)

This manuscript provides nice discussion related to design strategies that can be used to generate structural engineering solutions that are economical and have low architectural impact. The basic premise of this manuscript is very much in line with an objective of the present effort. One very important discussion given is related to the dynamic multiplier recommended in the GSA Guidelines (GSA 2003). A simple single degree of freedom model is used to illustrate that when nonlinear material is included in the analysis where instantaneous loading is applied, the dynamic displacement is 2.5 or greater. As the strength of the SDOF model considered was reduced (*i.e.* the plastic moment capacity of a cross-section reduces), collapse was shown to occur even though demand to capacity ratio limits stipulated (GSA 2003) are satisfied.

This behavior points out the problem with a single dynamic multiplier for forces and displacements within a structural system. While the displacement amplifier may be 2 or greater, the force amplifiers are limited when plastification within the system occurs. When plastic hinges form, the bending moments in the members are capped at the plastic moment capacity. The shear forces at the ends of the members are also capped as a result of member equilibrium. Furthermore, when the interaction surface is reached in a beam-column member, there are limited combinations of axial load and moment that can be supported by that member. Therefore, while one might argue that the 2.0 multiplier for displacements is too low, a second argument can be made that for forces, the multiplier will likely be less than 2.0.

The simple SDOF example illustrates concern with “blind” application of demand-to-capacity ratios because collapse mechanisms are not explicitly pointed out as they are when inelastic structural analysis is performed. If engineers are focused on component DCR’s, they are likely to miss collapse mechanisms that form within the structural system. Just as a collection of component DCR’s can lead an engineer to miss collapse mechanisms forming within the structural system, the authors’ single degree of freedom example also ignores system behavior and focuses too myopically on the traditional two-span continuous beam with missing internal support scenario.

A strong argument for the virtues of catenary behavior acting within a structural system to enhance robustness in steel framing systems is made. It is recommended that isolated catenary bands throughout the structure may lead to very robust framing systems. However, there is a problem in creating isolated bands of strength as this design philosophy is contrary to the philosophy of distributing robustness throughout the structural system (Shipe and Carter 2004). One would like to avoid the isolated strength provided by “transfer girders” and the associated failure that can occur when such framing systems are utilized (Corley 2002). It would be very useful to see what a system can support if its initial design was ignorant of catenary and membrane behavior. Perhaps a structural system has built-in capacity through activated inherent membrane strength that is not counted on at design time.

It is pointed out that the moment capacities at the ends of the members may not have to be at levels corresponding to the full moment capacity in order to provide collapse resistance (Hamburger and Whittaker 2004). While this may be true, if significant vertical deformations develop in the structural system, large rotation demand can be imparted to connected elements. Therefore, even though design may occur without moment capacity in mind, when the deformations required to generate catenary action occur, the rotations demanded of the ends of the beam member may lead to premature fracture at the connections. The present effort must not focus on components, but must consider the system first with a trickle-down effect to the components within that system. There is a synergy of all components acting together to resist collapse, but the facilitator for this cooperative activity is the structural system.

An example is provided which appears to illustrate that modest increase in simple framing member sizes and the addition of moment resisting connections throughout the framing plan at columns lines could support as many as 15 stories in catenary action. The inelastic deformations required to activate catenary action can be on the order of 10 percent or greater of the 60-foot span considered (6 feet or more). If one considers all this deformation to be inelastic, it implies 0.19 radians of expected rotation demands at the ends of the catenary member. Therefore, 2D catenary action alone requires careful consideration of its impact in all aspects of the structural system.

Iwankiw and Griffis (2004)

This relatively recent effort sought to examine the structural performance of major multistory structures subjected to abnormal loadings of blast, impact, and fire from several terrorist attacks. The objective of the effort was to provide “... a unified structural engineering review of this performance” (Iwankiw and Griffis 2004). Several general recommendations were made to improve structural performance in the wake of terrorist attack. The first is to mimic the Pentagon’s structural system and increase the building’s footprint to prevent occupancies from being concentrated in confined areas of the facility. Furthermore, spreading the

building's footprint will spread its weight in horizontal planes and demand more vertical supporting elements thereby increasing the inherent redundancy in the structural system. The number of floors requiring support will also decrease assuming that a target square footage requirement is needed.

The authors recommend utilization of a "leaning index" (Iwankiw and Griffis 2004) to provide a measure of the increased vulnerability risk in structural systems. The leaning index could be used to establish design objectives whereby the percentage of gravity only (leaning) columns to the total number of columns within the any story within the structural system would be minimized. The structural engineer could then incorporate this objective along with others traditionally considered in design to develop economical solutions to the problem of designing structural steel framing systems.

One point raised by the authors that should be heeded is that "...undue over-reaction..." to abnormal loading events should be avoided. The engineering community is trained to solve problems and identification of the problem is the first step in finding the solution. One might argue that to solve the problem of buildings collapsing during terrorist attacks, the engineering community should point to the development of heightened security measures to avoid terrorist attack on buildings. This may be more productive than additional design requirements to some, or all, buildings (Iwankiw and Griffis 2004).

Marchand and Alfawakhiri (2004)

This document is likely the most comprehensive review of recommendations related to the design of structural steel framing systems for blast loading and progressive collapse resistance. While excellent information regarding blast resistant design is contained in this document, the present study will not consider threat-specific design. As a result, the recommendations regarding mitigation of progressive collapse will be reviewed and synthesized.

The authors provide a very concise yet detailed review of indirect and direct design approaches for progressive collapse mitigation. The concept of providing vertical and horizontal ties within the structural system is also reviewed. A detailed discussion and overview of the GSA Guidelines (GSA 2003) and the DoD Unified Facilities Criteria (DOD 2002) is given. The authors also walk the reader through the steps that are required to conduct an analysis of a structural system for progressive collapse mitigation.

The emphasis of the document is providing designers and building owners the latest information regarding blast and progressive collapse and the guidelines that are available for carrying out designs for abnormal loading conditions. However, there is precious little discussion regarding inherent robustness in steel systems and the sources of redundancy that typical steel systems have to resist disproportionate collapse. However, the authors do provide the reader with key issues that they perceive need resolution:

- The structural mechanics by which a moment resisting framework evolves from a flexure-dominant resisting system to a membrane- or catenary-dominant system remains to be fully understood. Furthermore, the rotational demands on connections as this structural resistance evolves are not understood.
- What is the reserve tensile capacity of steel beam-to-column connections (*e.g.* flexible, partially-restrained, fully-restrained) after significant inelastic rotations are absorbed.
- What is the most appropriate analysis approach? Is dynamic analysis most appropriate? Is static linear analysis accurate and reliable for alternate load path analysis?

The present effort should provide answers or insight into answering these questions. Specifically, the structural mechanics phenomena that are activated during an abnormal loading event should be quantified. Furthermore, the rotational demands at the connections within the structural steel framing system during abnormal loading events should be quantified. The present effort will not be able to conduct experimental testing of typical steel connections. However, the present study can most certainly give insight into the magnitudes of forces and deformations that typical steel connections will have to support if robustness in the steel system is to be preserved. Finally, the present study should shed some light onto the types of structural analysis that may be undertaken and their accuracy in predicting response.

Liu et al. (2005)

The concept of tying a structural system together with vertical, horizontal and perimeter systems to prevent progression of collapse from a local instance to collapse of an entire structural system easily stands the test of structural engineering intuition. However, the magnitudes of tying forces recommended in U.K. design guidelines and building regulations have had very little evaluation in regard to structural steel framing systems. The objective of the reviewed research effort was to analytically evaluate the forces generated in a steel framed structure during an abnormal loading event (*e.g.* removal of a vertical column within the structural system). The analytical study evaluated the impact of the number of key elements (ODPM 2005) removed, the height of the structural system, and the period of time over which the building is damaged on the tying forces generated within the structural framing system.

The analytical evaluation of a 3-story and 7-story structural steel framework illustrated that joint stiffness and the rate that a key element is removed are influential factors in determining the tying force required in the structural system. The analysis conducted suggested that the tying force recommendations contained in the U.K. provisions were un-conservative for the framework considered. It should be noted that only two structural systems were considered. Recommendations for further work were provided.

Munoz-Garcia et al. (2005)

The work of Owens and Moore (1992) included experimental testing that implemented monotonically increasing (static) loading. This effort attempts to extend this previous experimental work to include dynamic loading and rate-dependent material properties on the assumption that dynamic strain rates will be present during abnormal loading events.

Nonlinear finite element analysis was utilized to reproduce the results seen in the experiments of Owens and Moore (1992) under four rates of loading; 1 ms, 10 ms, 100 ms, and 1,000 ms. Finite element models of high-strength bolts subjected to dynamic loading were compared with previously obtained experimental results and reasonable correlation was described. Dynamic tension forces were applied to finite element models of flexible end plate and web cleat connections. The connections considered in Owens and Moore (1992) were modeled. The tensile loading was applied in a ramped manner up to a constantly maintained level. The ramped segment of the loading history ranged from 1 – 1,000 ms. The partial end plate FE models were said to capture some of the phenomenological behavior seen in the experiments, but modifications to the models were in order. These modifications were not reported. The failure modes in the web cleat connection experiments were seen in the FE results. However, the loading rate did not appear to alter the failure mechanism from that seen in the static experimental results. The FE analysis also indicated that the web cleat connections were superior to the flexible end plate connection with respect to tensile capacity.

It should be noted that pure tensile loading was applied in the FE analysis. It is well known that a combination of shear, tension, and moment will be applied to connections within a structural steel system responding to an abnormal loading event. As a result, the present effort should shed light onto the expected force and deformation demands that are likely to be seen at connections in typical structural steel systems during abnormal loading events so that experiments and FE analysis models can be designed to shed light onto detailed performance.

2.6 Experimental Work

Experimental efforts related to the moment-rotation performance of structural steel connections have been numerous over the last three decades. A review of all these efforts is not possible in this research report as the focus of the present effort is elsewhere. Virtually all experimental efforts related to structural steel connections have been to determine moment-rotation response, shear-deformation response, or axial loading response. To the writers' knowledge there have been very few experimental efforts undertaken to evaluate the behavior of structural steel connections to the demands incurred during the system's response to abnormal loading events. The main reason for this is that there is precious little information related to what these

demands are. For example, what combinations of axial load, transverse shear, and bending moment must a connection support during one of these events? Also, what deformation/ductility demands are placed on steel connections during these events? The present section will review experimental work that most closely attempts to address these issues.

Owens and Moore (1992)

Researchers in the U.K. began to realize that structural steel systems needed to be evaluated with respect to their ability to support tying forces recommended by design regulations (BSI 2003; ODPM 2005). This research effort sought to develop understanding for the robustness present in structural steel systems contributed by the frequently used simple web-cleat connections (*i.e.* double-angle connections) and flexible end plates. An experimental study was undertaken as well as analytical efforts devoted to understanding the response seen in the experiments.

The focus of the effort was on double angle web cleat connections and end plate connections that are fillet welded to the web of the wide-flange shape. The experiments were undertaken to evaluate the ability of these two connection configurations to resist tying forces recommended in the design regulations: 75 kN (16 kips) for floor level framing; and 40 kN (9 kips) for roof level framing (BSI 2003). The web cleat connection in the U.K. is essentially the double angle flexible connection used in U.S. practice and therefore, it will be the focus of the present review.

The specimens tested consisted of 11 double-angle connections with variations in bolt gages and angle thicknesses. The angles used in the connections were very close to 4-inch equal-leg angles found in the United States. Two angle thicknesses were considered: 5/16" and 3/8". Thus, the experimental work will shed some light onto the capacity of connection tensile-force capacities for United States configurations. The experimental results exhibited significant axial deformations for the web cleats (on the order of 1-inch or more). A load deflection model for the angle connection was developed to help explain some of the behavior seen in the experiments and predictions made with this model compared favorably to the experimental results seen.

The research program was able to conclude that the web cleat connection provides significantly greater capacity in resisting tying forces than the comparable end plate connection. There was significantly greater ductility exhibited by the web cleat when compared to the end plate connection. The experimental evidence also revealed that when the large deformations occurred in the connections, prying forces of significant magnitude were generated in the bolts. Recommendations on bolt gages for the web cleat connection were made so that the minimum tying forces (BSI 2003) could be supported.

Girhammar (1980b)

The Swedish Research Council for Building Research sponsored yet another effort studying the response of structural steel systems to abnormal loading events. In this instance a two-span continuous system with lost interior support was simulated. The experimental testing done included two simply-supported (design intent) beam segments whose continuity after loss of the interior support were facilitated by a segment of column. The beam-to-column connections were made using flush end plates with bolting to the column flange. Flange stiffeners and web doublers did not exist in the connection. These connections were said to be capable of supporting "...25% degree of moment rigidity..." (Girhammar 1980b).

Dynamic testing of a two-span condition with uniformly distributed loading was conducted. The test arrangement included two beam spans connected at their ends to segments of steel column through flush end plates with seating blocks and a central column stub that facilitated connection of the two adjacent beam spans to one another. The presence of a concrete slab was not included in the experiments. The central segment of column was supported with a wire during gravity loading and this wire was subsequently cut to simulate dynamic loss of the interior support. The transient load deformation response included a capping effect on column force resulting from the finite capacity of the connections in the system limiting the loading that is transmitted. Furthermore, the dynamic testing illustrated fairly remarkable deflection magnitudes with the relatively innocuous steel end plate connections facilitating this behavior.

Rigid body models of the two-member system were utilized to predict behavior. It is interesting to note that the author states "...no effects of geometric nonlinearity need be considered" (Girhammar 1980b). This seemed to be a strange conclusion since it appeared catenary action was significant based on the deformations seen. However, the capping behavior seen in the response time-history suggests that catenary action may not have taken over from the flexural (moment) resistance. This indicates a synergy between flexural mechanism and catenary mechanisms. This synergy should be explored in the present effort.

Girhammar (1980a)

The tradition of Swedish Council for Building Research sponsored studies continued with an experimental examination of the behavior bolted "heel" connections and bolted end-plate connections in structural systems where catenary action is present. The "heel" connection is essentially a flush end plate welded to the supported beam that rests on a "bracket-type" support during erection. The end-plate connection considered in this study is essentially the extended end plate connection used in the U.S.

The experimental setup was essentially that of Girhammar (1980c) with a notable exception that static loading was considered and the loading direction was horizontal. Two beam segments were connected to column stubs at their opposite ends whereas their common end was connected to a segment of column to

complete the two-span condition. No member loading was considered and a hydraulic actuator loaded the centermost column thereby creating a two-span catenary where the beam segments essentially acted as rigid bodies.

The experimental results indicated a clear transformation from a bending mechanism to a catenary load resisting mechanism as the ultimate loading condition was approached. The (change in bending moments) measured at the ends of the beam segments were essentially zero at the ultimate condition (Girhammar 1980a). The experimental evidence also indicated that bolt punching through the end plates were a limit state to consider and to combat this, it was recommended that washers be used under the bolt head *and* the nut. Similar behavior was seen in the web cleat connections tested by (Owens and Moore 1992). The extreme deformations that occur in the extended end plate connection were found to place very large demand on the fillet welds that are normally utilized in these connections. It was recommended that additional research into sizing fillet welds in end plates which were thinner than the column flange should be completed.

Milner et al. (1998)

A rather unique experimental effort was undertaken at the Building Research Establishment Cardington test facility in the United Kingdom. A full-scale timber framed building, complete with brick cladding, was constructed. The experimental testing included removal of selected load bearing wall panels. The goal of the testing was to "...verify by 'test' that the inherent stiffness of standard cellular platform timber frame construction can provide adequate robustness so that, in the event of an accident or misuse, the building will not suffer collapse to an extent disproportionate to its cause" (Milner *et al.* 1998). Therefore, the testing completed would demonstrate that a typical timber/masonry structure could or could not meet the Building Regulations (ODPM 2005) without special design considerations.

The timber/masonry structure constructed was 6 stories in height and occupied a floor plan area of approximately 20 feet by 34 feet. By all accounts it was full-scale and the floor plans rising through the structure had interior wall layouts consistent with the type of building considered (multistory residential construction). Loading was applied to the floor system through engineered layout of sand bags. There were essentially two goals of the testing: (a) verify that standard timber frame construction with exterior brickwork would allow safe egress of people within a regulation-mandated timeframe when a length of load bearing wall was removed; (b) determine if, after load bearing elements were removed, the building could resist disproportionate collapse for up to eight hours to allow temporary shoring to be installed post-event. The experiments included removal of an interior wall segment and an exterior panel immediately adjacent to a corner of the structure. All wall segments removed existed at the first floor (ground) floor level.

In the case of an interior wall panel loss, the structure responded with approximately 1 inch of deflection in the floor system after 20 hours. Deformations in the walls above the compromised wall panel were not noticeable (Milner *et al.* 1998). In the case of exterior panel removal immediately adjacent to the corner of the building, the deformation in the floor system after 20 hours was less than 1/4" and less than 1/8" in the wall system above. The experimental effort revealed that when the timber framed construction is properly executed with the wall panels "...keyed into each intersection of the building and appropriately nailed together", there is very reasonable robustness inherent in the structural system. The researchers also recommended the Eurocode approach to ensure reasonable robustness. Furthermore, the traditional engineering practice of considering 2D behavior for robustness evaluation leads to conservative results when 3D behavior is the reality.

2.7 Analytical Methods for Assessing Performance

There have been a plethora of analytical methods proposed in recent years to address the sensitivity and performance of a structure to progressive collapse. Some analytical methods have been designed to utilize commercial software, some methods have been proposed for simple single degree of freedom models, while others have been complex explicit time history simulations complete with connection fracture and three-dimensional response simulation. The objective of the present section is to review the literature related to structural analysis methodologies that have been recently proposed to either simulate progressive collapse events or evaluate the sensitivity of a structural system to progressive collapse.

Rahamian and Moazami (2003)

This manuscript outlines a case study of a 35-story structural steel framing system whereby geometrically and materially nonlinear structural analysis is used to evaluate alternate load path development within a 3-dimensional framing system. This effort points out the difficulty in using 2D catenary behavior to model 3D reality. Detailed discussion of catenary and membrane action in the structural steel system is provided in Chapter 6 of this report, but suffice it to say that 3D membrane behavior can occur in steel systems with lower tensile force demands than that encountered in 2D modeling because of compression rings that can help to create force equilibrium with membrane tension.

The finite element analysis conducted included a 3D model of a single floor plate within the structural system. Two compromising scenarios were included in the study: (a) removal of an interior column; and (b) removal of an exterior column. The analysis included both floor slab and steel members, but detailed discussion of the FE modeling was not discussed. The tensile capacity of the metal deck was ignored. As is often the case, structural engineers do not correctly link slab finite elements to beam finite elements together in an FE model of the system and the results can be suspect. Furthermore, strains and stresses computed in

combined shell-beam finite element models are not accurate unless very special precautions are taken. These issues were not discussed and therefore, only qualitative judgments can be made using the results.

The FE analysis did not include deformation limits in the structural response. Instead, a 5% strain limit was imposed. The writers were confused as to what this limit meant. The FE analysis also indicated formation of tensile forces in the steel framing as well as bending moments. The in-fill framing in the system included flexible connections. A preliminary design was undertaken prior to conducting the compromised structure evaluation. The 3D FE analysis of the two abnormal loading scenarios indicated that the majority of the beam and girder members within the floor system were adequate for the lost column scenarios considered. The beams functioning as catenary members needed to have their connections designed for the full plastic capacity of the member. It was not clear if the full plastic capacity was tension capacity, or moment capacity. The slab system required that the mesh reinforcement be "...upgraded and additional rebars be placed at critical locations." (Rahamian and Moazami 2003).

Floor deflections seen in the structural analysis ranged from approximately 10 inches to 36 inches. The column spacing was said to be an average of 30 feet. The figures presented in the manuscript indicate that these vertical deflections were likely accumulated over the 30-foot span length. This implies that the total rotation demand (elastic rotation plus plastic rotation) at the connections in the system ranged from 0.0278 to 0.0997 radians. The upper-end of this range would likely create plastic deformations that exceed capacities for typical fully-restrained steel moment-resisting connections. Therefore, the connection demand present in steel systems needs further evaluation.

This effort indicates that the present study should consider 3D behavior in the modeling of the structural system. Furthermore, the tensile capacity of the metal deck should be included in the analysis as it can contribute to the membrane capacity of the floor system. The results regarding the concrete slab reinforcement required to gain membrane contribution to the resistance (Rahamian and Moazami 2003) indicate that it may be economical to provide simple increases in WWM reinforcement in composite slab systems or concentrated bands of reinforcing steel in the slab to enhance robustness.

Powell (2005)

As outlined previously in this review, there are several methods that can be used to evaluate a structural system's sensitivity to progressive collapse. Powell (2005) presents an overview and guidance to these methodologies and makes recommendations regarding relative accuracy of the approaches.

The concept of using energy in assessing progressive collapse is popular in the research community. In essence, if progressive collapse is likely during an abnormal loading event, there will be an imbalance of

energy in the system thereby indicating that equilibrium through the time history of the response cannot be maintained. Powell (2005) argues that energy procedures are exact for single degree of freedom systems, but the level of approximation increases as dynamic degrees of freedom are added to the analytical model.

It is successfully argued that nonlinear dynamic analysis with gravity loading applied first in a loading sequence and subsequent member removal is the most accurate methodology to evaluate progressive collapse tendencies in structural systems. It is also argued that conducting such an analysis requires little more effort than nonlinear static analysis. It is recommended that viscous damping can be ignored because only one half-cycle of deformation surrounding the peak displacement in the response is needed in the response analysis.

It is interesting to note that Powell (2005) recommends that structural engineers should be very cautious of using catenary effects in resisting abnormal loading events. It is argued that the adequacy of the anchorage at the ends of the catenary is very easy to “over-estimate” and presence of sufficiently strong and stiff anchorage is unreliable. The senior writer would agree with this statement, but would add that in multistory buildings, Vierendeel action of the floors above the compromised area in the framework are likely more important. Catenary behavior is likely to become more important as one moves upwards vertically in the framework to the levels with fewer floors above. These issues will be evaluated in the present research effort.

Powell (2005) presents a case study of a structural steel frame where a column located immediately adjacent to the corner column at the perimeter of the system is removed suddenly. Demand to capacity ratios for plastic hinge rotations, column strength, beam moment strength and floor beam connection strength were computed. Implied impact factors for column strength, beam moment strength, and floor beam connection strength ranged from below 2.0 to well above 2.0 indicating that the dynamic multiplier recommended in the GSA Guidelines (GSA 2003) can be conservative or un-conservative. The present research effort should try to utilize nonlinear dynamic time history analysis if at all possible.

Dusenberry and Hamburger (2005)

A simplified analysis procedure for evaluating the tendency for progressive collapse to occur in simple structural systems is proposed in this manuscript. The procedure is based upon a single degree of freedom model's response to loss of interior support. The procedure proposed uses lost potential energy and kinetic energy to determine the displacement at which the structure is able to stop its vertically downward travel after loss of support. This is sensed by determining when or if the kinetic energy becomes zero during the response. If the kinetic energy is not extinguished during the event (the velocity of the mass in the SDOF

system never becomes zero) then progressive collapse is likely because the system cannot arrest the motion of the mass.

The process used to carry out the energy-based procedure is demonstrated. The process is a set of linearized structural analyses whereby plastic hinges are inserted throughout the structure as yielding occurs. If a plastic hinge is inserted, then a concentrated moment is added into the analytical model and the end of the member where the hinge occurs has a friction-free pin inserted. The analysis approach is very simple and accurate for SDOF systems. However, the procedure will become very cumbersome and perhaps intractable if multistory systems are considered. However, the procedure gives the structural engineer a very good feeling for the problem and evaluation of simple systems can be readily accomplished.

Khandelwal and El-Tawil (2005)

Although not a design-analysis oriented contribution to the body of literature, this effort certainly illustrates the power of computer simulation in analyzing a structure's tendency to suffer from progressive collapse. An analytical model was developed for implementation in 3D transient analysis for a steel framing system after removal of an interior column at the ground floor level. An explicit time-history analysis code was utilized and the 3D model included two planar frames with the floor system linked with constraint equations. It should be noted that the slab conditions ignore membrane action and bending resistance is ignored. One of the two frames within the model has a column removed and the analysis illustrates the failed frame "pulling" its companion to the ground. The uncompromised framework contains reduced beam section (RBS) members and connections that appear to have fully welded webs and flanges.

There are several broad reaching statements made regarding potential concerns related to the robustness of the perimeter moment-frame structural steel system considered. The problems that were mentioned as cause for concern are the lack of out-of-plane stiffness and strength of the perimeter moment-resisting frames in typical economical structural systems designed to resist seismic loading and the related use of RBS beams within these systems as their out of plane capacity will also be reduced.

The authors point out the limitations in the simulation presented that resulted from the need to balance computational effort with the benefits of detailed simulation. These limitations are clearly illustrated and discussed in the manuscript. Of particular note are the assumptions and very complex boundary conditions used to simulate floor slab behavior and the synergy between the interior framing and exterior perimeter framing. As a result, the reader should temper the concerns expressed by the authors with the understanding that the simulation described is part of a much larger effort underway to understand the response of steel systems to compromising events.

Grierson et al. (2005a)

Moving in a direction that is quite to the contrary of the immediately preceding effort, (Grierson *et al.* 2005a) proposed several simplified methods for carrying out progressive collapse analysis (PCA) on building frames. The method proposed is a series of step-by-step re-analyses on models that have been modified as a result of plastification indicated during the previous analysis step. Debris loading is included in the analysis procedure. The procedure is intended to be implemented using commercial software. Each analysis within the procedure is linear elastic. However, prior to executing a step in the analysis, the structural model is altered to account for plastification and therefore, the stiffness of the system is changed as damage occurs. Accuracy of the proposed methodology is not evaluated, but an example analysis is provided. The example considered is a planar frame considered previously in the literature and the abnormal event considered is removal of a second story exterior column.

Grierson et al. (2005b)

A very recent contribution to the arsenal of structural analysis methods is the static nonlinear analysis methodology proposed by Grierson *et al.* (2005b). Planar structural analysis of damaged structures is considered in this work. Plastic hinges within the members in the analytical model can consider axial load-moment interaction and transverse shear-moment interaction. Gradual degradation of the member's stiffness through penetration of yielding is modeled using a two-level interaction surface and with transition between being described using the long-standing degradation multiplier method. Debris loading is included in the analysis method.

The structural analysis algorithm proposed requires some interaction by the user (mainly removal of failed members from the analytical model). A linearized static analysis algorithm is employed and the structural analysis is stopped when a user-defined load multiplier is reached, or the structure stiffness matrix becomes singular indicating structural instability. Two planar frame examples are given. The first is a two-story, two-bay structure and the second is a 9-story 5-bay system. The analysis procedure for both systems is described in detail. The process of debris formation and subsequent loading of a series of floors below the compromised portion of the structure can be clearly tracked using the method proposed.

The analysis method is limited to planar structural analysis and therefore, generalization of the results to real system is limited. However, the 9-story frame example chosen (Grierson *et al.* 2005b) demonstrates that failures in the upper-stories of a structural steel frame can propagate downward through the structure causing collapse of lower floors. This has some impact on how the present effort should be undertaken. For example, the upper stories of a steel frame can be subjected to damage from abnormal events. These upper stories will have limited opportunity to form Vierendeel action as there are few stories/floors above the

compromised region. Therefore, the robustness present in these upper stories should be evaluated in the present study.

2.8 Literature Synthesis and Research Objectives

One can argue that the literature review is not complete on a variety of grounds. However, it is felt that the review did indeed encompass many important works that have been generated subsequent to the NIST bibliography that covered years 1948 through 1973 (Leyendecker *et al.* 1976). There is much that can be learned from the ideas generated in this past work and the present section of the report seeks to synthesize this knowledge in a single location so that subsequent research objectives can be postulated.

The literature review has provided several very important points and ideas that can be carried forward in the present effort. First and foremost, the structural engineer should be allowed significant freedom in design to address structural integrity as he or she sees fit. Specification provisions should not prevent the structural engineer from exercising judgment. Design specifications should provide some minimum criteria that the structural engineer can include in his or her structural system that will provide “resistance” to progressive collapse after unforeseen events.

Several very interesting points were raised in the discussion following the Ronan Point Report (ISE 1969). The first is that one cannot design for every event and the second is that non-redundant systems are all too common in building systems. One participant went so far as to say: “Do we stop designing balconies?” Bridge structures are often classified as redundant or non-redundant and there are built-in penalties rewarding multiple-girder bridge systems over two- and three-girder systems. This begs the notion that provisions that reward redundancy should be built into design specifications. These specification provisions would guide the engineer toward enhanced structural integrity while providing the engineer with opportunities to meet elevated owner expectations.

The literature appears to be at a consensus in that all buildings should have some minimal level of robustness provided by code or specification provisions. In other words, if the engineer follows the provisions, there will be a minimal level of robustness present in the structure to give it resistance to progressive collapse. It won’t necessarily prevent progressive collapse because as the age-old saying goes – “accidents happen”. However, the structure will have built-in toughness to resist disproportionate collapse. The present research effort should strive to quantify what that inherent robustness is.

The literature review indicated that there is very little documented evidence for tying force magnitudes in structural systems. The precast concrete system perhaps has the most justification for tying force magnitudes. The research should investigate tying forces that are realistic for the structural steel

framing systems and evaluate anchoring and tying force recommendations. The structural steel system has built-in tension ties in an orthogonal layout in the form of beams and girders. The inherent robustness provided by typical framing scenarios in regard to tying forces should be addressed in the effort. The splice forces in columns under abnormal event loading should be studied and it appears that the U.K. recommendation that these splice forces be capable of resisting the loading from one floor tributary to a column warrants validation. Minimum tying forces and column splice forces seem like very simple provisions for structural integrity assurance.

Any attempt in quantifying robustness in the structural steel framing system should be done using 3D structural models whenever possible and the effort cannot ignore the presence of the concrete slab and steel deck. Furthermore, the tensile capacity of the metal deck should be included in the analysis as it can contribute to the membrane capacity of the floor system. The research effort should also strive to quantify the capabilities of the secondary load carrying mechanisms that are present in the structural steel framing systems and examine ways to ensure these mechanisms are present or enhance their presence. Once these secondary sources are identified and their contribution quantified, they can be used to define minimum levels of ductility and strength such that indirect design can be carried out through inclusion of these minimum levels in design specifications. It may be appropriate to recommend design provisions that provide minimum tie force magnitudes and bending moment capacities at connections in the steel framework. In some ways this is analogous to providing minimum levels of frame action as done in ACI 318. The results regarding the concrete slab reinforcement required to gain membrane contribution to the resistance (Rahamian and Moazami 2003) indicate that it may be economical to provide simple increases in WWM reinforcement in composite slab systems or concentrated bands of reinforcing steel in the slab to enhance robustness.

Recommendations should be made regarding targeted experimental and analytical efforts that can ensure the presence of secondary load-carrying mechanisms in the steel skeleton. There is limited test data generated for structural steel connections that are subjected to axial, shear, and bending moment demands and deformation demands that are likely to occur during events where key load carrying elements are rendered ineffective. “As a result, the exemption process criteria have been designed to be conservative and therefore, there will be very few exemptions for steel frame structures” (GSA 2003). The present study should contribute to the knowledge base such that this conservative nature to the exemption process can be relaxed. The structural analysis conducted as part of this research project should provide the community with loading and deformation demands that are likely to be present in typical steel structures during these abnormal loading events and therefore, proper analytical efforts can be designed to provide justification for allowing more steel structural systems to be exempt from progressive collapse evaluation. In an ideal world, it would be very beneficial if the typical structural steel system could be shown to follow the shaded paths through the exemption process in the flowcharts of Figures 2.3 through 2.7.

With regard to development of minimum structural integrity provisions, there are very good points made in Leyendecker and Ellingwood (1977). First of all, the alternate load path method conducted with removal of key structural elements (*e.g.* major load carrying beams, floor slabs between supports, columns) can be considered "... a feasible means of determining minimum requirements for strength and continuity which can result in buildings said to possess structural integrity" (Leyendecker and Ellingwood 1977). The authors emphasize that the reasons for the minimums should be clearly illustrated in any code provisions and that these provisions would likely need to be developed for different construction types. Precast concrete panelized systems have been addressed (Fintel and Schultz 1979) and reinforced concrete slab systems have also received consideration (Hawkins and Mitchell 1979; Mitchell and Cook 1984). Structural steel systems are notably absent at present and the WTC research effort (NIST 2005) did not address structural integrity provisions for steel systems. The present research effort therefore, should seek to fill the void and propose structural integrity provisions for typical structural steel framing systems. These provisions should be developed using the alternate load path philosophy and this in turn will address one-half of the design flowchart proposed in Figure 2.3 through 2.7.

The present study should seek to quantify the benefits of distributing moment-resisting frameworks throughout the perimeter of the structural steel system and internally, and provide quantitative data and recommendations with respect to what effective tying means in the typical steel framing system and how one might enhance membrane and catenary action in floor framing. Repetitive framing should be incorporated in the frames used for robustness evaluation, and traditional serviceability constraints should be applied in the design of evaluation frames so that the added robustness due to the likely increased member sizes is included in the systems evaluated. Therefore, the present study should utilize pre-designed framing systems. Filling the web of the girder with bolts (*e.g.* providing 6 rows in a W21 section rather than 4 rows) is an economical method of attaining additional shear strength as well as axial loading strength for catenary action and bending moment strength at what are traditionally assumed to be pin connections (Shipe and Carter 2004). These sources of redundancy and robustness in the steel framing system are felt to be very important. Therefore, the present study should seek to illustrate the beneficial effect of this type of enhancement in structural systems. Finally, the present effort must include enhanced material strengths not counted on in design.

The present effort should provide insight into the structural mechanics phenomena that are activated during an abnormal loading event. Furthermore, the rotational demands at the connections within the structural steel framing system during abnormal loading events should be quantified. The present effort will not be able to conduct experimental testing of typical steel connections. However, the present study can most certainly give insight into the magnitudes of forces and deformations that typical steel connections will have to support if robustness in the steel system is to be preserved. Finally, the present study should shed some light onto the types of structural analysis that may be undertaken and their accuracy in predicting response.

Trying to develop design provisions for specific threats (*e.g.* blast loading) is very difficult. Furthermore, the event that renders members ineffective can take place very rapidly. Therefore, if one were to quantify the robustness inherent in structural steel systems, the analysis conducted should not consider specific threats (*e.g.* blast loading). Furthermore, evaluation of strain-rate effects during the structure's response to such events should be considered in the research effort. Powell (2005) presented a case study of a structural steel frame where a column located immediately adjacent to the corner column at the perimeter of the system is removed suddenly. Demand to capacity ratios for plastic hinge rotations, column strength, beam moment strength and floor beam connection strength were computed. Implied impact factors for column strength, beam moment strength, and floor beam connection strength ranged from below 2.0 to well above 2.0 indicating that the dynamic multiplier recommended in the GSA Guidelines (GSA 2003) can be conservative or un-conservative. The present research effort should try to utilize nonlinear dynamic time history analysis if at all possible.

The 9-story frame example analyzed in Grierson *et al.* (2005b) demonstrated that failures in the upper-stories of a structural steel frame can propagate downward through the structure causing collapse of lower floors. This has some impact on how the present effort should be undertaken. For example, the upper stories of a steel frame can be subjected to damage from abnormal events. These upper stories will have limited opportunity to form Vierendeel action as there are few stories/floors above the compromised region. Therefore, the robustness present in these upper stories should be evaluated in the present study.

Chapter 3

Three-Story SAC Frame

3.1 Introduction and Building Description

Evaluating the robustness and structural integrity inherent with the steel structural framing system is a relatively daunting task given the fact that there are limitless combinations of shapes, connections and framing configurations present in steel structures. It was therefore, decided the SAC-FEMA suite of buildings would be selected as base topologies for the research effort (FEMA 2000d). These buildings were designed using a variety of base assumptions regarding location, loading, and topology. The pre-Northridge configurations located in Boston were chosen for this effort. The present chapter of the report will focus on the three story building.

The building consists of structural steel wide-flange shapes with lower-bound yield stress equal to 50 ksi typical of A992. Moment resisting frames (MRF's) are located on the perimeter of the building and not all bays are part of the MRF system. The typical framing plan for the structure is shown in Figure 3.1.

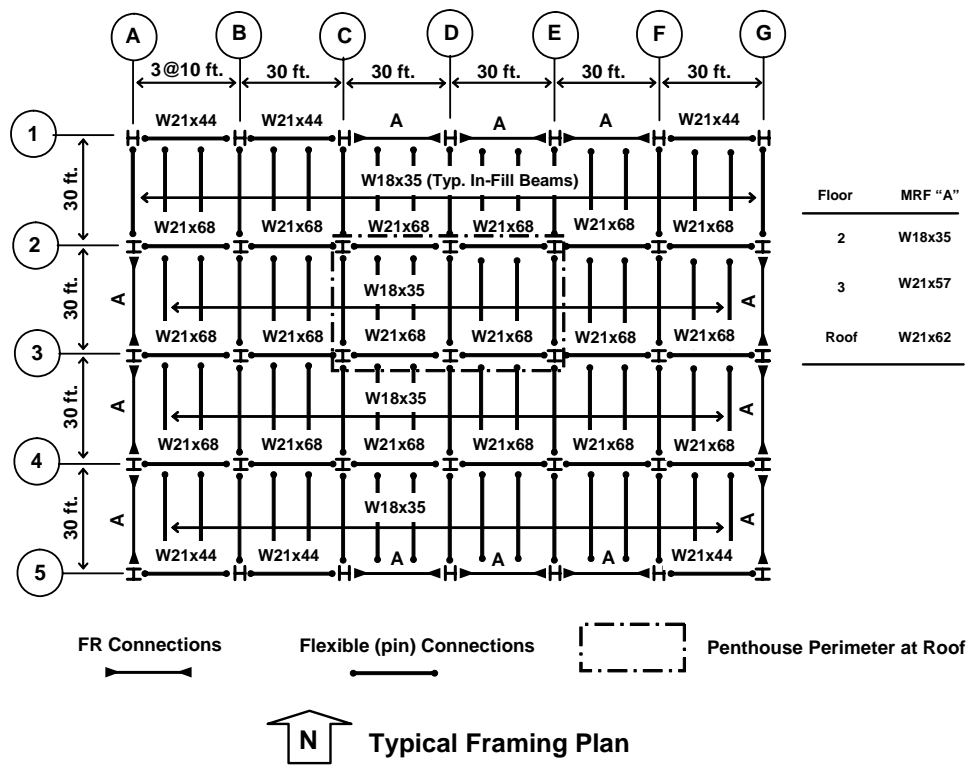


Figure 3.1 Framing Plan Used for SAC 3-Story Modified Boston Building Frame.

All members in the frame consisted of wide-flange shapes. Interior beams and girders were all assumed to be connected using *flexible* connections of negligible moment capacity. These connections are indicated using solid circles at the beam ends. The moment-resisting (rigid or fully-restrained) connections at the ends of the beams in the MRF's are indicated by triangles at the beam ends. The typical MRF in the building system consists of three-bay, three-story frame configurations. The beams within the MRF's vary with location and the small table to the right of the framing plan in Figure 3.1 provides wide-flange shape sizes for these members. Column orientations are also indicated in the framing plan. A penthouse was located at the roof level and its location is indicated in Figure 3.1.

A column schedule indicating member sizes is given in Figure 3.2. As indicated, the relatively short overall height of the framing system dictated that splices in the column stacks were not necessary.

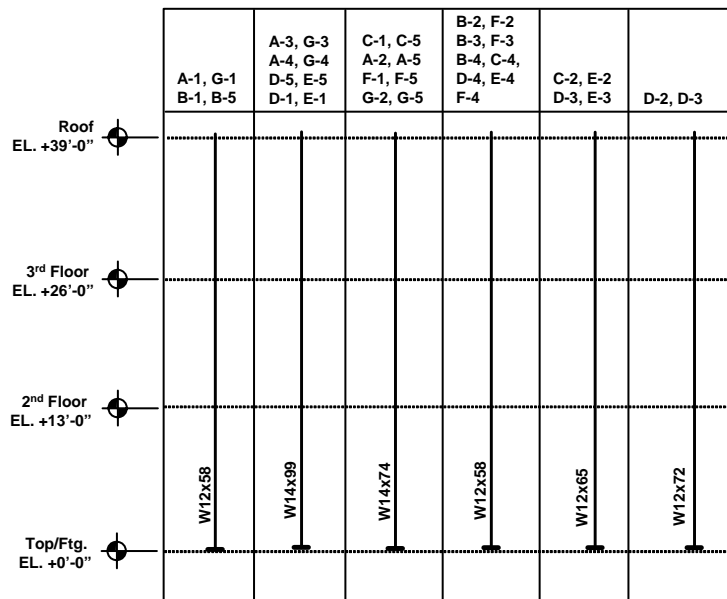


Figure 3.2 Column Schedule for SAC 3-Story Boston Modified Boston Building Frame.

The configuration of the moment resisting frames and their proximity to the simple framing adjacent to them is illustrated in Figures 3.3 and 3.4. The bases of all columns in the system are taken to be pinned (friction-free) and flexibly-connected beam members have their connections indicated with hollow circles. These connections were assumed to be friction-free pins in relation to bending about the member's major axis, but were considered fully-restrained or rigid with regard to bending about the member's minor and longitudinal axes (torsion) to reflect the presence of concrete floor slab. Moment-resisting (fully-restrained or rigid) connections are indicated with filled-in triangles. The floor-to-floor heights shown in the elevations are assumed to be taken from centerline of beam/girder to centerline of beam girder. No rigid offsets or flexible panel zones were considered. Centerline-to-centerline dimensions were considered throughout.

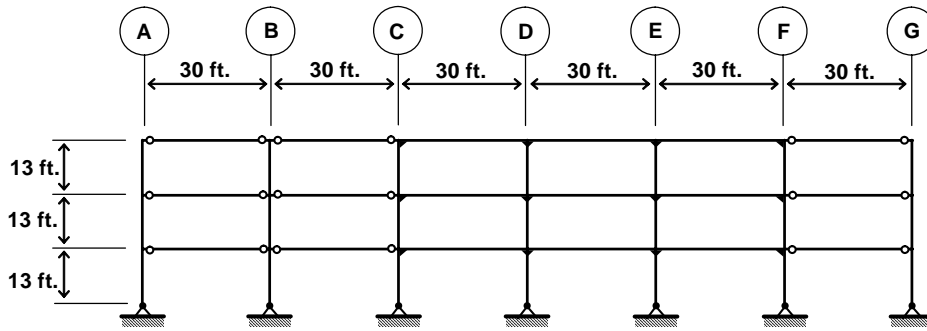


Figure 3.3 Framework Elevation Along Column Lines 1 and 5 Looking North.

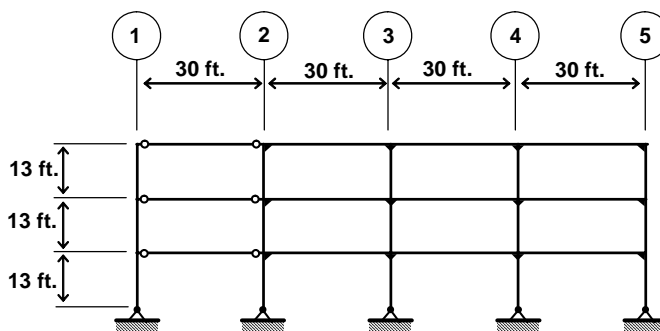


Figure 3.4 Framework Elevation Along Column Lines A and G Looking West.

A relatively simplistic loading scenario was used for the structure considered. The floors were assumed to support a superimposed dead loading of **83 psf**. This dead loading was taken to include concrete-steel composite slab, steel decking, ceilings/flooring/fireproofing, mechanical/electrical/plumbing systems and partitions (20 psf). The live loading applied to the floors was assumed to be typical office occupancy with a magnitude of **50 psf**. The region of the roof in the penthouse area was assumed to have a superimposed dead loading of **96 psf** applied. The live loading in this area was taken to be **50 psf**. The roof in regions outside of the penthouse area was assumed to support a superimposed dead loading of **63 psf** and a live loading of **50 psf** (one could argue for 30 psf – snow). Exterior cladding was assumed around the perimeter of the building. This cladding was assumed to weight **25 psf** over the wall area and a 3.5-foot high parapet at the roof level. The self-weight of the structural steel framing members was computed automatically by the computer software.

A three-dimensional structural model was developed for the 3-story building considered. The 3D nature of the model was needed in case orthogonal tying members were needed in the framing system. A schematic of the initial 3D model is shown in Figure 3.5. The SAP2000 analysis program was used (CSI 2004).

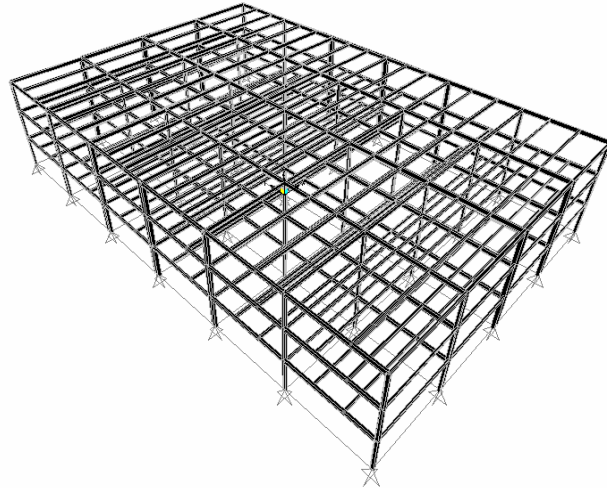


Figure 3.5 Extruded View Illustrating Basic SAP2000 Model of Uncompromised SAC 3-Story Modified Boston Framework Without Diaphragm X-Bracing.

Conveying the loading applied within this 3D model to the reader is likely best done via tabular description. Table 3.1 describes the superimposed dead loading and live loading used for the members within the framing system. It should be re-emphasized that the self-weight of the members was computed via software.

Table 3.1 Uniformly Distributed Superimposed Dead Loading and Live Loading Magnitudes (kips per linear foot) Applied to Members in the Structural Analysis.

Member	2 nd Floor		3 rd Floor		Roof	
	DL (klf)	LL (klf)	DL (klf)	LL (klf)	DL (klf)	LL (klf)
In-Fill Beams	0.83	0.50	0.83	0.50	0.63	0.50
Exterior Beam	0.74	0.25	0.74	0.25	0.57	0.25
Exterior Girder	0.33	-	0.33	-	0.25	-
Penthouse Beam (Beams in between lines C through E)	0.83	0.50	0.83	0.50	0.80	0.50
Penthouse Beam (Beams on lines C through E)	0.83	0.50	0.83	0.50	0.96	0.50

3.2 Critical Load Analysis and Diaphragm Modeling

In order to assess the need for nonlinear geometric analysis, the elastic critical loads for the frame were determined using eigenvalue analysis. The first two critical buckling modes were evaluated for the 3D

framing model developed. A factored loading combination, $1.2w_D + 1.6w_L$, consistent with LRFD was used. The critical load factors are therefore, applied to this loading combination as follows,

$$\gamma_{cr} \cdot (1.2w_D + 1.6w_L)$$

It should be noted that the self-weight of the system was not increased in the eigenvalue analysis. The critical buckling mode shapes for this loading combination are giving in Figure 3.6 and 3.7.

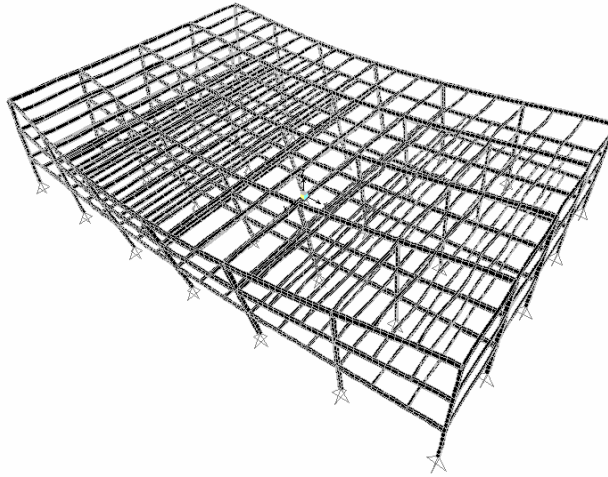


Figure 3.6 SAP2000 Displaced Shape Plot Illustrating Buckling Mode Shape Corresponding to the First Buckling Mode: $(\gamma_{cr})_1 = 0.200$.

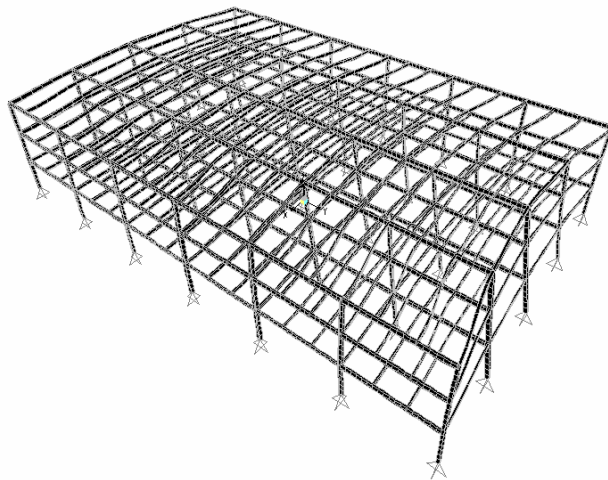


Figure 3.7 SAP2000 Displaced Shape Plot Illustrating Buckling Mode Shape Corresponding to the Second Buckling Mode: $(\gamma_{cr})_2 = 0.364$.

The flexibly-connected infill framing results in two rather unexpected buckling modes of very low magnitude. The lack of a “rigid” diaphragm in the system at the floor levels causes buckling modes that are not consistent with the reality of the framing system. As a result, the diaphragm action in the framing system required modeling. An x-braced system of weightless diaphragm members was developed to simulate the effect of the concrete floor slab (*i.e.* its shear stiffness) in the structural analysis conducted. The x-bracing is required to maintain tensile forces in panel perimeter framing. If rigid diaphragm models are utilized, the tensile forces in the beam members are removed.

Shear-racking deformation that will occur in a floor framing panel during the unrealistic buckling modes as shown in Figures 3.6 and 3.7, or during deformations subsequent to a column member within the framing system becoming ineffective is schematically shown in Figure 3.8.

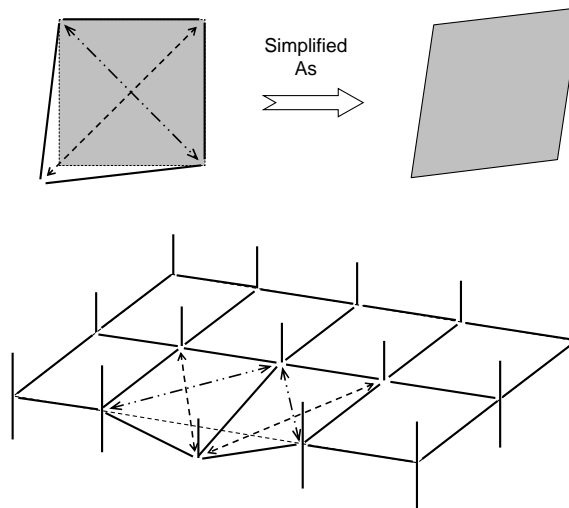


Figure 3.8 Conceptualization of Diaphragm Behavior with a Compromised Building.

As the originally square panel deforms (omitting the bending components orthogonal to the plane of the floor plate implied in Figure 3.8) tension and compression stress trajectories will develop along lines of principal stress within the panel. In a nutshell, x-bracing members that are used to simulate the presence of a composite-steel concrete deck diaphragm at the floor and roof levels are developed through the assumption that the lines of principal tension and compression can be replaced with discrete weightless diagonal wide-flange shape members that provide an equivalent shear racking stiffness to that of the concrete-steel deck system. This concept is very similar to that used by (Mahendran and Moor 1999) in the analysis of three-dimensional metal buildings.

The floor system assumed to be present in the development of the x-bracing members is given in Figure 3.9. Any panel that is considered to have x-bracing member replacement will always be bounded by either girders or columns at its perimeter. For the present 3-story structure considered, this will result in a 30-foot by 30-foot panel.

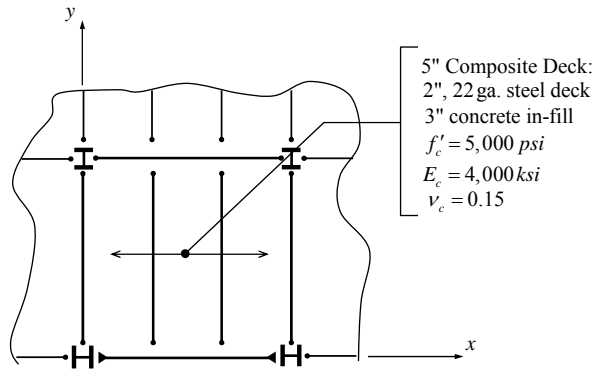


Figure 3.9 Typical Steel Floor Framing System Used as Basis for Diaphragm Model.

The panel shear racking can be modeled using isotropic material behavior. It is understood that the steel deck will likely manipulate the behavior in a manner that would make it non-isotropic, but the present model will assume that only the concrete above mid-height of the deck flutes is effective. The shear racking behavior and pertinent material model data is given in Figure 3.10.

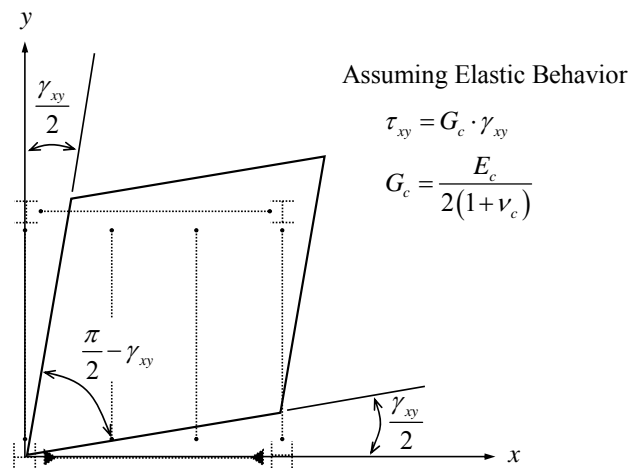


Figure 3.10 Floor Panel Shear Deformations Assumed to be Present in Diaphragm Model.

It is a little more convenient to model the diaphragm shear strain as occurring on one side only of the panel. In this manner, a pure shear racking behavior can be maintained and the angle changes are more

manageable. Furthermore, the lines of principal tension and compression that will form in the panel will contain discrete wide-flange shapes that maintain the same shear racking stiffness in the floor panel. The shear racking stiffness of the concrete floor panel can be computed by assuming a 1-inch shear racking deformation in the panel as shown in Figure 3.11.

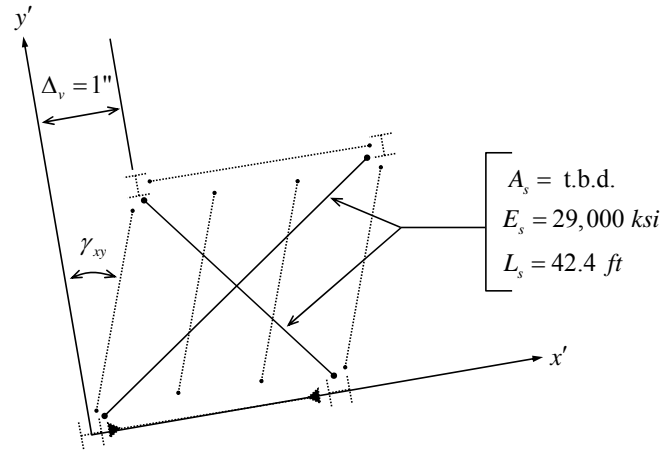


Figure 3.11 Diagonal Bracing Members Used to Model Diaphragm Shear Deformations.

Using the material properties given in Figure 3.9, the shear modulus of the concrete computed using the assumption of isotropy is approximately 1,700,000 psi. The shear strain, γ_{xy} , can then be computed using geometry as 0.00139 radians. Hooke's law for elastic behavior results in the following elastic shear stress,

$$\tau = G \cdot \gamma_{xy} = 2,363 \text{ psi}$$

Assuming that this shear stress exists along the entire edge of the shear panel (uniformly distributed) a shear force that creates the 1-inch racking deflection can be computed as,

$$V = (2,363 \text{ psi})(360 \text{ in})(4 \text{ in}) = 3,402,720 \text{ lbs}$$

The shear stiffness of the concrete panel then follows: 3,402,720 lbs/in. A 4-inch uniform thickness concrete floor slab is assumed (3-inch concrete in-fill plus 1-inch depth into the 2-inch steel deck flutes).

If the concrete in the panel is replaced with two discrete diagonal members along the lines of action of principal tension and compression for the square panel ($\theta = 45$ degrees), the shear stiffness of these two discrete members can be written as,

$$k = \frac{AE}{L} \cos^2 \theta + \frac{AE}{L} \sin^2 \theta = \frac{AE}{L} (0.707)^2 + \frac{AE}{L} (0.707)^2 = \frac{AE}{L}$$

With the lengths of the diagonal members given in Figure 3.11 as 42.4 ft, an area of the steel member required to maintain the panel's shear racking stiffness can be computed by setting the shear stiffness of the concrete panel equal to the stiffness of the diagonal x-braced panel. This results in the following cross-sectional area;

$$A = \frac{L}{E}(3,402,000 \text{ psi}) = \frac{(42.4)(12)}{29,000,000}(3,402,000) = 60 \text{ in}^2$$

Thus, the panel shear-racking stiffness can be maintained if two members with cross-sectional area equal to 60 square inches are placed along the diagonals. It should be noted that in order to maintain correct loading within the analysis software, these members should be input with no density and therefore, *will contributed zero mass and dead loading in the transient and static analysis*. The present analysis assumed a W14x159 diagonal member with cross-sectional area of 47 square inches. Several structural analyses indicated that the axial stiffness of these members were sufficient to prevent unrealistic buckling modes.

The orientation of the diagonal members within the framing plan at the two floor and roof levels are shown in Figure 3.12.

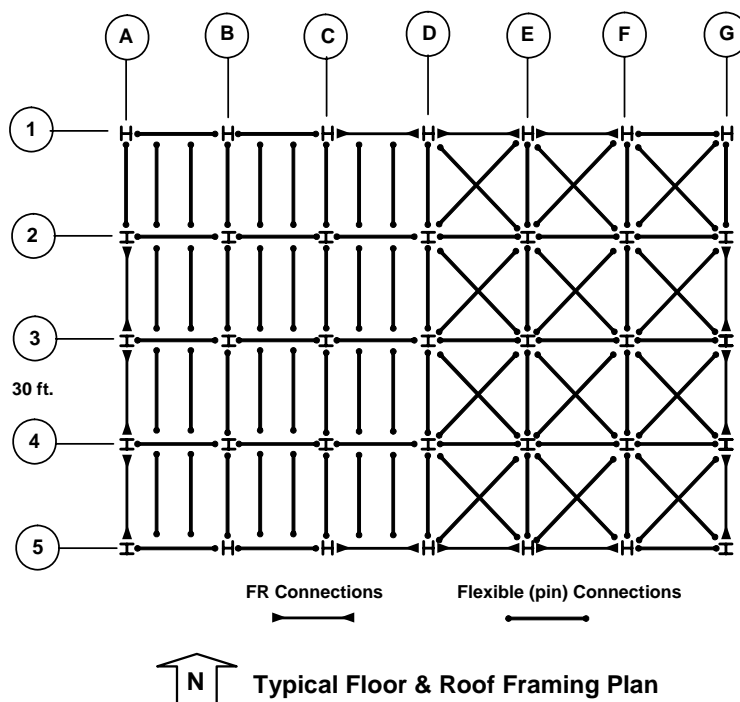


Figure 3.12 Schematic Illustrating Locations for Diaphragm X-Bracing within Framework.

Figure 3.12 does not show all x-bracing members due to prevent clutter. The W14x159 x-bracing members simply pass through all infill framing members without connectivity. The x-brace diaphragm members are only connected at the columns that lie on the boundary of the panel. As mentioned previously, they are

considered to have zero mass and contribute only stiffness in the analysis. The members are connected to the columns using friction-free pins and the moment release is only about the major axis.

An extruded view of the SAP2000 model for the building including x-brace diaphragm members is shown in Figure 3.13. This model was then used to evaluate the change in critical buckling modes for the framework. The critical loads for the revised models and the shapes of the critical buckling modes are shown in Figures 3.14 and 3.15.

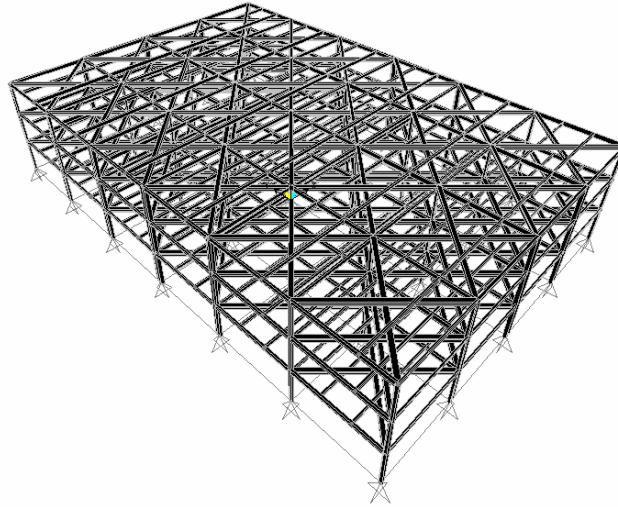


Figure 3.13 Extruded View Illustrating Basic SAP2000 Model of Uncompromised SAC 3-Story Modified Boston Framework With Diaphragm X-Bracing In Place.

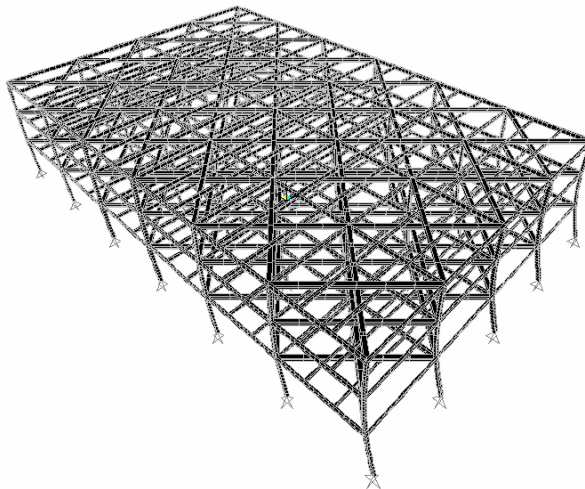


Figure 3.14 SAP2000 Displaced Shape Plot Illustrating Buckling Mode Shape Corresponding to the First Buckling Mode: $(\gamma_{cr})_1 = 1.226$.

The critical modes are now very much in line with engineering intuition regarding manner in which these 3D frames will become unstable. The two modes are now sway modes in orthogonal directions. This behavior follows from the use of perimeter moment resisting frames in the two orthogonal directions. The critical load factors for the frames are essentially the same for the two orthogonal buckling modes. As a result, the x-bracing members have preserved the proper behavior for the three-dimensional frame.

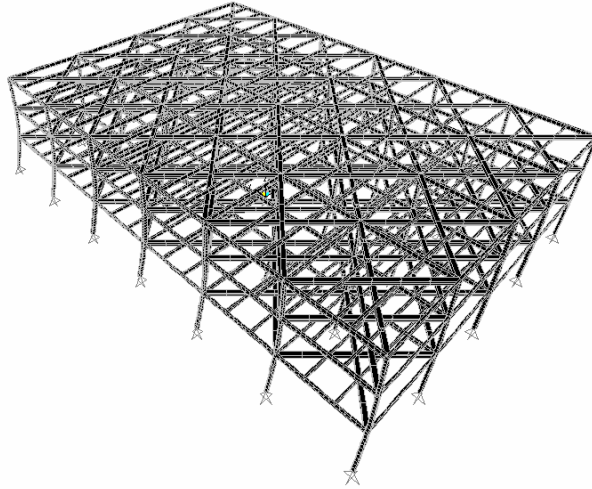


Figure 3.15 SAP2000 Displaced Shape Plot Illustrating Buckling Mode Shape Corresponding to the Second Buckling Mode: $(\gamma_{cr})_2 = 1.367$.

3.3 Elastic Analysis of Compromised Frame

As outlined in the literature review and synthesis, there are several approaches that can be used to evaluate the impact of compromising events on steel structures. Furthermore, the present study is focused on examining the inherent structural integrity and robustness in steel framing systems and making recommendations to enhance robustness in these systems. As a result, the present analysis effort will assume that one of the columns at the first-floor level become *ineffective*. The event that renders the column ineffective is immaterial. Only the fact that a column's load carrying capacity is compromised is considered important.

The GSA guidelines provide several recommended procedures that can be used to demonstrate that compromising events can be withstood by the framing system without disproportionate collapse. These procedures were reviewed in the literature review and the linear elastic dynamic analysis approach is used in the present effort. The loading combination applied to the frame at the time of the compromising events is;

$$1.0w_D + 0.25w_L \quad (3.1)$$

The event that renders a member ineffective is modeled using loading functions that vary with time. These will be described later in this subsection.

The live loading used in equation (3.1), $0.25w_L$, is intended to simulate the live loading present at the time the compromising event occurs. The uniformly distributed live loads, w_L , applied in the analytical models are based upon 50-psf office live loading (ASCE 2006). The usual live load models used as the basis for U.S. structural engineering involve two components: (a) sustained loading; and (b) extraordinary loading. The sustained portion is assumed to be continuously present (with varying magnitude) and it represents ordinary office furniture, bookcases, desks, safes, their contents, and normal personnel (McGuire and Cornell 1974). A change in the sustained loading magnitude would likely be generated by tenant occupancy changes. The extraordinary portion of the live loading is intended to simulate those instances where people group during office parties, or cases where office furniture is temporarily stacked during remodeling (McGuire and Cornell 1974).

The present study assumes that the live loading present when the structural system is compromised is the *expected arbitrary point-in-time sustained live loading* (Ellingwood and Culver 1977). Extraordinary live loading components are not considered. If one were to consider design for progressive collapse mitigation, then the *expected maximum sustained live loading* may be desired. Surveys and analysis of office live loading (Culver 1976; Ellingwood and Culver 1977) have indicated that the mean or expected arbitrary point-in-time sustained live loading is on the order of 11 psf. Assuming a moderate influence area (*e.g.* 300 square feet), the expected value of the maximum sustained live loading generated by common live loading models is on the order of 26 psf (Ellingwood and Culver 1977). The present study utilizes 50-psf office live loading with the 0.25 multiplier and therefore, the sustained live loading present at the time of the compromising event is 12.5 psf. This live loading magnitude is therefore, a little higher than the expected point-in-time sustained live loading found in office live loading surveys (Culver 1976). It should be noted that no live load reduction is utilized.

An examination of the framing system leads to several *a-priori* conclusions regarding the inherent robustness of the system. The assumption that all interior framing is simply supported results in limited ability of the system to overcome an interior column becoming ineffective without activating load resisting mechanisms that aren't considered at present (*e.g.* two-way catenary/membrane action in the floor slab). Several nonlinear elastic static analyses were run with first-floor interior columns removed (*e.g.* column D4). The analysis with beam end fixity (springs) consistent with flexible connections constructed using bolted double web angles resulted in very large deformations and instability. In general, compromising events for the interior columns are best handled via orthogonal tension tying as done in the U.K. provisions. As a result, interior columns becoming ineffective were not considered in this frame analysis. Corner columns at locations A1 and G1 have pin connected framing members. With stiffness and moment capacity typical of web-cleats, the corner columns in this framing configuration are vulnerable. Orthogonal tying with framing

members located along the column lines would be a very effective system, but this is not considered. The issue of orthogonal framing acting as ties and slab membrane action is discussed in other sections of this report.

It was decided to examine a scenario whereby an exterior column at the first floor level in the building was rendered ineffective. The moment-resisting frame layout in the building considered suggested the following compromised column events could be handled with a single analysis. These events are highlighted in Figure 3.16.

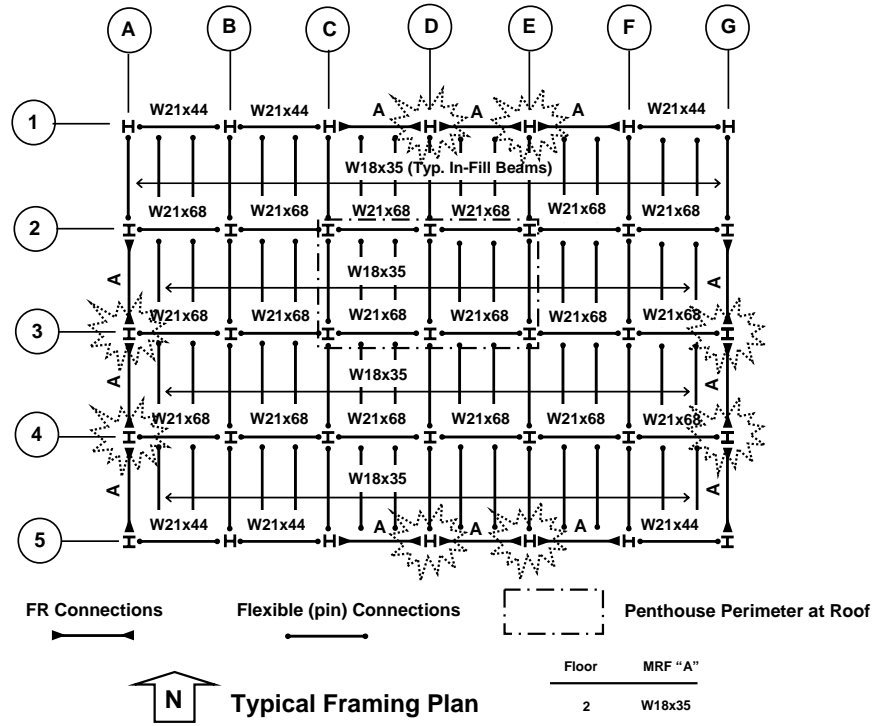


Figure 3.16 Ineffective Columns (one column at a time) Considered with the Analysis Conducted.

The second floor plan is illustrated in Figure 3.16 and the ineffective column is located immediately below the second floor level. It should also be noted that only one column at a time is considered to be ineffective. The analytical model described in this chapter will provide insights into what happens within this 3D framing system when columns A3, A4, D1, E1, G3, G4, D6, and E6 are independently rendered ineffective.

The SAP2000 model used to analyze this framework for these compromising events is created by simply removing the column in question and replacing it with a loading equivalent to that present with the column in place. The base SAP2000 frame model is shown in Figure 3.17.

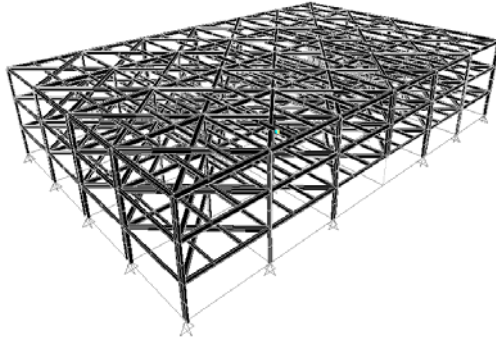


Figure 3.17 Extruded View Illustrating Basic SAP2000 Model of Compromised SAC 3-Story Modified Boston Framework With Diaphragm X-Bracing In Place and Column D-5 Removed.

In order to gain an engineering “feel” for the system in the compromised state, an elastic buckling load analysis on the framework was conducted. The following loading combination and critical load multiplier was used;

$$\gamma_{cr} \cdot (1.0w_D + 0.25w_L)$$

The first critical elastic buckling mode for the frame is shown in Figure 3.18 below.

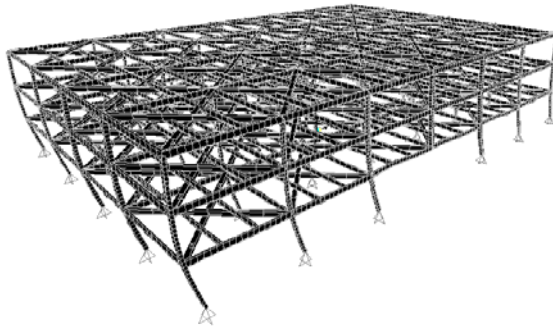


Figure 3.18 SAP2000 Displaced Shape Plot Illustrating Buckling Mode Shape Corresponding to the First Buckling Mode with Column D5 at First Floor Level Removed: $(\gamma_{cr})_1 = 2.064$.

It can be seen that the first critical mode is a sway mode in the direction parallel to the long dimension of the building. The applied load ratio of 2.064 indicates that the structure is in no danger of becoming unstable under static gravity loading assumed to be present at the time of the event. The second, third, and fourth buckling modes are shown in Figures 3.19, 3.20, and 3.21.

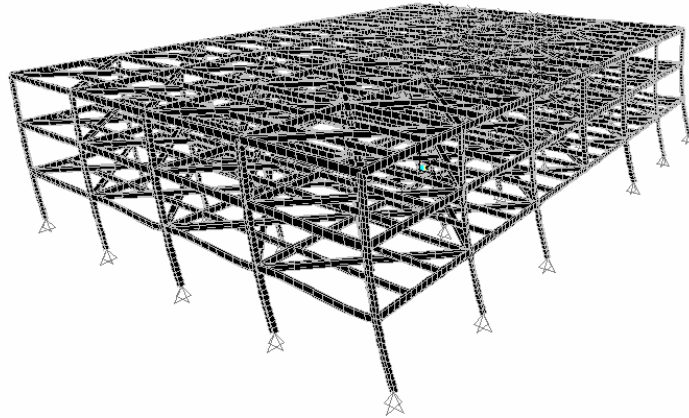


Figure 3.19 SAP2000 Displaced Shape Plot Illustrating Buckling Mode Shape Corresponding to the Second Buckling Mode with Column D5 at First Floor Level Removed: $(\gamma_{cr})_2 = 2.469$.

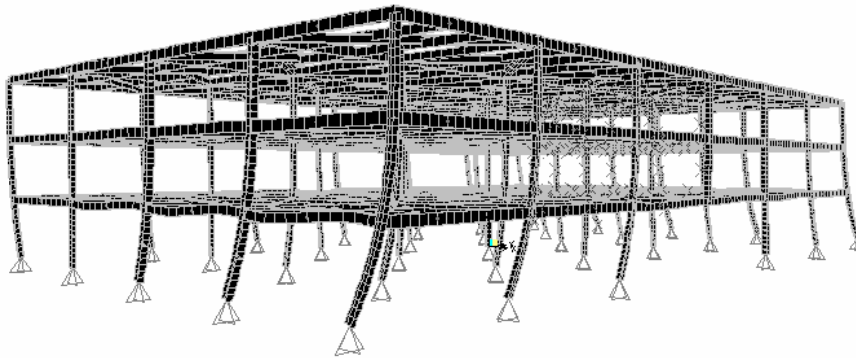


Figure 3.20 SAP2000 Displaced Shape Plot Illustrating Buckling Mode Shape Corresponding to the Third Buckling Mode with Column D5 at First Floor Level Removed: $(\gamma_{cr})_3 = 4.857$.

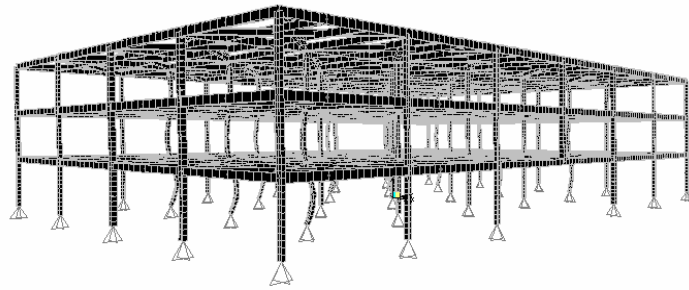


Figure 3.21 SAP2000 Displaced Shape Plot Illustrating Buckling Mode Shape Corresponding to the Fourth Buckling Mode with Column D5 at First Floor Level Removed: $(\gamma_{cr})_4 = 6.061$.

Figures 3.18 and 3.19 illustrate that the first two elastic buckling modes continue to correspond to sway modes in orthogonal directions. The critical load factors (applied load ratios) for these modes are also relatively close to one another. The fact that these buckling load factors exceed 2.0 is a result of the reduction in live and dead load factors in the combination. Figure 3.20 illustrates a torsional buckling mode for the framework and Figure 3.21 illustrates the first of many individual column buckling modes for the interior framing.

The process by which a column in the framework becomes ineffective is modeled in a time history analysis. Both the gravity loading and column loading are applied as time-history functions within the SAP2000 analysis as shown in Figure 3.22.

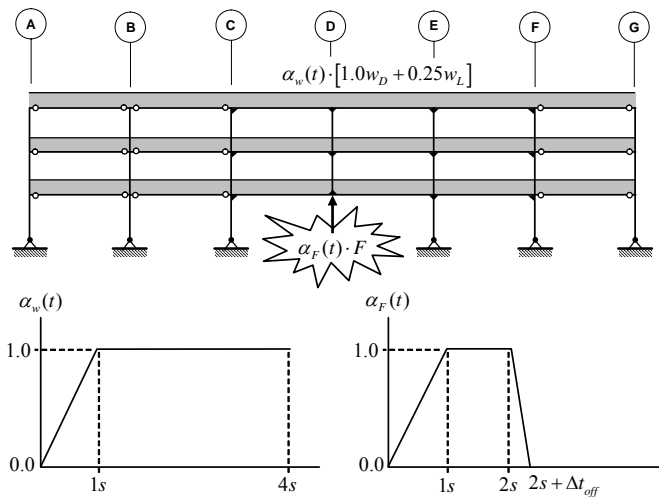


Figure 3.22 Conceptualization of Column Death Loading Scenario Implemented in the SAP2000 Time History Analysis of the Compromised Framework.

The axial loading present in the column to be removed (column D5 in this case) is determined using a simple linear geometric analysis of the structural system. This column's axial load is then applied in an upward direction to the joint at the second floor. The gravity loading present during this analysis is that given by equation (3.1). The symmetry of the spans on either side of the column considered ineffective results in very little (negligible) bending moments in the compromised column under gravity loading.

The event rendering this column ineffective is simulated by applying the gravity loading and upward loading at the ineffective column location as functions of time with multipliers that vary as shown in Figure 3.22. The duration of the event that renders the column ineffective is modeled with the upward force being *turned off* over a time interval, Δt_{off} . The entire analysis duration (4-sec. in this case) was determined via trial and error. The gravity loading and column's resisting force are applied over a 1-sec. duration as indicated in the Figure. The 1-sec. interval that follows is used to have the frame *settle* in place with the gravity loads applied. The column's resisting axial load is then *turned off* and the frame is allowed to dynamically respond to this event.

Damping is important in a dynamic analysis. Damping can preserve numerical stability of the solution algorithm as well as generate reduced peak displacements during the dynamic event as damping levels increase. One can argue that damping levels during an event whereby beams and/or columns in the framing system become ineffective will be higher than levels during seismic events (*i.e.* significant deformations, cracking etc..., will occur). However, the present structural analysis assumes damping at a level equal to 5% of critical. Default magnitudes of material-level damping in SAP2000 were also used (CSI 2004). In order to attain a better distribution of mass through the framing system (Powell 2005), all in-fill beams were divided into two elements. Columns in the moment resisting frames were divided into two elements in the attempt to better simulate $P-\delta$ effects when only $P-\Delta$ effects can be modeled.

The GSA Guidelines recommend that member "turn-off" rates be done with duration equal to $1/10^{\text{th}}$ of the natural frequency of the framing system (GSA 2003). The fundamental vibration frequencies of the framework in vertical mode indicated that 0.01 second "turn-off" interval would be sufficient to meet these guidelines. However, it was desired to examine the impact of turn off rate on the response of the framing system to the ineffective column. Figure 3.23 illustrates the response of the framework to three column turn off rates and the difference between nonlinear geometric and linear geometric response. Material nonlinearity is not considered.

The turn off interval is important in determining the response. There is very little difference in peak displacement and the period of the response with turn off rates equal to $\Delta t_{off} = 0.05 \text{ s.}$ and $\Delta t_{off} = 0.01 \text{ s.}$ As a result, the analysis conducted in this study utilizes a turn off rate of 0.01 second. The damping present in the

system is also apparent in the response and the number of large cyclic deformations after column removal could give rise to concerns with regard to low-cycle fatigue. However, one must keep in mind that this analysis is elastic and the 5% damping is a rational estimate for damping inherent in the system during response to an instantaneously lost column. It is likely that damping would be higher than 5% of critical during such an event and the low-cycle fatigue concerns can be alleviated somewhat.

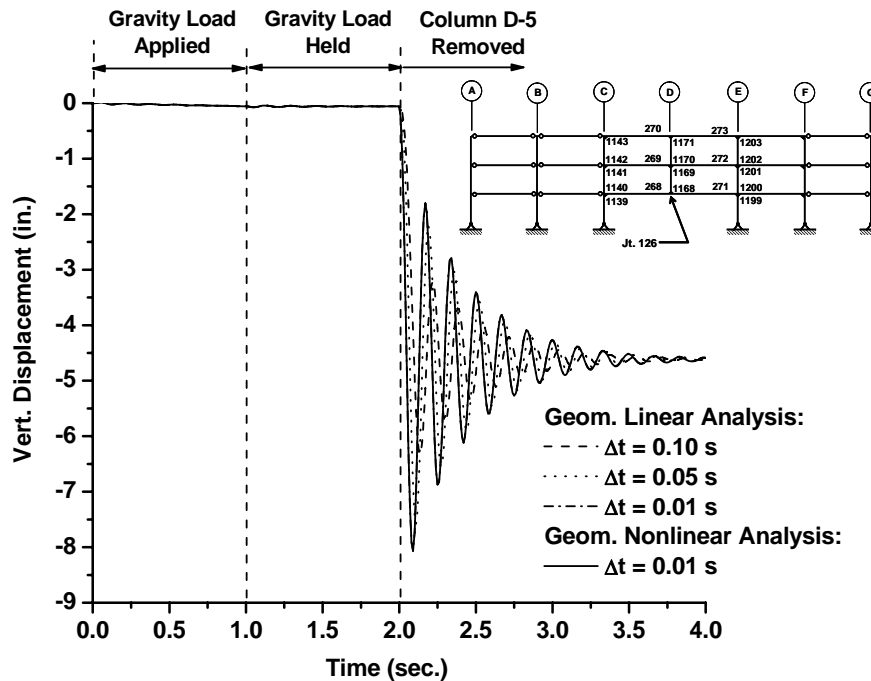


Figure 3.23 Impact of Column Death Rates on Elastic Linear and Nonlinear Geometric Response of the Modified SAC 3-Story Framework Used (displacement is immediately above lost column).

Nonlinear geometric analysis is also not an issue in the response. The nonlinear geometric response utilized the 0.01-second turn off rate and the response is identical to the linear geometric response. This is expected since the live loading is very small relative to the usual factored load levels implemented in design. There is no tendency for the columns in the frame to be subjected to interstory sway. As a result, the $P-\Delta$ effects are very small and deflections of the beam member ends relative to one another are not large enough to activate significant contribution of geometric stiffness. All columns remaining in the main load resisting systems in the vicinity of the ineffective column are connected to beams with moment-resisting connections. Thus, the $P-\delta$ effects are expected to be very, very small as well. Therefore, the analysis conducted in the study of the 3-story frame omits nonlinear geometric effects.

The SAC-FEMA study of moment-resisting connections (FEMA 2000c; FEMA 2000a) pointed out the importance of strain rates on connection response. It is well known that the toughness of steel material decreases and the yield stress of the material increases with increase in the strain rate (Barsom and Rolfe 1999). To this end, the elastic strain rates for axial loading, shear loading and bending moment were computed for the ineffective column scenario previously described. Linear geometric response, 5% damping, and a turn off rate of 0.01 seconds were utilized in this analysis. Figures 3.24 through 3.32 contain strain-rate responses for the framework.

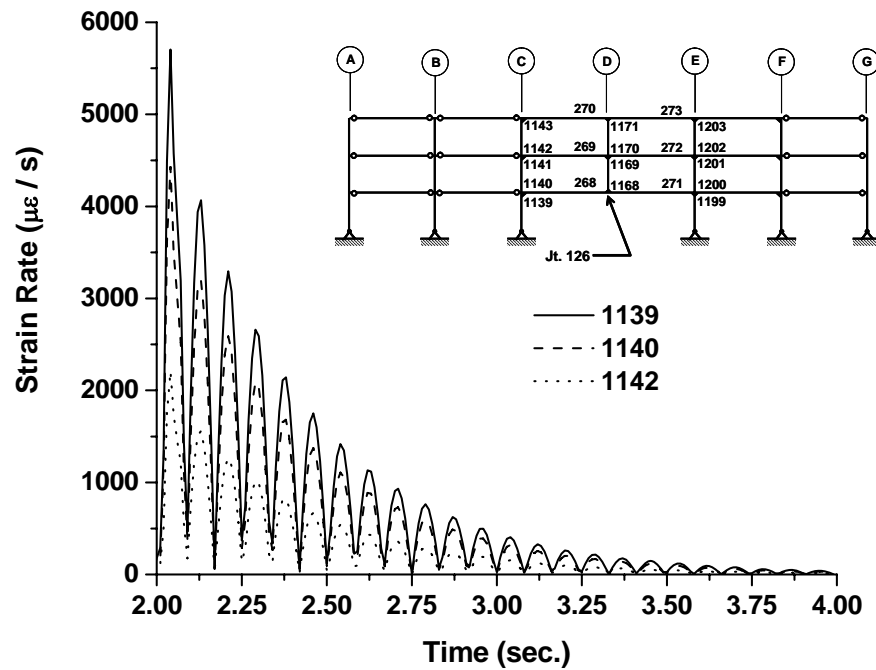


Figure 3.24 Axial Load Strain Rates (micro-strain per second) for Columns Along Line C in the Moment-Resisting Frame.

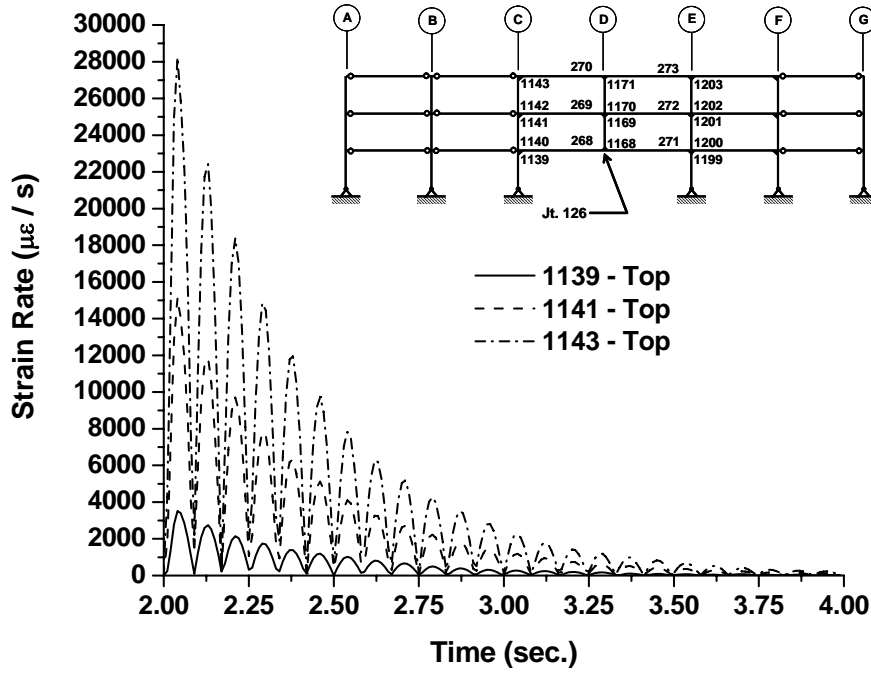


Figure 3.25 Shear Strain Rates (micro-strain per second) for Columns Along Line C in the Moment-Resisting Frame.

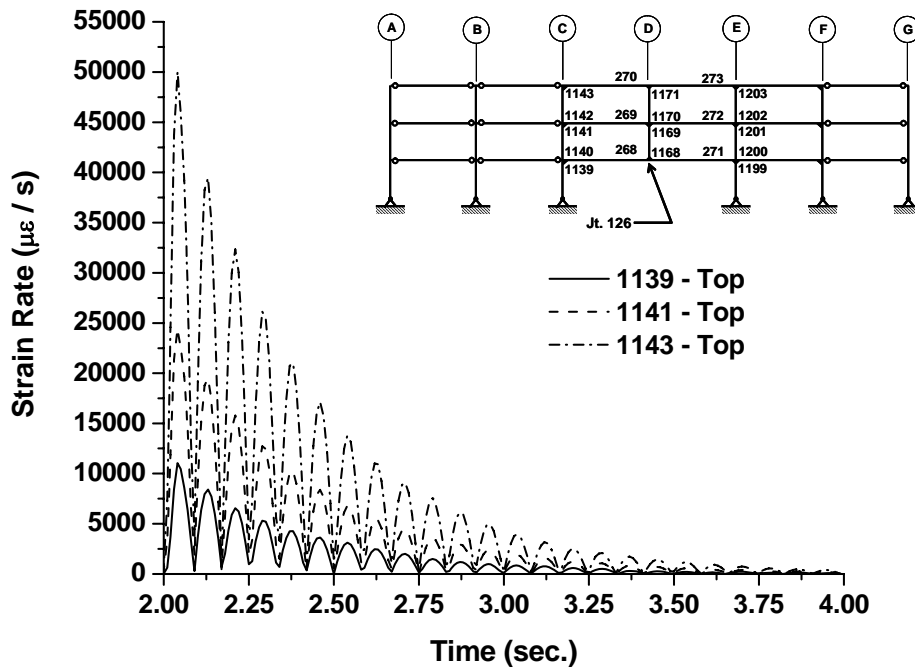


Figure 3.26 Bending Moment Strain Rates (micro-strain per second) for Columns Along Line C in the Moment-Resisting Frame.

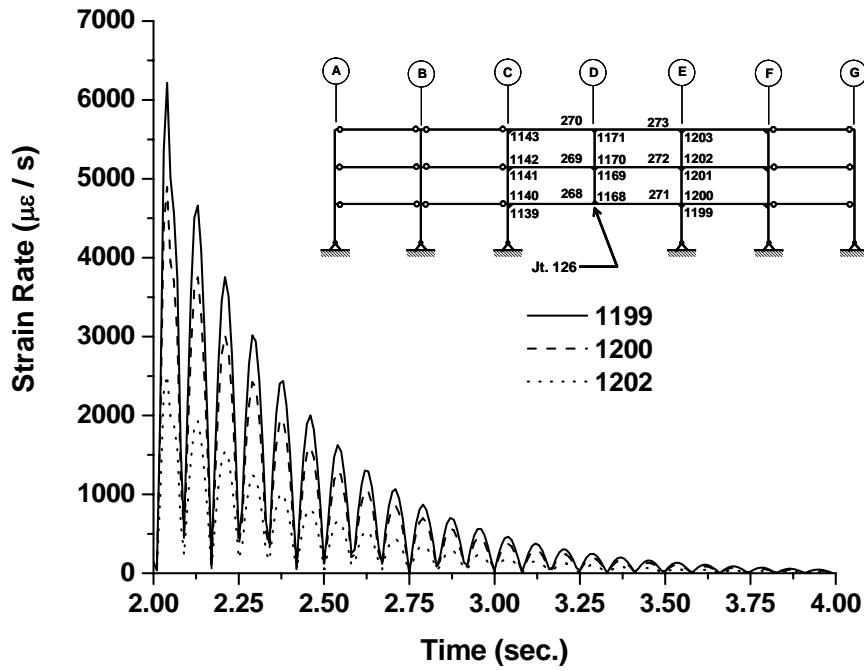


Figure 3.27 Axial Load Strain Rates (micro-strain per second) for Columns Along Line E in the Moment-Resisting Frame.

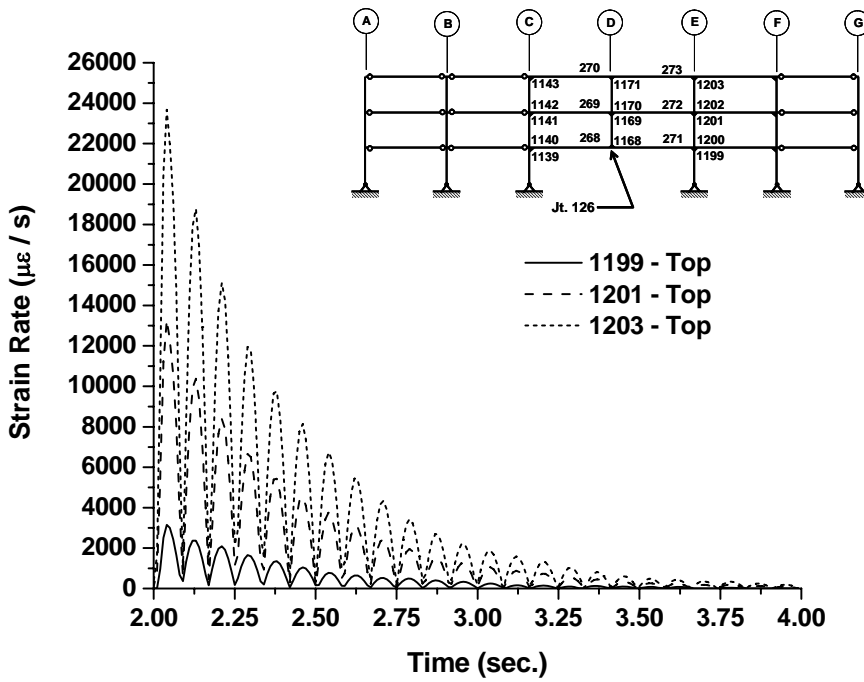


Figure 3.28 Shear Strain Rates (micro-strain per second) for Columns Along Line E in the Moment-Resisting Frame.

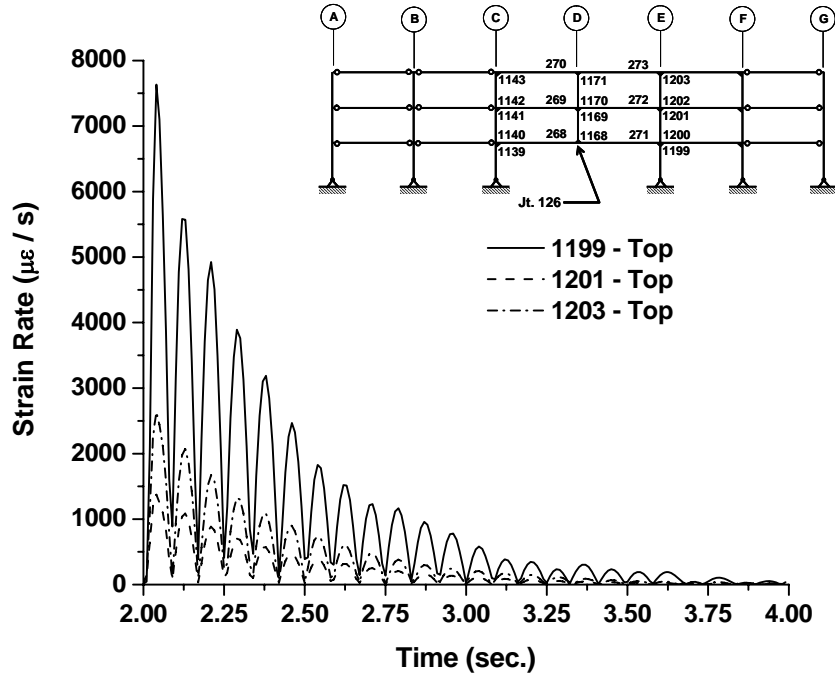


Figure 3.29 Moment Strain Rates (micro-strain per second) for Columns Along Line E in the Moment-Resisting Frame.

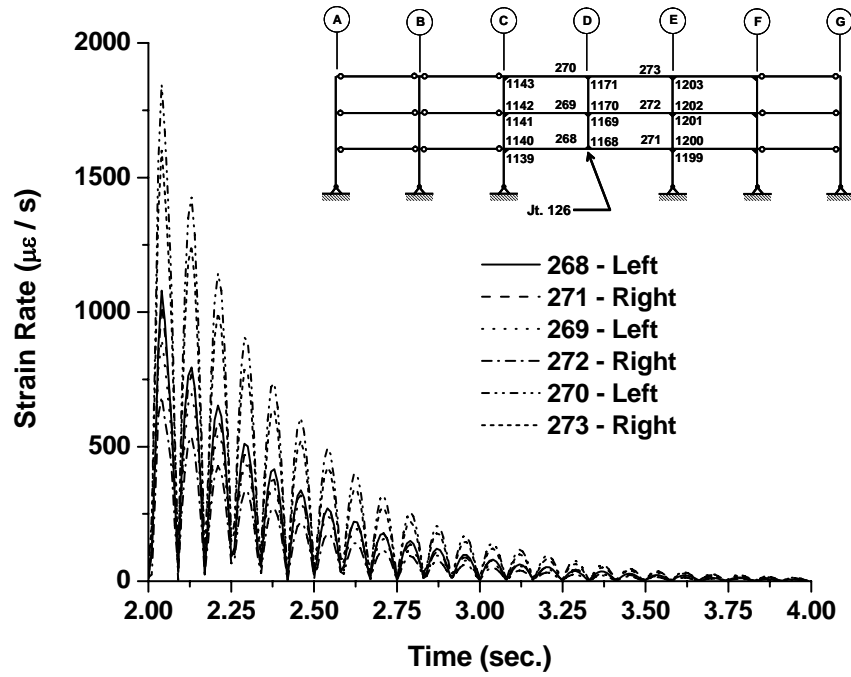


Figure 3.30 Axial Load Strain Rates (micro-strain per second) in the Beams of the Moment-Resisting Frame with Ineffective Column.

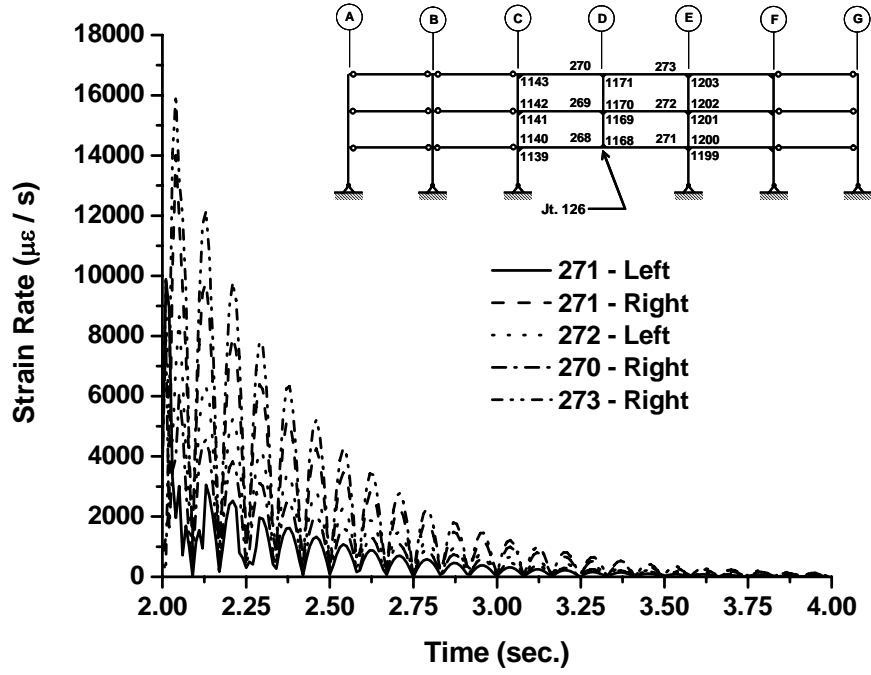


Figure 3.31 Shear Strain Rates (micro-strain per second) in the Beams of the Moment-Resisting Frame with Ineffective Column.

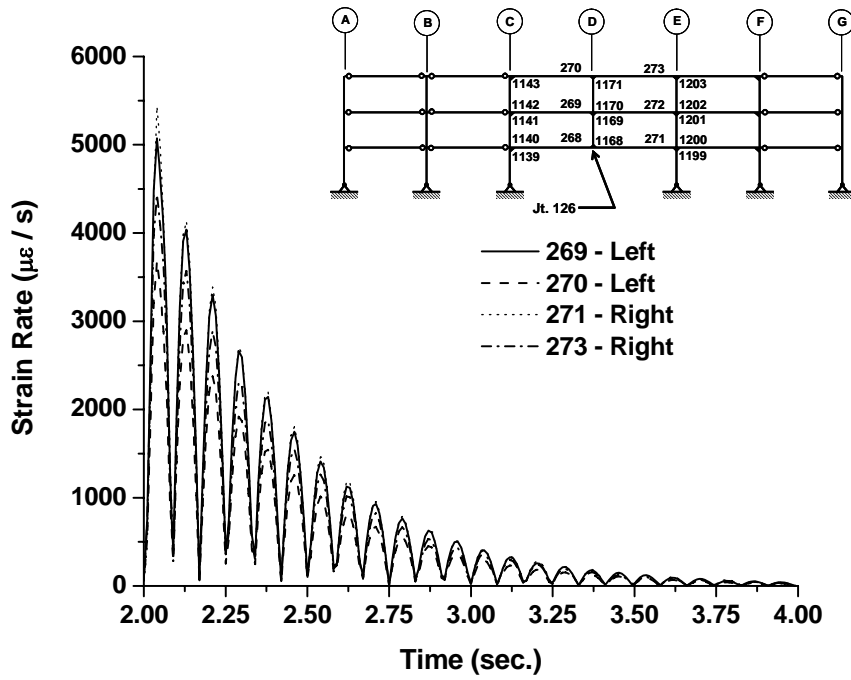


Figure 3.32 Bending Moment Strain Rates (micro-strain per second) in the Beams of the Moment-Resisting Frame with Ineffective Column.

The elastic strains in the material were computed using simple mechanics theory and procedures commonly employed in the analysis of structural steel framing systems. The expressions for computing strains at each instant in time during the analysis are;

$$\varepsilon_{axial} = \frac{P}{A \cdot E} \quad (3.2)$$

$$\varepsilon_{shear} = \frac{V}{A_w \cdot G} = \frac{V}{(d - 2t_f) \cdot G} \quad (3.3)$$

$$\varepsilon_{bending} = \frac{M}{S \cdot E} \quad (3.4)$$

The strains at each instant of time during the response are computed using equations (3.2) through (3.4). With the solution increment $\Delta t = 0.01$ sec, an estimate for the rate of change in strain at any instant of time can be computed using the following *difference formula*,

$$\dot{\varepsilon}(t) = \frac{d\varepsilon}{dt}(t) \approx \frac{1}{2 \cdot \Delta t} [\varepsilon(t + \Delta t) - \varepsilon(t - \Delta t)] \quad (3.5)$$

The axial strain rates in the columns and beams range from a low of $1,875 \mu\varepsilon/s$ (0.0019 in/in/s) and a high of $6,250 \mu\varepsilon/s$ (0.0062 in/in/s). The shear strain rates are significantly higher in all members of the framework. Peak shear strain rates occur in the columns of the framework at the top of the 3rd story columns. These rates are on the order of $28,000 \mu\varepsilon/s$ (0.028 in/in/s). Bending strain rates are comparable to the axial and shear rates. A similar exception to that found with the shear strain rates is element 1143 which is a 3rd story column at column line C. The bending strain rate for this member is also relatively rapid compared to other members. This member has an applied peak bending strain rate of $50,000 \mu\varepsilon/s$ (0.05 in/in/s).

Figure 3.26 illustrates significant differences in bending moment strain rates among the columns at line C. The bending moments in the beams at each floor level at column line C vary with stiffness of the column members at line C. Furthermore, the bending moment in the roof beam at column line C must be carried exclusively by element 1143 (the column). However, the bending moments in the beams at other floor levels at line C are able to distribute among multiple columns connected to the beam. Therefore, there is a significantly smaller bending moment strain rate in the lower story columns along column line C than at the roof level.

The fracture toughness of steel materials can be affected by loading rate. In order to evaluate the tendency for the materials in the members to fracture prematurely as a result of loading rates, the strain rates computed during the time history required analysis. The fracture toughness of steel materials can be reduced as the loading rate increases from that used in determining the fracture toughness according to ASTM E 399 (ASTM 1997; Barsom and Rolfe 1999). Dynamic loading rates (*e.g.* strain rates seen in CVN impact testing)

are often taken to be on the order of $10 \text{ } \varepsilon/s$ and intermediate loading rates are often taken to be on the order of $0.001 \text{ } \varepsilon/s$ (Barsom and Rolfe 1999). The bending and shear strain rates seen in the elastic time history analysis lie in between these values.

The time to maximum bending moment or maximum shear determined with the current elastic time history analysis is on the order of 0.15 seconds. This is a little more rapid than the intermediate loading rate and orders of magnitude slower than the dynamic loading rate (Barsom and Rolfe 1999). For A36 steel, one could argue that the difference between slow-bend and impact toughness at 75 degrees F is diminished significantly (Barsom and Rolfe 1999). Therefore, if it is assumed that the event rendering the column ineffective occurs when the steel's temperature is near room temperature, the loading rates found in the elastic time history analysis give no indication that fracture toughness of the constituent materials will be significantly diminished. It is understood that local strain concentrations resulting from connection details and flaws that may be generated through welding have been ignored. These issues need further evaluation.

It should be noted that the absolute value of the strain rates reported have been taken and this is the reason for the data residing in a single quadrant of strain rate versus time space. The results also indicate that the strain rates decrease quite rapidly with time as a result of damping in the system. In general, the columns in the system are subjected to higher strain rates than the beams. The beams in the system have the highest shear strain rates of all members in the framework (on the order of 0.016 in/in/s).

The members within the 3D framework are subjected to a variety of axial, shear and bending loads when column D5 (at first floor) is rendered ineffective. As a result, there is a need to measure the effect of these three load effects acting simultaneously on the members and then these forces can also be used to evaluate demand placed on connections. The research conducted after the Northridge earthquake has provided pertinent evaluation tools to carry out these types of activities (FEMA 2000b).

It has been known for decades that the interaction of axial load and bending moment can be conservatively modeled as linear. Therefore, one can consider the following interaction to be conservative,

$$\frac{P}{P_n} + \frac{M}{M_n} \leq 1.0 \quad (3.6)$$

where: P_n is the nominal axial capacity of the member; and M_n is the nominal bending moment capacity of the member. The addition of transverse has not been as thoroughly studied, but the interaction of shear and moment has been modeled using the following interaction equation,

$$\left(\frac{V}{V_y} \right)^2 + \frac{M}{M_p} \leq 1.0 \quad (3.7)$$

It was decided to utilize a combination of equations (3.6) and (3.7) to define a demand to capacity ratio (DCR) for the present elastic analysis that would give indication that the yield surface for a member has been breached. The DCR used to assess member strength and stability using the results of the present elastic time history analysis in the present study is,

$$DCR = \frac{P}{P_n} + \left(\frac{V}{V_n} \right)^2 + \frac{M}{M_n} \leq 1.0 \quad (3.8)$$

where: P_n is the flexural buckling capacity of the wide-flange member (defined using both major- and minor-axis buckling); V_n is the shear strength of the member; and M_n is the flexural capacity of the member considering the limit states of yielding (*i.e.* plastic moment strength) and lateral torsional buckling. Equation (3.8) is very similar to equation (H3-6) in the AISC Specifications for HSS shapes (AISC 2005a). Expected yield strengths (55 ksi) were used to define all member capacities.

The AISC specifications (AISC 2005a) are utilized to determine the nominal axial capacities, shear capacities and bending moment capacities for use in equation (3.8). The nominal axial capacities of the vertical elements in the framework are defined using an effective length factor for both axes of flexural buckling equal to 1.0 and a C_m factor of 1.0. Moment amplification for $P - \delta$ effects was ignored because the axial loading in the members will be much less than the Euler critical load. Furthermore, elastic nonlinear geometric analysis conducted also indicated that $P - \Delta$ effects were very small and therefore, moment amplification for these effects was ignored. The unbraced length of the member was taken to be the story height (13 feet) and flexural buckling of about both major- and minor-axes was considered. Horizontal element axial strengths (*i.e.* beams) were taken to be full yield strengths using expected yield stress. In compression, the concrete slab is likely to take a significant amount of compression force, thus limiting axial compression carried by the beam and the full yield strength in tension is assumed possible (assuming connections are adequate). A major motivation for this study is to determine the demands placed on connections within frames subjected to compromising events.

The bending moment capacity for the vertical elements in the system are defined using pure-bending modifiers of $C_b = 1.0$, which is conservative, and an unbraced length equal to the story height (13 feet). Horizontal element bending capacity is determined assuming the fully-braced condition. Local buckling was considered in the definition of bending capacity for all elements in the system.

The shear strength of the member is defined using the height of the web in the cross-section (depth minus two flange thicknesses) and the web thickness. The shear capacity of the web is taken from the specifications (AISC 2005a).

Elastic time history analysis using a column turn off rate of 0.01 seconds was conducted for the frame and loading described previously. The response time history data was then used to define DCR's for all elements in the framework using equation (3.8). Figures 3.33 through 3.35 illustrate the response history of the DCR's for members within the moment-resisting framework. Each figure contains a key to the output data. Both columns and beams were considered. It should be noted that the columns along line D were not considered in the graphical output, but their response data is summarized in a table that follows.

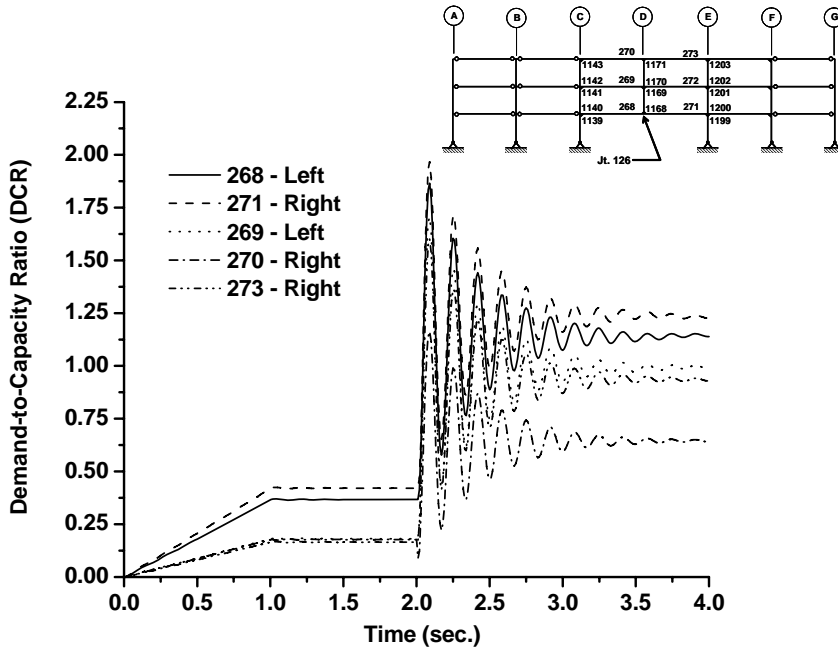


Figure 3.33 Demand to Capacity Ratios for Beams in Frame Affected by Ineffective Column at D-5.

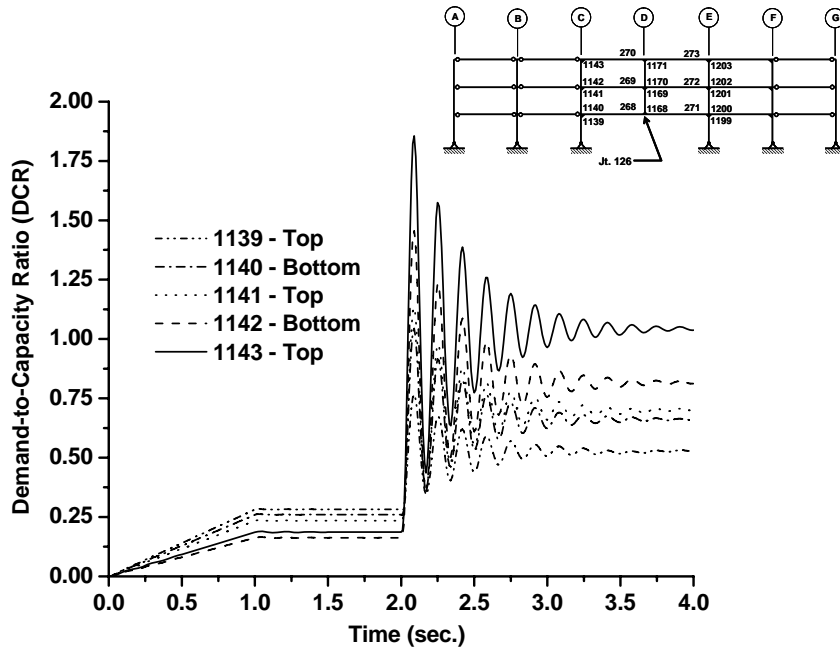


Figure 3.34 Demand-to-Capacity Ratios (DCR's) Assuming Elastic Response for Columns Along Line C in Frame.

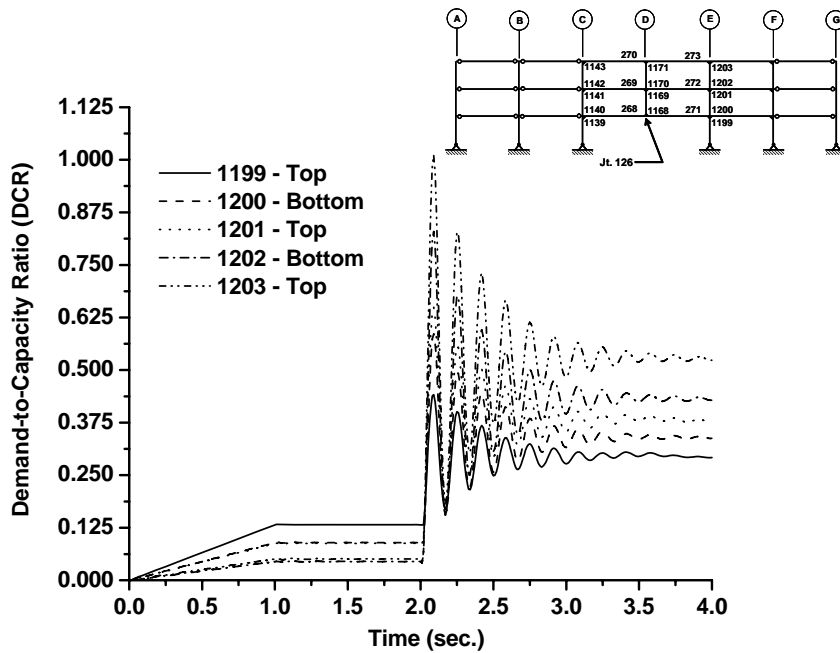


Figure 3.35 Demand-to-Capacity Ratios (DCR's) Assuming Elastic Response for Columns Along Line E in the Frame.

The elastic analysis indicates that the largest DCR's occur in the beams within the framework. The largest of the beam member DCR's occurs in the second floor beam at column line E. The columns at column line E all have DCR's less than 1.0 and therefore, one can say that these members in the framework are adequate if column D5 becomes ineffective at the first floor level. The columns along line C have DCR's that exceed 1.0 in virtually all cases. In general, the simply-supported beams adjacent to this column stack results in this behavior. If one utilized moment-resisting connections (*i.e.* FR or rigid connections), the DCR's for these members would likely decrease.

Table 3.2 provides the peak component demands (*i.e.* axial, shear, moment) and the peak DCR's for the members in the frame.

Table 3.2 Peak Non-Dimensional Member Demands and Demand-to-Capacity Ratios for Elastic Response to Ineffective Column at Location D-5.

Member (1)	$\frac{P}{P_n}$ (2)	$\frac{V}{V_n}$		$\frac{M}{M_n}$		$DCR = \frac{P}{P_n} + \left[\left(\frac{V}{V_n} \right)^2 + \frac{M}{M_n} \right]$		
		Left/Bot. (3)	Right/Top (4)	Left/Bot. (5)	Right/Top (6)	Left/Bot. (7)	Right/Top (8)	
B E A M S	268	0.030	0.283	0.110	1.755	0.807	1.866	0.838
	271	0.028	0.105	0.291	0.851	1.854	0.879	1.967
	269	0.024	0.284	0.100	1.602	1.195	1.707	1.230
	272	0.018	0.117	0.300	1.281	1.751	1.314	1.859
	270	0.058	0.259	0.090	1.144	1.098	1.269	1.164
	273	0.049	0.127	0.291	1.210	1.467	1.275	1.601
C O L M N S	1139	0.389	-	0.068	-	0.372	-	0.766
	1140	0.279	0.272	-	0.692	-	1.044	-
	1141	0.279	-	0.272	-	0.781	-	1.133
	1142	0.129	0.479	-	1.096	-	1.455	-
	1143	0.129	-	0.478	-	1.498	-	1.856
	1168	0.098	-	-	-	-	0.098	-
	1170	0.038	-	-	-	-	0.038	-
	1199	0.273	-	0.044	-	0.167	-	0.441
	1200	0.200	0.200	-	0.346	-	0.586	-
	1201	0.200	-	0.200	-	0.409	-	0.649
	1202	0.098	0.366	-	0.598	-	0.830	-
1203	0.098	-	0.365	-	0.780	-	1.012	

In general, the axial load demand is less than 0.40 for all members. When the axial demand increases, the bending moment and shear demands are small. The majority of the demand in the beam members is due to bending moment and more often than not, these demands are the reason that the DCR's are elevated beyond 1.0. Reducing this bending moment demand can be done by providing orthogonal moment resisting framing in the 3D system to help “drag” forces in alternate directions. The DCR's that are greater than 1.20 gave significant concern that the elastic time history analysis would be invalid and therefore, the distribution of demand throughout the frame was examined as well.

The axial, shear, and bending moment demand distribution within the framework is shown in Figures 3.36 through 3.38.

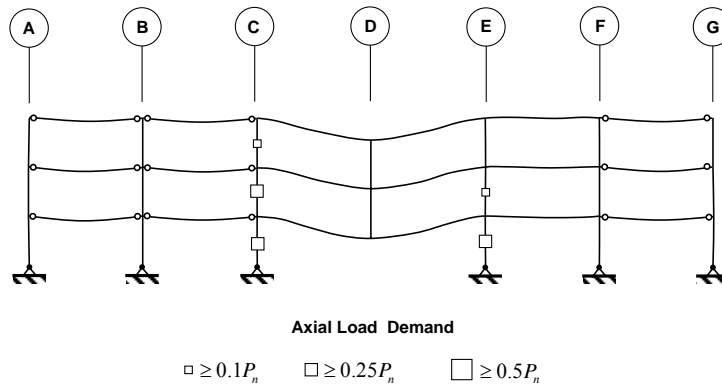


Figure 3.36 Axial Load Demand for Members in Moment-Resisting Frame Containing Ineffective Column.

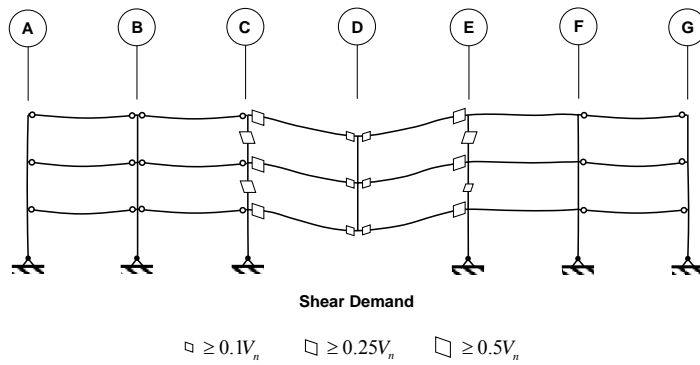


Figure 3.37 Transverse Shear Demand for Members in Moment-Resisting Frame Containing Ineffective Column.

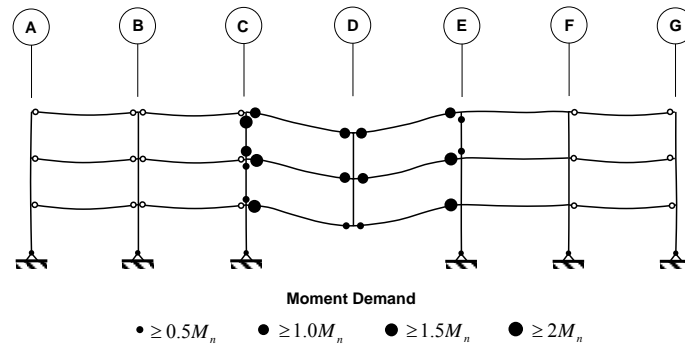


Figure 3.38 Bending Moment Demand for Members in Moment-Resisting Frame Containing Ineffective Column (no moment demands exceed $2M_n$).

If one were to examine the dominant terms that define the DCR used here in light with what is seen in these figures, it can be said with certainty that the bending moment demands in the beams are the most important indicator of the adequacy of the frame during the compromising event. Furthermore, the behavior exhibited in the response gives confidence that the linear interaction expression is reasonable and conservative. The bending moment demand, however, indicates that a plastic hinge analysis of the framework is likely needed to make final judgments. Therefore, an analytical model that incorporates plastic hinges (moment-only) was developed.

The moment demand distribution shown in Figure 3.38 suggests that all columns in the framework should have moment hinges inserted at their top and bottom locations. Furthermore all beams left of column line E should have moment hinges inserted. Finally, it would be prudent to incorporate hinges to the immediate right of column line E in the beams in case moments distribute significantly after yielding. The moment hinge model used in the subsequent inelastic analysis of the framework is shown in Figure 3.39.

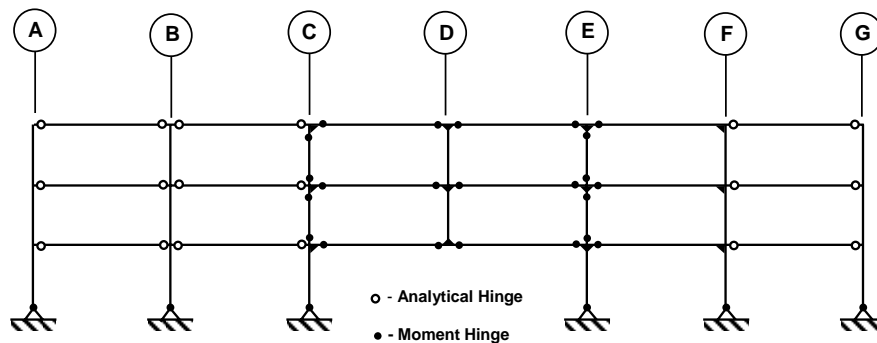


Figure 3.39 Moment Hinge Insertions to Frame Model Using Results of Elastic Time History Analysis.

The development of the hinge models in a manner that is suitable for implementation in SAP2000 is now described in the next section. A discussion of the inelastic response of the frame is also included in this section.

3.4 Inelastic Time History Analysis of Framework

The SAP2000 program has the capability of defining a variety of hinges (*e.g.* axial load, shear, bending moment) in addition to interaction surfaces. Shake down analysis on benchmark problems led to concerns that SAP2000 was unable to properly follow axial load moment interaction surfaces and therefore, hinges used in nonlinear material analysis for the present study were limited to moment only hinges with subsequent checks pertaining to the validity of this modeling assumption.

SAP2000 expects moment hinges to be input using non-dimensional moment rotation curves where the bending moment defining arrival at full plastification of the cross-section corresponds to the plastic moment capacity of the cross-section. The interaction surface assumed in the present study utilizes nominal moment capacities that include limit states of lateral torsional buckling and yielding. In those cases where the nominal moment capacity is less than the plastic moment capacity of the cross-section the moment hinge used in SAP2000 incorporates a yield moment that is less than the plastic moment capacity. Figure 3.40 illustrates the moment hinges defined for the inelastic analysis of the three dimensional framework. Locations of these hinges are as illustrated in Figure 3.39.

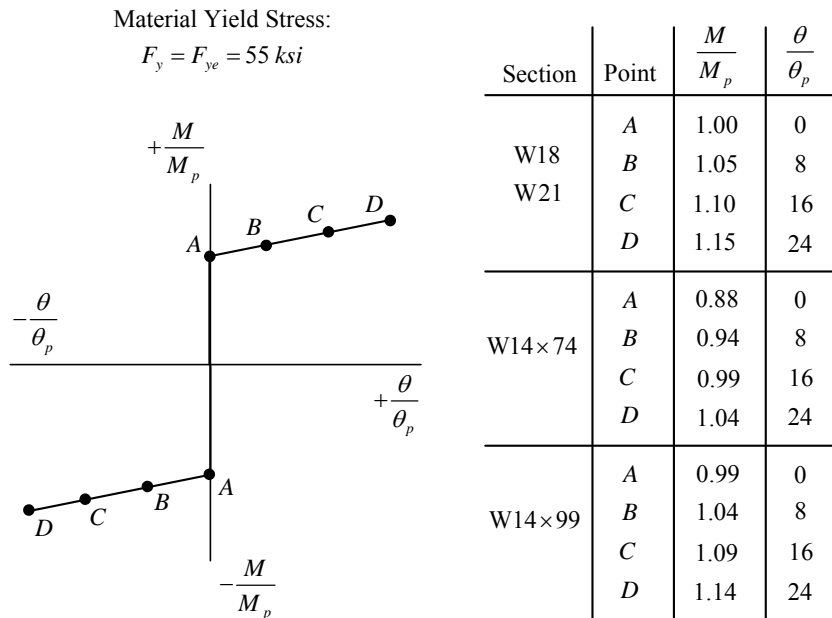


Figure 3.40 Moment Hinge Parameters Used for SAP2000 Frame Hinge Properties.

As indicated in the figure, the moment capacities of the W14x74 and W14x99 cross-sections are limited by flange local buckling. It is for this reason that the ratio M/M_p for the cross-section is less than 1.0. The moment hinges were defined using the expected yield stress of the material. Points B, C, and D are defined with a small amount of hardening to aid in convergence during the nonlinear solution.

The ratio of rotation to plastic moment rotation is used by SAP2000 to assign acceptance criteria for rotation in the hinges (CSI 2004). However, these demand measures were not used in the present analysis. Plastic rotation demand in the members of the framework was computed manually using data output during the analysis run. Therefore, these ratios were simply defined to make sure that no hinge would rotate beyond the point D.

The inelastic time-history analysis was carried out by starting with a model that was a modification of the elastic analysis model. The appropriate plastic hinges were attached to the members in the locations shown in Figure 3.39 and the time step increments during the Newmark solution were reduced to 0.001 seconds. The convergence tolerance was then relaxed slightly from the default values and the event tolerance parameter was set to 0.01. The same time history functions and column upward axial load magnitudes were used in the inelastic analysis. Since the elastic time history analysis (Figure 3.20) demonstrated nonlinear geometric effects were negligible a first-order materially nonlinear analysis was executed here. The system deformations seen in the inelastic analysis support this assumption.

A key to output is contained in Figure 3.41. This key was present in previous time history response graphs.

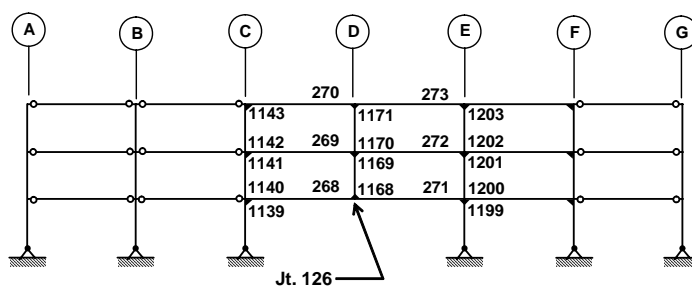


Figure 3.41 Frame Elevation Illustrating Key to Output Information for Nonlinear Material Analysis of the SAC 3-Story Framework.

A comparison of the elastic versus inelastic response of the frame is given in Figure 3.42. As one can see, the peak inelastic displacement is 50% greater than the elastic displacement.

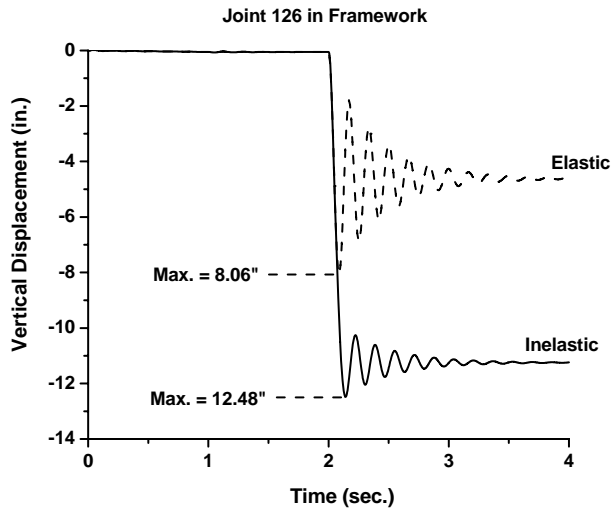


Figure 3.42 Elastic Versus Inelastic Response Comparison for Frame with Ineffective Column at First Floor and Location D-5.

The peak inelastic displacement of 12.5 inches is essentially 1.7% of the 60-foot span length in the compromised system. This is not large enough to activate geometric stiffness in the beam members or catenary action in this frame. Therefore, the use of geometrically linear analysis is justified.

The loading combination recommended in the GSA guidelines is multiplied by 2.0 to simulate dynamic loading effects in static analysis (GSA 2003). The results for the elastic analysis in Figure 3.42 appear to indicate that this is slightly conservative as suggested by others (Marchand and Alfawakhiri 2004). It should be noted that this factor should be evaluated for axial load, bending moment, and shear effects as well. The “permanent” displacement after the compromising event in the materially nonlinear analysis is roughly three times the static elastic displacement under the same loading.

The bending moment response history for three members coming together at the second floor at column line C is shown in Figure 3.43.

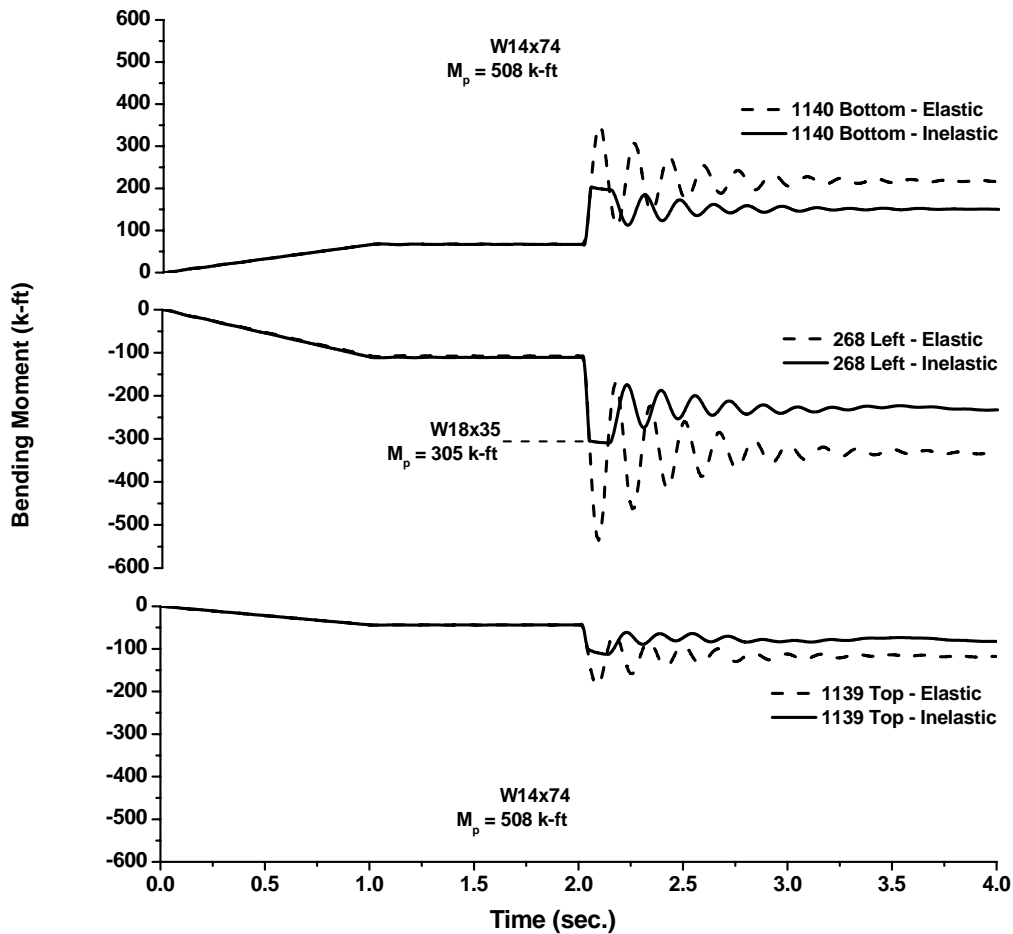


Figure 3.43 Bending Moment Time-History Response for Members Framing Together at the Second Floor Beam-to-Column Connection at Column Line C.

At shortly after two seconds into the response a plastic hinge forms in beam 268. The formation of this hinge serves to cap the bending moment that can be supported at its corresponding beam-to-column joint. As a result, the bending moments in adjacent columns are “capped” as well. Thus, the hinging in beam 268 serves to protect the columns framing into the common joint. This figure also illustrates that the bending moments in the all members are much lower when inelastic response characteristics are utilized and therefore, inelastic analysis techniques are likely the most accurate and least conservative approaches for structural integrity analysis. When elastic analysis is utilized, the forces present in the system are overestimated.

Bending moment time histories for the members framing into the column at line C at the third floor are shown in Figure 3.44.

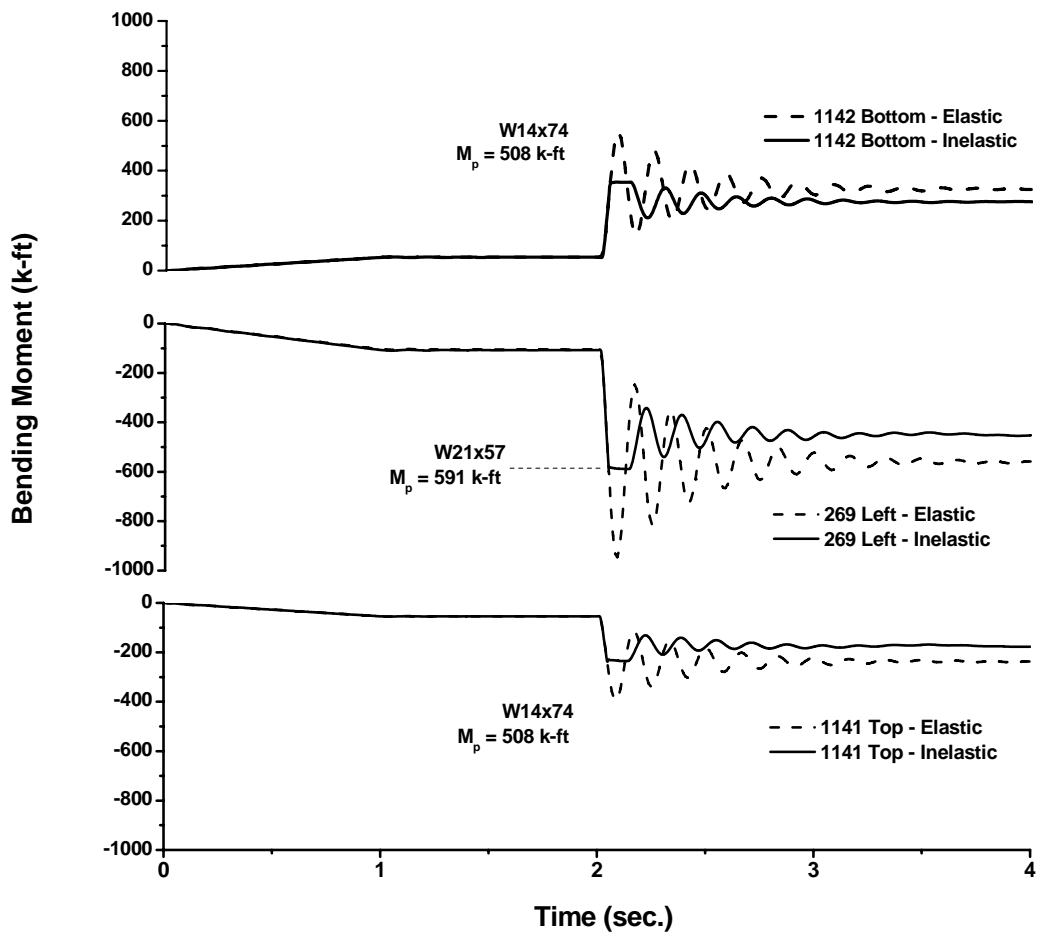


Figure 3.44 Bending Moment Time-History Response for Members Framing Together at the Third Floor Beam-to-Column Connection at Column Line C.

Similar behavior is seen in this case as well. The plastic hinge forms in member 269 and this again serves to limit the moment that is required of the column members framing into that joint.

The final comparison that will be made is with the joint at the roof level at column line C. Bending moment response histories for members 270 and 1143 are shown in Figure 3.45. In this case, the column forms the plastic hinge first and the demand in the adjacent beam is immediately capped to that moment magnitude to preserve equilibrium of the joint.

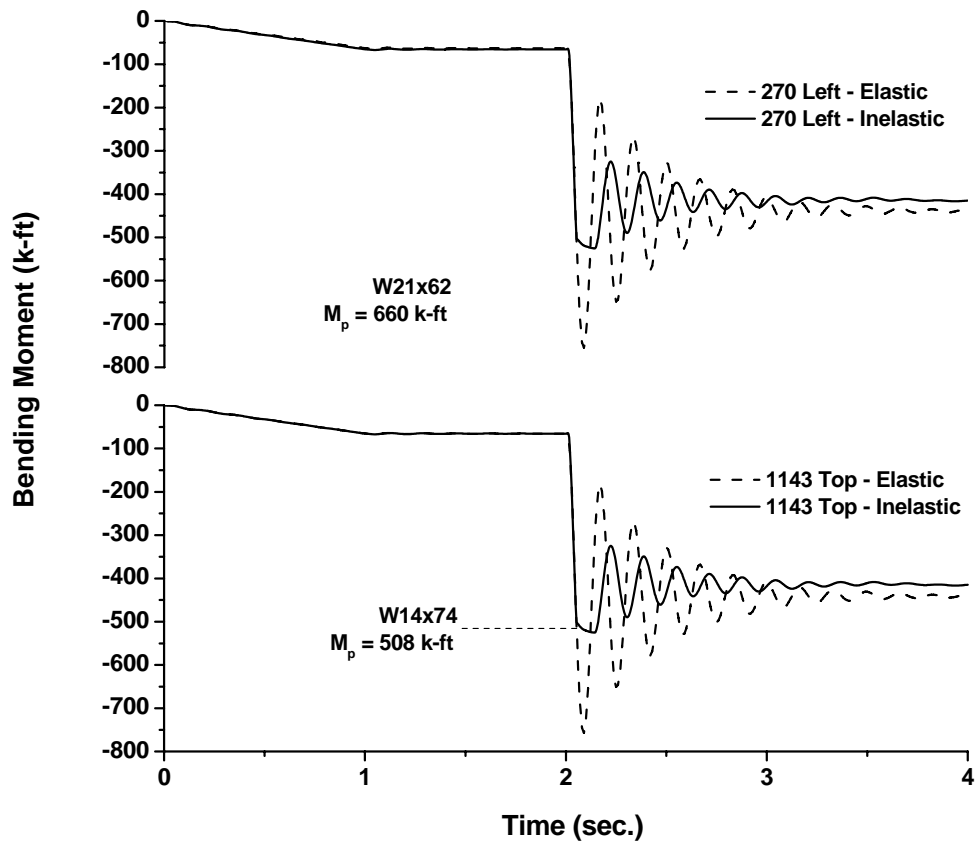


Figure 3.45 Bending Moment Time-History Response for Members Framing Together at the Roof Beam-to-Column Connection at Column Line C.

It is interesting to note that the elastic and inelastic response tend to dampen out to essentially the same static bending moment capacity as required by equilibrium and yielding is temporary.

The final aspect to the inelastic behavior that will be evaluated is the formation of hinges in the beam members and the bending moment time histories. The response histories for these members are given in Figures 3.46 through 3.48.

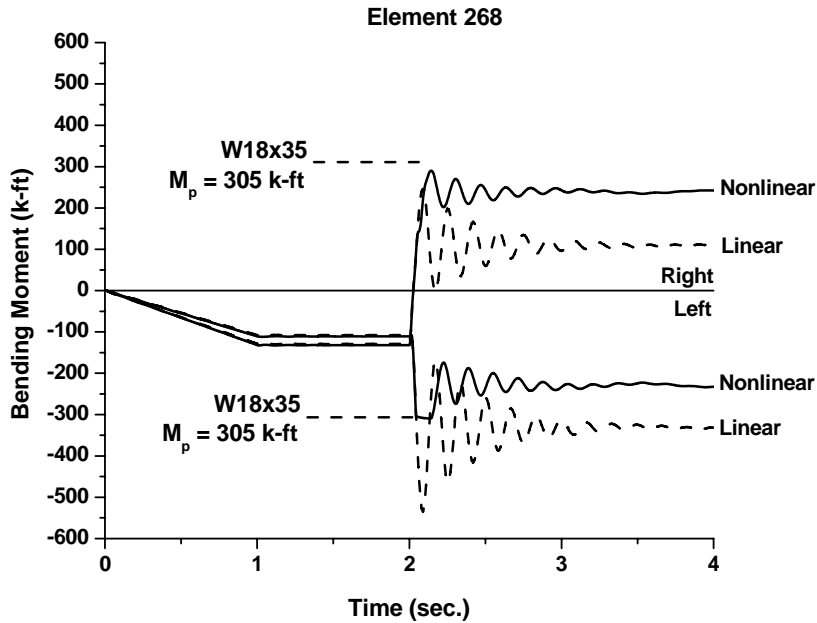


Figure 3.46 Bending Moment Time-History Response for Second Floor Beam (Element 268) Spanning from Column Line C to D.

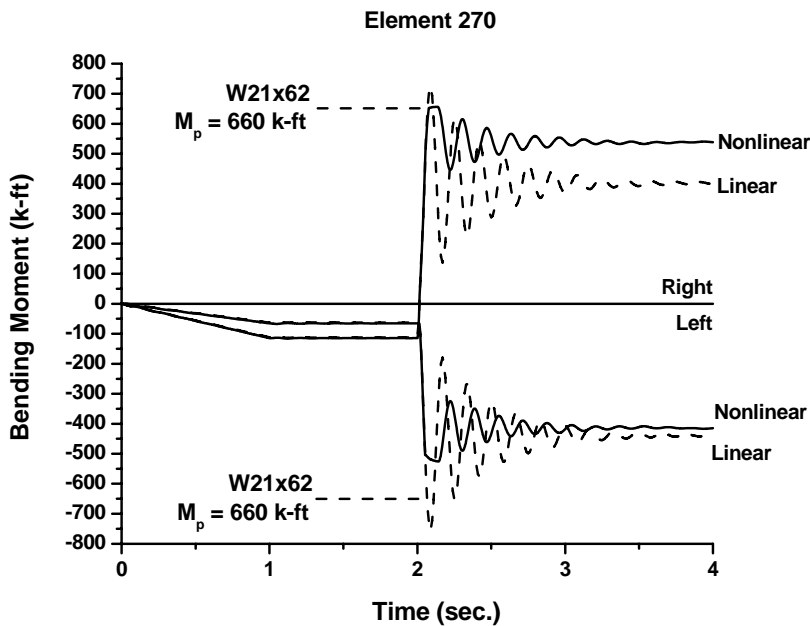


Figure 3.47 Bending Moment Time-History Response for Roof Beam (Element 270) Spanning from Column Line C to D.

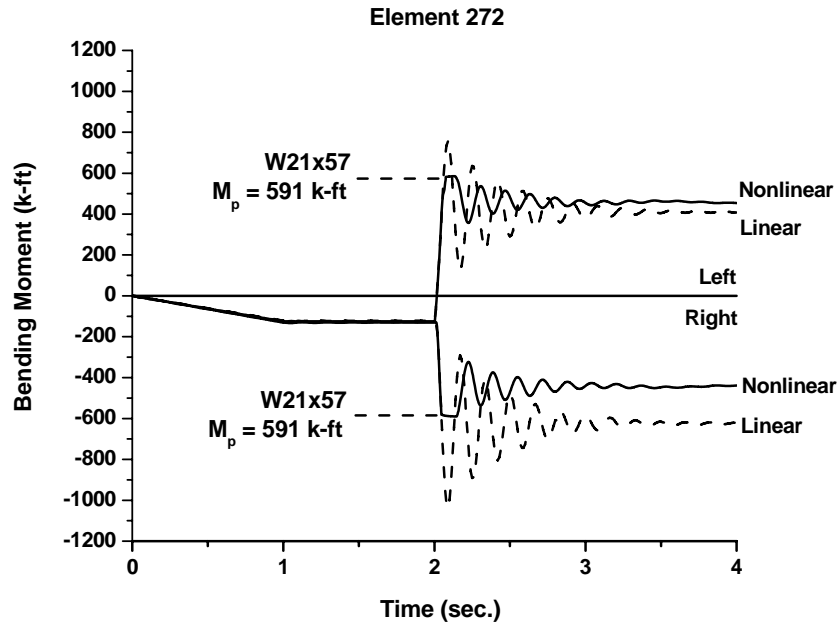


Figure 3.48 Bending Moment Time-History Response for Third Floor Beam (Element 272) Spanning from Column Line D to E.

The materially nonlinear response of the beam members in these figures illustrates the system's desire to equalize moments at both ends of the beam members at the plastic moment capacities. The deflected shapes shown in Figures 3.36 through 3.38 would lead one to the conclusion that the beams will form plastic moment hinges at both ends and catenary action will NOT develop until significant vertical deformation occurs (*e.g.* 15% of the beam spans or 9 feet). The 12.5" deflection at the location of the ineffective column should result in suspicion of catenary action. In fact, as shown by this framework, it is not needed to maintain structural integrity.

The response shown in Figures 3.45 through 3.48 also stresses the importance of designing connections for reversal of moment. Robustness in the structural steel framing system cannot easily be attained using unidirectional moment-resisting connections. It is recommended that all moment resisting connections be designed for equal moment magnitudes in positive and negative bending.

The symmetry in the inelastic response histories indicates that plastic hinges are forming at both ends of the beam members. Previous results related to the columns and the immediately preceding results related to the beams indicate plastic hinges will form in the members of the framing system after loss of column D5 at the first floor as shown in Figure 3.49. A collapse mechanism would have occurred if the final hinges formed at the right end of element 268 and the left end of element 271. Keep in mind that this frame was not

designed for compromising events, but simply reacts to a compromising event the best way it knows how (force redistribution). The fact that this framework did not collapse indicates that the steel structural system has a great deal of inherent resiliency and robustness even if seismic detailing is not utilized.

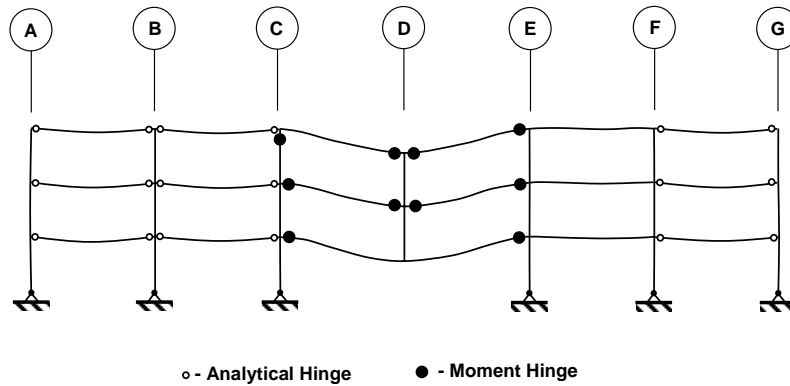


Figure 3.49 Moment Hinge Formation Computed During Response of Frame to Ineffective Column at the First Floor at Location D-5.

The demand to capacity ratios (defined previously) that result when plastic (moment) hinges are included in the analysis can now be evaluated. If a plastic moment hinge forms during the analysis M/M_n may exceed 1.0 because the hardening after point A on the moment hinge will cause the moment capacity to continue to climb. Thus, our analysis really is now limited to where do moment hinges form and how far past 1.0 do we go when hinges do indeed form. The only real unknowns once the moment hinges form are the axial and shear demands. Inelastic rotational demand after yielding is also very important and is evaluated.

The reader is once again referred to Figure 3.41 for the key to member response data. Time histories of axial load, shear, bending moment, and demand to capacity ratios are given for several members in the framework in Figures 3.50 through 3.54. These figures illustrate the expected result that the majority of the DCR is contributed by the bending moment demand. All DCR's for the members in these figures exceed the 1.0 limit. The worst violation is member 1143 shown in Figure 3.51, where the DCR is approximately 1.28. In general, the DCR's have reduced considerably when one compares them to those in Table 3.2. A summary of DCR's for all members in the moment-resisting framework are given in Table 3.3.

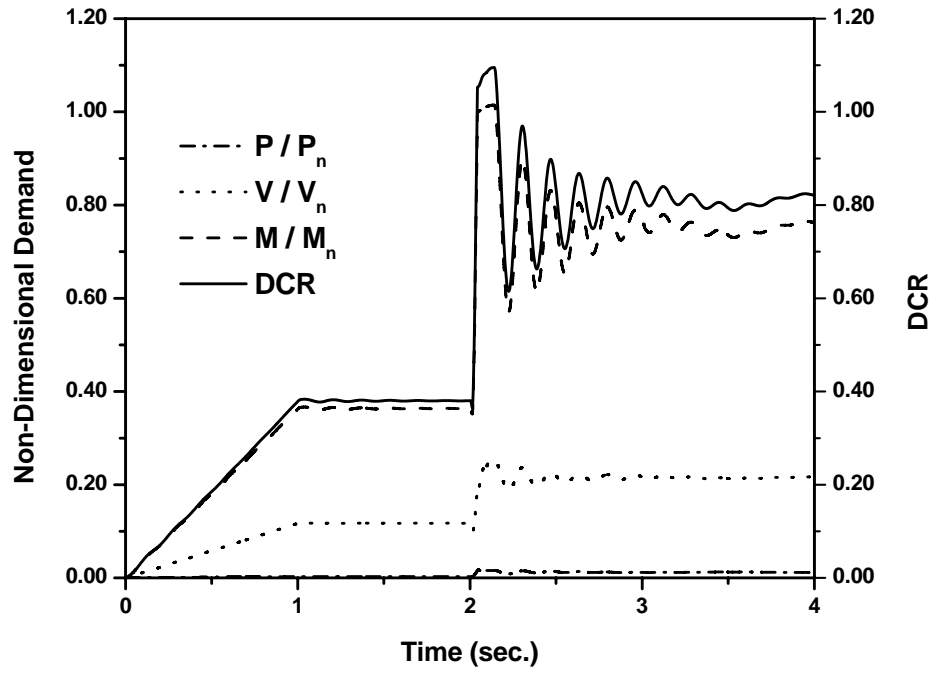


Figure 3.50 Non-Dimensional Force Demands and Demand-to-Capacity Ratio Time Histories for Element 268 at the Left End (Column Line C).

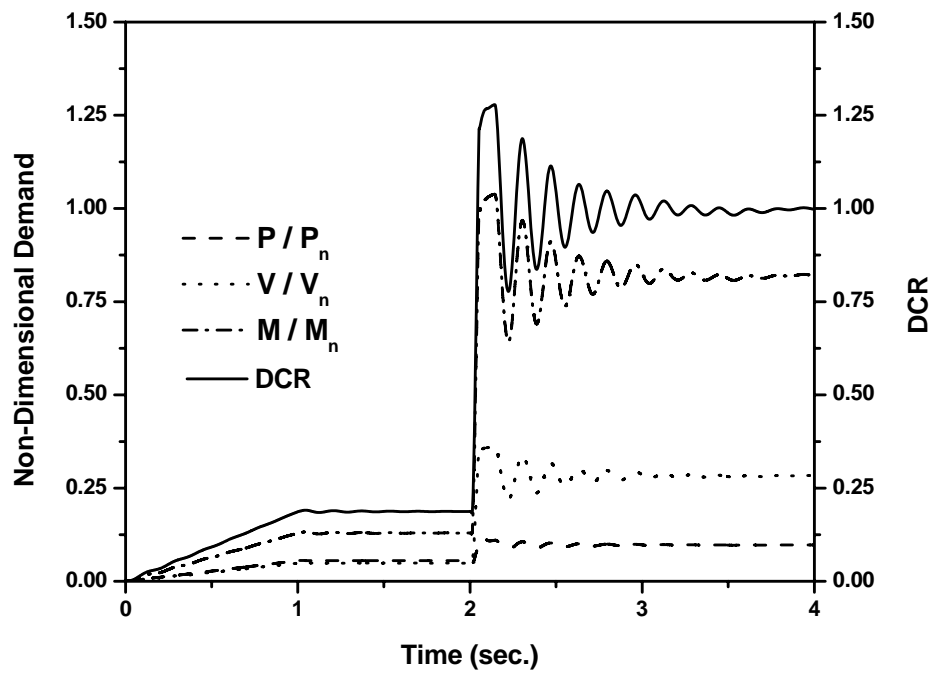


Figure 3.51 Non-Dimensional Force Demands and Demand-to-Capacity Ratio Time Histories for Element 1143 at the Top (Roof Level).

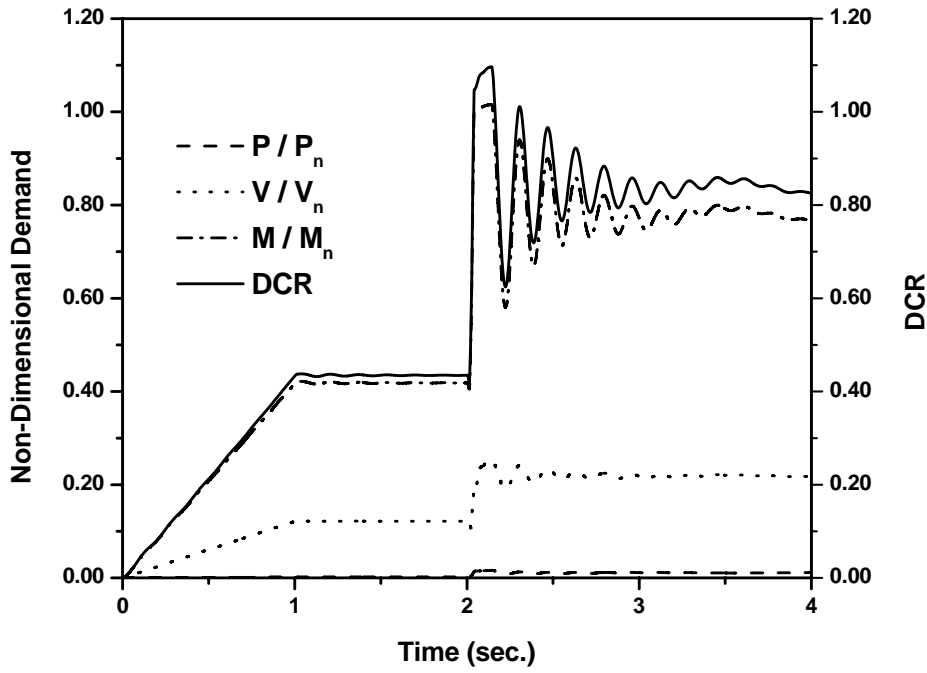


Figure 3.52 Non-Dimensional Force Demands and Demand-to-Capacity Ratio Time Histories for Element 271 at the Right End (Column Line E).

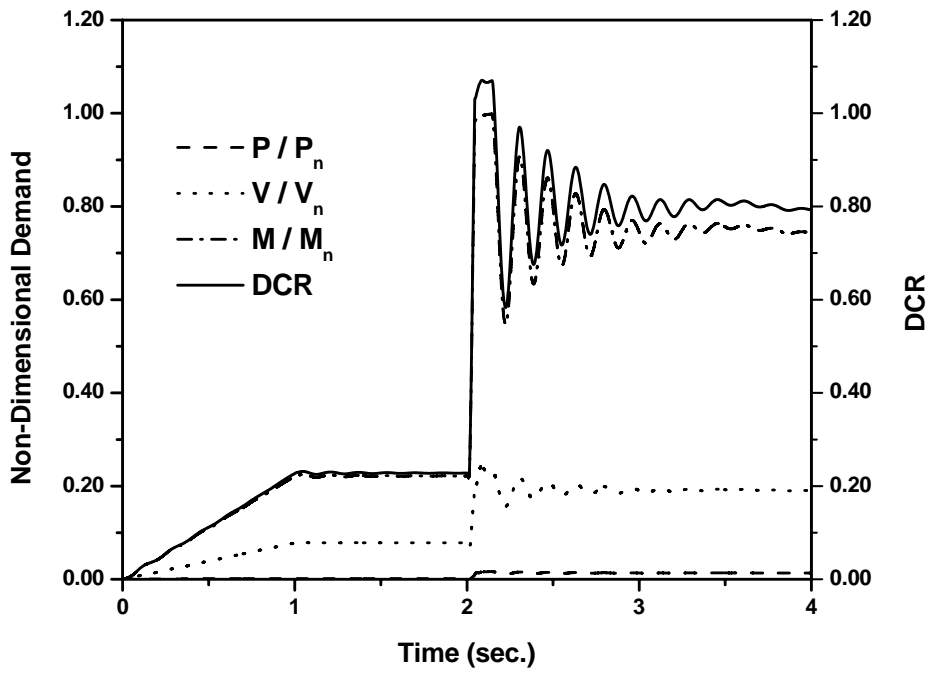


Figure 3.53 Non-Dimensional Force Demands and Demand-to-Capacity Ratio Time Histories for Element 272 at the Right End (Column Line E).

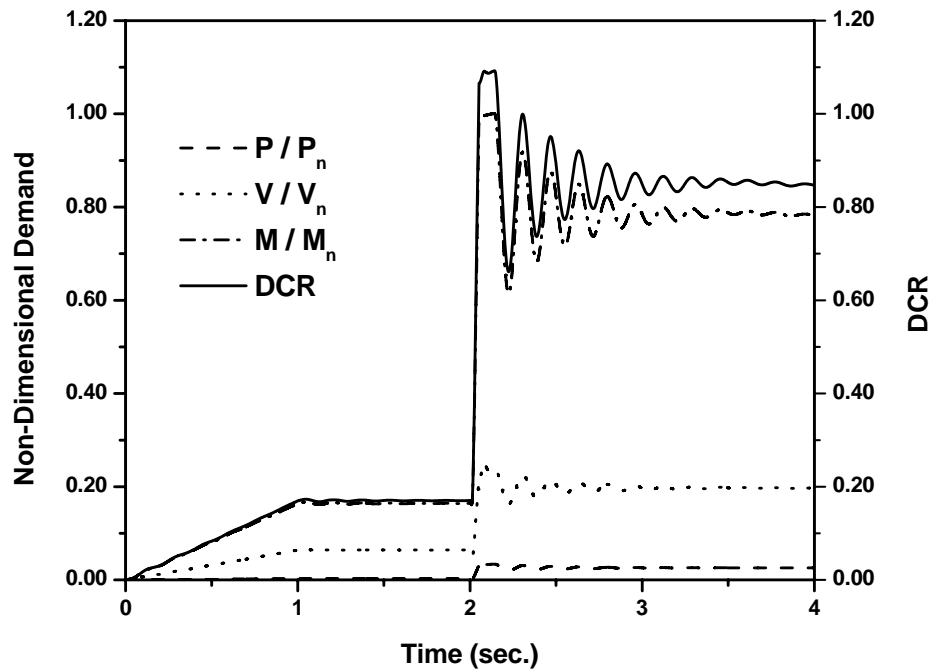


Figure 3.54 Non-Dimensional Force Demands and Demand-to-Capacity Ratio Time Histories for Element 273 at the Right End (Column Line E).

The majority of members within the framework now have DCR's less than 1.10. The exception is member 1143. The beam immediately to the left of the beam-to-column joint at column line C does not have a moment resisting connection (it is analytically pinned). Furthermore, the bending moment capacity of beam 270 exceeds that of 1143 by a wide margin. As a result, member 1143 has to take the brunt of the bending moment demand caused by the ineffective column on its own. A similar situation with better result occurs at column line E at the connection of members 273 and 1203. In this instance, the beam immediately to the right of 1203 (column line E) has a fully-restrained (rigid) connection. As a result, as moment demand is sent to the connection through beam 273, column 1203 has the help of an adjacent beam in accommodating that demand. As a result, the DCR for 1203 is only 0.647. Therefore, if one were to take anything away from the inelastic analysis carried out here, it is the importance of providing some moment restraint at all beam-to-column connections in an area where ineffective members may occur. Since the friction-free pin connections assumed in the present analytical model do not exist in real structures, the magnitude of this moment capacity needed to even out demands is worthy of further study.

A comparison of the data in Tables 3.2 and 3.3 illustrates that the inelastic analysis has adjusted many of the member DCR's downward. Some of these reductions due to redistribution of forces within the system were significant (*e.g.* member 268, 269, 272). It should also be noted that in some instances the left and right

sides of the members sought to balance demand and the DCR at one end went down while the DCR at the other end went up. This is the natural way the structural system wants to perform and an elastic analysis prevents (hides) this behavior. As a result, elastic analysis can give misleading results when attempting to define the inherent robustness in a structural system.

Table 3.3 Peak Non-Dimensional Member Demands and Demand-to-Capacity Ratios for Inelastic Response to Ineffective Column at Location D-5.

Member (1)	$\frac{P}{P_n}$ (2)	$\frac{V}{V_n}$		$\frac{M}{M_n}$		$DCR = \frac{P}{P_n} + \left[\left(\frac{V}{V_n} \right)^2 + \frac{M}{M_n} \right]$		
		Left/Bot. (3)	Right/Top (4)	Left/Bot. (5)	Right/Top (6)	Left/Bot. (7)	Right/Top (8)	
B E A M S	268	0.018	0.255	0.126	1.014	0.950	1.095	0.967
	271	0.016	0.121	0.256	0.959	1.015	0.976	1.097
	269	0.019	0.244	0.082	0.997	0.990	1.071	1.012
	272	0.017	0.077	0.245	0.990	0.998	1.011	1.071
	270	0.037	0.231	0.080	0.796	0.994	0.882	1.037
	273	0.034	0.103	0.251	0.997	1.000	1.039	1.092
C O L U M N S	1139	0.336	-	0.046	-	0.223	-	0.558
	1140	0.240	0.182	-	0.403	-	0.665	-
	1141	0.240	-	0.181	-	0.470	-	0.605
	1142	0.113	0.361	-	0.701	-	0.942	-
	1143	0.113	-	0.361	-	1.038	-	1.278
	1168	0.133	-	-	-	-	0.133	-
	1170	0.038	-	-	-	-	0.038	-
	1199	0.227	-	0.020	-	0.067	-	0.285
	1200	0.166	0.102	-	0.158	-	0.328	-
	1201	0.166	-	0.101	-	0.196	-	0.358
	1202	0.083	0.253	-	0.347	-	0.491	-
	1203	0.083	-	0.253	-	0.503	-	0.647

One observation can be used to justify that the framework considered has sufficient structural integrity and robustness to allow an ineffective column without disproportionate collapse for the loading magnitude and compromising event considered. When the plastic hinge was defined in SAP2000, there was hardening employed to aid in preventing convergence failures due to numerical instabilities. This in effect allowed the moment capacity to exceed the true plastic moment capacity and in the instance of member 1143, the DCR would have likely been closer to 1.0 than the 1.278 exhibited. For example, if one considered the

demands and DCR's in Table 3.2 and 3.3, one would see that as the moment in the column is capped, moments and forces are required to redistribute. The initial redistribution from the elastic to inelastic analysis saw the DCR go from 1.856 to 1.278. The moment demand for this member went from 1.498 in the elastic analysis case to 1.038 in the inelastic analysis. The axial load and shear demands also reduced when the moment capacity in this member was limited by hinge formation. Thus, it is reasonable to expect that if the hardening in the hinge were not present, the DCR for this member would reduce from the 1.278 value shown. The magnitude of this reduction was not evaluated; however, a reduction to 1.20 is not unrealistic. The friction-free pin beam-to-column connection in the beam immediately to the left of column 1143 is also not reflective of reality. If this connection had a moment capacity equal to 10% of the column's plastic moment capacity (a likely scenario for typical clip angle connections), then the DCR for element 1143 would be reduced. Therefore, this element was assumed to be adequate to support the demands imposed.

As a result, the demand to capacity ratios seen in the inelastic analysis leads one to believe that for the compromising event considered (*i.e.* ineffective column D5 at the first floor), no additional structural engineering need be done to prevent disproportionate collapse. It is also likely that the slab and orthogonal framing will contribute to carrying the load after losing this column and that has been omitted in the present analysis.

One additional item of importance in the assessment of the frame's ability to compensate for an ineffective column and prevent disproportionate collapse is the plastic rotation demands that are placed on the connections at the ends of the beams. The plastic rotations at the ends of the beams were computed using the displacement results taken from the inelastic time history analysis. A schematic describing what was done is given in Figure 3.55.

First the displacements at the ends of all beams were recorded. The difference between the vertical displacement at column lines C and D; and D and E; were then computed at all time steps in the analysis. These displacement differences establish the chord angle, θ , at each step in the analysis. The bending moment demand data was then examined to determine the time instant, t_e , and chord rotation when M/M_n first exceeded 1.0. The data was again examined to determine a second time instant, $t_{p,peak}$, when the peak chord rotation occurred after this initial attainment of the plastic moment capacity. Unloading of a hinge was not considered in the definition of plastic rotation. These two chord rotations were then used to define peak plastic rotations. The chord angles corresponding to these times were then located. These chord angles were used to define the plastic rotation as follows,

$$\theta_p = \theta(t_{p,peak}) - \theta(t_e) \quad (3.9)$$

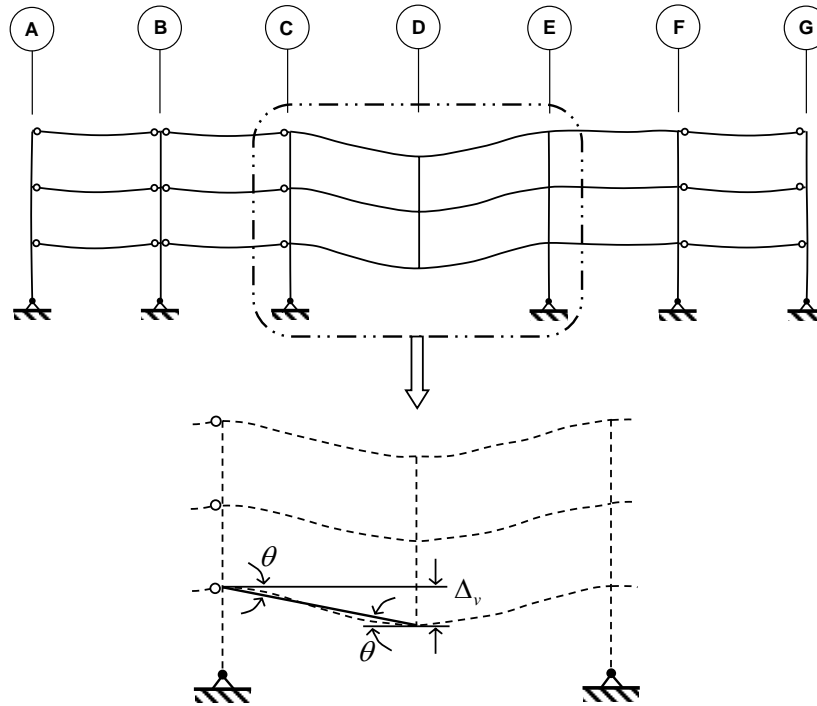


Figure 3.55 Illustration of Beam Member Angle Generated During Time History Response.

The displacement and moment demand data indicated plastic rotation demands that were fairly consistent across all members. In the beams, the plastic rotation demands were on the order of 0.022 radians. If the plastic rotation at the top of member 1143 is assumed to provide all rotation at the joint facilitating vertical movement of column line D, then the plastic rotation in this member is on the order of 0.016 radians. There is no reason to believe that a properly detailed fully-restrained connection cannot support a plastic demand of 0.022 radians (FEMA 2000c; FEMA 2000d; FEMA 2000b). It is also expected that a plastic hinge forming in the W14x74 member can also sustain 0.016 radians of plastic rotation prior to significant moment capacity degradation. The time history analysis indicated that the plastic capacity of the cross-section was temporarily reached and inelastic re-loading did not occur.

The plastic rotations computed indicate that the column member (*i.e.* member 1143) will likely have a ductility demand of approximately 1.9 if all rotation after initial yield is provided by the top of this column at column line E. This is less than the ductility ratio assumed for compact shapes in non-seismic design and therefore premature fracture or local buckling is not expected (omitting localized concentrations of stress and strain in the connections).

The axial peak demand-to-capacity ratios found during the response for the beam members found in Table 3.3 give an indication of the peak tying and compression forces that will form in the framing system when the interior column is compromised. The peak tying forces are approximately 3.7% of the axial tension yield load of the beam member. These are found in the rows corresponding to members 270 and 273. Beam-to-column connections were also subjected to peak compression demands equal to approximately 1.9% of the axial compression capacity of the beam member. The compression demands are found in the rows corresponding to members 268, 271, 269, and 272. It is expected that these tension and compression demands on the connections will vary with the ability for Vierendeel action to form within the structural system. In the present building, Vierendeel action is limited when compared to the 10-story and 20-story frames subsequently considered. Thus, of the three frames considered in this present study, the tying forces and compression forces applied to the beam-to-column connections are expected to be the most severe in the present frame.

3.5 Concluding Remarks and Recommendations

The elastic and inelastic analysis conducted on the SAC 3-story building frame allows several conclusions to be drawn and recommendations to be made. The first is that robustness and inherent structural integrity cannot be easily guaranteed if unidirectional moment connections are utilized. All connections intended to be moment resisting within a framework should be designed assuming complete reversal is possible. End plate connections with bolt arrangements that are unsymmetrical about the beams axis of bending should not be allowed unless structural integrity of the framing system with these connection types can be demonstrated.

A comparison of elastic and inelastic analysis results for the framework demonstrates that elastic time history analysis can lead to moment, shear, and axial load demands that differ considerably from inelastic analysis. The demand-to-capacity ratio defined for the present study is also significantly different when these two approaches are utilized. One can certainly argue that this is expected.

The plastic rotation demands within the system considered indicate that there is no reason to believe that a moment resisting connection detailed to the latest steel design specifications cannot support a plastic rotation demand of 0.022 radians with only one cyclic excursion to that magnitude. The plastic rotation demand in a column member within the framework was 0.016 radians. This rotational demand indicated a ductility multiplier of 1.9, which is much less than the 3.0 limit assumed when defining compact shapes. It is believed that the W14x74 member can sustain a ductility demand ratio of 2.0 without issue. As a result, connection ductility will not limit the robustness or inherent structural integrity in the framing system analyzed.

It is recommended that moment resisting connections be used across all columns at the perimeter of the framework. The response of column 1143 in the inelastic analysis indicates that one simply needs to provide moment capacity in the connection to the left of column line C and the demand on 1143 will be alleviated as indicated by behavior of column 1203 at column line E. The magnitude of this moment may only need to be a fraction of the moment capacity of the adjacent column. This connection moment capacity can then help to alleviate demand on 1143 such that the DCR returns to levels close to 1.0 or lower. The magnitude of this moment required and the contribution of orthogonal framing moment capacities should be quantified. It is thought that partial-stiffness and partial-strength connections at the perimeter may be a very desirable scenario rather than flexible connections. In other words, more realistic estimates for flexible beam connections (traditionally modeled as friction-free pins) and orthogonal framing can be very important to fully understanding general structural integrity.

The strain rates that arose in the members of the framework considered with column death of 0.01 second duration indicates that intermediate strain rates are being seen and a reduction in fracture toughness of the steel material need not be considered when evaluating inherent structural integrity and robustness. It should be noted, however, that geometric considerations (stress raisers) in the connections were not considered in the present study.

The analysis conducted on this framework was limited to consideration of very few column members becoming ineffective. Most notably missing from the evaluation were columns at which one or both beams have pinned beam connections at the column. These columns are located at B, C, and F along columns lines 1 and 5; and at 2 along column lines A and G. The corner columns and intermediate columns are also notable missing from evaluation. The analytical model that includes pin connections will not support removal of these columns as a failure mechanism forms, or the pin connections lead to a mechanism right from the beginning. Therefore, these situations require special consideration. It is likely that the moment resisting beam connections should be distributed throughout the perimeter of the framing system. In this manner, it is expected that the moment resisting connections at the beam to column connections will help to establish structural integrity. Orthogonal moment resisting frames dispersed throughout the framing plan will also foster robustness and structural integrity in the event that both interior and exterior columns are ineffective.

The inelastic analysis conducted indicated that beam-to-column connections would likely be subjected to axial force demands that were less than 5% of the axial tension or axial compression capacity of the beam members. Therefore, it would be conservative to design the connections for axial demands equal to 5% of the beam cross-section's tensile capacity and assume that this force (tension or compression) acts

simultaneously with the beam's plastic moment capacity. Designing for this additional *tying force* (in the case of tension) would enhance the robustness of the steel framing system.

It may be prudent to relate this tying force to the gravity loading applied at the floor level where the tying member exists (in this case, an exterior girder). A tie force can be estimated using procedures (DOD 2005) reviewed in Chapter 2 of this report. For example, for an interior tie element, the required tie force is computed using,

$$F_t = 0.50 \cdot [GRAV] \cdot (s_t \cdot L_s)$$

If an exterior tie element is considered, the required tie force is computed using,

$$F_t = 0.25 \cdot [GRAV] \cdot (s_t \cdot L_s)$$

The gravity loading, $GRAV$ (psf), is taken as $1.2D + 1.6L$; s_t is the spacing between ties; and L_s is the beam or girder span. The interior tie force computed must be at least 16.9 kips, and the exterior tie force must be at least 8.4 kips.

In the 3-story framework considered, slight modifications need to be made because a specific tie member arrangement is not generated *a-priori*. However, if one looks at the previous tie force equations, the tie force is a fraction of the gravity loading applied. The axial demands contained in Table 3.3 can be restated as axial forces shown in Table 3.4.

Table 3.4 Peak Axial Tie Forces Computed in Beams Using Inelastic Analysis (T – tension; C – compression).

Member (1)	P (kips) (2)	
B E A M S	268	10.0 (T)
	271	9.2 (T)
	269	17.5 (T)
	272	15.3 (T)
	270	33.5 (C)
	273	30.9 (C)

The peak tension forces occur in the floor beams immediately above those adjacent to the compromised floor level. The maximum tension force is 17.5 kips. It should be noted that compression force will likely be carried by the floor slab and beam in a symbiotic manner.

The gravity loading applied to girder A at this level is a combination of 83-psf superimposed dead loading; mean point-in-time sustained live loading ($0.25 \cdot 50 = 12.5 \text{ psf}$); and 25-psf cladding loading. If these loads are converted to uniformly distributed loading along column lines 1 and 5, we have;

$$w_D = 83 \text{ psf} \cdot 30 \text{ ft} \cdot 0.5 = 1,245 \text{ plf}$$

$$w_L = 12.5 \text{ psf} \cdot 30 \text{ ft} \cdot 0.5 = 187 \text{ plf}$$

$$w_{clad} = 25 \text{ psf} \cdot 13 \text{ ft} = 325 \text{ plf}$$

The total uniformly distributed loading on the girder is $1,757 \text{ plf} = 1.78 \text{ klf}$. The total loading applied to the girder spanning between column lines is therefore, $1.78 \text{ klf} \cdot 30 \text{ ft} = 52.7 \text{ kips}$.

The peak tension force (or tying force) in the girders of the 3-story framework considered is 33% of the total gravity loading applied to the girder considered. A tie force expression analogous to those in the UFC criteria can therefore be generated,

$$F_t = 0.33 \cdot [GRAV] \tag{3.10}$$

where *GRAV* is the total gravity loading applied to the tie member (girder in this case).

The ability for the framework to form Vierendeel action across the ineffective column was made possible by having multiple stories above the compromised framing system. If a column in one of the upper stories becomes ineffective, this bridging action may not be possible and catenary action in the system will be required. This topic is investigated in the section of the report devoted to catenary action in the slab system.

The results of the inelastic time history analysis also indicated that columns were not subjected to tensile loading demand of any appreciable amount. As long as the floor framing members in the system remain active contributors to the resistance of vertical movement in the system, column splices are likely not needed to be designed for tensile (hanging) forces. The axial force demands seen in Table 3.3 for members 1168 and 1170 do indicate that the compression demands do get quite low (*e.g.* 3.8% of the nominal capacity). Since tensile forces were not seen in any columns in the present analysis, it is difficult to recommend any minimum splice force magnitudes to elicit enhanced robustness in the system.

Chapter 4

Ten-Story SAC Frame

4.1 Introduction and Building Description

As with the three-story building, the SAC-FEMA suite of buildings (FEMA 2000d) was again selected for base building topologies. These buildings were designed using a variety of assumptions regarding location, loading, and topology. The pre-Northridge configurations located in Boston were again chosen. The present chapter of the report will focus on the analysis of the ten-story building.

The building consists of structural steel wide-flange shapes with lower-bound yield stress equal to 50 ksi typical of A992. Moment resisting frames (MRF's) are located on the perimeter of the building and all bays are part of the MRF system. The typical framing plan for the structure is shown in Figure 4.1.

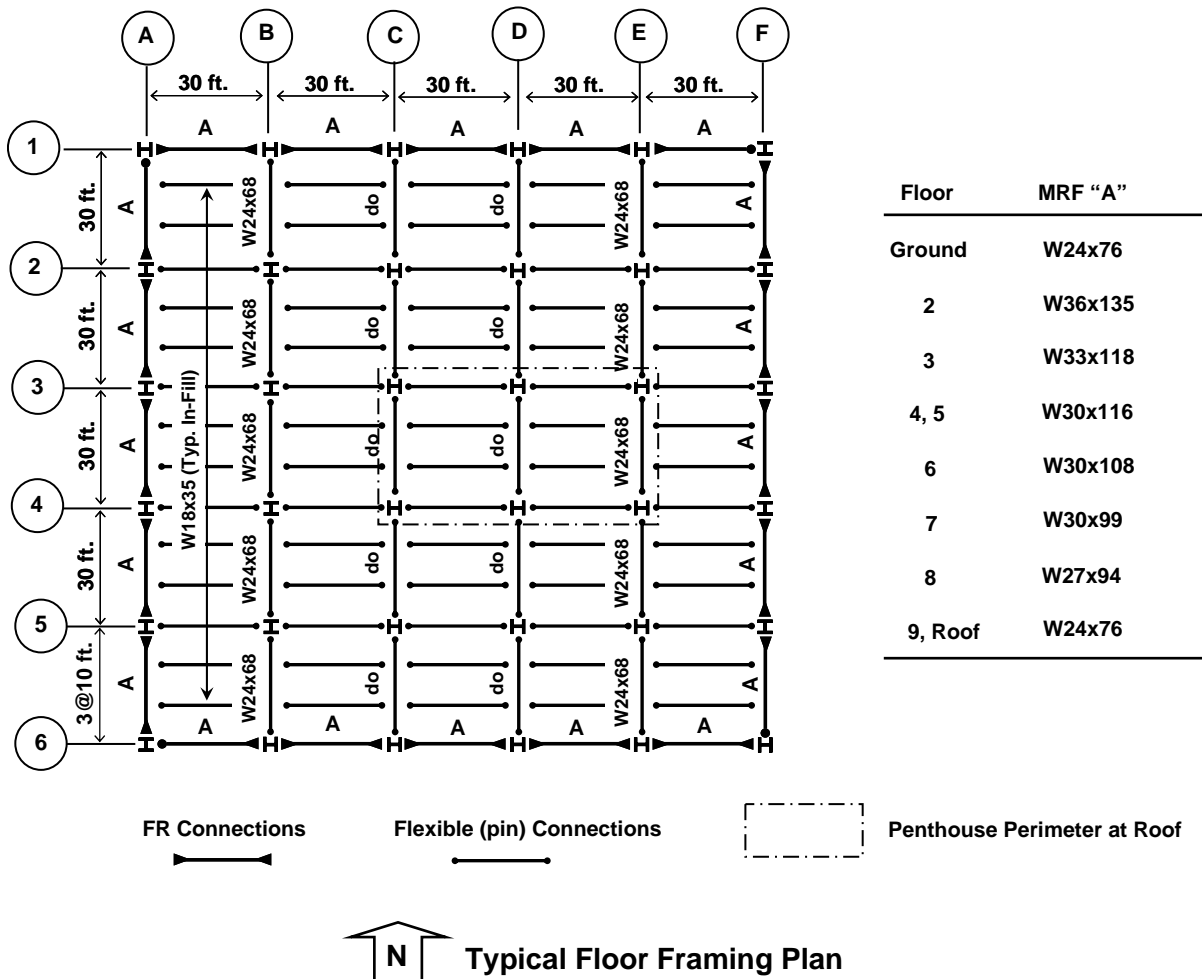


Figure 4.1 Framing Plan Used for SAC 10-Story Modified Boston Building Frame.

All members in the frame consisted of wide-flange shapes. Interior beams and girders were all assumed to be connected using *flexible* connections of negligible moment capacity and stiffness. These connections are indicated using solid circles at the beam ends. The moment-resisting (rigid or fully-restrained) connections at the ends of the beams in the MRF's are indicated by solid triangles at the beam ends. The typical MRF in the building system consists of five bay, ten story frame with a pin at one end of the frame. The beams within the MRF's vary with location and the small table to the right of the framing plan in Figure 4.1 provides wide-flange shape sizes for these members. Column orientations are also indicated in the framing plan. A penthouse was located at the roof level and its location is indicated in Figure 4.1.

A column schedule indicating member sizes is given in Figure 4.2. The height of the building and changing of column shapes requiring splices in the columns is indicated.

	A-1, A-6; F-1, F-6	A-2, A-3, A-4, A-5; B-2, B-6; C-1, C-6; D-1, D-6; E-1, E-6; F-2, F-3, F-4, F-5	B-2, B-3, B-4, B-5; C-2, C-5; D-2, D-5; E-2, E-5	C-3, C-4; E-3, E-4	D-3, D-4
Roof EL. +39'-0"	W14x61	W14x120	W8x48	W12x53	W12x58
9 th Floor EL. +26'-0"					
8 th Floor EL. +26'-0"	W14x90	W14x176	W12x65	W12x79	W12x79
7 th Floor EL. +26'-0"					
6 th Floor EL. +26'-0"	W14x132	W14x211	W12x96	W14x99	W12x106
5 th Floor EL. +26'-0"					
4 th Floor EL. +26'-0"	W14x159	W14x233	W12x120	W12x120	W14x132
3 rd Floor EL. +26'-0"					
2 nd Floor EL. +13'-0"			W14x145	W14x145	W14x159
Ground Floor EL. 0'-0"					
Top/Ftg. EL. -13'-0"	W14x211	W14x283	W14x176	W14x176	W14x176

Figure 4.2 Column Schedule for SAC 10-Story Boston Modified Boston Building Frame.

The configuration of the moment resisting frames is illustrated in Figures 4.3. The bases of all columns in the system are taken to be pinned (friction-free) and flexibly-connected beam members have their connections indicated with hollow circles. These connections were assumed to be friction-free pins in relation to bending about the member's major axis, but were considered fully-restrained or rigid with regard to bending about the member's minor and longitudinal axes (torsion) reflecting the presence of the concrete floor slab and positive attachment to the girders and beams. Moment-resisting (fully-restrained or rigid) connections are indicated with filled-in triangles. The first floor was considered to be below grade and the ground floor nodes were taken to be pinned around the perimeter. A roller condition is indicated, but strict modeling (*i.e.* allowance of the structure to separate from the surrounding soil) would have required compression-only (non-linear) elements and it was decided that bi-directional restraint would not sacrifice modeling accuracy. Centerline to centerline dimensions are used for floor-to-floor heights. No rigid offsets or flexible panel zones were considered in the modeling.

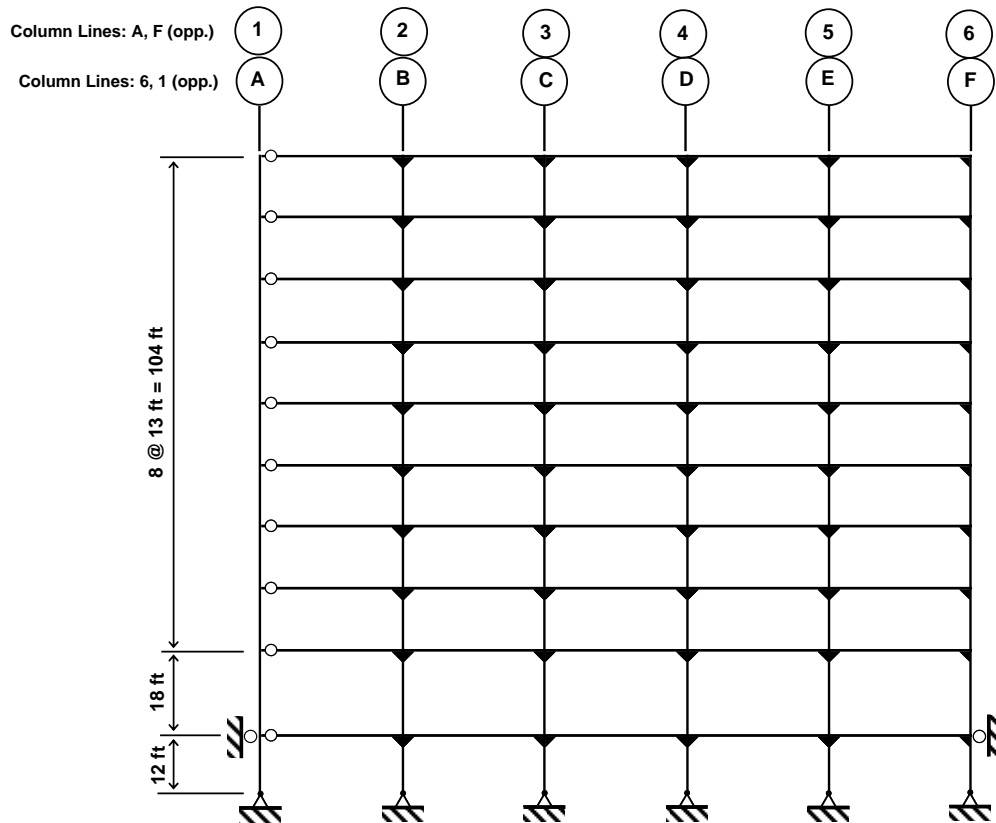


Figure 4.3 Framework Elevation Along Column Lines 1 and 5 or A and F Looking North.

The same loading as the three story building described in chapter 3 (see Table 3.1) was used for the ten story building with the self weight of the members calculated by computer software.

A three-dimensional structural model was developed for the 10-story building considered. The 3D nature of the model was needed in case orthogonal tying members were needed in the framing system. A schematic of the initial 3D model (without diagonal diaphragm bracing) is shown in Figure 4.4. The SAP2000 analysis program was used (CSI 2004).

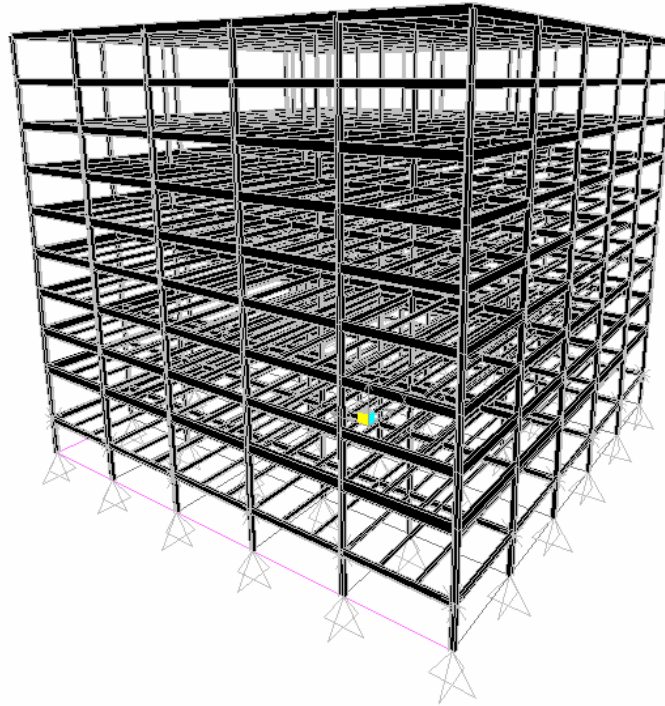


Figure 4.4 Extruded View Illustrating Basic SAP2000 Model of Uncompromised SAC 10-Story Modified Boston Framework Without Diaphragm X-Bracing.

4.2 Critical Load Analysis and Diaphragm Modeling

In order to assess the need for nonlinear geometric analysis, the elastic critical loads for the frame were determined using eigenvalue analysis. The first two critical buckling modes were evaluated for the 3D framing model developed. A factored loading combination, $1.2w_D + 1.6w_L$, consistent with LRFD was used. The critical load factors (applied load ratios) are therefore, applied to this loading combination as follows,

$$\gamma_{cr} (1.2w_D + 1.6w_L)$$

The critical buckling mode shapes for this loading combination are giving in Figure 4.5 and 4.6.

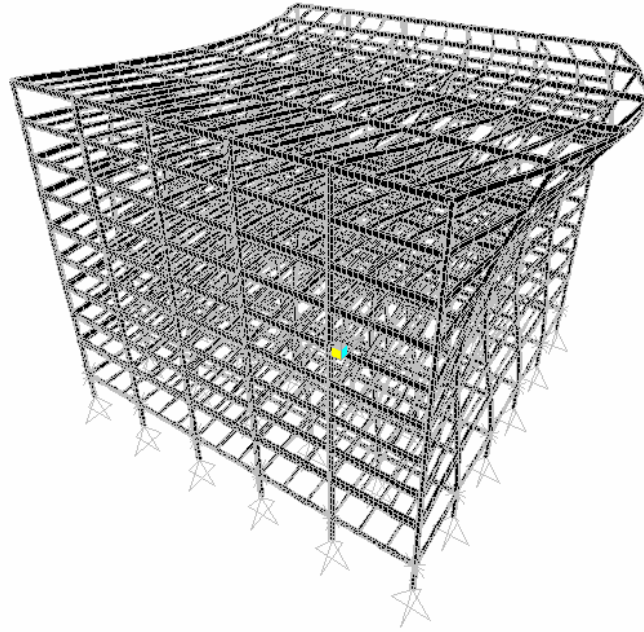


Figure 4.5 SAP2000 Displaced Shape Plot Illustrating Buckling Mode Shape Corresponding to the First Buckling Mode: $(\gamma_{cr})_1 = 0.413$.

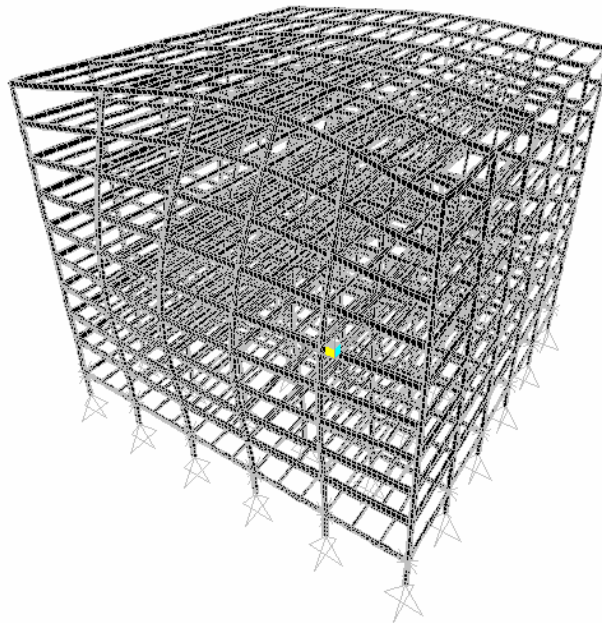


Figure 4.6: SAP2000 Displaced Shape Plot Illustrating Buckling Mode Shape Corresponding to the Second Buckling Mode: $(\gamma_{cr})_1 = 0.582$.

The flexibly-connected infill framing results in buckling modes of very low magnitude similar to the three story building. The critical load factors shown in Figures 4.5 and 4.6 are below 1.0. The lack of a “rigid” diaphragm in the system at the floor levels causes buckling modes that are not consistent with reality. As a result, the diaphragm action in the framing system required modeling as was done in the 3-story building analysis. An x-braced system of weightless diaphragm members developed previously for the 3-story building is again used to simulate the effect of the floor system in the structural analysis. The orientation of the diagonal members within the framing plan at the two floor and roof levels are shown in Figure 4.7.

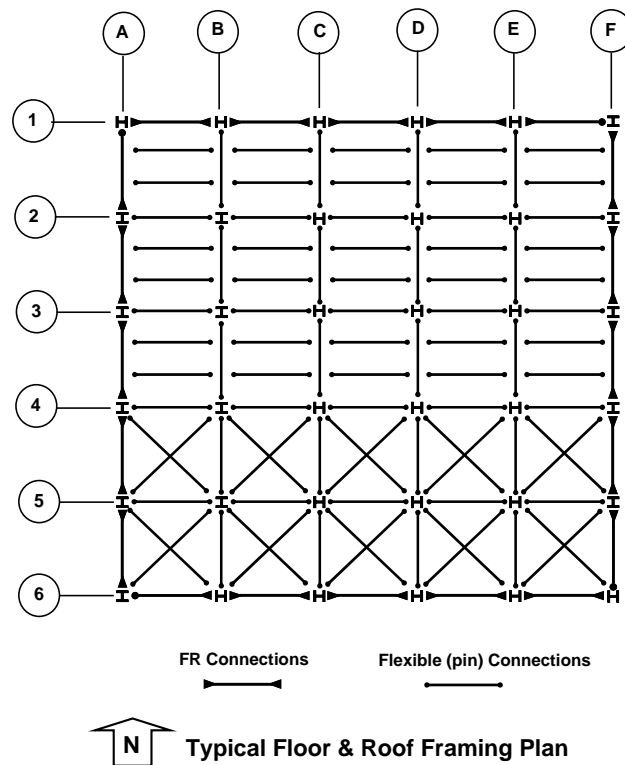


Figure 4.7 Schematic Illustrating Locations for Diaphragm X-Bracing within Framework.

Figure 4.7 does not show all x-bracing members to prevent clutter. Similarly to the three story building, the W14x159 x-bracing members simply pass through all infill framing members without connectivity. The x-brace diaphragm members are only connected at the columns that lie on the boundary of the panel. As mentioned previously, they are considered to have zero mass and contribute only stiffness in the analysis. The members are connected to the columns using friction-free pins and the moment release is only about the major axis.

An extruded view of the SAP2000 model for the building including x-brace diaphragm members is shown in Figure 4.8. This model was then used to evaluate the change in critical buckling modes for the framework. The critical loads for the revised models and the shapes of the critical buckling modes are shown in Figures 4.9 and 4.10.

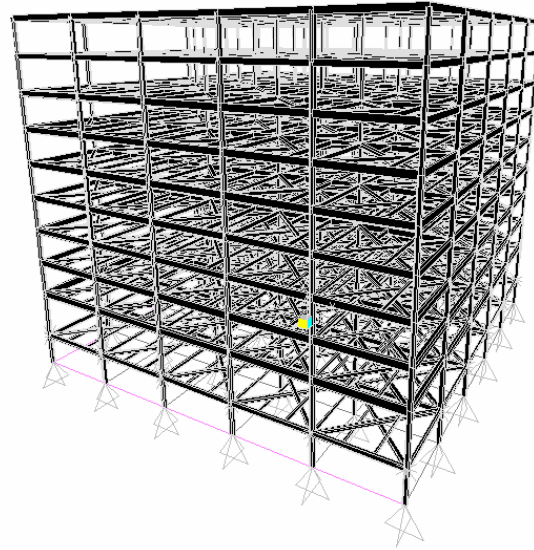


Figure 4.8 Extruded View Illustrating Basic SAP2000 Model of Uncompromised SAC 3-Story Modified Boston Framework With Diaphragm X-Bracing In Place.

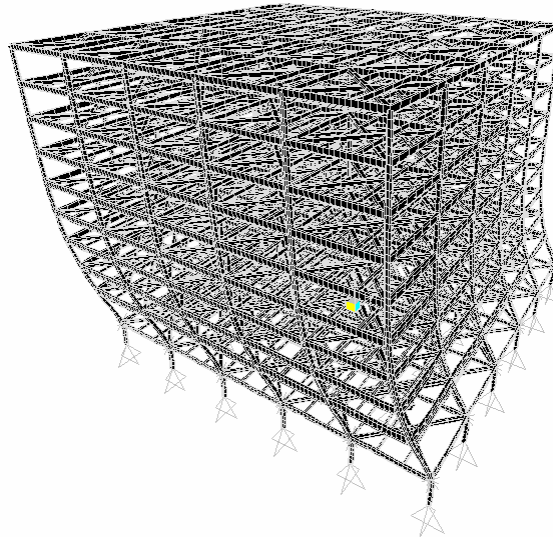


Figure 4.9 SAP2000 Displaced Shape Plot Illustrating Elastic Buckling Mode Shape Corresponding to the First Buckling Mode: $(\gamma_{cr})_1 = 3.712$.

As happened with the three story model, the critical modes are now very much in line with engineering intuition regarding the manner in which these 3D frames will elastically buckle. The two modes are now sway modes in orthogonal directions. This behavior follows from the use of perimeter moment resisting frames in the two orthogonal directions. The critical load factors for the frames are essentially the same for the two orthogonal buckling modes as would be expected for the framework with near-symmetric layout of moment-resisting components. As a result, the x-bracing members have preserved the proper behavior for the three-dimensional frame.

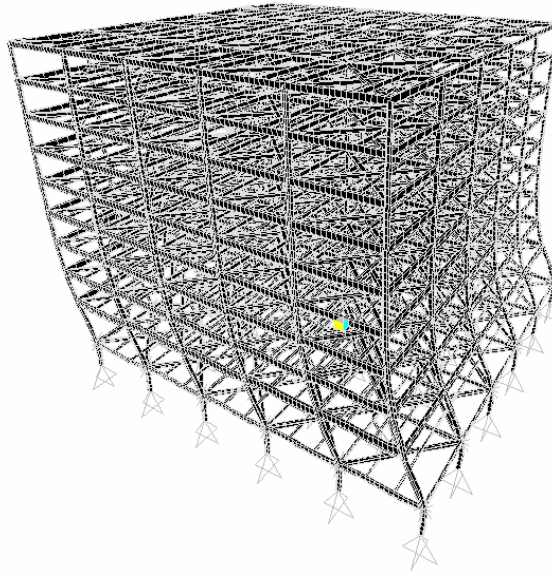


Figure 4.10 SAP2000 Displaced Shape Plot Illustrating Buckling Mode Shape Corresponding to the Second Buckling Mode: $(\gamma_{cr})_2 = 3.878$.

4.3 Elastic Analysis of Compromised Frame

As discussed in Chapter 3.3 of the three story building, the elastic analysis effort for the ten story building assumes that one of the columns at the ground floor level becomes ineffective. Again, the event that compromises the column's load carrying abilities is immaterial. Similarly to the three story building, the interior columns were not considered in this study. The moment-resisting frame layout in the building considered suggested the following compromised column events could be handled with a single analysis. These events are highlighted in Figure 4.11.

As with the three story building, the GSA recommended load combination for compromising events was used:

$$\gamma_{cr} (1.0w_D + 0.25w_L)$$

The event that renders a member ineffective is modeled using loading functions that vary with time and application of the loading over time. These will be described later in this subsection.

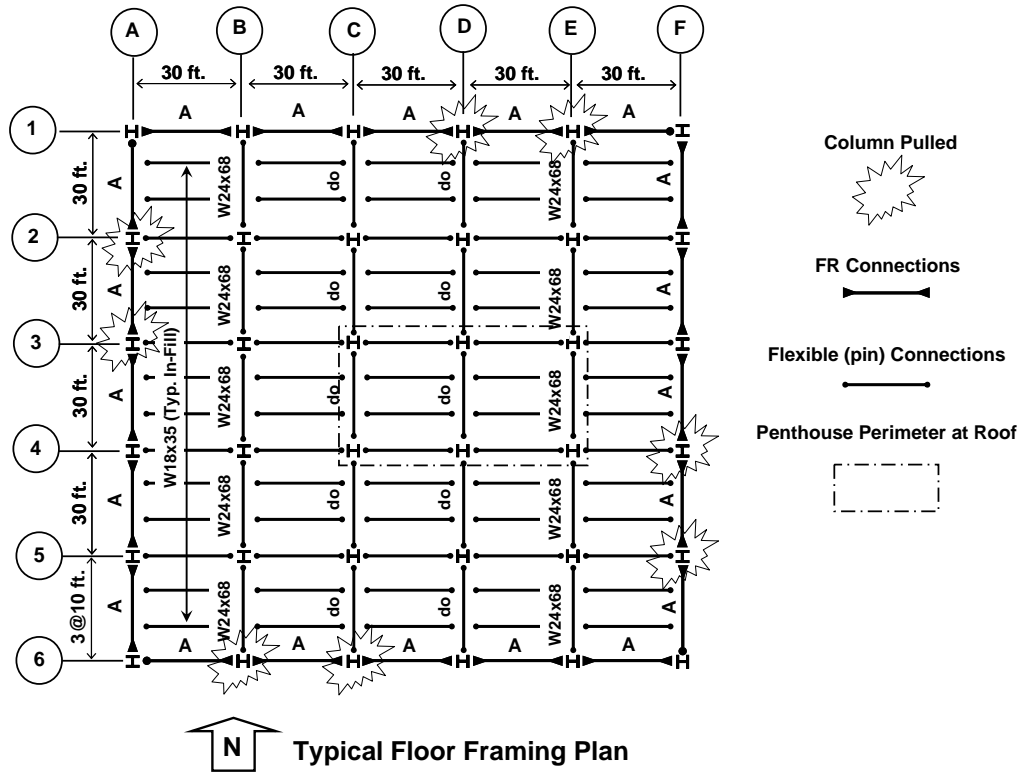


Figure 4.11 Ineffective Columns (one column at a time) Considered with the Analysis Conducted.

The second floor plan is illustrated in Figure 4.11 and the ineffective column is located immediately below the second floor level. As with the three-story building, only one column at a time is considered to be ineffective. The analytical model described in this chapter will provide insights into what happens within this 3D framing system when columns A2, A3, D1, E1, F4, F5, B6, and C6 are independently rendered ineffective.

The SAP2000 model used to analyze this framework for these compromising events is created by simply removing the column in question from the model and replacing it with a loading equivalent to that present with the column in place. The base SAP2000 frame model is shown in Figure 4.12.

In order to gain an engineering “feel” for the system in the compromised state, an elastic buckling load analysis of the framework was conducted. The following loading combination and critical load multiplier was used;

$$\gamma_{cr} (1.0w_D + 0.25w_L) \quad (4.1)$$

The first elastic critical buckling mode for the frame is shown in Figure 4.13.

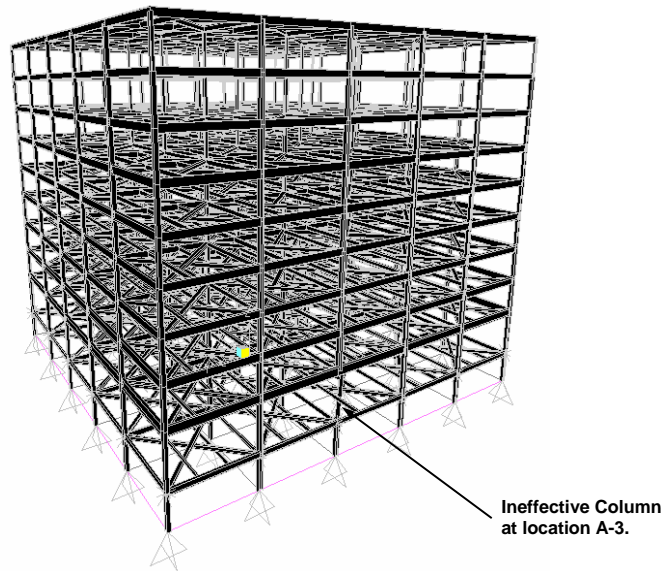


Figure 4.12 Extruded View Illustrating Compromised SAC 10-Story Modified Boston Framework With Diaphragm X-Bracing In Place and Column A-3 Removed.

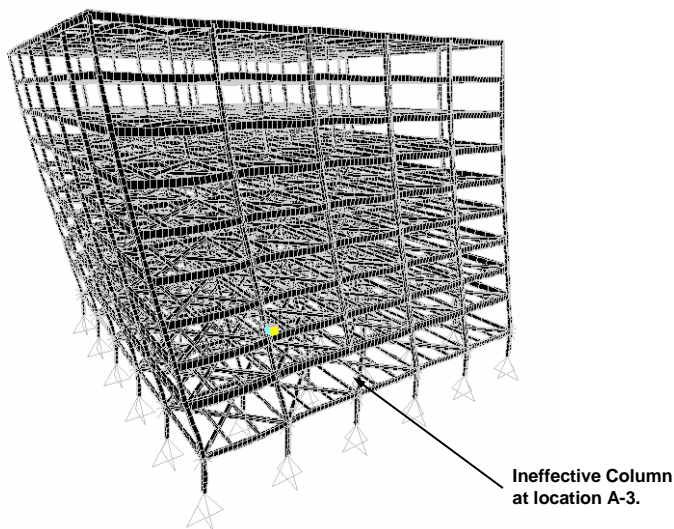


Figure 4.13 SAP2000 Displaced Shape Plot Illustrating Buckling Mode Shape Corresponding to the First Buckling Mode with Column A-3 at First Floor Level Removed: $(\gamma_{cr})_1 = 6.128$.

It can be seen that the first critical mode is a sway mode of the same type seen previously in the uncompromised framework. The applied load ratio of 6.13 indicates that the structure is in no danger of becoming elastically unstable under the static gravity loading assumed to be present at the time of the event. The significantly reduced live loading magnitude results in the increased applied load ratio at buckling

The process by which a column in the framework becomes ineffective is modeled in a time history analysis. Both the gravity loading and column loading are applied as time-history functions within the SAP2000 analysis as shown in Figure 4.14.

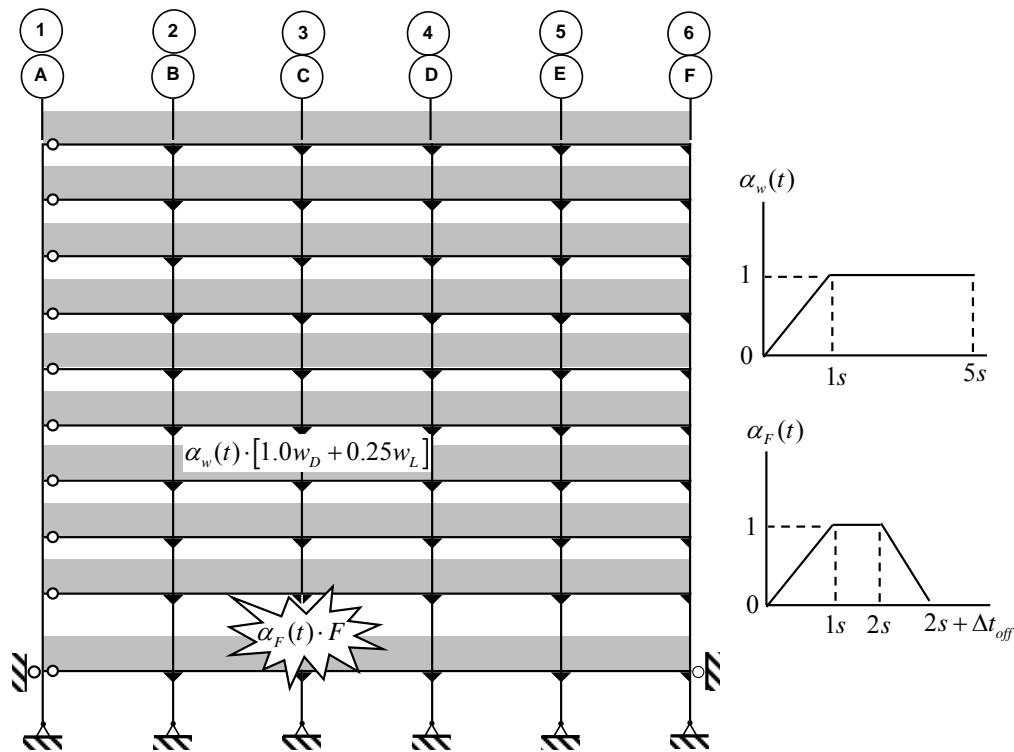


Figure 4.14 Conceptualization of Column Death Loading Scenario Implemented in the SAP2000 Time History Analysis of the Compromised Framework.

The process of rendering a column *ineffective* is essentially the same as that done in the 3-story building described in Chapter 3. The axial loading present in the column to be removed is determined using an elastic analysis of the structural system with the gravity loading given by equation (4.1). This column force is then applied as a concentrated load to the joints above and below the member in subsequent analyses. The column is then *turned off* over the ineffectiveness interval, Δt_{off} , after the gravity loading and column forces are applied simultaneously in a ramped manner over a 1-second interval and then held constant with 1-second

“settling period” as seen in Figure 4.14. At 2-seconds, the column is rendered ineffective and the entire system is allowed to respond over a 5-second analytical duration. This duration was found to capture all pertinent response and also allowed a sufficient time-lapse to allow damping to return the structure to the statically deformed configuration. As discussed in Chapter 3, 5% damping was assumed and all default magnitudes of material-level damping in SAP2000 were implemented (CSI 2004).

The GSA Guidelines recommend that member “turn-off” rates be done with duration equal to 1/10th the natural frequency of the framing system fundamental vibration period (CSI 2004). The lowest vibration frequencies of the framework in vertical mode indicated that 0.01 second “turn-off” interval would be sufficient to meet these guidelines. One can argue that in many, many cases that this turn off rate is very conservative. This issue will be discussed in other chapters of the report.

The impact of geometric nonlinearity (*i.e.* $P-\delta$ or $P-\Delta$ effects) on the response was evaluated. Columns in the framework were subdivided into two elements in the vicinity of the removed column (*e.g.* adjacent two column lines and three stories in height). This would allow the SAP2000 program to provide a measure of modeling $P-\delta$ effects in the response. Figure 4.15 illustrates the difference between nonlinear geometric and linear geometric response. Material nonlinearity is not considered.

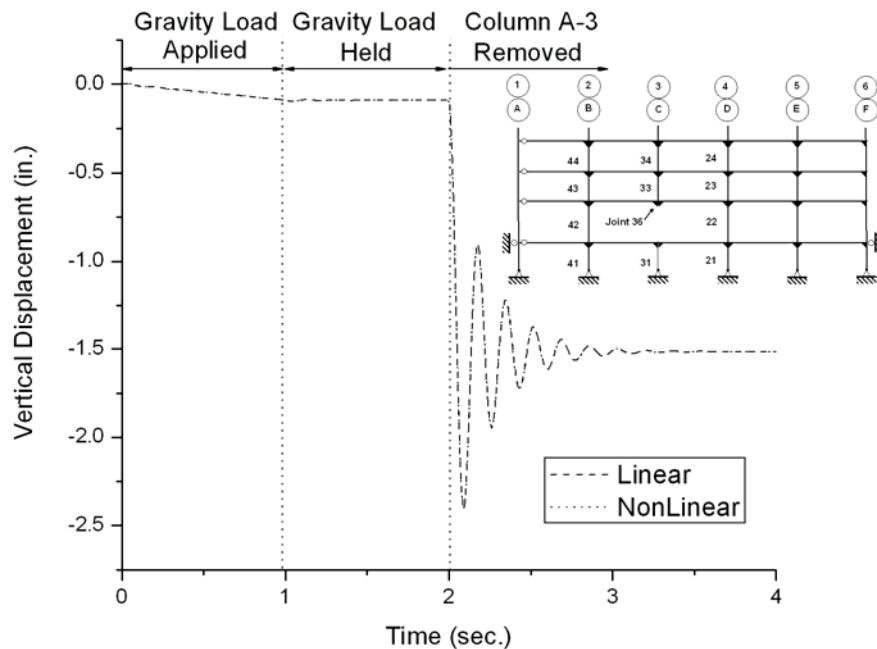


Figure 4.15 Elastic Linear and Nonlinear Geometric Response of The Modified SAC 10- Story Framework Used (displacement is immediately above lost column).

Figure 4.15 illustrates that nonlinear geometric analysis is not required to evaluate response. The nonlinear geometric response utilized the 0.01-second turn off rate and the response is identical to the linear geometric response. As discussed in Chapter 3, this is expected since the live loading is very small relative to the usual factored load levels implemented in design. With no tendency for the columns in the frame to be subjected to inter-story sway, $P - \Delta$ effects are very small as well as the $P - \delta$ effects. Therefore, the analysis conducted in the study of the 10-story frame omits nonlinear geometric effects. Displacements of the beam ends relative to one another are also quite small leading to negligible geometric stiffness contribution.

The SAC-FEMA study of moment-resisting connections (FEMA 2000c; FEMA 2000d; FEMA 2000a) pointed out the importance of strain rates on connection response. It is well known that the toughness of steel material decreases and the yield stress of the material increases with increase in the strain rate (Barsom and Rolfe 1999). To this end, the elastic strain rates for axial loading, shear loading and bending moment were computed for the ineffective column scenario previously described. Linear geometric response, 5% damping, and a turn off rate of 0.01 seconds were utilized in this analysis. Equations 3.2, 3.3, and 3.4 in Chapter 3 were used again to calculate strain rates for critical members in the ten story building. Figures 4.16 through 4.29 contain strain-rate response for these members within the framework.

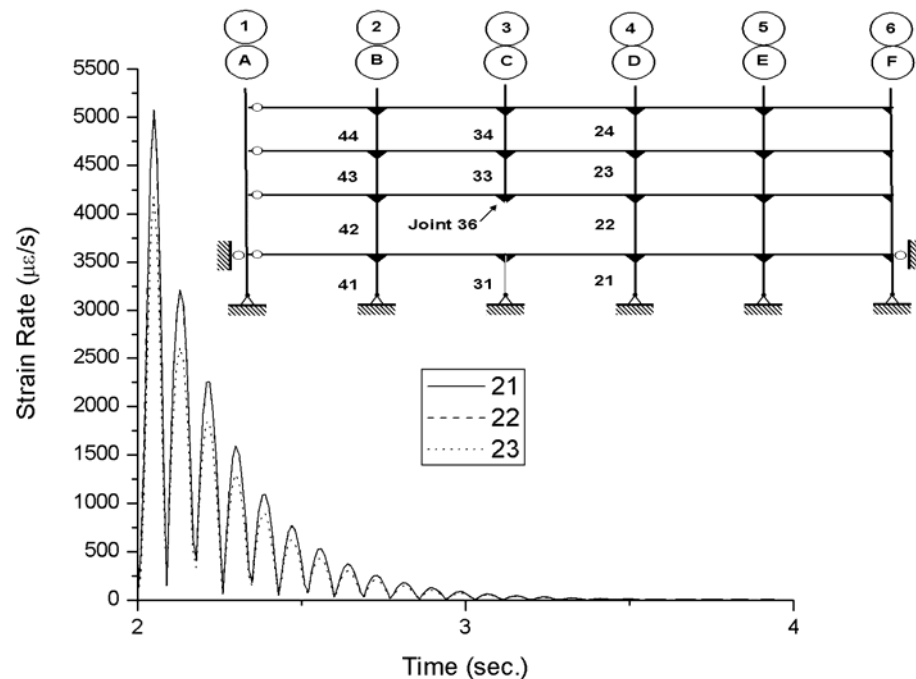


Figure 4.16 Axial Load Strain Rates (micro-strain per second) for Columns Along Line D in the Moment-Resisting Frame.

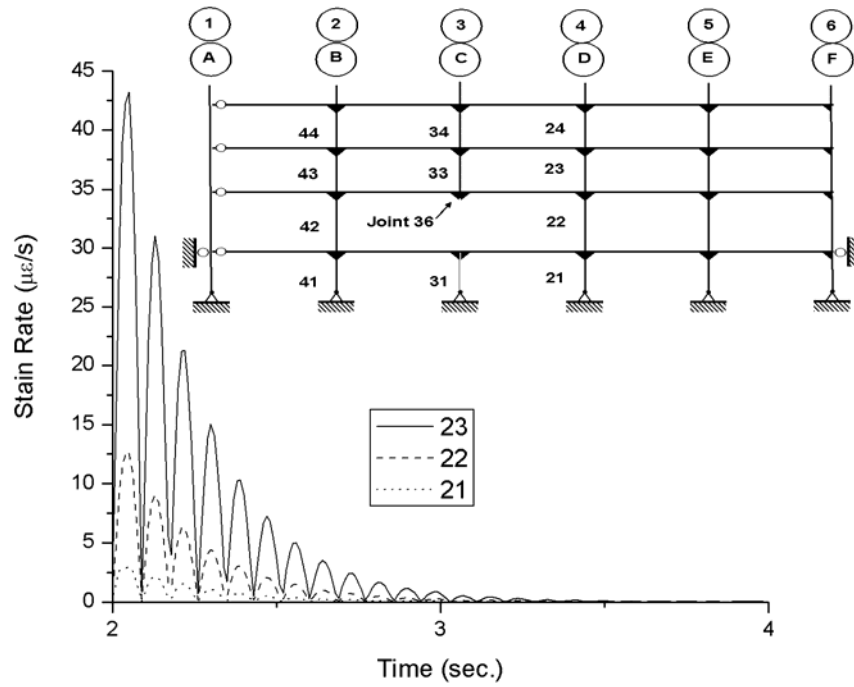


Figure 4.17 Shear Strain Rates (micro-strain per second) for Columns Along Line D in the Moment-Resisting Frame.

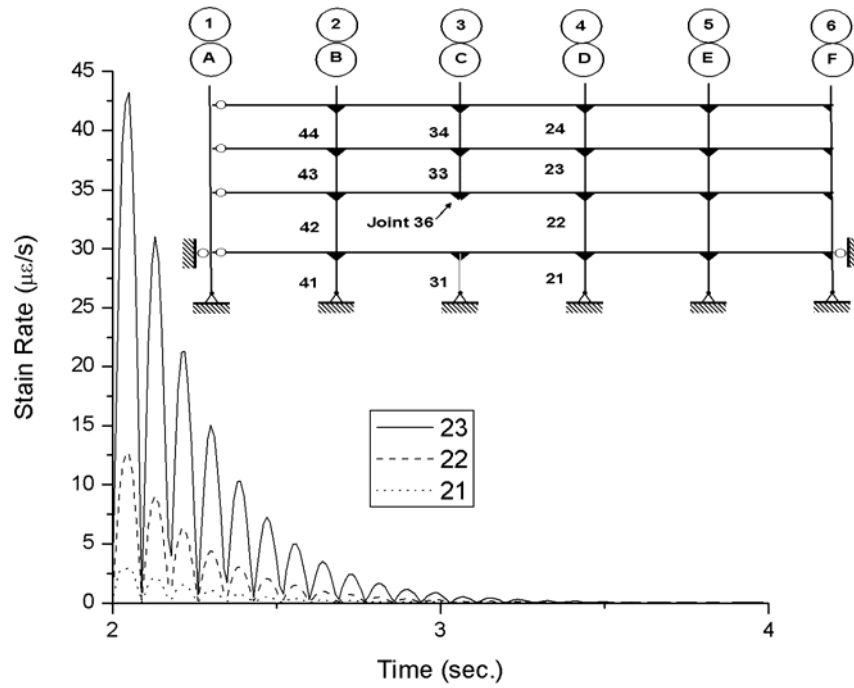


Figure 4.18 Bending Moment Strain Rates (micro-strain per second) for Columns Along Line D in the Moment-Resisting Frame.

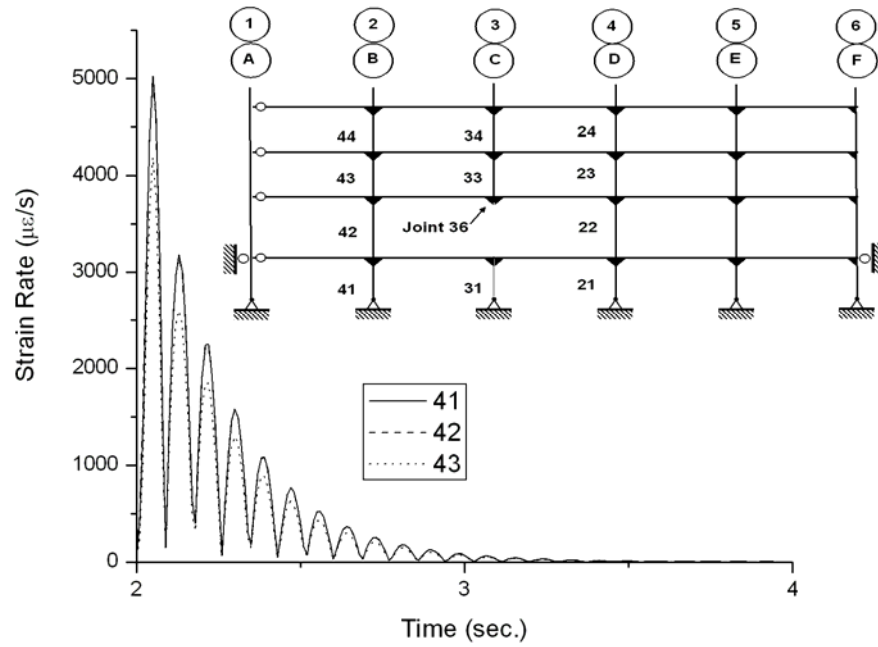


Figure 4.19 Axial Load Strain Rates (micro-strain per second) for Columns Along Line B in the Moment-Resisting Frame.

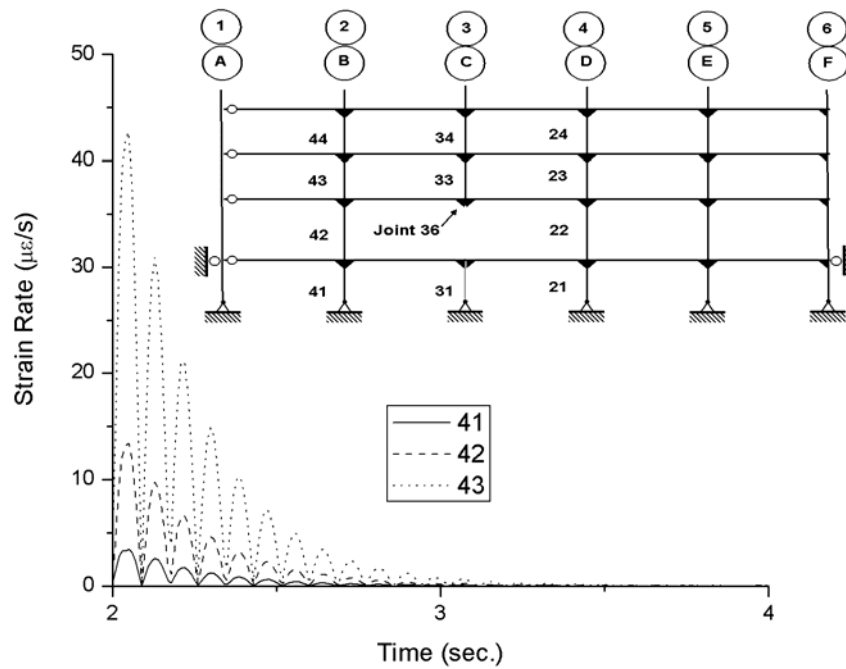


Figure 4.20 Shear Strain Rates (micro-strain per second) for Columns Along Line B in the Moment-Resisting Frame.

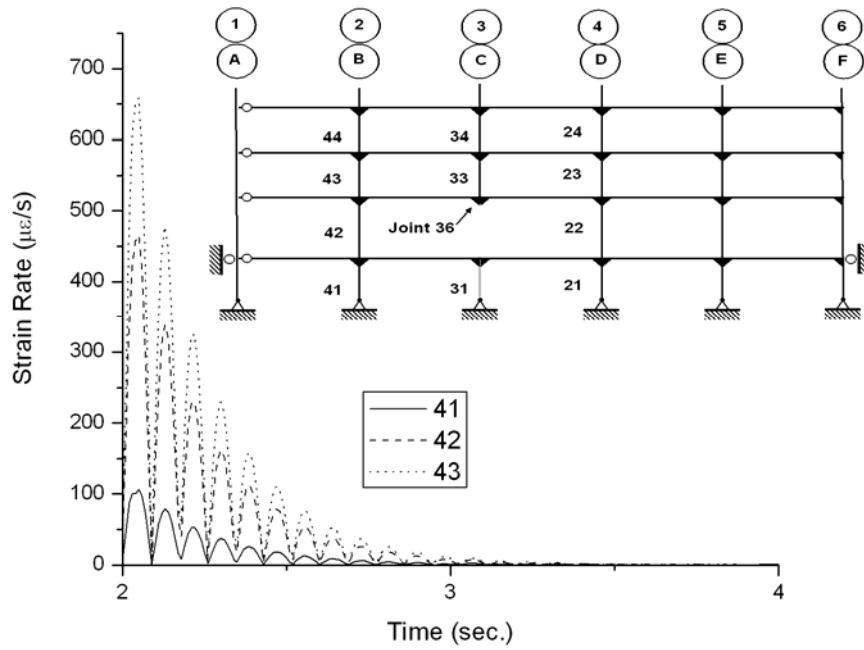


Figure 4.21 Moment Strain Rates (micro-strain per second) for Columns Along Line B in the Moment-Resisting Frame.

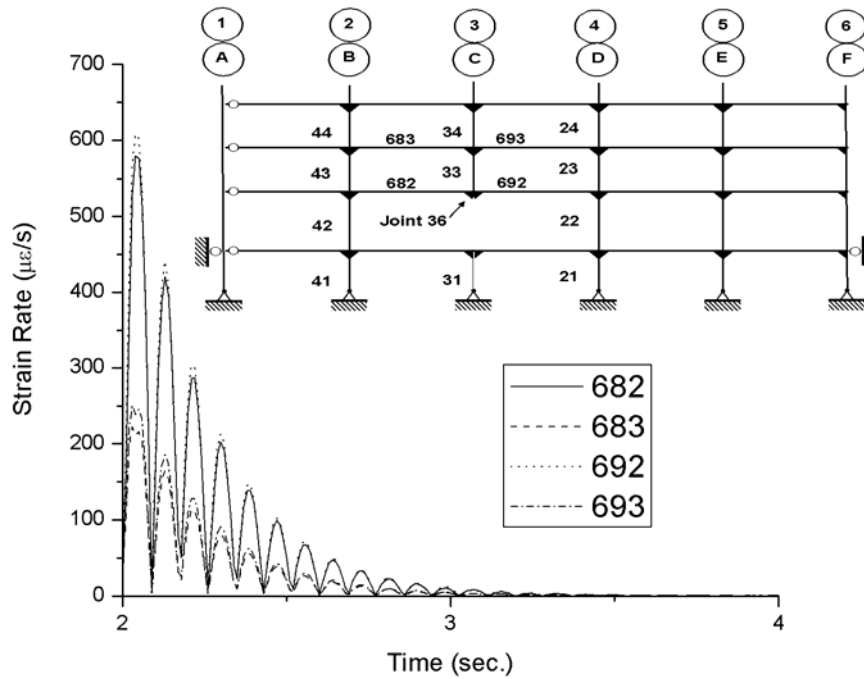


Figure 4.22 Axial Load Strain Rates (micro-strain per second) in the Beams of the Moment-Resisting Frame with Ineffective Column.

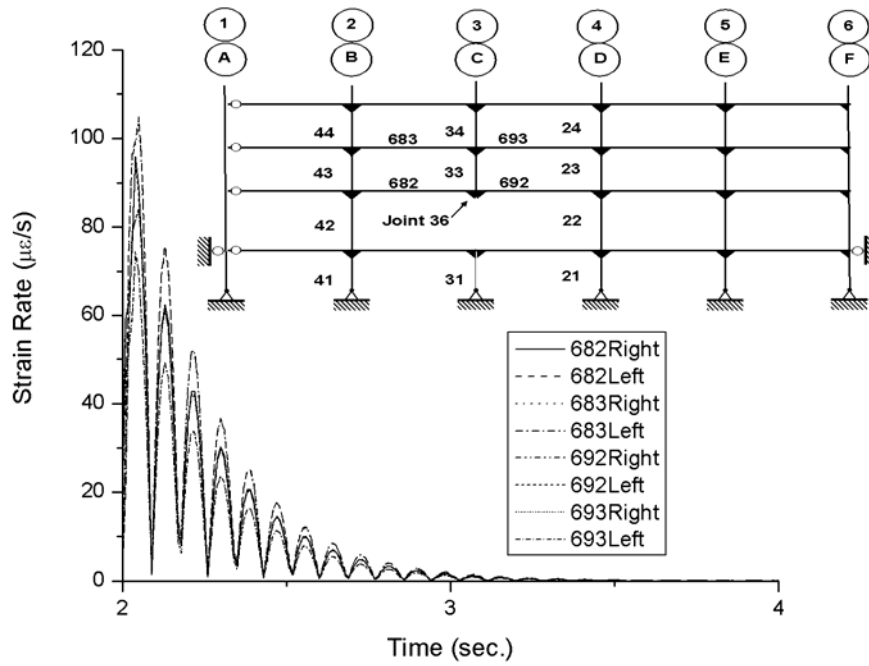


Figure 4.23 Shear Strain Rates (micro-strain per second) in the Beams of the Moment-Resisting Frame with Ineffective Column.

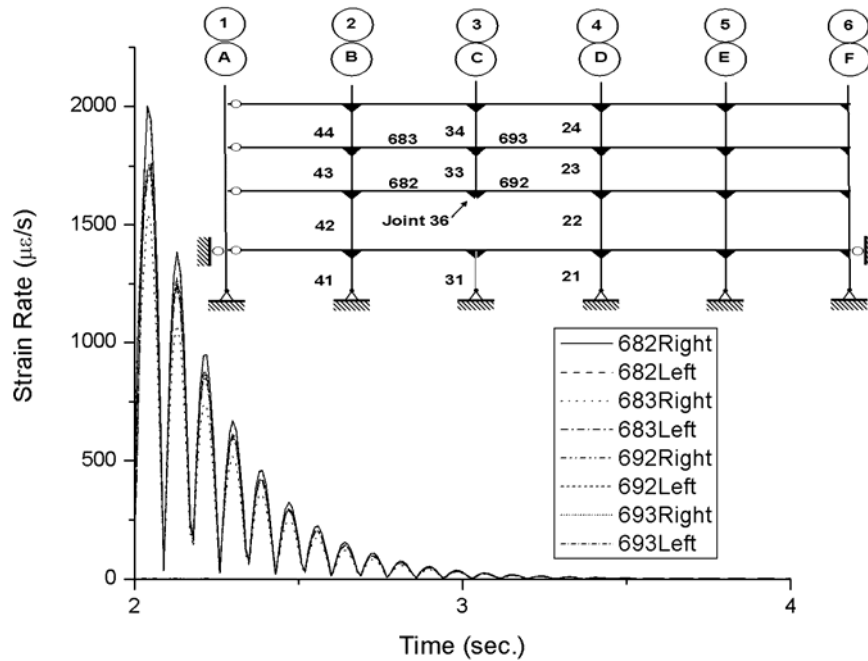


Figure 4.24 Bending Moment Strain Rates (micro-strain per second) in the Beams of the Moment-Resisting Frame with Ineffective Column.

The axial strain rates in the columns and beams range from a low of $218 \mu\epsilon/s$ (0.00022 in/in/s) and a high of $5,650 \mu\epsilon/s$ (0.0057 in/in/s). The shear strain rates are lower in all members of the framework. Peak shear strains occur in the columns of the framework at the top of column 23 on the interior of the moment resistant frame. These rates are on the order of $105 \mu\epsilon/s$ (0.00011 in/in/s). Bending strain rates in the columns are comparable to the axial rates with a maximum of $2,000 \mu\epsilon/s$ (0.002 in/in/s).

As seen in the 3-story building analysis outlined in Chapter 3, the strain rates seen in this structure are only slightly more than the intermediate loading rate and orders of magnitude lower than the dynamic loading rate (Barsom and Rolfe 1999). The loading rates found in the elastic time history analysis give no indication that fracture toughness of the constituent materials will be insufficient, or the elevated yield strength resulting from increased load rate should be considered. It should be emphasized again that stress raisers caused by connection geometry have been ignored. Again, it should be noted that the absolute value of the strain rates reported have been taken and this is the reason for the data residing in a single quadrant of strain rate versus time space. The results also indicate that the strain rates decrease quite rapidly with time as a result of damping assumed in the system.

The need to determine if inelastic time history analysis is warranted was performed by evaluating demand to capacity ratios (DCR's) for the members in the framework. As discussed in Chapter 3, in order to incorporate shear, moment, and axial load, the DCR used to assess member strength and stability using the results of the present elastic time history analysis is given by,

$$DCR = \frac{P}{P_n} + \left(\frac{V}{V_n} \right)^2 + \frac{M}{M_n} \leq 1.0 \quad (4.12)$$

where all terms have been defined previously in Chapter 3. All assumptions discussed in Chapter 3 were carried forward for the ten-story building.

Linear elastic time history analysis using a column turn off rate of 0.01 seconds was conducted for the frame and loading described previously. The response time history data was then used to define DCR's for all elements in the framework using equation (4.12). Figures 4.25 through 4.27 illustrate the response history of the DCR's for members within the moment-resisting framework. Each figure contains a key to the output data. Both columns and beams were considered.

The elastic analysis indicates that the largest DCR's are found in the beams, though those values hover around 0.68. The largest DCR occurs in beam 693 on the right end, away from the ineffective column. The columns on either side of the ineffective column have DCR's less than 0.63. With those DCR's, one could assess that the beams and columns in the building are adequate with one ineffective column.

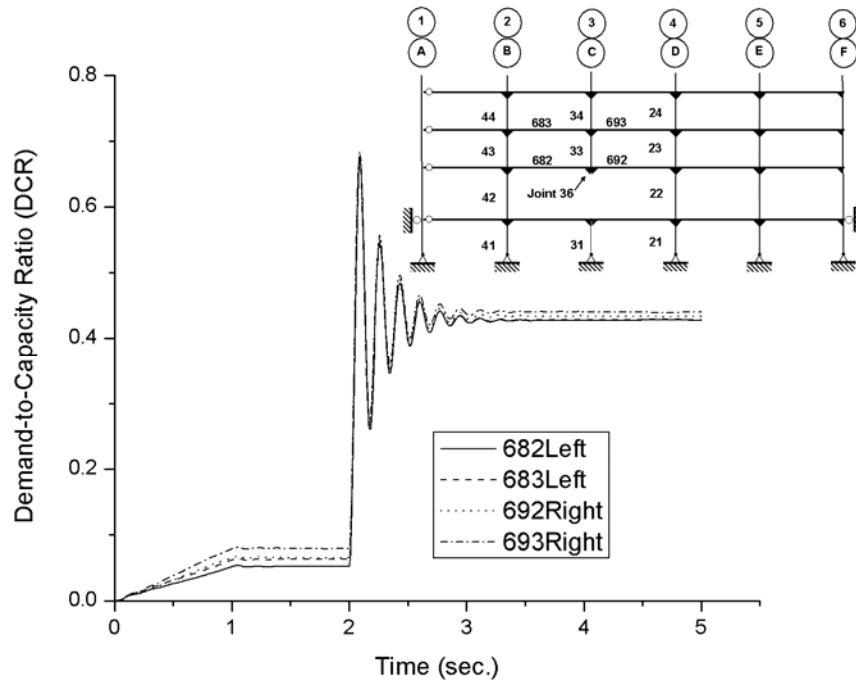


Figure 4.25 Demand to Capacity Ratios for Beams in Frame Affected by Ineffective Column at A-3.

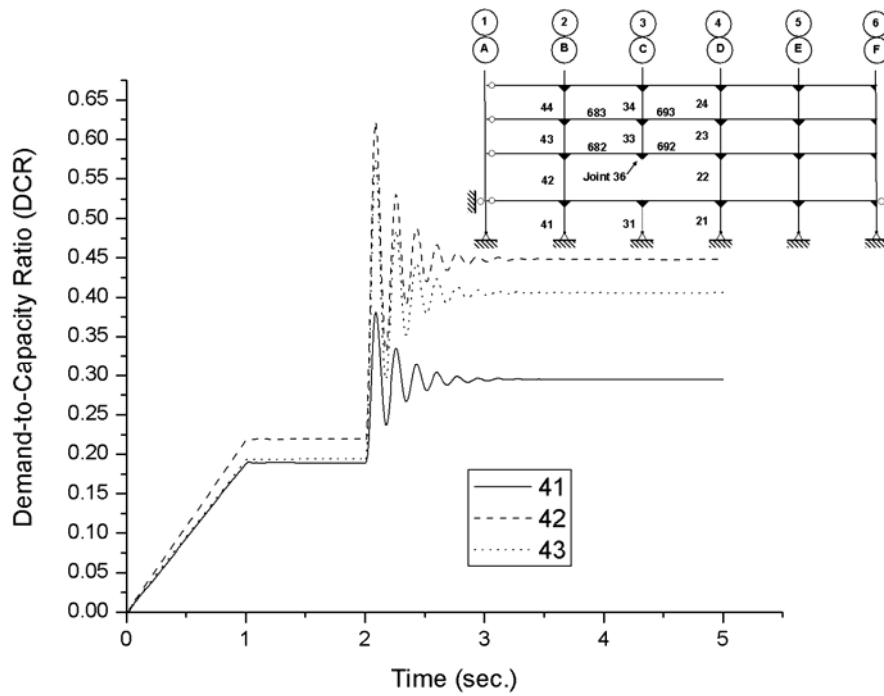


Figure 4.26 Demand-to-Capacity Ratios (DCR's) Assuming Elastic Response for Columns Along Line B in Frame.

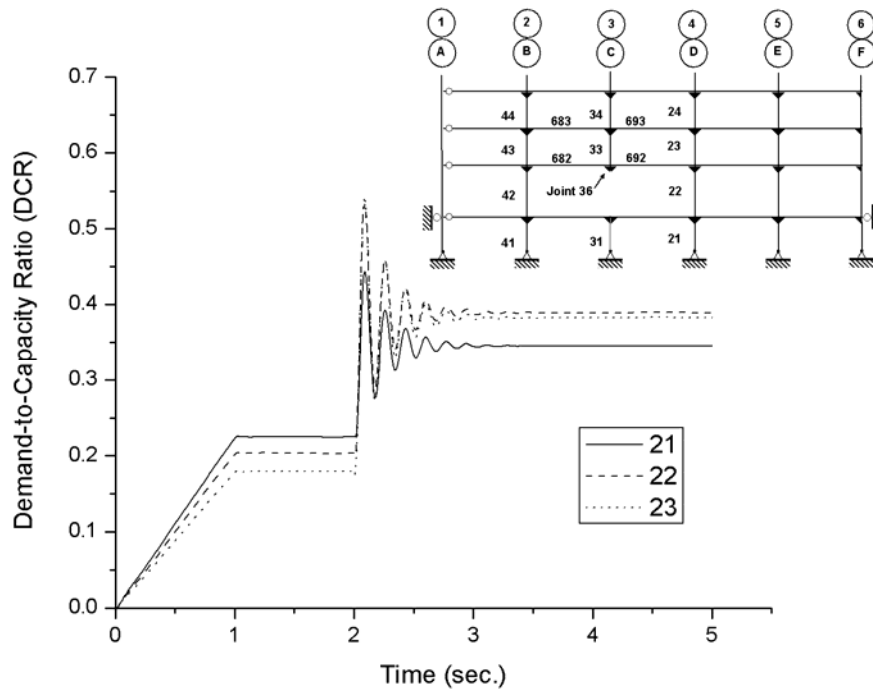


Figure 4.27 Demand-to-Capacity Ratios (DCR's) Assuming Elastic Response for Columns Along Line D in the Frame.

Table 4.1 provides peak component demands (*i.e.* axial, shear, and moment) and peak DCR's for the members in the frame. In general, the axial load demand in the beam members is very small (*e.g.* less than 2% of the axial capacity). The bending moment demand is relatively large for these members (*e.g.* at least 60% of capacity) and the shear demand is moderate. When comparing the beam results to the 3-story building, the axial, bending, and shear demands for the beams in the 10-story framework are much lower due to the Vierendeel action occurring in the floors above the compromised column. The axial load demands in the columns in the vicinity of the ineffective column member are moderate (*e.g.* 45% or less). The bending moment demands and shear demands in these members are relatively small as well. The effect of Vierendeel action of the upper stories is evident in this framework. The results of the 20-story building frame show similar behavior as will be seen in the next chapter of the report. Overall, the peak DCR's for the critical members in the vicinity of the ineffective column indicate that inelastic response is unlikely in this frame when single columns around the perimeter of the system become ineffective.

The axial, shear, and bending moment demand distribution within the framework is shown in Figures 4.28 through 4.30. If one were to examine the dominant terms in equation (4.12) in light with what is seen in these figures, the bending moment demands are by far the most important indicator of the adequacy of the frame during the compromising event. The results in Table 4.1 confirm this.

Table 4.1 Peak Non-Dimensional Member Demands and Demand-to-Capacity Ratios for Elastic Response to Ineffective Column at Location A-3.

Member		$\frac{P}{P_n}$	$\frac{V}{V_n}$		$\frac{M}{M_n}$		$DCR = \frac{P}{P_n} + \left(\frac{V}{V_n}\right)^2 + \frac{M}{M_n}$	
			Left/Bot.	Right/Top	Left/Bot.	Right/Top	Left/Bot.	Right/Top
Beams	682	0.020	0.170	-	0.624	-	0.673	-
	683	0.008	0.162	-	0.637	-	0.672	-
	692	0.020	-	0.171	-	0.637	-	0.679
	693	0.009	-	0.165	-	0.649	-	0.685
Columns	21	0.415	-	0.008	-	0.029	-	0.444
	22	0.392	-	0.034	-	0.140	-	0.533
	23	0.330	-	0.120	-	0.200	-	0.544
	41	0.330	-	0.014	-	0.051	-	0.381
	42	0.408	-	0.037	-	0.212	-	0.622
	43	0.346	-	0.121	-	0.212	-	0.573

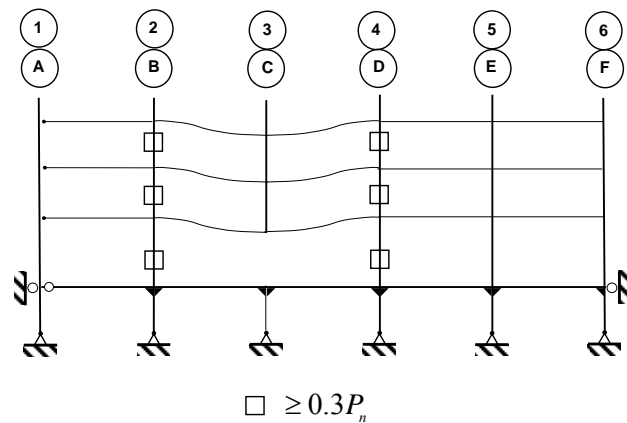


Figure 4.28 Axial Load Demand for Members in Moment-Resisting Frame Containing Ineffective Column.

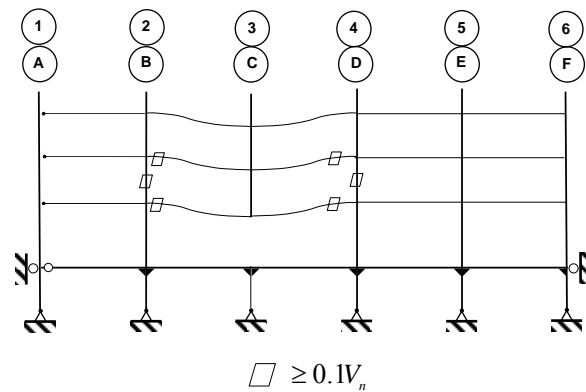


Figure 4.29 Transverse Shear Demand for Members in Moment-Resisting Frame Containing Ineffective Column.

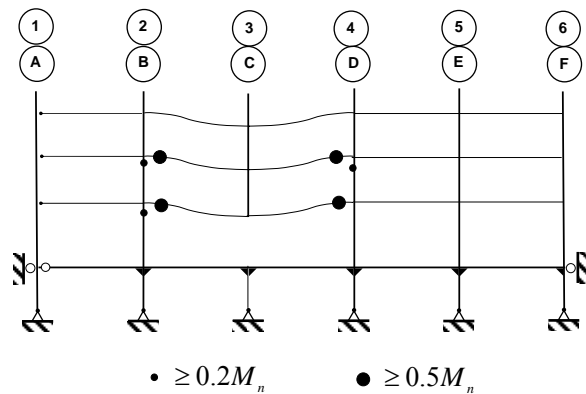


Figure 4.30 Bending Moment Demand for Members in Moment-Resisting Frame Containing Ineffective Column.

The DCR data in Table 4.1 indicates that no plastic hinges are expected to form in the 10-story frame when single exterior columns at the ground floor level are rendered ineffective. It should be noted that corner columns becoming ineffective were not considered. As a result, elastic analysis is sufficient to describe frame behavior under the event considered. The benefits of having multiple stories above the compromised column are evident in these results when compared to those of the 3-story framework.

4.4 Concluding Remarks

A steel framework based upon the 10-story SAC pre-Northridge Boston building has been analyzed using elastic time history analysis when subjected to a variety of ineffective column scenarios. Columns at the

ground floor level around the perimeter of the structure were rendered ineffective in the structural analysis using a “column death” process described previously for the 3-story SAC building framework. A corner column becoming ineffective was not considered.

The configuration of the framework; the lack of interstory drift of the column member ends relative to one another; and the very small vertical deformation of the beam ends relative to one another leads to the conclusion that geometric nonlinear effects are not significant in this framework. It should be noted that the maximum vertical deflection of the floor system immediately above the column rendered ineffective was approximately 3 inches. This is extremely small given the span of 60 feet and therefore, catenary action is not possible in the beam members. The load carrying mechanism at work for this framework is Vierendeel action of the stories above the compromised column.

Tension tying forces for this framework are much smaller than those found for the 3-story framework. Therefore, the tension/compression recommendation from the 3-story frame analysis can carry forward to similar frames to those considered in this chapter.

Axial demands for the columns in this frame (30-40% of the compression capacity of the column member) indicated that splices would not be subjected to tension forces. As in the case of the 3-story frame, as long as the beams participate in resisting the gravity loading, the columns above the compromised member maintain significant compression force levels. Thus, splices in the columns are not expected to be subjected to significant tension forces.

The connection demands at the ends of the beam members in the framework are non-remarkable. The bending moment and shear demands appear to be well within the limits of modern ductile moment-resisting connections that are designed to support the plastic moment capacity of the beam member. The axial load demands in the beam members are negligible (at least when there are sufficient floor levels above the compromised column) and the combination of the previously recommended tying forces with these shears and moments does not appear to be unduly punishing to the connections.

The beneficial action of Vierendeel action in the floors above the level containing the compromised column diminishes as one rises in the framework. In general, one would expect similar behavior to that of the 3-story framework when columns at the seventh level are rendered ineffective. If columns at the ninth and eighth floor levels are rendered ineffective, then Vierendeel action is likely not possible and the load carrying mechanism is likely to be catenary action in the framing members as well as membrane action in the floor system. This behavior is considered in another chapter of the report.

Strain rates in members in the immediate vicinity of the ineffective column were found to be in the intermediate rate category and therefore, a reduced fracture toughness and elevated yield of the material can be ignored. However, it should again be emphasized that connection geometric effects were not considered.

Demand-to-capacity ratios for all members in the frame configuration analyzed did not lead to yielding in members near the compromised column. Beams and columns are expected to respond to ineffective columns at the ground floor level in an elastic manner. This conclusion must be tempered with the knowledge that Vierendeel action plays a large role. The three-story SAC building analysis indicates that when there are three-stories (or less) above the compromised or ineffective column, inelastic behavior should be expected.

Chapter 5 Twenty-Story SAC Frame

5.1 Building Description

Similar to that of the three- and ten-story buildings, a 20-story structure was taken from the SAC-FEMA project documents (FEMA 2000d). As done previously, the Boston design was used. The pre-Northridge configuration was also assumed. Initially, the building model was constructed using the member sizes specified by the SAC-FEMA documents. Orientation of all members also followed the SAC recommendations and all steel material used assumed a lower-bound yield strength of 50 ksi. It is of note that while the entire exterior perimeter of the model frame consists of moment-resisting frames, the interior framing (infill beams, girders and interior columns) are modeled with flexible (pinned) connections. No major axis rotational restraint in these connections is assumed. A typical floor plate is shown in Figure 5.1.

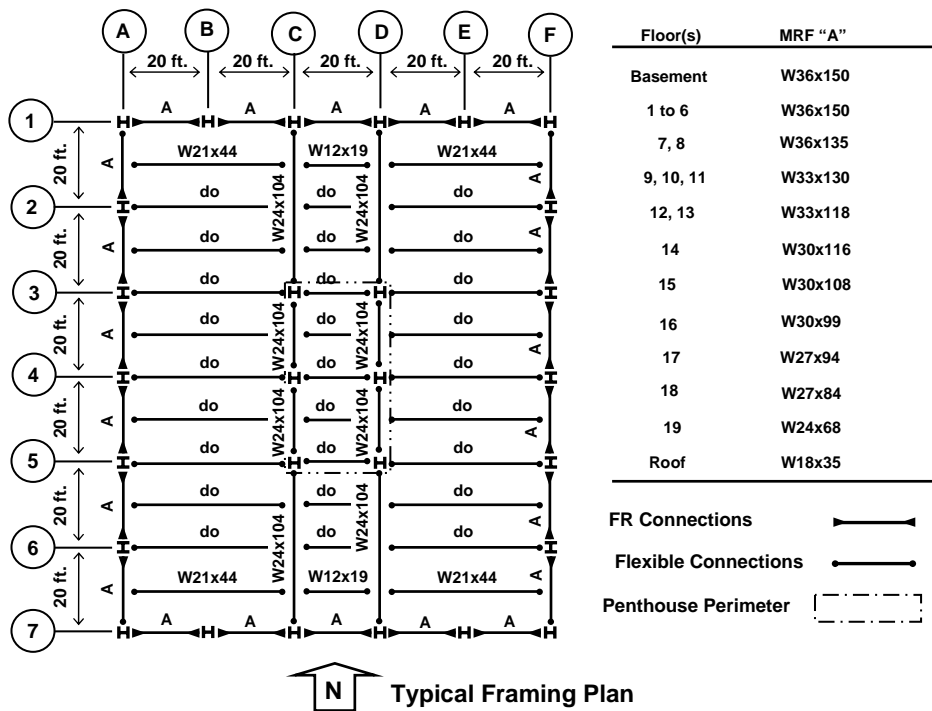


Figure 5.1 Typical Floor Plan With Orientation Of Columns.

Load magnitudes are similar to those used for the three- and ten-story buildings (Chapters 3, and 4). The twenty-story model was subjected to full factored gravity loading of $1.2w_D + 1.6w_L$ without live load reduction to validate its performance under design-level loads. With this analysis, it became apparent that several members were incapable of carrying gravity loading at the factored load levels. The members that

were found to be inadequate were resized for gravity load resistance using the AISC specifications (AISC 2005a) and replaced. Overall, minor changes were made to the frame found in the SAC document (FEMA 2000d). These changes were mainly focused in the sizes of the in-fill beams and several column members in the interior of the framework. A column schedule for the framework is shown in Figure 5.2.

	A-1, A-7; F-1, F-7	A-2, A-6; B-1, B-7; E-1, E-7; F-2, F-6	A-3, A-4, A-5; C-1, C-7; D-1, D-7; F-3, F-4, F-5	C-3, C-5; D-3, D-5	C-4; D-4
Roof 249'-0"	W14x61	W24x68	W24x68	W10x49	W8x48
20 th 236'-0"	W14x82	W27x94	W24x131	W12x72	W10x60
19 th 223'-0"	W14x109	W30x99	W27x146	W12x96	W12x72
18 th 210'-0"	W14x132	W30x116	W27x161	W14x120	W14x90
17 th 197'-0"	W14x159	W36x135	W30x173	W14x145	W14x120
16 th 184'-0"	W14x193	W36x150	W30x173	W14x176	W14x176
15 th 171'-0"	W14x233	W36x160	W33x201	W14x211	W14x145
14 th 158'-0"	W14x283	W36x170	W33x201	W14x233	W14x159
13 th 145'-0"	W14x331	W36x182	W33x221	W14x257	W14x176
12 th 132'-0"	W14x342	W36x182	W33x221	W14x283	W14x193
11 th 119'-0"	W14x370	W36x210	W36x260	W14x342	W14x233
10 th 106'-0"					
9 th 93'-0"					
8 th 80'-0"					
7 th 67'-0"					
6 th 54'-0"					
5 th 44'-0"					
4 th 41'-0"					
3 rd 28'-0"					
2 nd 15'-0"					
Ground 0'-0"					
Sub. 1 -13'-0"					
T/Ftg. -26'-0"					

Figure 5.2 Column Schedule for Modified SAC 20-Story Building Used in the Present Study.

All heights indicated in the column schedule are from centerline of beam to centerline of beam.

The development of unrealistic buckling load magnitudes and buckled shapes for the framework were anticipated and a system of x-bracing diaphragms were placed in the floor plates in a manner that was similar to that done in the 3- and 10-story frames. There is a noticeable difference in the present 20-story building framing system when compared to that of the 10- and 3-story buildings. Using the column arrangement given in the floor plan in Figure 5.1, the x-bracing arrangement in Figure 5.3 was selected.

The non-square floor panels in the current building made the computations previously used to size the x-bracing diaphragm members inconsistent. While the diagonal members are installed across square bays for the other two building models, the twenty-story frame incorporates rectangular bays. The computations that

suggested using W14x159 diaphragm members were based upon 30-ft by 30-ft bays. The following rationale was used to maintain W14x159 (massless) diaphragm members in the present structure. First of all, the square 20-ft by 20-ft panels in the central region of the frame will be stiffer than the panels in the 30-ft by 30-ft panels used previously if W14x159 diagonal members are utilized.

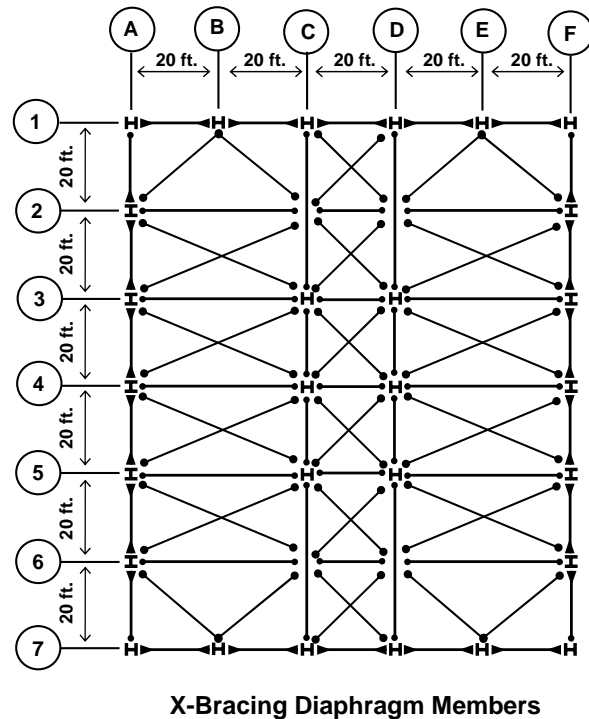


Figure 5.3 Typical Floor Plan With Diagonal Members.

The chevron braces in the corner bays will have the same stiffness as the 20-ft by 20-ft bay arrangement and will again be stiffer than the 30-ft by 30-ft bays with respect to east-west shear racking behavior. With regard to shear racking deformations in the north-south direction, the chevron braced bays will be less stiff when compared to the previous 30-ft by 30-ft braced bays. The rectangular bays will be less stiff than the 30-ft by 30-ft. All these issues will conspire to lead the W14x159 braces in the 20-story building to a diaphragm stiffness that is less than those used in the 3-story and 10-story framework. Several test runs (eigenvalue buckling analysis) were conducted to evaluate the adequacy of these members and it was felt that using W14x159 wide-flange sections of zero mass with flexible (pin) connections is justified.

As noted previously, the exterior perimeter of the model building contains moment-resisting frames. Exterior frames in the North-South elevations have rigidly connected beams, while frames in the East-West elevations have rigidly connected beams between column lines 2 and 6, but contain flexible connections at column lines 1 and 7. The building is also restrained from lateral movement at the lowest two floor plates,

but vertical movement and rotation is allowed. At the bottom of each column, restraint from translation only is provided. It should be noted that the lateral restraint provided on levels one and two is both outward and inward. While the adjacent earth would resist any outward movement, this condition is not truly valid for inward movement, as tie-backs or other system of anchorage would be required to limit movement away from the soil wall. Figure 5.4 provides elevations of the model building.

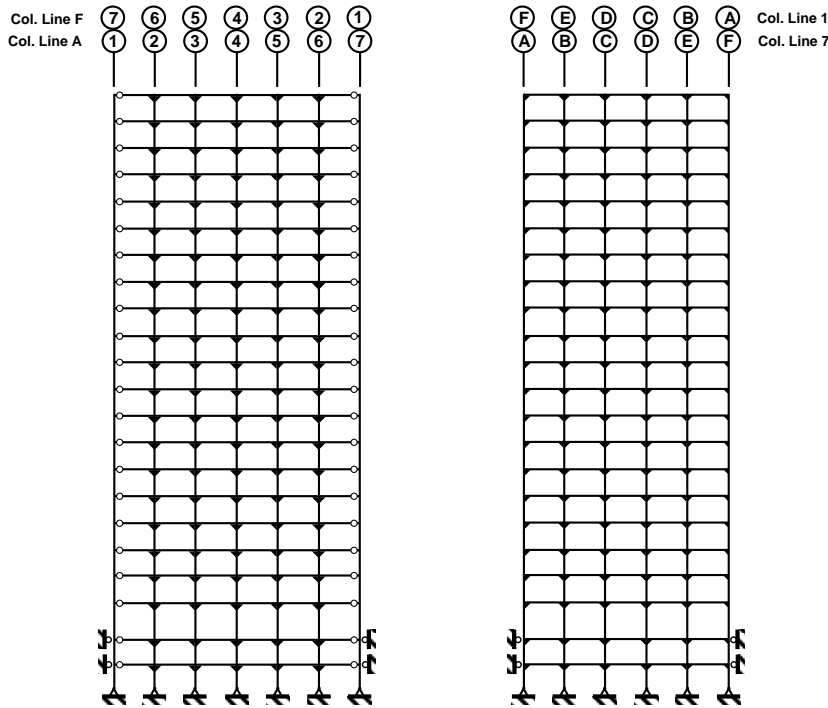


Figure 5.4 Elevations Of The 20-Story Building With Fixities And Member Releases.

The open circles in Figure 5.4 indicate the presence of major moment releases at the end of the girders.

The critical loads and buckling mode shapes for the framework were computed using the elastic buckling (eigenvalue) analysis found in SAP2000 (CSI 2004). Full factored gravity loading of $\gamma_{cr}(1.2w_D + 1.6w_L)$ was used. The first buckling mode occurred at an applied load ratio of $(\gamma_{CR})_1 = 3.123$ and is illustrated in Figures 5.5 and 5.6. Minor axis buckling of several of the columns within the 3D frame is seen to occur. The buckling modes that correspond to lateral sway of the system occur with larger applied load ratios. It should be noted that the graphics capability of SAP2000 is unable to illustrate twisting in the girders connected to the buckled column. The extruded view mode cannot illustrate the torsional deformation of the girder needed for deformation compatibility with the column even though it is actually present.

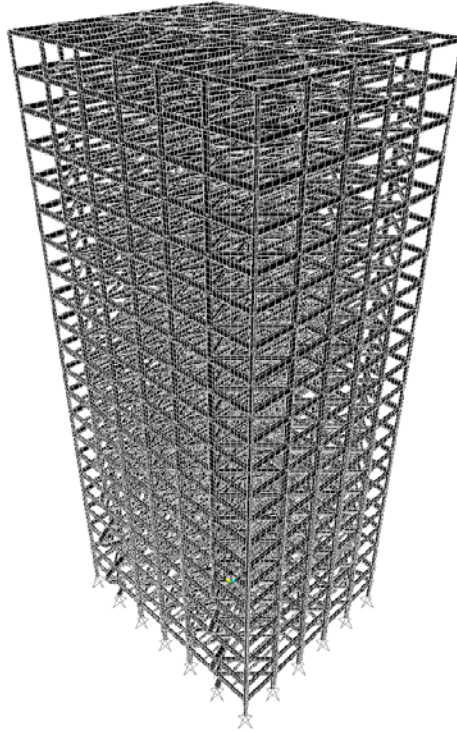


Figure 5.5 First Elastic Critical Buckling Mode. (Note The Minor-Axis Buckling Of Lower, Next-To-Corner Columns.)

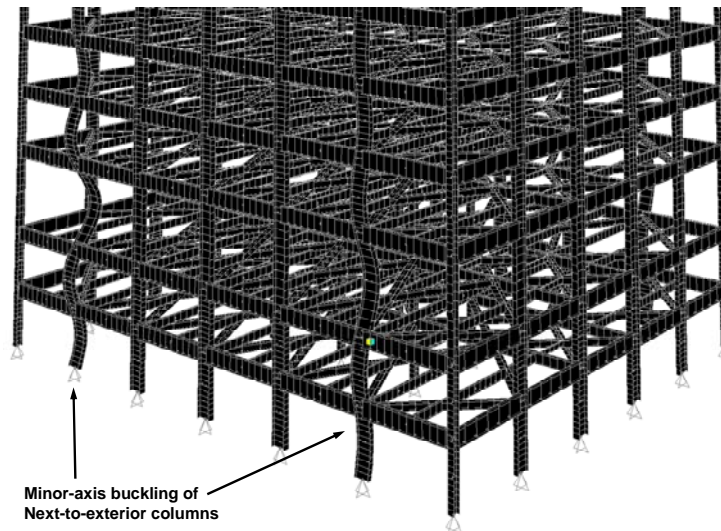


Figure 5.6 Detail Of First Critical Buckling Mode.

The full factored gravity loading was applied to the frame as a mechanism to shake down the analytical model. The resulting axial load, shear, and major-axis moment diagrams for frame elevations along

column lines A and F are shown in Figure 5.7. Although not indicated in the graphic, there axial loading in the exterior columns. Similar diagrams for elevations along column lines 1 and 7 are in Figure 5.8.

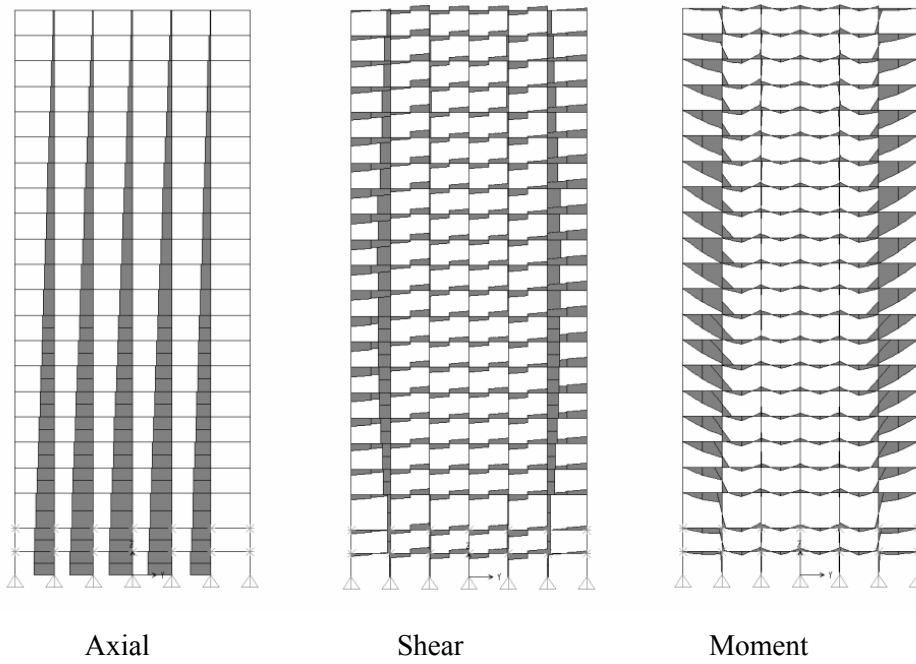


Figure 5.7 Axial Load, Shear and Moment Diagrams for Elevations along Column Lines A and F.

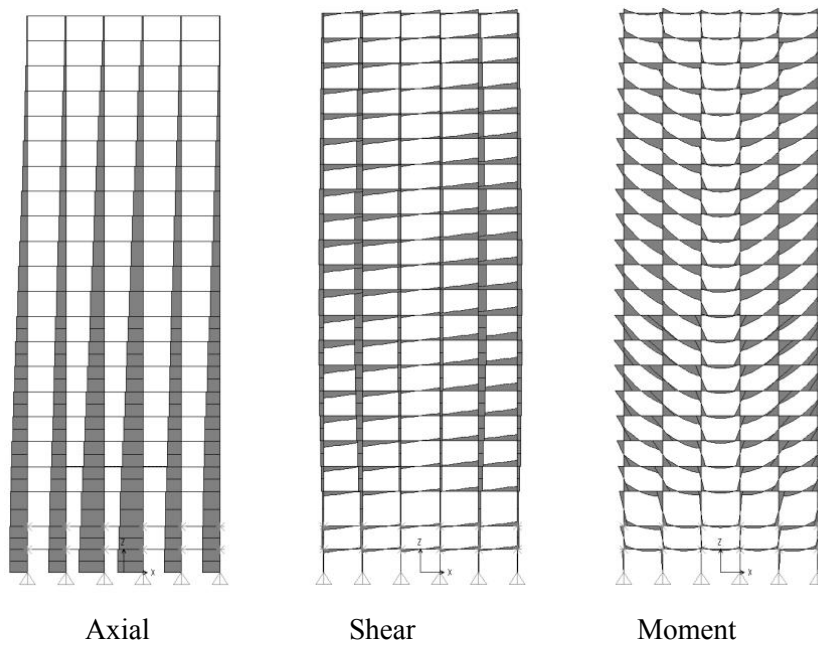


Figure 5.8 Axial Load, Shear and Moment Diagrams for Elevations along Column Lines 1 and 7.

By inspection, the axial load distributions appear ordinary. However, it is of interest to note the rather large increase in axial loads in columns C7/C1 and D7/D1 when compared to others along column lines 1 and 7. The framing plan (refer to Figure 5.1) contains girders framing into these columns and they have very large tributary areas relative to the remaining columns in these framing lines. This disparity in axial loading also leads to some rather interesting behavior in relation to shear and moment diagrams. A similar disparity in axial loading along column lines A and F also exists. The corner columns have very small tributary areas when compared to the interior columns.

The distribution of axial loading within the columns of the framing system leads to some rather interesting nuances in the shear and moment diagrams. The very heavy loading at the interior of the frame elevations leads to significant column shortening for these interior columns. The shortening that is occurring is so significant (relative to the outer columns) that it is skewing the bending moment diagrams in the beams away from the expected parabolic variation from negative to positive to negative moment. In some instances the increase in loading at the interior columns relative to others in the frame elevation is nearly 50%.

The exterior girders have bending moment diagrams that look like cantilevers resulting from the interior end of the girder translating downward with the remaining interior portions of the framing system. The bending moment diagrams for the girders in Figure 5.7 between column lines 2 and 6 have the expected shape because the shortening is more consistent among these columns and relative deformation between the ends is minimized. If one examines the bending moment diagrams for the beams in Figure 5.8 it almost appears as though the expected shape of the moment diagram (*e.g.* negative-positive-negative moment) extends from one end of the building to the other. There is very little gravity loading applied to the girders along column lines 1 and 7 and therefore, virtually all the moment in these members (at least under gravity loading) is a result of column shortening. The two central-most columns along lines C and D shorten the most and therefore, the girder spanning between C and D has very small (mostly gravity load) moment. The columns at lines B and E will be subjected to much less shortening than those along column lines C and D and also those at A and F. Thus, the beams spanning from A-B, B-C and from D-E, E-F will have moment diagrams that look like they result from vertical deformations of the beam ends relative to one another. This is in effect what is happening in the system. It should also be emphasized that the live loading applied has no reduction to reflect probability of all floors being loaded simultaneously.

5.2 Column Removal (Ineffectiveness) Rates

In order to instigate a progressive collapse scenario, rapid removal of a column was simulated. Consistent with the other model buildings studied, this rapid removal is performed by rendering a member ineffective, which compromises the structure. Discussion of this procedure is described in the SAC 3-story building

analysis chapter as well as the literature review chapter. According to the GSA guidelines, the time in which a member should be removed is approximately one-tenth of the period associated with the lowest vertical vibration mode for the structure (GSA 2003). A modal analysis was conducted on the uncompromised model frame. There were no vertical vibrational modes for the system in the first 10 modes of vibration. A typical (realistic) higher-mode vibrational shape with period of 0.495 seconds is shown in Figure 5.9.

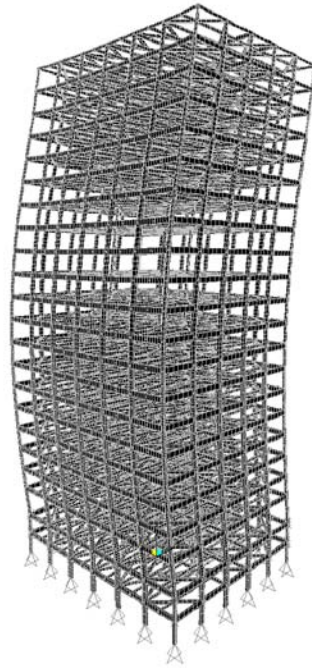


Figure 5.9 Highest Realistic Vibration Mode Of Model Structure ($T = 0.495$ sec.).

Since the only vibrational modes of engineering usefulness were lateral and torsional modes, it was decided to explore column ineffectiveness rates that were similar to those used in the previous two frame studies.

Investigation of progressive collapse may be conducted through a number of methods. While it may be valid to conduct static, linear analyses of structures with appropriate load factors that intend to account for dynamic effects; dynamic analysis was selected again for the 20-story framework. It is important to reiterate that the twenty-story building has two main areas of focus – the moment-resisting frame at the perimeter and the gravity frame at the core. Progressive collapse can theoretically be initiated anywhere within the structure, the interior gravity frame contains flexible (pinned) beam-to-girder and girder-to-column connections. As outlined previously, this condition requires that the framing rely on catenary and membrane action in the slab and steel framing system to avoid a progressive failure. Investigation related to this behavior with structural steel framing system is left for another chapter in this report. The present chapter focuses on response when perimeter columns are rendered ineffective.

It has been argued that the “correct” method of analysis is to apply gravity loadings then remove, or render ineffective, the specified member (Powell 2005). This approach has been used in the analysis of all frameworks in the present study. However, the duration of the time-history analysis has varied with the frame being considered. The loading simulation and response history analysis resulting from several column ineffectiveness rates was conducted in a manner similar to that done for the 3-story and 10-story frameworks. The time-history variation in the column load to be turned off and the gravity loading, $1.0w_D + 0.25w_L$, is shown in Figure 5.10. A gravity loading of $1.0w_D + 0.25w_L$ is applied simultaneously with the simulated column loading (*i.e.* concentrated forces) in a ramped fashion to the structure over a two second time interval. The column loads are the axial load in the column under an applied gravity load of $1.0w_D + 0.25w_L$ and their application is shown in Figure 5.11.

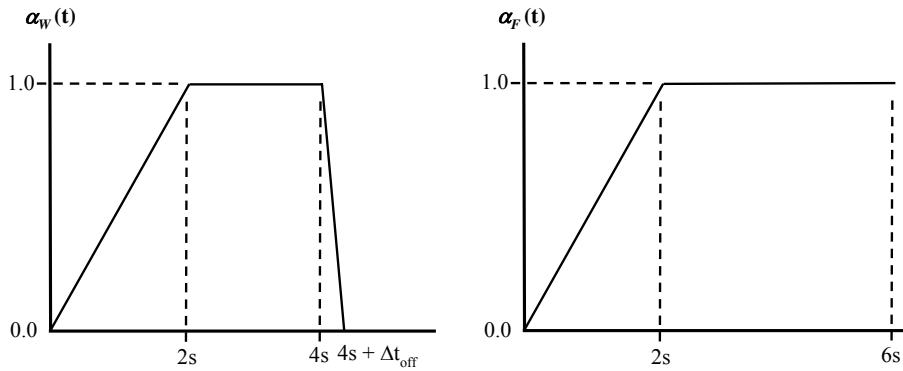


Figure 5.10 Time-History Functions Used In Analysis Of The Twenty-Story Building.

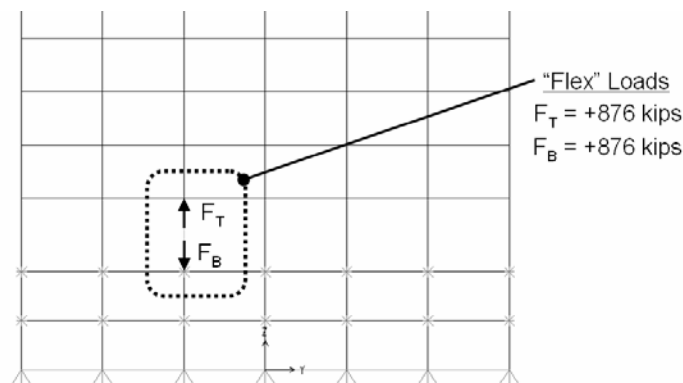


Figure 5.11 Column Loads Used to Simulate Ineffective Column.

There is an important difference in the concentrated forces used to simulate columns in this frame when compared to that used in the 3-story framework. In the present analysis, an upward force is applied at the top node of the removed column and a downward force is applied to the bottom node of the same column. This is done because a ground-floor column is rendered ineffective and statics demands that the column exert equal and opposite forces to the floors.

Once gravity and concentrated column loads have been applied, a two second “settling period” is enforced. This fixed loading period allows the structure to come to rest after the ramped gravity and column loadings are applied. Test analyses indicated that this duration was sufficient to allow the 5% damping to bring the structure to a steady state displacement. The concentrated loading used to simulate the presence of a column was then “turned-off” over a turn-off period; Δt_{off} . The time-history analysis continues with the gravity loading function held fixed at 1.0. The time history analysis carried out in this manner simulates the presence and removal of a column within the framework. Test runs indicated that a total analysis duration of 6 seconds was suitable to allow the damping levels to bring the structure to rest in a statically deformed configuration.

In order to evaluate the effect of removal rate, Δt_{off} , on the structure’s response to columns being rendered ineffective, dynamic, time-history analyses were conducted with 5% damping of the structure and a series of ineffectiveness rates. Figure 5.12 illustrates the peak displacement at a floor immediately above an ineffective column for a series of three ineffectiveness rates: 0.1, 0.05, and 0.01 seconds. The column chosen was A3 at the ground floor level.

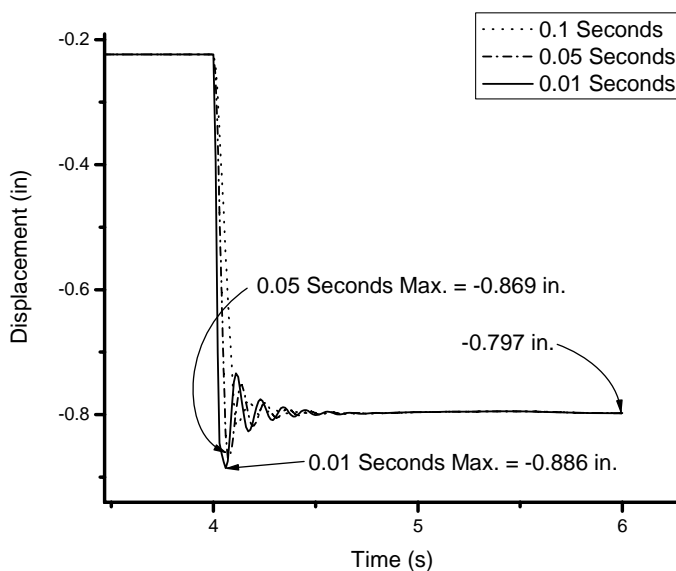


Figure 5.12 Comparison Of Turn-Off Intervals.

The results shown in Figure 5.12 indicated that ineffectiveness rates of 0.01, 0.05 and 0.10 seconds yielded significantly different results with a maximum static displacement to peak displacement ratio of 1.11. A decision was made to select the conservative removal rate of 0.01 seconds and use this ineffectiveness rate for the time-history analysis of the 20-story framework. This duration maintains consistency with the three and ten story buildings studied.

Comparison between linear and non-linear behavior was conducted at a turn off interval of 0.01 seconds to examine the impact that nonlinear geometric behavior ($P-\Delta$ and $P-\delta$) had on the response. All columns were subdivided into a minimum of two frame elements to allow the SAP2000 analysis formulation to capture $P-\delta$ effects. Figure 5.13 shows a comparison of nonlinear and linear elastic response of the structure to removal of column A3 at the ground floor level.

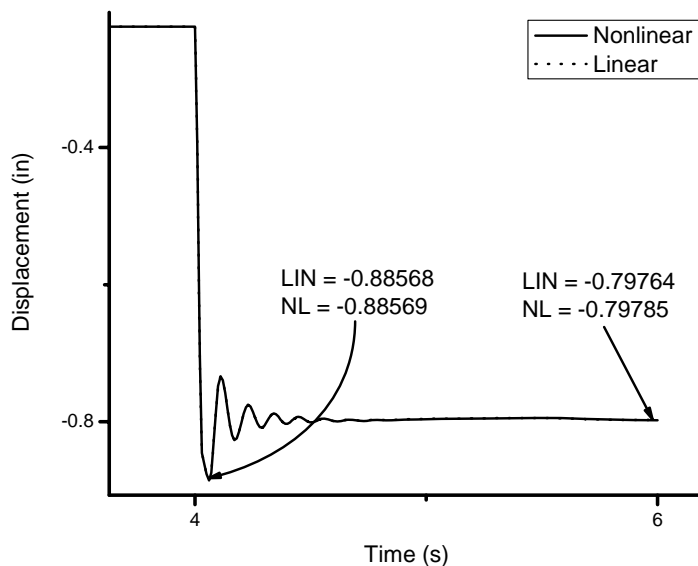


Figure 5.13 Comparison Of Linear And Non-Linear Behavior For Column A3 Removal at Ground Floor with Ineffectiveness Rate Of 0.01 Seconds.

Figure 5.13 illustrates that there is virtually no difference between the linear and nonlinear response of the system. As result, linear analysis can be used to assess demand-to-capacity ratios for members within the framework.

5.3 Time History Analysis Results for 20-Story Frame

The time history analysis conducted for the 20-story frame considered a variety of column removal scenarios at the ground floor level. Because the perimeter framing contained moment resisting frames where all girders and beams were rigidly connected to the columns (with the exception of the corner columns in the east and

west frame elevations), six column removal scenarios were identified for analysis. Each involved rendering one column at the ground floor level ineffective. The columns were chosen based on symmetry of the floor plan their ability to represent the entire structure. The ineffective columns chosen are shown in Figure 5.14.

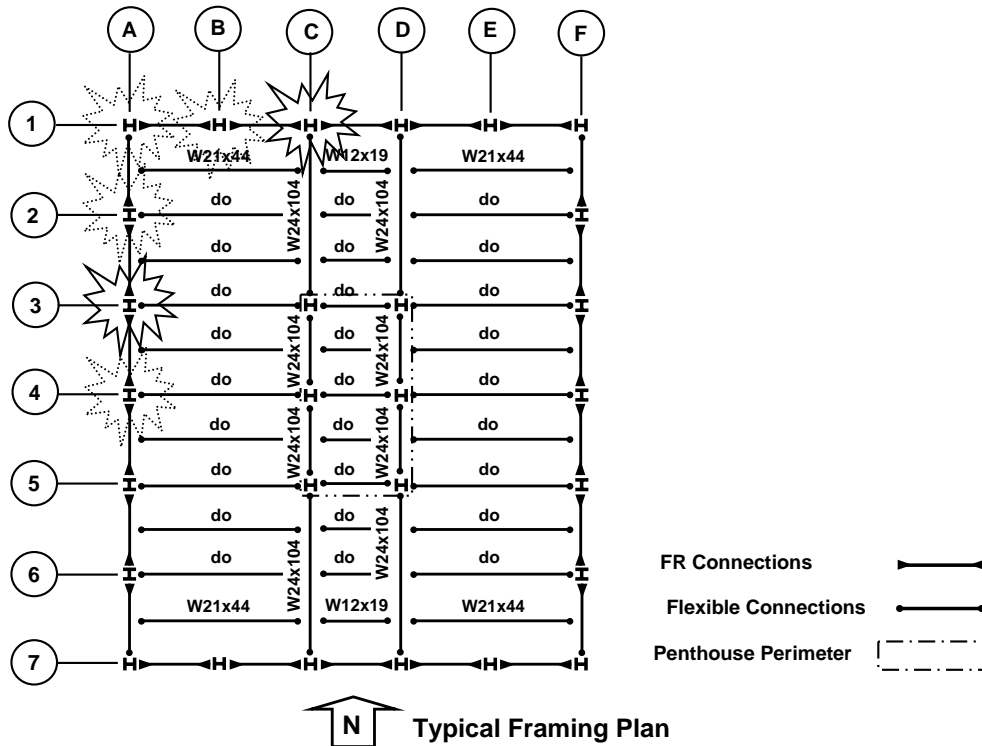


Figure 5.14 Typical floor plan with column removals. Columns A3 and C1 were found to produce maximum results.

Figure 5.13 and the preliminary analysis indicated that linear geometric analysis was sufficient to assess response of the frames if elastic material was assumed. The initial analyses conducted did assume linear material response and validity of this analysis is subsequently evaluated through use of demand-to-capacity ratios for members.

Preliminary analyses were conducted for the ineffective column scenarios shown in Figure 5.14, yielding two events that provide a representative envelope of maximum response. The removal of columns A3 and C1 were found to produce the most significant results and these scenarios were selected for detailed analysis. The framing plan used in this structural system results in very low levels of axial loading in the corner columns and therefore, loss of column A1 was not critical. Maximum vertical displacements at the floor level immediately above the ineffective column occurred between 0.0 and 0.25 seconds after column was rendered ineffective. Table 5.1 illustrates the peak vertical displacements seen during the time-history analysis, the final “settled” static displacements and a ratio of peak dynamic to static displacements. It is

important to note that nearly all the maximum axial, shear, and moment loadings occurred at the same time as maximum displacement as well.

Table 5.1 Maximum Vertical Displacements (Downward) After Column Indicated Is Rendered Ineffective.

Ineffective Column	$[\Delta_{v,max}]_{THA}$ (in.) (2)	$[\Delta_{v,max}]_{static}$ (in.) (3)	$\frac{[\Delta_{v,max}]_{THA}}{[\Delta_{v,max}]_{static}}$ (4)
A3	0.89	0.80	1.11
C1	0.81	0.73	1.11

Acknowledging the importance of strain rates in connection and member response, the time history analysis results were utilized to compute elastic strain rates for axial load, shear loading, and bending moment in the members after columns A3 and C1 were rendered ineffective over the 0.01-second interval. The procedure used in computation of strain rates is outlined in section 3.3 of the report and utilizes the central difference approximation found in Figure 5.15. Similar magnitudes for strain rates were found when removing column A3 and are not discussed herein. Figures 5.16 through 5.24 illustrate strain rates for the twenty-story frame with column C1 is compromised.

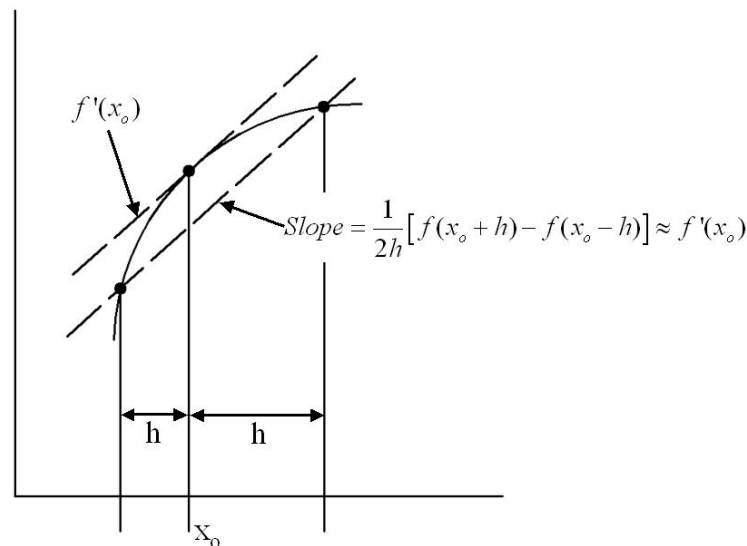


Figure 5.15 Central-Difference Numerical Approximation Used to Compute Strain Rates.

Maximum overall strain rates when column C3 is removed relative to axial load, shear and bending moment are found in Table 5.2. Figure 5.25 illustrates the locations of peak strain rates found in members

located in close proximity to the compromised column. The largest moment and shear rates were found in the beams directly above the column removed and this is reflective of the deformed shape of the structure that occurs after the column is rendered ineffective. The largest axial load strain rate was found in the column directly above and in line with the removed member. These occurrences are expected as the nodes attached to those members were subjected to the greatest displacements and also largest load reversals when the column is rendered ineffective.

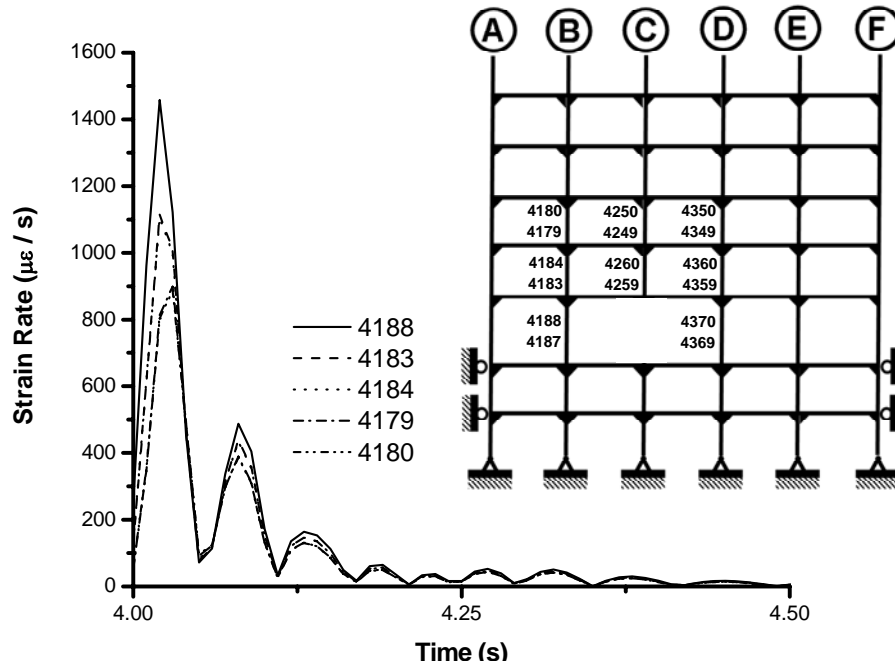


Figure 5.16 Axial Load Strain Rates For Column Stack at Line B when Column C1 Is Compromised.

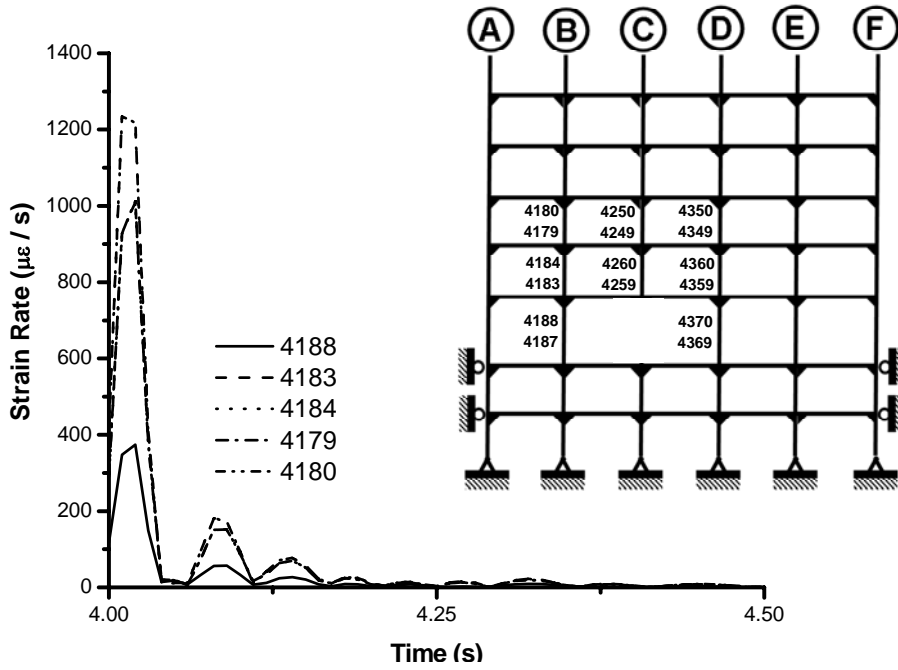


Figure 5.17 Shear Strain Rates For Column Stack at Line B When Column C1 Is Compromised.

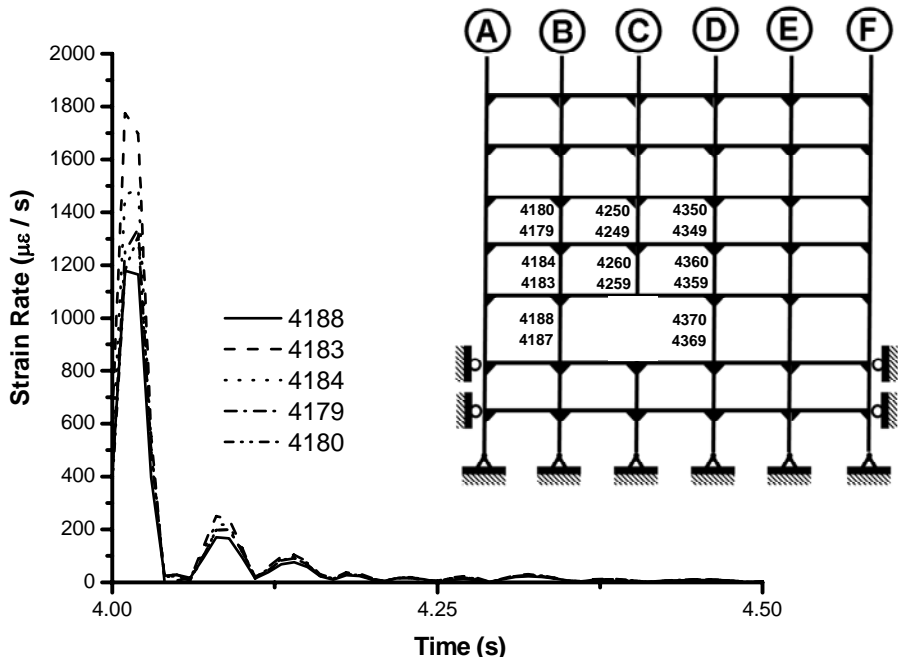


Figure 5.18 Bending Moment Strain Rates For Column Stack At Line B When Column C1 Is Compromised.

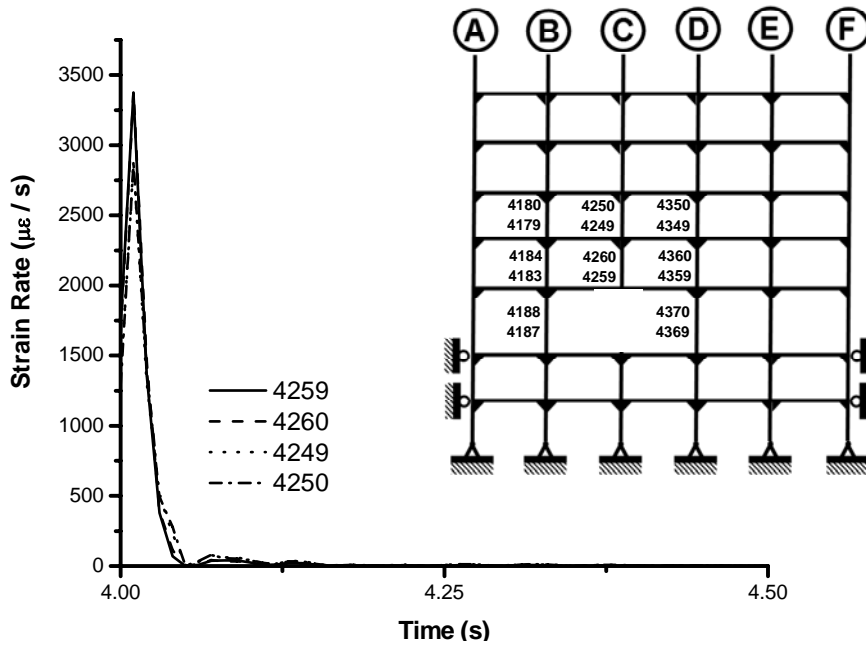


Figure 5.19 Axial Load Strain Rates For Column Stack At Line C When Column C1 Is Compromised.

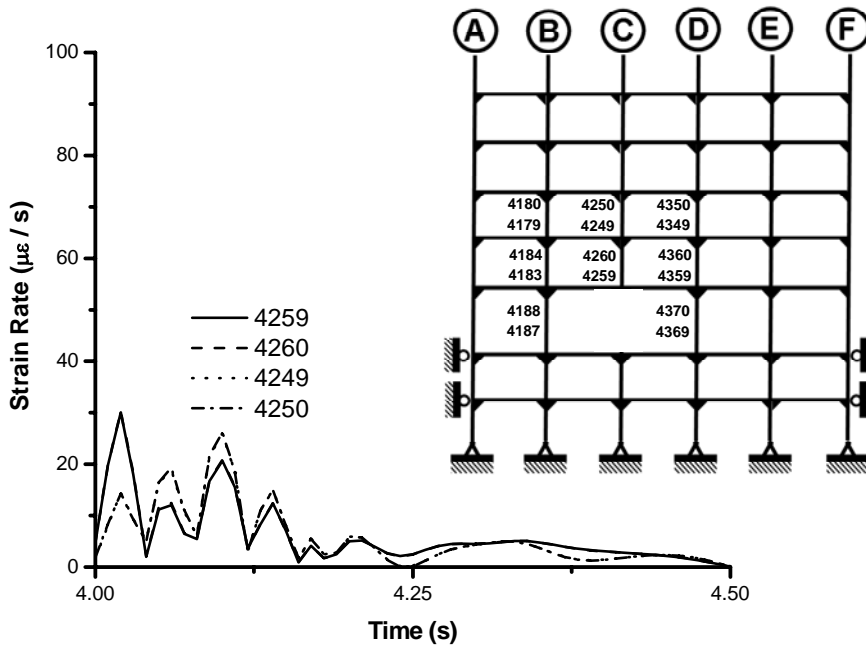


Figure 5.20 Shear Strain Rates For Column Stack At Line C When Column C1 Is Compromised.

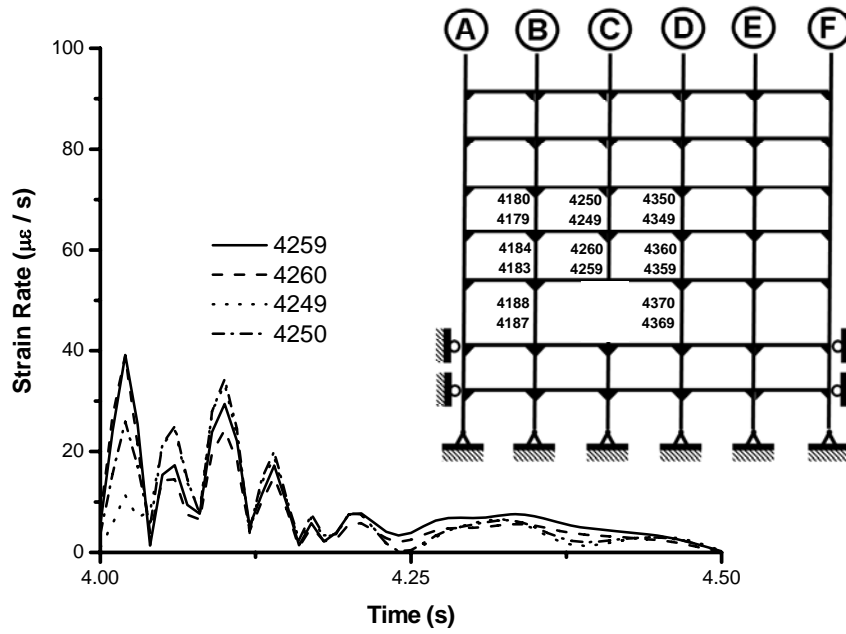


Figure 5.21 Bending Moment Strain Rates For Column Stack At Line C When Column C1 Is Compromised.

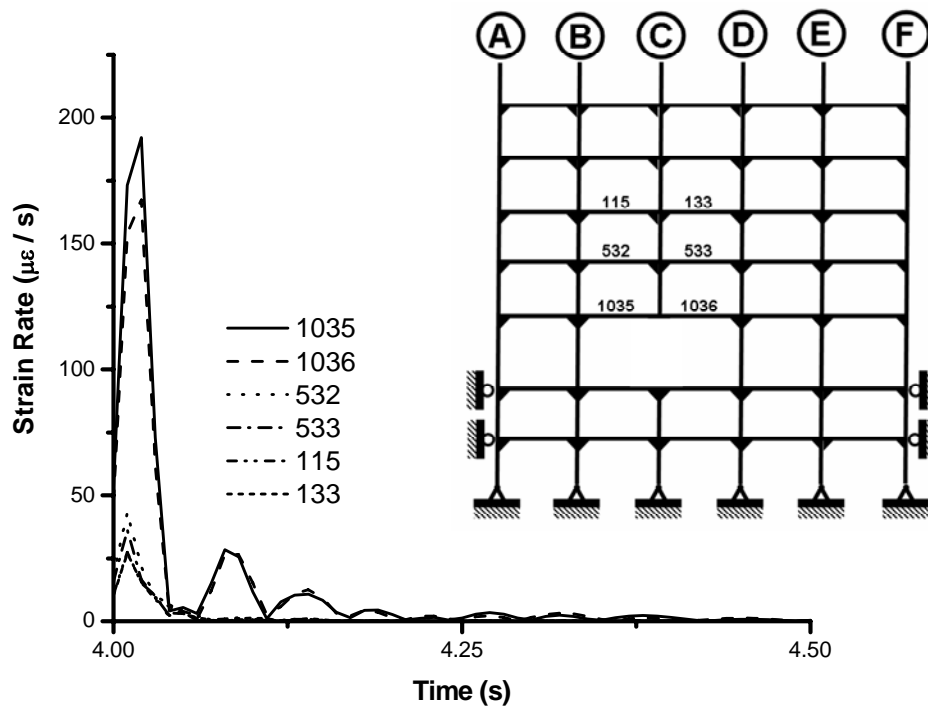


Figure 5.22 Axial Load Strain Rates For Beams When Column C1 Is Compromised.

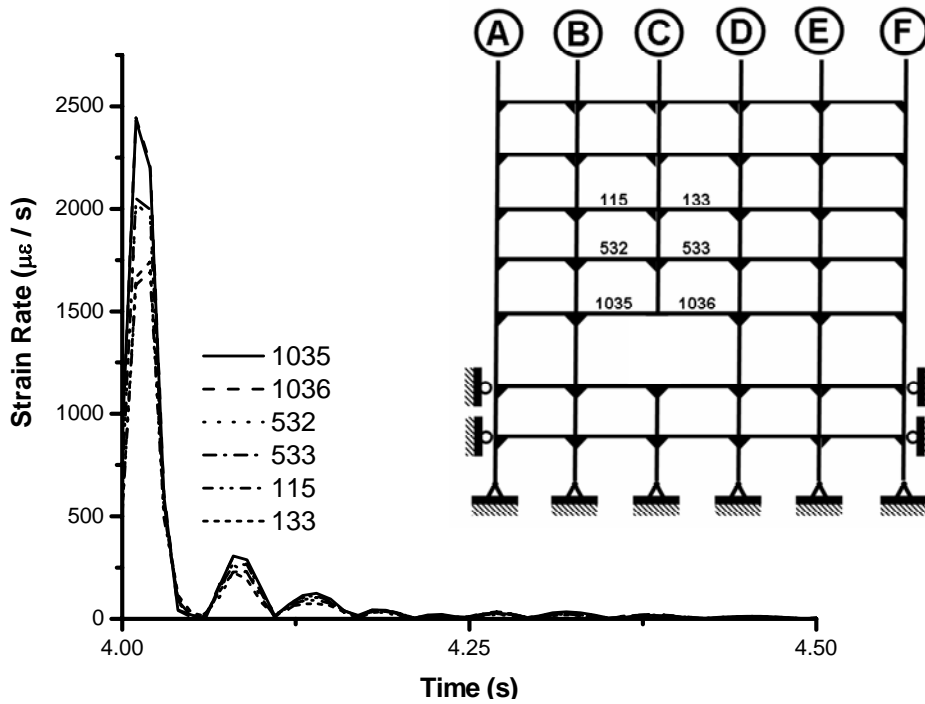


Figure 5.23 Shear Strain Rates For Beams When Column C1 Is Compromised.

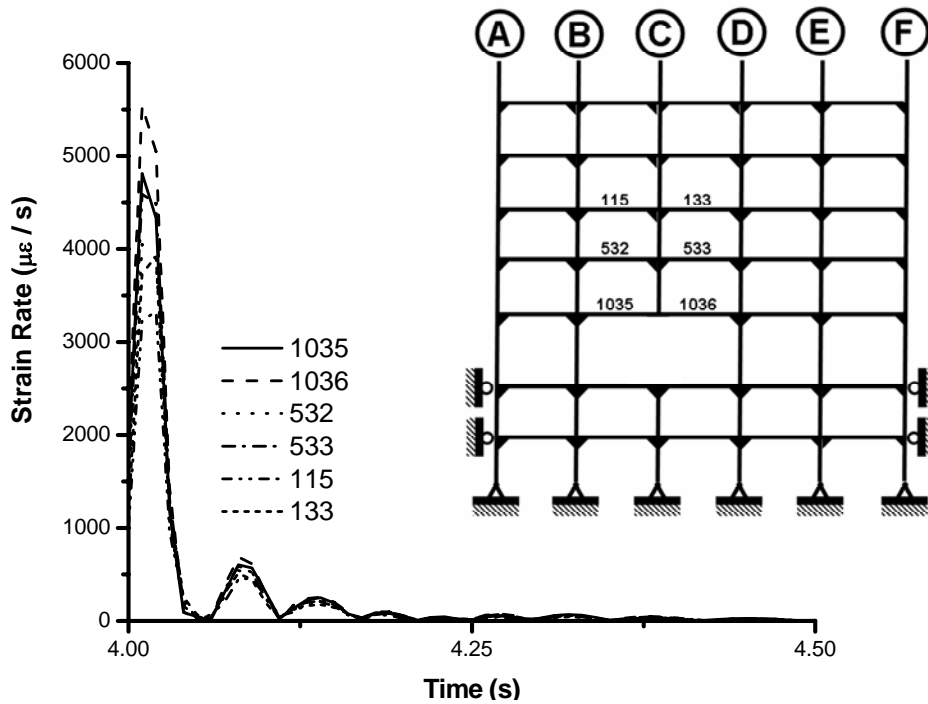
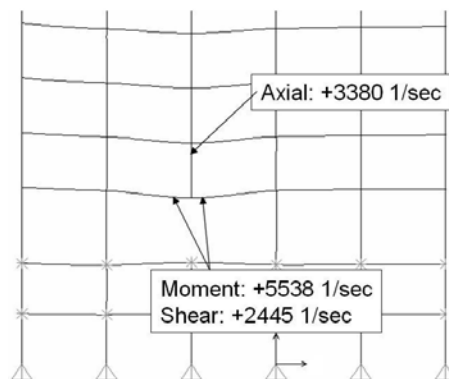


Figure 5.24 Bending Moment Strain Rates For Beams When Column C1 Is Compromised.

Table 5.2 Peak Strain Rates When Column C1 Is Compromised.

Member (1)	$\left(\frac{\mu\epsilon}{s}\right)_{axial}$ (2)	$\left(\frac{\mu\epsilon}{s}\right)_{shear}$ (3)	$\left(\frac{\mu\epsilon}{s}\right)_{bending}$ (4)
Beams	192	2445	5538
Column on Line B	1458	1238	1776
Column on Line C	3380	30	39
Column on Line D	1229	1206	1727

Recalling the discussion of strain rate effect on material fracture toughness from section 3.3, the magnitudes observed for the elastic dynamic analysis of the twenty-story model building do not generate a great deal of concern. The maximum calculated value is on the order of $0.006\epsilon/s$, which is only slightly larger than the value indicated for intermediate loading rates (Barsom and Rolfe 1999). Magnitudes to be considered dynamic loading rates ($10.0\epsilon/s$ or greater) are not observed. In general, the beams experience elevated strain rates from shear loading and bending moments. The columns adjacent to the compromised column line (B and D) observed similar strain rates due to re-distribution of all loads while the ineffective column line experiences significant straining only in an axial manner. The axial load strain rates in the column stack along column line C are elevated, but not of concern.

**Figure 5.25** Locations Of Largest Strain Rates When Column C1 Compromised.

One interesting item of note is that since the ground floor columns are rendered ineffective, there is actually a “rebounding” of the floor upward after the column is removed. The rebound is created by the build up of internal compressive strain energy in the framing below the column being rendered ineffective. This phenomenon can be seen in Figure 5.25. In the chapter related to the SAC 3-story building analysis, it was

recommended that moment resisting connections be designed for moment reversal. This rebounding effect suggests that moment resisting connections at the ends of beams (be they in-fill or otherwise) should be designed for reversal of moments and should not be designed as unidirectional.

The strain rates are relatively inconsistent among all frames considered in the study. In general, the strain rates in the 3-story frame had the largest strain rate magnitudes and the 10- and 20-story frames had much smaller strain rate magnitudes (order of magnitude less). The reason for this can be qualitatively appreciated through consideration of the peak displacements that the floor levels are undergoing and the time duration over which this displacement change occurs. The 3-story frame nodes undergo much larger displacements (nearly an order of magnitude larger) over nearly the same time frame as the nodes in the 10- and 20-story frame. Thus, the strain rates for the members in the 3-story frame are much larger. As done in the previous frames, the geometric effects in the connections were ignored when evaluating strain rates.

Similar to the three- and ten-story frame analyses, demand-to-capacity ratios (DCR) for individual members were developed to provide a venue for evaluating the variety of axial, shear and bending loads in the members of the twenty-story frame. The DCR's were again defined as,

$$DCR = \frac{P}{P_n} + \left(\frac{V}{V_n} \right)^2 + \frac{M}{M_n} \quad (5.1)$$

The nominal axial, shear and moment capacities of each member were calculated using the recommendations of AISC (AISC 2005a). Resistance factors of 1.0 were used. It should be noted that flexural buckling about both major and minor axes, lateral torsional buckling, and local buckling effects were accounted for in capacity computations. Shear capacity was calculated using the area of each member's web, including any contribution of flange thicknesses. Also, the expected yield strength, not lower-bound strength, was used for computations. A majority of the steel shapes used in the twenty-story model frame are classified as Group 1 or 2 shapes, and thus, a 10% increase in the expected yield strength was used (FEMA 2000b). The unbraced lengths for determining bending moment capacities of the columns were taken as the story height from centerline to centerline of the beams. Preliminary analysis indicated that the beams were subjected to tensile forces when the column becomes ineffective and therefore, the axial capacity of the beams were taken to be the tensile capacity based upon gross cross-section area. Finally, the buckling mode shapes seen in the eigenvalue analysis indicated that the effective length factors for all members could be taken as 1.0.

An elastic time history analysis (linear geometric effects were assumed as justified previously) with column ineffectiveness rate equal to 0.01 seconds was used to generate axial loads, shear loads, and bending moments throughout members in the framework. Two ineffective column scenarios were considered: column

C1 removed and column A3 removed. Keys to member results for these scenarios are given in Figures 5.26 and 5.27.

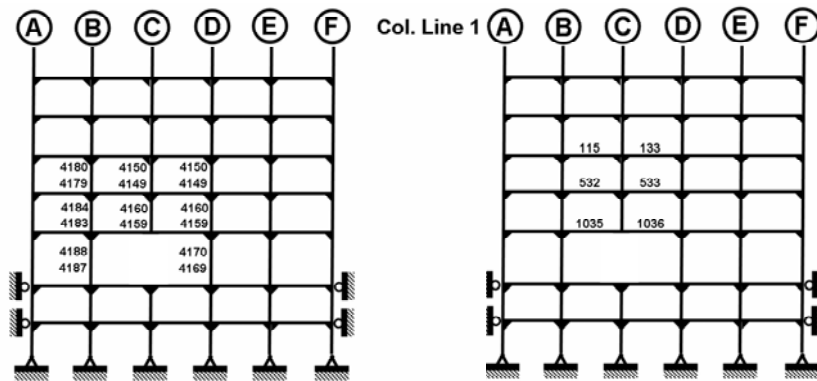


Figure 5.26 Member Numbers When Column C1 Is Rendered Ineffective.

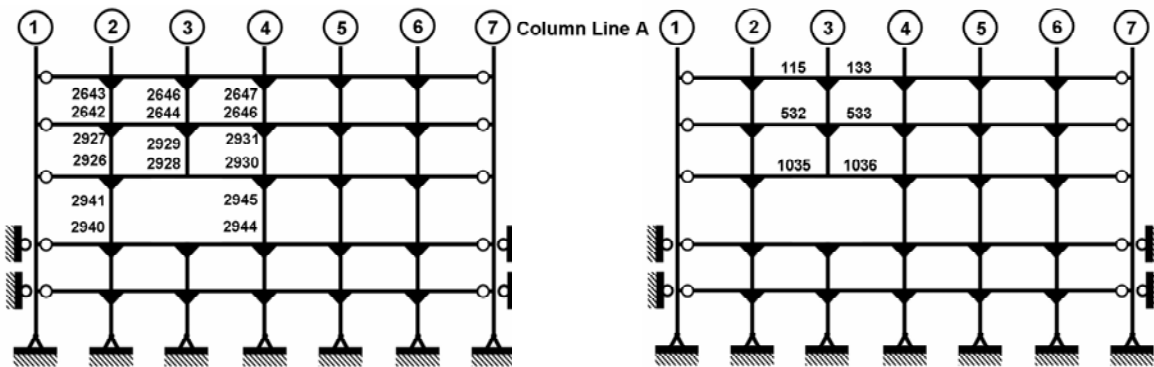


Figure 5.27 Member Numbers When Column A3 Is Rendered Ineffective.

Figures 5.28 through 5.33 illustrate member DCR's when columns C1 and A3 are rendered ineffective. It can be seen that in no instance for the twenty-story frame do the computed DCR's exceed 1.0. As a result, non-linear material analysis incorporating load-limiting hinges similar to that conducted for the 3-story frames is not required. In addition, it was found that the load levels in most members were similar to those levels found in the uncompromised structure. This indicates a very high degree of redundancy and robustness within the frame. One should keep in mind that the compromising scenario is loss of a single column.

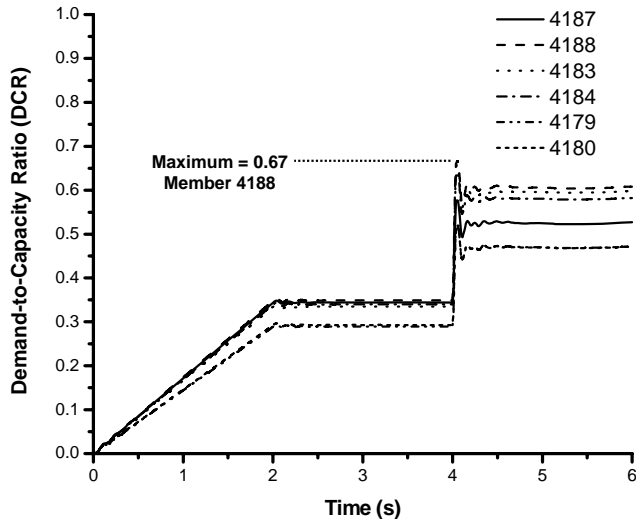


Figure 5.28 Demand-To-Capacity Ratios Along Column Line B When Column C1 Is Rendered Ineffective.

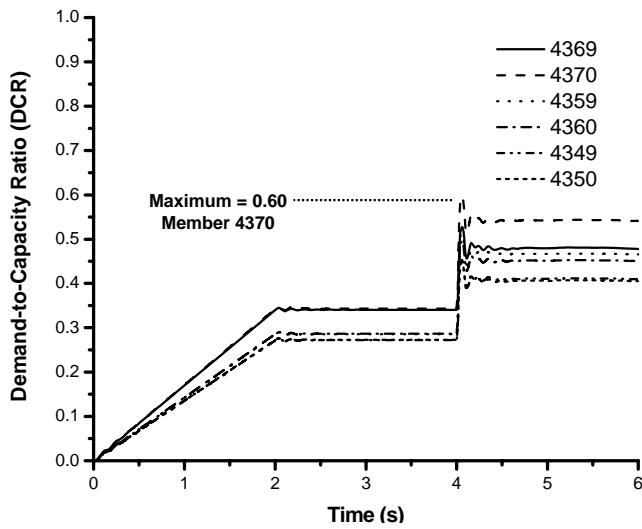


Figure 5.29 Demand-To-Capacity Ratios Along Column Line D When Column C1 Is Rendered Ineffective.

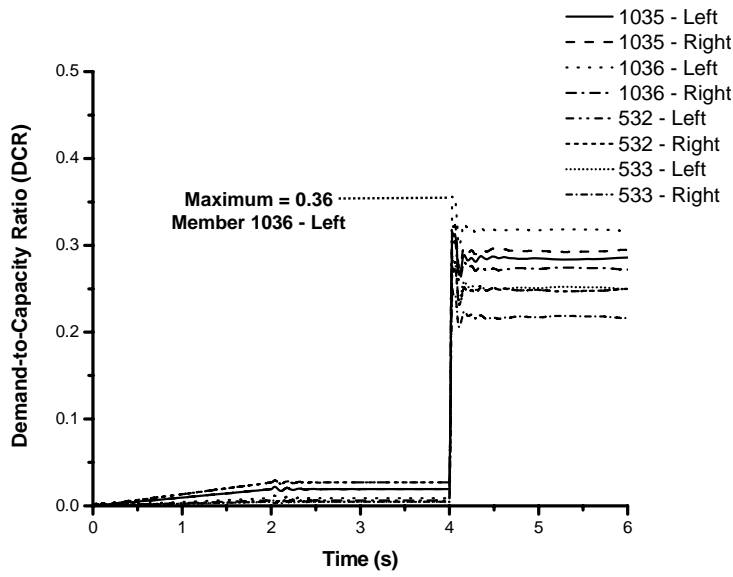


Figure 5.30 Demand-To-Capacity Ratios In Exterior Beams When Column C1 Is Rendered Ineffective.

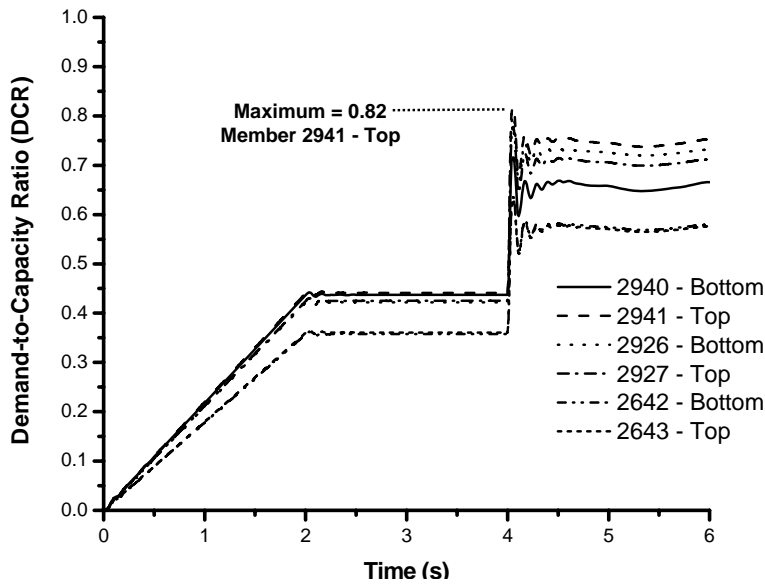


Figure 5.31 Demand-To-Capacity Ratios Along Column Line A2 When Column A3 Is Rendered Ineffective.

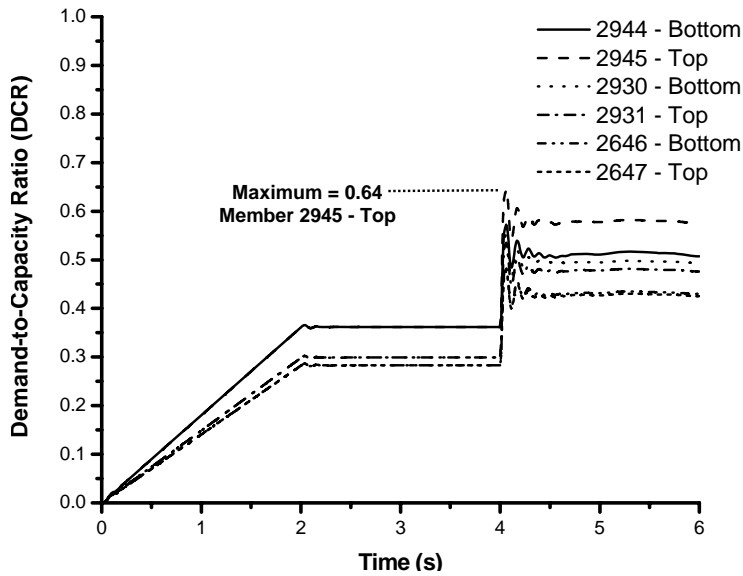


Figure 5.32 Demand-To-Capacity Ratios Along Column Line A4 When Column A3 Is Rendered Ineffective.

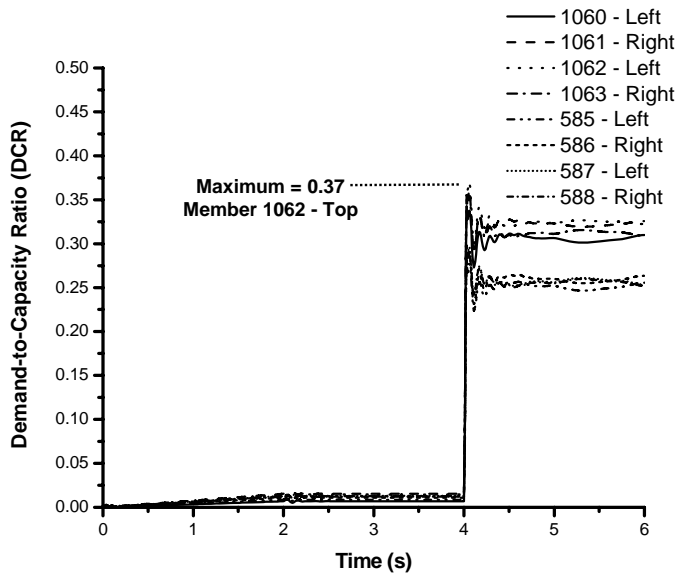


Figure 5.33 Demand-To-Capacity Ratios In Beams When Column A3 Is Rendered Ineffective.

5.4 Concluding Remarks

It is apparent that the twenty-story model frame contains a significant degree of redundancy through the computed strain rates of connections and demand-to-capacity ratios of members. Admittedly, this was expected going into the analysis. When a compromising event occurs in the exterior perimeter frame (*e.g.* a single column becomes ineffective), the model engages a large number of adjacent members in the vicinity of

the event to distribute the loading to other members within the framework. As the twenty-story building has a large number of members relative to the three- and ten-story model buildings, the frame is able to sustain a significant event without much difficulty. Of course, rendering multiple columns within any given story would change the conclusions drawn here, but as outlined in the literature synthesis and review, the objectives of the present study were to attempt to quantify robustness and recommend general structural integrity provisions for steel systems. Removal of multiple columns in story would imply threat-specific knowledge and that is best handled with threat-specific design provisions.

A number of connections within the frame experienced a loading reversal (e.g. connection immediately above compromised column; and connections immediately below due to rebound) indicating that all rigid connections within moment-resisting frames be designed for complete moment reversal. That is to say, if a moment connection is to be used in a structural system, it should be capable of resisting positive and negative moments of the same magnitude.

It is also apparent that significant dynamic load increases are not present from the compromising events considered. The dynamic response of the structure indicates only an 11% increase in deflection due to the ineffectiveness of a column. This suggests that the 2.0 multiplier for loads present during the compromising event to simulate dynamic effects may be appropriate for a limited number of frame configurations and types (e.g. the three-story framework considered in this study). Again, the significant redundancy of the frame can be attributed to limiting the dynamic effect. Through the previous two model buildings studied, it can be concluded that less redundant frames exhibit greater dynamic effects.

Strain rates resulting from column ineffectiveness rates of 0.01 seconds were found to be very close to those strain rates classified as intermediate or below (Barsom and Rolfe 1999). The 5% damping magnitude (felt to be conservatively low) was also seen to be sufficient in reducing these strain rates very rapidly with time after the “event”. Again, connection geometric effects were ignored.

The axial forces present in the beam members resulting from activation of Vierendeel action in the frame are of minor consequence. The number of stories available above the compromised portion of the framework is directly related to the required tie forces generated to span the compromised regions of the structure. For the present 20-story frame and compromising scenario considered, these tying forces can be taken as those computed for the 3-story framework.

This analysis of the twenty-story frame was limited to independent removal of two ground level columns. While preliminary analyses ruled out the study of more columns in the ground level of the structure, other compromising events may have more significant effects. For instance, had members been compromised at higher levels within the structure, greater dynamic effects and strain rates would be expected.

The effects seen with this alternate event would be expected to be similar to those found in the three-story frame. While upper level columns of the structure support a lesser magnitude of load, fewer members are available to distribute loading after the compromising event. Additionally, the events leading to ineffective members at the interior of the frame were not studied. The presence of flexible connections between interior columns and beams/girders suggests an inherent instability in the event that a column becomes ineffective (*i.e.* if pinned connections are assumed, a mechanism is created *a-priori* once an interior column is rendered ineffective). The development of catenary action internal to the perimeter frame warrants further consideration and detailed analysis. These issues are addressed in a separate chapter of the report.

Chapter 6

Membrane and Catenary Action

6.1 Introduction

The chapters of the report devoted to the SAC 3-, 10-, and 20-story buildings provided many insights into the inherent robustness and inherent structural integrity of the steel framing system and the manner in which the steel skeleton redistributes loading when critical load carrying components become *ineffective*. However, the analyses carried out and synthesized in these sections did not consider what may happen at locations within the steel skeleton outside the perimeter at the ground floor level, and did not attempt to quantify inherent structural integrity contributed by components other than the steel skeleton. Furthermore, the analytical models assumed that pin-connected beams and girders existed at interior columns and these analytical models did not support analysis considering ineffective interior columns, interior girders, exterior girders, or in-fill beams. If robustness in the structural steel framing system is to be quantified, the analyses must go beyond the simple removal of columns around the perimeter of the framework.

The objectives of this chapter in the report are three-fold: (a) provide a targeted review of literature pertaining to catenary and membrane action in the floor plate and floor framing members within the structural steel building system; (b) provide a brief overview of the methodologies that have been proposed and validated via experimental testing for quantifying the catenary and membrane mechanisms in concrete floor framing systems; and (c) outline a new methodology for quantifying the membrane and catenary capacity in structural steel floor framing systems along with high-level provisions for ensuring structural integrity through the preservation of catenary and membrane action in the floor system.

6.2 Tension Action in Concrete Floor Systems

Researchers in the field of reinforced concrete have had a long history of attempting to understand the tensile behavior of structural concrete floor framing systems and proposing methodologies for quantifying the beneficial effects of catenary action and membrane action in concrete floor plates. Much of the research conducted in this regard has made its way into ACI 318 provisions for structural integrity (Hawkins and Mitchell 1979; Mitchell and Cook 1984). Researchers studying the response of structural steel systems to fire have also begun in earnest to understand and capitalize on the inherent robustness present in steel framing systems that is contributed by the concrete deck (Allam *et al.* 2000; Bailey *et al.* 2000; Huang *et al.* 2003a; Huang *et al.* 2003b).

The objective of this section is to review the findings of these past research efforts and extract pertinent information and procedures from them that can support a methodology for quantifying the membrane and catenary action in the steel system floor plate and provide a basis for the development of simple structural integrity provisions that can lead to enhanced robustness.

It has been long recognized that flat plate concrete floor systems have the potential to suffer from disproportionate collapse from a rather simplistic event: punching shear failure at interior and exterior columns (Hawkins and Mitchell 1979; Mitchell and Cook 1984). There was a series of systematic efforts carried out to develop design procedures that could limit the probability of a punching shear failure leading to progressive collapse. The first of such efforts was that conducted by Hawkins and Mitchell (1979). The result of this effort pertinent to this section is the proposed method for quantifying the membrane capacity of an orthogonally-reinforced concrete floor plate. Mitchell and Cook (1984) enhanced this methodology to include procedures that allow quantifying the role of catenary action in the behavior of the floor system and its partnering with membrane action to mitigate progressive collapse in concrete floor systems.

Hawkins and Mitchell (1979) provide a very nice description of the development of membrane action in the concrete flat-plate floor system and it is prudent to parallel that discussion here as it lays a foundation for much of the theory and assumptions for the equations that quantify membrane capacity to follow. When a concrete floor plate is loaded to the point of inelastic behavior, there is a tendency for the bottom fibers (assuming loading is from the top) to lengthen. This lengthening, however, is restrained by the concrete slab at the perimeter of the panel being loaded. Of course, steel beams in the systems considered in the present study will provide restraint to this movement. In the purely theoretical sense, the concrete slab will have a load versus vertical deflection response that exhibits snap through prior to the formation of membrane tension in the system. This *hanging net* effect cannot take place without significant vertical deformation. In the hanging configuration, all sections through the floor plate are subjected to tensile forces and it is imperative that properly developed tension reinforcement exists in the slab. In the usual structural steel floor system, there is welded wire fabric/mesh present as well as the steel form- or composite-deck.

The beauty of the work of Hawkins and Mitchell (1979) is that the expressions for computing the membrane capacity of concrete floor panels are rather simplistic and include a significant amount of *engineering feel*. More complicated methods for computing membrane capacity of slab systems are available (Park 1964; Regan 1975; Park and Gamble 1980). The fundamental assumption of the proposed methodology is that the deformed membrane between supports follows a circular shape. This makes the mathematics tractable and errors are minor when compared to the more correct catenary parabola. The basic slab system and membrane forces considered are schematically shown in Figure 6.1.

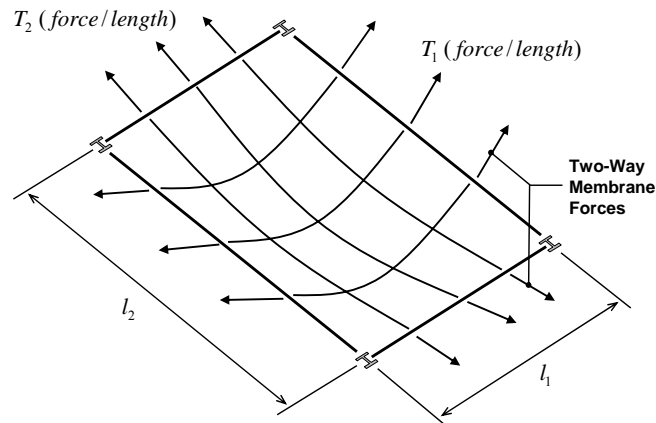


Figure 6.1 Two-Way Membrane Action in Reinforced Concrete Slab.

Two slab span directions are assumed. The first is defined as the short direction; l_1 . The second is termed the long direction; l_2 . Reinforcement is assumed to be present in both directions. The reinforcement area on a per unit length basis in the short and long directions are A_{s1} and A_{s2} , respectively. The normal strains in the fibers of the membrane are assumed to be uniform over the membrane thickness and are functions of the curvature in the membrane. Uniformly distributed loading over the surface of the membrane is assumed and positive loading is taken to be downward. Membrane tension forces (edge tensions) per unit length parallel to the short and long directions are T_1 and T_2 , respectively. These forces are assumed to be in the direction tangent to the deformed membrane's mid-surface at the edges.

Some of the fundamental membrane and catenary behavior principles should be reviewed at this point because they do have significant impact on the forces to expect with this type of behavior as well as the deformations to be expected. At this point, we will simply discuss catenary action because the membrane behavior that will be outlined is simply two-way catenary behavior. The fundamental free body diagram for catenary behavior is shown in Figure 6.2. The tension force in the membrane follows a tangent to the deformed shape at any point along the catenary's deformed shape. At the edge of the catenary, there is a tension force resultant, T_{\max} , and a force at the centerline of the catenary, T , when the uniformly distributed loading, w_o , is applied. A major structural engineering-related issue that needs to be considered when examining catenary and membrane behavior in floor systems is the trade-off between allowing significant catenary deflection, h , and the peak tension force.

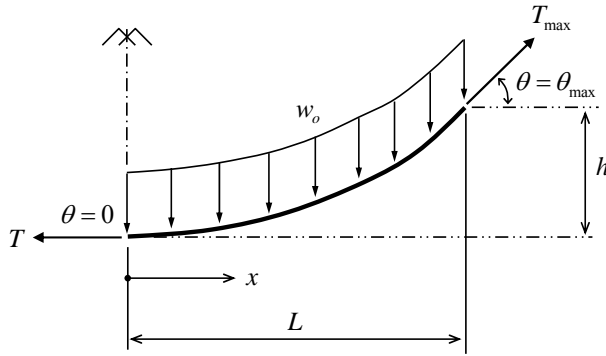


Figure 6.2 Fundamental Representation of Catenary Action.

The catenary forces will significantly increase if the shape of the catenary is held close to the horizontal plane (*e.g.* a tight-rope). If one does not allow significant deflection in the catenary to occur, tension forces can become very large, thus rendering catenary action infeasible. If one allows significant deflection in the catenary and the strains in any deflected shape assumed will not exceed those corresponding to rupture, these tensile forces can be reduced. This is the fundamental dilemma that needs to be addressed with catenary and membrane action.

Attention can now be turned to membrane action in the concrete floor system illustrated in Figure 6.1. A typical structural mechanics solution procedure (*e.g.* imposition of vertical equilibrium, ensuring compatibility of deformations, and adherence to constitutive laws for the material) is employed to develop a relationship for the capacity of the tensile membrane that is a function of the edge tension, strain in the membrane (and therefore, vertical deflection) and the panel dimensions. When the panel dimensions differ (*i.e.* they are rectangular) the membrane capacity of the panel based upon the tensile reinforcement capacity at the edges can be written as (Hawkins and Mitchell 1979),

$$w_{edge} = \frac{2T_1 \sin(\sqrt{6\varepsilon_x})}{l_1} + \frac{2T_2 \sin\left(\frac{l_1}{l_2} \sqrt{6\varepsilon_x}\right)}{l_2} \quad (6.1)$$

where: ε_x is the tensile strain in the membrane fibers parallel to the short direction, which is the dominant direction. If the slab panel is square, there is no dominant direction. As l_2/l_1 increases, the slab panel begins to behave as a single direction membrane (*i.e.* a catenary).

Concrete slab systems quite often have different reinforcement patterns at the edges than that found in the *middle strip* areas within the panel span. This difference can be better appreciated by examining Figure

6.2 and noting the difference in catenary forces at the mid-span and edge. As a result, if the mid-span reinforcement controls the tensile capacity of the membrane, the vertical load carrying capacity is (Hawkins and Mitchell 1979),

$$w_{pos} = 2\sqrt{6\varepsilon_x} \cdot \left[\frac{T'_1}{l_1} + T'_2 \cdot \frac{l_1}{l_2^2} \right] \quad (6.2)$$

where: T'_1 and T'_2 are the tensile membrane forces per unit length within the mid-span (positive moment) regions of the panel parallel to the short- and long-directions, respectively.

The tensile membrane forces in equations (6.1) and (6.2) are nothing more than the forces in the reinforcement per unit length around the perimeter of the panel. These forces must take into account the stress-strain relationships for the steel reinforcement. Furthermore, the strain in the direction parallel to the short and long dimensions of the panel are related to one another as a result of the assumed circular shape of the membrane. If one knows the strain in the direction parallel to the long dimension, the strain in the direction parallel to the short dimension is computed using (Hawkins and Mitchell 1979),

$$\varepsilon_1 = \varepsilon_2 \cdot \left(\frac{l_2}{l_1} \right)^2 \quad (6.3)$$

Therefore, once the strains in the two directions are computed (long direction assumed, then short direction computed), the constitutive laws for the reinforcement can be used to determine the state of stress and then the tensile membrane forces on a per foot basis follow.

Hawkins and Mitchell (1979) provide comparison of the membrane capacity predictions made using equations (6.1) and (6.2) with experimental testing. The comparison is quite favorable given the relative simplicity of these equations.

An expression for the central deflection in the panel has been provided by Mitchell and Cook (1984). Once the strain in the direction parallel to the short direction is known, the maximum deflection within the panel can be computed using (Mitchell and Cook 1984),

$$\delta = \frac{3l_1\varepsilon_1}{2\sin(\sqrt{6\varepsilon_1})} \quad (6.4)$$

The vertical deflection is important when assessing the capacity of the membrane. Assuming end anchorage is present, the membrane is capable of carrying more loading in a highly deflected configuration for a fixed tensile force capacity. Therefore, if a large amount of loading is present and there is a fixed tensile capacity for the reinforcement in the membrane (assuming no rupturing of the reinforcement), then there is a tendency

for the membrane to continue to deflect vertically to generate greater vertical components in the catenary forces. Therefore, the vertical deflection given by equation (6.4) can be used to determine if a slab panel will become debris loading for a panel below, or will impede modes of egress from the structure. The horizontal component of the maximum tensile force at the edge of the catenary/membrane shown in Figure 6.2 indicates that if this horizontal force can be resisted by compression rings in the slab system by providing proper edge restraint to the slab panel (*e.g.* a steel beam with positive connection to the slab system) the slab system can generate much of the needed membrane action itself.

Mitchell and Cook (1984) provide an enhanced description of the post-failure response of concrete slab structures that is pertinent to situations that are encountered in the present study. It was felt that reviewing several observations of experimental behavior outlined in this effort was important. The response of a slab structure after initial failure depends upon the amount and details of the steel reinforcement, the vertical support conditions and the horizontal restraint conditions at the panel edges (Mitchell and Cook 1984). When the slab panel has vertical support surrounding its edges (*e.g.* steel beams at the perimeter of the panel), the slab is capable of providing its own in-plane compression ring restraint conditions at the perimeter. This compression ring helps to resist the horizontal component of the maximum tensile force shown in the free-body-diagram in Figure 6.2. If the edges of the panel are allowed to deform vertically, then this compression ring cannot form.

When “stiff” beams are present at the perimeter of the slab panel, the membrane action in the slab panel facilitates the slab system hanging off the perimeter beams. When an interior slab panel is considered, the adjacent regions of the floor system will help to restrain the edges of the overloaded panel. Edge or corner panels can develop the necessary compression ring behavior if the edges are supported by beams that have significant flexural stiffness when compared to the slab itself.

A situation where formation of the compression ring restraint is unlikely in a concrete slab system is an edge panel in a two-way slab system without beams. The vertically stiff beam is not present in this situation and therefore, a one-way membrane is likely to form. This one-way membrane attempts to activate the in-plane restraint offered by adjacent panels that are not overloaded. When the beams of significant relative stiffness are not present at the edges of the panel, the one-way membrane is supported with catenary action between columns in a direction orthogonal to the one-way membrane’s spanning direction. Corner panels behave in a similar manner with the catenary action occurring diagonally between columns.

When one-way catenary action is present in the floor framing system, the fundamental structural mechanics theory related to catenary behavior can be utilized. The catenary subjected to uniformly distributed loading, w_o , shown in Figure 6.2 will be utilized as a basis for the following discussion. The

catenary sag is denoted as h . One-half the catenary span is defined as L . Two catenary capacities can be computed. The first is controlled by the maximum tensile force at the edge of the catenary panel, T_{\max} . In this case the uniformly distributed loading capacity of the catenary can be computed using (Hibbeler 2006),

$$w_{ou,1} = \frac{T_{\max}}{L} \cdot \left[1 + \left(\frac{L}{2 \cdot h} \right)^2 \right]^{-0.50} \quad (6.5)$$

The second considers the catenary tension force at mid-span as the controlling force. In this case, the uniformly distributed loading capacity of the catenary can be computed as (Hibbeler 2006),

$$w_{ou,2} = \frac{2 \cdot T \cdot h}{L^2} \quad (6.6)$$

The uniformly distributed forces that are applied to the catenary arise from either one-way or two-way membrane action in the slab system. The load paths within an overloaded slab system must be studied in order to determine these uniformly distributed loading magnitudes.

Equations (6.5) and (6.6) indicate that the loading capacity of the catenary is tied to the *sag*. One should keep in mind that as the sag increases, the length of the catenary relative to the horizontal span increases. In the case of steel floor systems an originally horizontal element (*e.g.* a light-gauge deck panel, a bar within welded-wire mesh) will become a sagging – catenary – element. Therefore, the change in length between the initial horizontal configuration and catenary configuration will lead to significant straining in the components. Therefore, the length along the profile of the catenary is very important and, if known, will allow computation of strains in the catenary components.

The fundamental theory of the parabolic catenary can be used to develop a relationship for the length along the catenary parabola using a simple line integral. The equation of the parabola given in Figure 6.2 is (Hibbeler 2006),

$$y = \left(\frac{h}{L^2} \right) \cdot x^2 \quad (6.7)$$

Using equation (6.7) in an expression for the length along the catenary (application of the Pythagorean Theorem), the length of the catenary can be easily computed by evaluating the integral along the line-length of the parabola. It should be noted that one-half the length of the parabola is considered. The length of the catenary is given by,

$$L' = \int_0^L \left[\sqrt{1 + \frac{4h^2}{L^4} x^2} \right] dx \quad (6.8)$$

Equation (6.8) can be used to compute the length of the components in the catenary in its deformed position and this length can be used along with the initial length to compute strains for estimates of ductility demand in the catenary system.

6.3 Membrane Action in Composite Deck Structural Steel Systems

Although structural steel floor framing systems are significantly different in many ways than that of a two-way flat plate or flat slab cast-in-place concrete system, there are enough similarities to justify using the theory and expressions developed by Hawkins and Mitchell 1979 and Mitchell and Cook (1984) in assessing the robustness of structural steel framing systems. This section of the report will outline the assumptions made regarding the composite concrete-steel deck floor framing system, and its impact on membrane and catenary behavior.

It is felt that membrane and catenary action are indeed possible within the structural steel framing systems commonly found in buildings. More importantly, it is felt that this catenary and membrane behavior, to a large extent, is inherent in the systems typically constructed. The tension reinforcement present in these systems will need to be quantified and their anchorage discussed prior to detailed examination of ineffective supporting member scenarios.

In composite steel-concrete floor systems, there is typically welded-wire mesh and light gauge steel deck that can be utilized as tension reinforcement within the slab system should membrane and/or catenary action be needed. However, one must understand the usefulness of these components as reinforcing mechanisms in the slab system before one can count on this reinforcement as being inherent sources of membrane and catenary reinforcement for the floor system.

The light-gauge steel deck is essentially a uni-directional spanning entity. In the direction parallel to the flutes in the deck, the steel deck is highly likely to be a very useful form of tension reinforcement for facilitating catenary action. However, in the direction orthogonal to the flutes, the steel deck likely has puddle welds or TEK screws that are unlikely to preserve tensile forces within the deck in this orthogonal direction. Furthermore, the fluted nature of the deck results in a tension force that has two distinct elevations at the floor deck soffit. This makes relying on the steel deck providing tensile membrane or catenary reinforcement in two directions questionable. Therefore, the present analysis assumes that the steel deck provides one-way reinforcement within the floor framing system. It is recommended that the two-way spanning capability of the concrete-steel composite deck system be evaluated in future efforts. If this is done, this conservative assumption can be relaxed. It should be noted that if the steel deck panels are not continuous over the supporting beam, a force-transfer mechanism is questionable.

The welded-wire fabric present in the floor system is also a source of membrane and catenary tension reinforcement. This steel fabric generally has a slightly elevated yield stress when compared to the usual mild-steel reinforcement. Furthermore, the spacing of the wires in the mesh can change with direction. This reinforcement will be assumed as sufficient to develop catenary and membrane forces if it is considered continuous through the panel perimeter.

In the steel building system considered in this study, a panel is defined as having in-fill beams and/or girders bounding a panel of concrete slab. In most cases, the perimeter of the slab panel will have puddle welds or even steel studs connecting the steel deck to the perimeter beams/girders. Furthermore, these perimeter members will have significantly greater flexural stiffness when compared to that of the slab. As a result, the slab system can be assumed to develop compression ring anchorage if the perimeter members and perimeter connectivity remain in tact during a compromising event.

The basic process used to assess and quantify the membrane and catenary action present in structural steel floor framing system is to use equations (6.1) through (6.4) to describe two-way membrane behavior in the floor framing system and equations (6.5) and (6.6) to describe one-way catenary behavior. The strains in both one-way and two-way catenary systems must be compared to rupture strains for the elements participating. This is done using equation (6.3) in the case of two-way behavior and equation (6.8) in conjunction with the initial horizontal length for one-way behavior. The following sections in this chapter of the report proceed with evaluating several ineffective element scenarios and make recommendations regarding the levels of inherent robustness in the floor system, or make recommendations regarding simple measures that can be taken to enhance structural integrity in these systems.

6.4 Ineffective Element Scenarios

An ineffective element scenario as considered in this study is a situation where the following occurs in the structural steel framing system: an interior column in the framing system is rendered ineffective; an interior in-fill beam is rendered ineffective; an edge in-fill beam is rendered ineffective; two adjacent in-fill beams (one at the edge and the other interior) are rendered ineffective; and finally, a spandrel girder is rendered ineffective, thus rendering one or more in-fill beams ineffective as well. The 30-foot framing bays of the SAC 3-story and 10-story frameworks are considered as the base topologies for the study. This section of the report provides an outline of methods that can be used to assess the membrane and catenary action in the structural steel floor system and the magnitudes of the floor system capacities given an ineffective member scenario.

6.4.1 Ineffective In-Fill Beam(s)

The first scenario(s) considered is an instance where a single in-fill beam is rendered ineffective. The situation is schematically described in Figure 6.3.

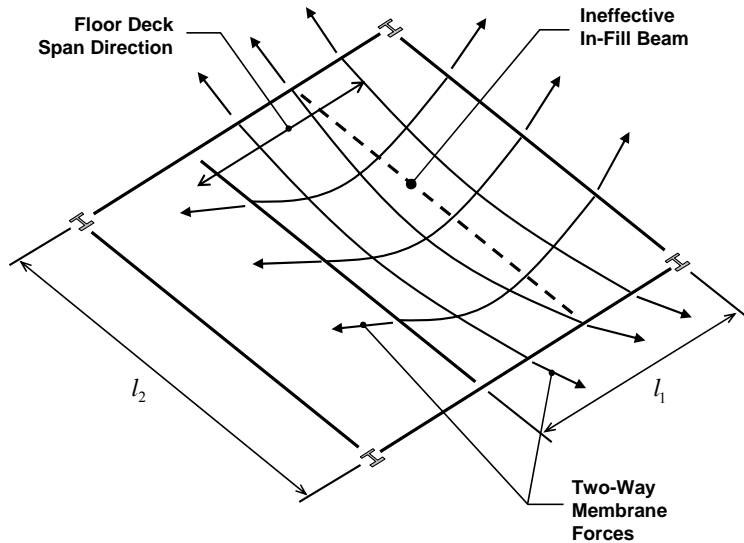


Figure 6.3 Schematic of Two-Way Membrane Action in Composite Steel-Concrete Floor System when One In-Fill Beam is Rendered Ineffective.

This scenario corresponds to the two-way membrane action considered by Hawkins and Mitchell (1979) and Mitchell and Cook (1984) where the panel dimensions are 20-feet by 30-feet. For the present evaluation, 2VLI22 steel deck is assumed to span between the in-fill beams and provide formwork and tension reinforcement for the concrete deck. Typically recommended shrinkage and temperature reinforcement is assumed to be present: 6x6-W1.4xW1.4. The steel deck is assumed to provide membrane tension reinforcement in the short direction and the welded-wire fabric is assumed to provide reinforcement in orthogonal directions.

The two-way membrane reinforcement is assumed to have elastic perfectly plastic stress strain behavior. The yield stress of the welded wire mesh is taken as 65-ksi and the tension area provided on a unit length basis is 0.00233 sq. in. per in. (ACI 1997). The steel deck is assumed to have yield stress equal to 40-ksi and the cross-sectional area on a unit length basis is 0.03542 sq. in. per in. (Vulcraft 2005).

If the full cross-sectional area of the steel deck is at yield, the tension force that can be developed is 1.42 kips per linear inch. If the steel deck panel ends at the beam considered, the horizontal component of this force will have to be carried by puddle welds or shear studs discretely located along beams or girders supporting the two-way membrane. If studs or puddle welds are located at 6 inches on center, a conservative

estimate of the force carried at each discrete connection becomes 8,500 lbs. This force was felt to be too large for typical puddle welds and is close to the capacity of most shear studs welded to steel flanges.

As a result, the area of the steel deck considered effective as tensile reinforcement for the membrane was limited so that the force at each connector around the perimeter of the panel was limited to approximately 550 lbs/in. The nominal strength of a typical 5/8-in. arc spot weld to structural steel substrate through 2VLI22 steel deck is 1.64 kips (AISI 2001). Therefore, 5/8-in puddle welds at 3 inches on center would yield 550 lbs/in capacity. As a result, 40% of the steel deck cross-sectional area on a per unit length basis was assumed to be effective. It should be noted that better information regarding this anchoring strength would yield very good and reliable estimates for the two-way membrane strength of the steel-concrete composite floor plate. It should also be noted that the connections may not only be puddle welds, but may include shear studs facilitating composite action in the beams and girders.

A MathCAD (MathSoft 2005) worksheet was developed for computing two-way membrane capacity for general situations found in steel framing systems. The worksheet for the current scenario is given in Appendix 6.1. One in-fill beam is assumed to be lost in a 30-ft by 30-ft framing system with in-fill framing at 10-ft on center. When the single in-fill beam is rendered ineffective, the two-way membrane dimensions are 20-ft by 30-ft. The forces are made up of a percentage of the total steel deck cross-sectional area at yield and the welded wire mesh (WWM) cross-sectional area in the short-span direction. The cross-sectional area of the WWM is the only tensile reinforcement assumed in the long direction. The force at the perimeter of the panel in the steel deck is 566 lbs/in and one can appreciate the near one-way membrane behavior because the force in the long-direction is only 152 lbs/in. This panel does indeed behave with two-way membrane action. The panel's uniformly distributed load carrying capacity is approximately 110 psf with nearly 7 inches of vertical deflection ($\sim L/34$). As long as the deflection does not exceed the story height (thus causing debris loading); the rotations at the perimeter are not sufficient to cause rupture to the components at these locations; and the strains in the membrane reinforcement do not exceed the rupture strain of the material, the system should be capable of supporting the loading magnitude computed.

It should be noted that the strain in the long direction reinforcement is assumed and the strain that corresponds to the short direction (assuming circular membrane deformed shape) is computed. The strain in the reinforcement spanning in the short direction is 0.00225 in/in, which is approximately 2 times the yield strain for the deck and much less than the yield strain for the WWM. Keeping the yield strain in the steel deck to $\leq 2\varepsilon_y$ was felt to be sufficient to prevent rupture. The connections at the ends (*e.g.* puddle welds or shear studs) needs to be evaluated with regard to this ductility capacity.

In order to qualify the panel's capacity within the realm of typical floor loadings and dynamic effects that are likely to occur as a framing member becomes *ineffective*, the following loadings were assumed to be present on the panel:

Concrete-Steel Composite Deck	50 psf
Ceiling/Flooring/Fireproofing	3 psf
Mechanical/Electrical/Plumbing	7 psf
Partitions.....	20 psf
Percentage of Live Loading (25% of 50 psf)	12.5psf

The total loading present on the panel at the instant the in-fill beam is rendered ineffective is approximately 93 psf. If current progressive collapse mitigative guidelines are employed (GSA 2003), this would require that the two-way membrane be capable of supporting;

$$2 \cdot [1.0D + 0.25L] = 2 \cdot [93] = 186 \text{ psf} > 110 \text{ psf}$$

The membrane is not capable of carrying this loading and therefore, the system as assumed requires additional structural engineering to resist disproportionate (progressive) collapse at GSA-level loading. It should be noted, however, that the system can carry the system self-weight and mean point-in-time sustained loading with a moderate dynamic multiplier: $(110/93) \approx 1.2$. This implies that the system definitely has inherent resistance to disproportionate collapse, but can only tolerate a small dynamic amplification in loading.

The MathCAD template allows evaluation of other reinforcement or steel deck scenarios with respect to two-way membrane capacity. If the 2VLI22 gauge deck is to remain, but mild-steel reinforcement of #3 at 12-inch spacing (60-ksi yield strength) is used, the two-way membrane capacity will be approximately 189-psf. All previous scenarios resulted in membrane deflections of approximately 7 inches and strains $\leq 2\varepsilon_y$. A brief summary of the previous analysis is;

2VLI22 and 6x6-W1.4xW1.4.....	110 psf ($\beta_{dynam} \approx 1.2$)
2VLI22 and #3 at 12-inches on center	189 psf ($\beta_{dynam} \approx 2.0$)

Therefore, the slab system typically present in a structural steel system appears to be capable of carrying its own weight and mean point-in-time sustained live loading in the event a single in-fill beam is rendered ineffective. This illustrates the *inherent* structural integrity or robustness in the system. The membrane action in the slab system is most effectively enhanced by increasing the mild steel reinforcement in the system because the steel deck connections have limited strength.

The 10-foot framing module can be used to evaluate other ineffective in-fill beam scenarios using the calculation methodology developed. A second scenario involving two ineffective in-fill beams is shown in Figure 6.4.

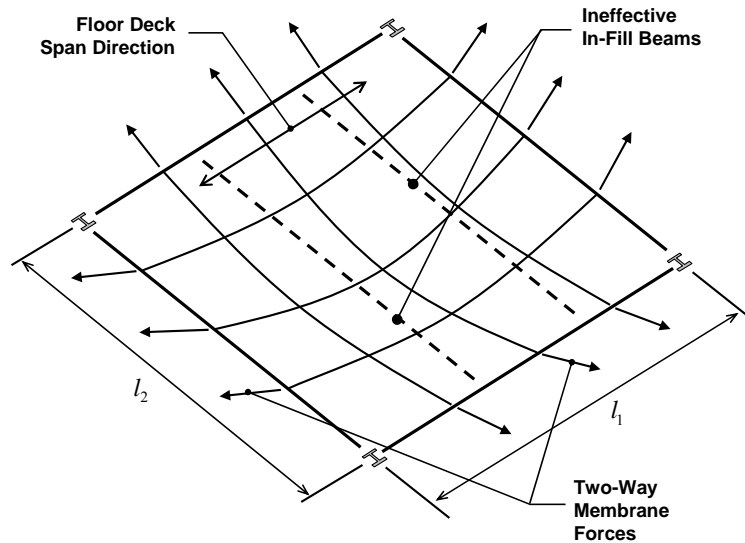


Figure 6.4 Schematic of Two-Way Membrane Action in Composite Steel-Concrete Floor System When Two In-Fill Beams are Rendered Ineffective.

This scenario is quite interesting because the panel is now square, but the tensile membrane reinforcement is orthotropic: deck plus WWM in l_1 direction and WWM in l_2 direction.

Appendix 6.2 includes a MathCAD worksheet for the scenario described in Figure 6.4. As might be expected, the loading capacity of the 30-ft by 30-ft membrane utilizing 6x6-W1.4xW1.4 welded wire mesh with 2VLI22 steel deck is lower than the previous scenario. The two-way membrane capacity is approximately 93 psf with 12 inches of membrane deflection. The typical panel found in structural steel floor systems cannot support the required 2.0 multiplier for dynamic effects required by current guidelines (GSA 2003), but is capable of supporting its self-weight and mean point-in-time sustained live loading likely at the time the two in-fill beams are rendered ineffective. The strain present in the steel deck is approximately $2.2 \cdot \epsilon_y$.

The same MathCAD worksheet was used to study alternate reinforcement schemes to the welded wire mesh scenario provided. It was assumed that either #3 or #4 mild-steel reinforcing bars would be used in the slab system in lieu of WWM. The 2VLI22 steel deck was still utilized at 40% cross-sectional area. The yield stress for the mild-steel bars was defined to be 60 ksi, instead of the 65 ksi used for the WWM. This study yielded the following:

#3 at 24 in. on center; $0.00458 \text{ in}^2/\text{in}$	119 psf at 12-in. defl. ($\beta_{\text{dynam}} \approx 1.3$)
#3 at 18 in. on center; $0.00611 \text{ in}^2/\text{in}$	140 psf at 12-in. defl. ($\beta_{\text{dynam}} \approx 1.5$)
#3 at 12 in. on center; $0.0092 \text{ in}^2/\text{in}$	178 psf at 12 in. defl. ($\beta_{\text{dynam}} \approx 1.9$)

Comparing the previous results for the single in-fill beam being lost, it can be said that the best balance in providing robustness for both one and two in-fill beams being lost would be to provide #3 mild-steel reinforcing bars at 12 inches on center. One might assume that *inhibiting* progressive collapse can be achieved by assuming that the 93-psf loading can be carried by the panel and therefore, the system inherently has this resistance and structural integrity.

6.4.2 Ineffective Spandrel Beam

The second scenario that is considered is that when a spandrel beam is rendered ineffective within the framing system. This situation is shown in Figure 6.5.

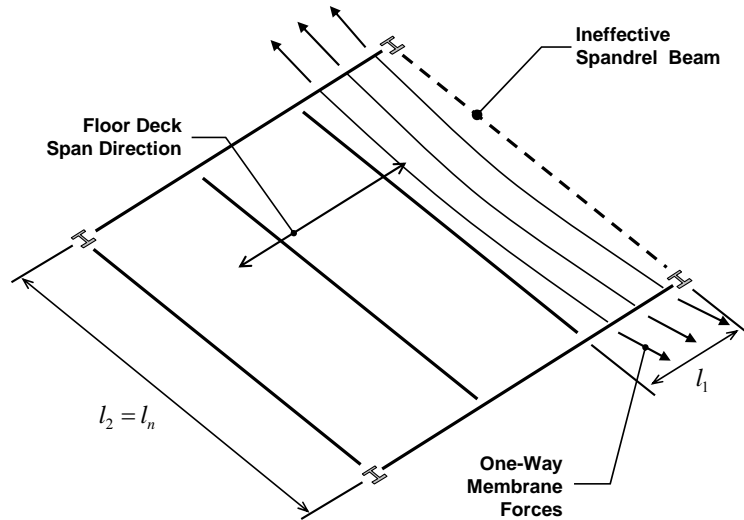


Figure 6.5 Schematic Illustrating Ineffective Spandrel Beam Scenario.

In this case, the support for the steel-concrete composite deck is ineffective and any anchoring at the slab edge (including membrane compression rings) is non-existent. Furthermore, the deck flutes will be running perpendicular to the direction of assumed catenary action and the deck is not considered to provide tension reinforcement to the catenary. It is assumed that catenary action will not create an overload condition at the girder connections framing into the columns. These connections are likely designed for a shear force computed on the basis of a tributary width equal to $l_n/2$ if an edge girder and l_n if an interior girder with uniformly distributed loading applied over the entire girder length. The case of one in-fill beam as shown

above may result in concentrated loadings being used. Finally, any exterior cladding that is being supported by the spandrel element is assumed to “fall” from the slab with the spandrel beam.

There are two possibilities for creating structural integrity and robustness if this ineffective member scenario arises. The first involves lumping catenary tensile reinforcement at the perimeter of the slab system (*i.e.* immediately above the ineffective spandrel in-board of the columns); and the second involves distributing catenary tensile reinforcement throughout the slab. If the catenary steel is concentrated at the perimeter, the tributary width of slab for the catenary will be 5 feet in this case (1/2 the deck span). If the catenary steel is distributed throughout the panel, then the tributary width of slab will simply be 1 foot. Equations (6.5) and (6.6) are used to evaluate the load carrying capacity of the catenary if the yield stress in the reinforcement is achieved (strains will be compared to the tensile rupture strain for the material).

Appendix 6.3 contains a MathCAD template illustrating the computations for a lumped mild-steel catenary reinforcement scenario: 4 – #4 Gr. 60-ksi reinforcing bars continuous at the perimeter. The catenary span is 360-inches (30 feet) and the tributary width of deck perpendicular to the catenary is 5 feet. As indicated, the loading capacity of the catenary is approximately 100 psf. The strains present in the catenary reinforcement with the assumed catenary sag of 14 inches is $\sim 2\varepsilon_y$. One could argue that the 5 foot tributary width is conservative since it is likely that the steel deck could carry much more than 2.5 feet of width to the interior in-fill beam. If the tributary width of slab carried by the catenary drops to 3 feet (assuming that the steel deck and WWM acting together move the bending inflection point further outboard of the first-interior in-fill beam), the 4 – #4 bars are capable of supporting 168-psf loading, which allows for a dynamic multiplier of 1.8.

A second mild-steel reinforcement scenario that can be considered is distributing reinforcement throughout the slab, thus creating one-way membrane action. This creates a tributary width to the catenary of one foot, but the one-way membrane’s span remains 30 feet. Utilizing the MathCAD template in Appendix 6.3 a variety of reinforcement scenarios can be considered. A summary of these are given in Table 6.1 (it should be noted that the static loading present is assumed to be 93 psf).

The results in Table 6.1 indicate that the typical WWM in a steel-concrete composite floor system is not capable of carrying the expected 93-psf loading. The loss of the steel deck as reinforcement in the situation considered is very punishing to load carrying capacity. If one were to consider disproportionate collapse *resistance* a dynamic load modifier of 1.0 would be needed and #4 bars at 18-inches on center appear to be appropriate. If progressive collapse *prevention* is desired a dynamic multiplier of 2.0 is appropriate (GSA 2003) and #4 at 9-inches on center is required. It should be noted that more capacity is gained as the catenary is allowed to sag, but one should recognize that with sag comes strain and the rupture strain may be

exceeded. All results reported in Table 6.1 have strains that are below the expected rupture strain for mild-steel reinforcement.

Table 6.1 One-Way Catenary Reinforcement Capacities with Variation in Distributed Slab Reinforcement.

Reinforcement Scenario (1)	h (in.) (5)	A_s (in^2/ft) (2)	q_u (psf) (3)	β_{dynam} (4)	$\mu = \frac{\epsilon_s}{\epsilon_y}$ (6)
6x6-W1.4xW1.4	16.2	0.028	21.5	0.23	2.4
#3 at 24-in. o.c.	16.2	0.055	39	0.42	2.6
#4 at 18-in. o.c.	16.2	0.133	94	1.01	2.6
#4 at 14-in. o.c.	16.2	0.1714	122	1.31	2.6
#4 at 9-in. o.c.	16.2	0.2667	189	2.03	2.6
#4 at 14-in. o.c.	18.0	0.1714	135	1.45	3.2
#4 at 12-in. o.c.	18.0	0.20	157	1.68	3.2

The #4 at 14" reinforcement rows indicate that if greater sag is allowed, there is an associated increase in membrane capacity if the rupture strain is not exceeded. The increase is roughly 11% corresponding to an additional 2 inches of membrane sag.

A second ineffective spandrel beam scenario considered is that where the spandrel beam is lost as well as the first interior in-fill beam. This scenario is shown in Figure 6.6. In this situation, two-way action is not considered because the supporting element at the edge of the panel is ineffective. Furthermore, catenary action at the edge of the panel as considered in the previous scenario has been deemed ineffective due to the increased tributary width of slab for the catenary. The reason for this is that at least 12-#4 bars will be required at the edge to create the one-way catenary behavior capable of carrying 10-feet of tributary slab and provide a dynamic multiplier of 2.0. With #4 bars at 9-inches on center, there are 13 bars in the panel. This appears to be a break-even point. Figure 6.6 and the previous results indicate that if #4 bars are provided at 9 inches on center throughout this bay, the spandrel beam, and any number of interior in-fill beams in this bay can be rendered ineffective. One-way membrane action in the slab system can be developed to provide progressive collapse prevention. If resistance to progressive collapse is desired, Table 6.1 indicates that the spacing can be doubled to 18 inches.

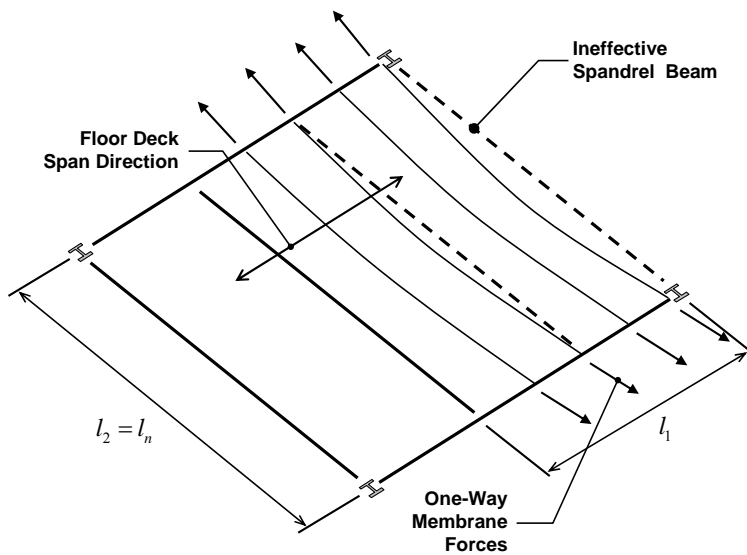


Figure 6.6 Schematic Illustrating Ineffective Spandrel and Immediately Adjacent Beam Scenario.

6.4.3 Ineffective Spandrel Girder

The 30-ft by 30-ft framing bays considered also contain situations where a spandrel girder may be rendered ineffective. This situation is schematically illustrated in Figure 6.7.

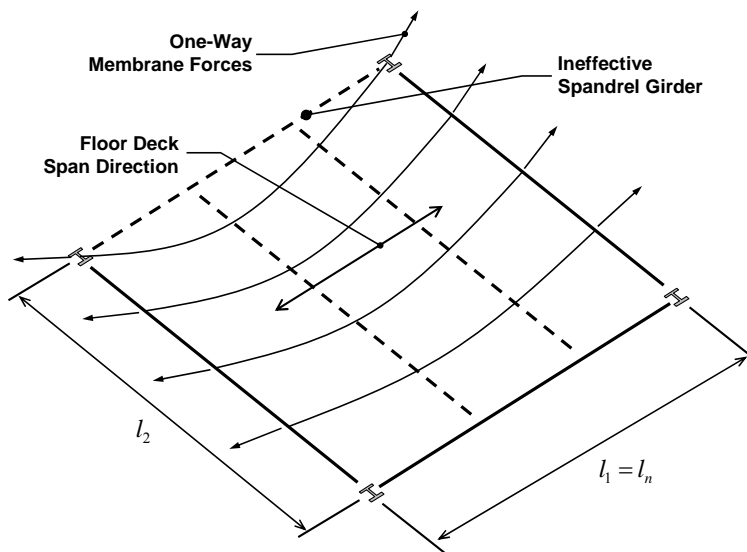


Figure 6.7 Schematic Illustrating Ineffective Spandrel Girder Scenario.

It will be assumed that when the spandrel beam is rendered ineffective, any exterior cladding attached to this member falls off the structure. This situation benefits from the presence of composite steel deck in the direction of the one-way membrane action. Therefore, this reinforcement must now be considered in the

analysis. It should be noted that since the vertical supporting element at the edge of the panel is lost, two-way action is not considered.

Appendix 6.4 contains a MathCAD template that is used to evaluate the capacity of the one-way membrane action in the slab panel. If one assumes that 50% of the steel deck is considered anchored at the end of the catenary and that 2VLI22 composite steel deck is used along with the typical shrinkage and temperature reinforcement (6x6-W1.4xW1.4), the one-way membrane capacity of the system is shown to be 102 psf with 13.5 inches of sag in the membrane. The strains in the WWM and steel deck are $\leq 2.7\varepsilon_y$. If 50% of the steel deck is considered “anchored” or effective in developing catenary action, the connections at the ends of the catenary must support a tensile force equal to;

$$\begin{aligned} T_{end} &= A_{deck} \cdot f_{dy} \\ &= (0.50 \cdot 0.425 \text{ in}^2/\text{ft}) \cdot (40 \text{ ksi}) = 8.5 \text{ k/ft} \end{aligned}$$

This is a significant anchoring force. Steel studs at 1-foot spacing are likely able to develop this force, but it is unknown if the deck is capable of channeling this force to discrete connection points. In the case of continuous panel edges and continuous deck panels over the support, this connection is of only moderate concern.

The previous calculations indicate that the slab system may be capable of supporting the 93-psf self-weight and mean point-in-time sustained live loading. However, if the dynamic load multiplier of 2.0 is desired, additional reinforcement will likely be required. The MathCAD template in Appendix 6.4 was used to explore mild-steel reinforcing bars as a supplement to the composite steel deck.

Table 6.2 One-Way Membrane Reinforcement Capacities with Variation in Distributed Slab Reinforcement (2VLI22 steel deck).

Mild-Steel Reinforcement (1)	h (in.) (5)	A_s (in ² /ft) (2)	q_u (psf) (3)	β_{dynam} (4)	$\mu_{max} = \frac{\varepsilon}{\varepsilon_y}$ (6)
#3 at 9-inches o.c.	13.5	0.1467	171	1.84	2.7
#4 at 14-inches o.c.	13.5	0.1714	186	2.0	2.7

Two arrangements appear sufficient: #3 at 9 inches and #4 at 14 inches on center. Both are very close to providing the 2.0 multiplier required by the GSA guidelines (GSA 2003). Therefore, the original system has resistance to progressive collapse, but enhancement can be attained through addition of mild-steel one-way membrane reinforcement in lieu of the welded wire mesh.

6.4.4 Ineffective Interior Column

The analyses of the SAC buildings covered loss of exterior columns at the perimeter of the framework. However, the “simple” interior framing led the analysis to breakdown because the pin connections at all in-fill and interior framing would theoretically not support removal of a column at any level. The 3-, 10-, and 20-story SAC building analyses also indicated that as one rises through the framework and loses the beneficial effects of Vierendeel action in the stories above an ineffective column, the floor system may be required to develop catenary and/or membrane action in addition to flexural capacity in order to maintain structural integrity.

The robustness inherent in structural steel simply-connected framing systems was evaluated through consideration of the typical interior framing bays present in the 3-story and 10-story SAC buildings and the assumption that an interior column would become ineffective. In this situation, the ineffective column facilitates activation of two-way membrane action in the concrete floor framing system and two-way flexure/catenary action in the structural steel framing. There is a synergy between these two component systems that has only recently been studied in relation to fire (Allam *et al.* 2000; Bailey *et al.* 2000; Huang *et al.* 2000a; Huang *et al.* 2000b; Burgess *et al.* 2001; Cai *et al.* 2002; Huang *et al.* 2003a; Huang *et al.* 2003b). In the present analysis, a deformation compatibility approach is used in conjunction with two separate static analyses: the first considering two-way membrane action in the slab; and the second considering two-way-grillage catenary/flexure action in the steel framing. These two analysis components are described in the schematics in Figures 6.8 and 6.9.

As the interior column is rendered ineffective, the slab and grillage of steel members is forced to deform in a compatible manner and they both resist vertical deformation to the extent that their strength and stiffness allow. The two-way membrane behavior in the slab is assumed to follow the theory described and used previously. Two way grillage (catenary/flexure) behavior in the steel framing can be computed using nonlinear structural analysis theory. These two theories can be used together to evaluate the robustness present in the typical 30-ft by 30-ft simple structural steel framing system.

The framing connections that are assumed for the present example are considered flexible and are double web angles (*i.e.* web cleats). In order to assess the capabilities of double angle connections in facilitating the 3D grillage behavior shown in Figures 6.8 and 6.9, the web cleat moment capacity, tension capacity, and shear capacity need to be determined. This process can be started by looking at the web cleat connection as being composed of bolt elements as shown in Figure 6.10. The transformation shown in Figure 6.10 is nothing new. Researchers have been studying methodologies for determining moment and tension capacities of bolted angle connections for quite some time (Wales and Rossow 1983; Astaneh-Asl *et al.* 1989a; Astaneh-Asl *et al.* 1989b; DeStefano and Astaneh-Asl 1991; DeStefano *et al.* 1991; DeStefano *et al.*

1994; Shen and Astaneh-Asl 1999; Liu and Astaneh-Asl 2000b; Liu and Astaneh-Asl 2000a; Shen and Astaneh-Asl 2000; Astaneh-Asl *et al.* 2002; Liu 2003).

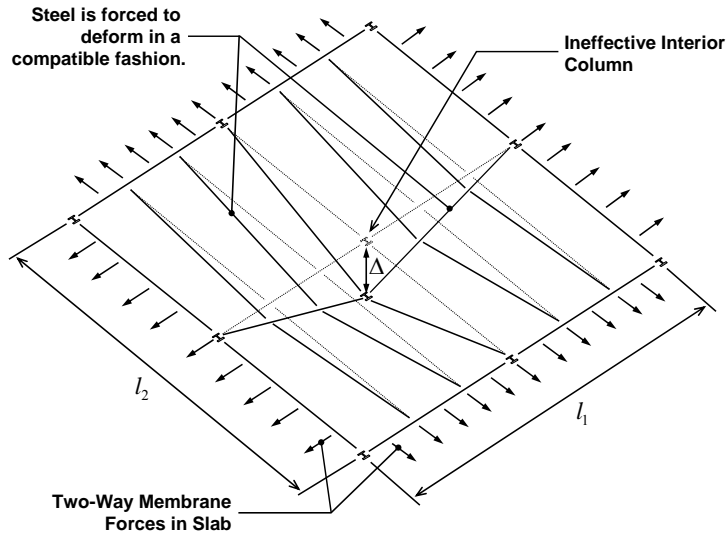


Figure 6.8 Two-Way Membrane Action Resulting from Ineffective Interior Column.

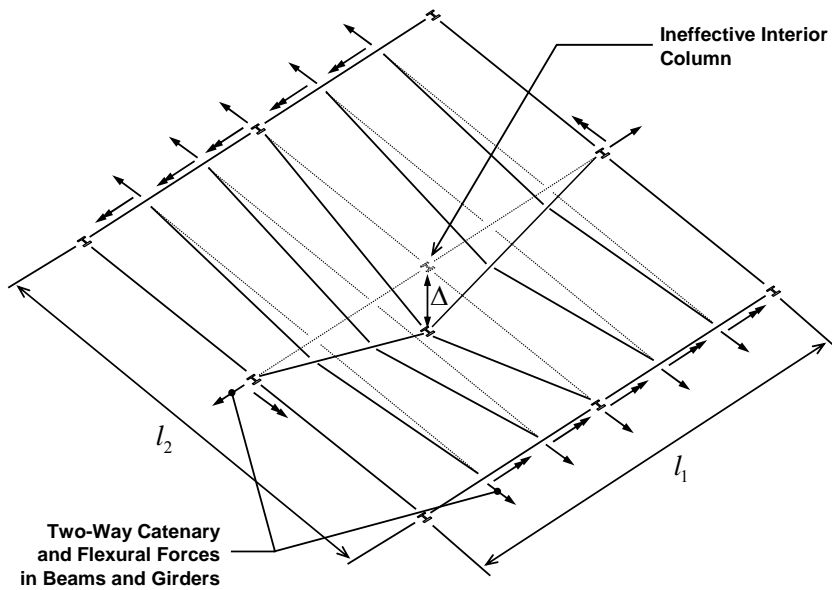


Figure 6.9 Two-Way Catenary/Flexure Action Resulting from Ineffective Interior Column.

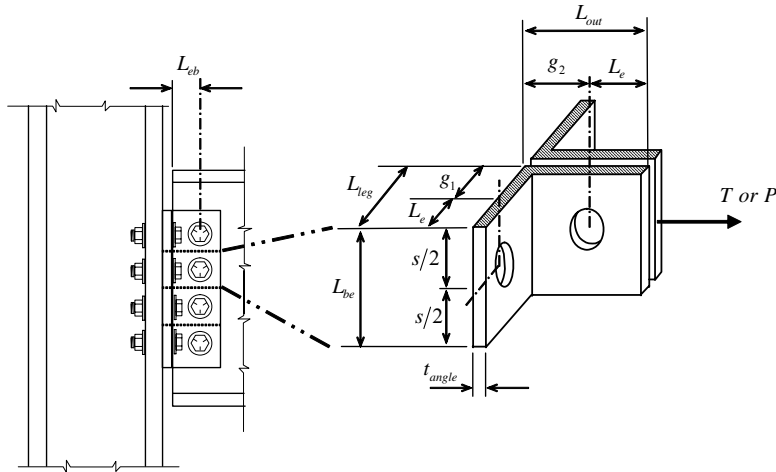


Figure 6.10 Web-Cleat to Bolt Element Transformation.

The present study uses the approach of Shen and Astanceh-Asl (2000) and Liu and Astanceh-Asl (2000b) to develop nonlinear tension and compression behavior for bolt elements. These bolt elements can then be assembled to form web cleats whereupon moment-rotation behavior of the connections or tension/compression response of the connection can be developed.

The parameters that affect the strength and stiffness of the bolt element are shown in Figure 6.10. The bolt element modeling approach can be used to determine the pure moment-rotation response of the double angle connection and the pure tension-deflection response of the double angle connection. The process begins with developing tension-deflection and compression-deflection response of the double angle bolt elements. A tri-linear tension-deformation response for the bolt element is derived using the procedure suggested by Shen and Astanceh-Asl (1999), Liu and Astanceh-Asl (2000a), Liu and Astanceh-Asl (2000b), and Shen and Astanceh-Asl (2000) with slight modification. The tri-linear response is shown in Figure 6.11.

Three characteristic points on the response are generated using procedures recommended by Shen and Astanceh-Asl (2000) with slight modification. Point (P_{T1}, δ_{T1}) is defined using the yield moment in the legs of the angle. The initial stiffness, K_{T1} , is essentially the linear elastic stiffness of the bolt element considering bending of the legs perpendicular to the beam web and the axial extension of the leg parallel to the beam web. Point (P_{T2}, δ_{T2}) corresponds to the plastic mechanism capacity of the angle legs perpendicular to the beam web. The post-yield mechanism stiffness is defined as K_{T2} . The final point on the tension-deformation response is (P_{TU}, δ_{TU}) . This point corresponds to the ultimate loading for the bolt element exclusive of bolt tension rupture or bolt shear rupture. It is defined through consideration of the angle legs perpendicular to the

beam web forming catenary tension between the bolts in the support and the legs parallel to the beam web. The tension in the catenary at this ultimate loading is taken to be the loading corresponding to fracture on the net area through the angle leg perpendicular to the beam web. The final stiffness in the response is defined as K_{T3} .

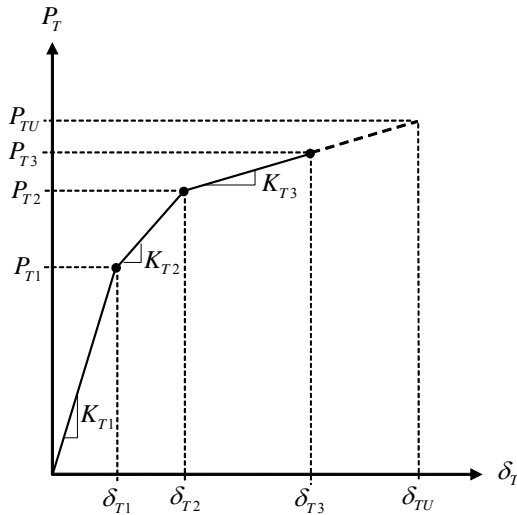


Figure 6.11 Double Angle Bolt Element Tension-Deformation Response.

The catenary tension force may or may not be able to form. For example, the bolts in the bolt element may fracture in tension prior attaining the catenary tension limit state. Therefore, a third point (P_{T3}, δ_{T3}) is defined. The loading, P_{T3} , is defined through consideration of the following bolt-element limit states;

- catenary tension fracture in the angle legs perpendicular to the beam web;
- tear-out bearing failure of the bolts in the beam web;
- tear-out bearing failure of the bolts in the angles;
- tension fracture of the bolts including prying action (Thornton 1985);
- tension fracture of the bolts excluding prying (superfluous);
- shear fracture of the bolts.

The final point is located along the response defined using the third stiffness, K_{T3} . This stiffness, along with P_{T3} defines the deformation capacity of the bolt element, δ_{T3} .

The bolt element compression-deformation response is assumed to be bilinear as indicated in Figure 6.12. The yield point (P_{C1}, δ_{C1}) is defined by considering three strength limit states;

- yield in the angle legs parallel to the beam web;
- yielding in the beam web;
- shear fracture of the bolts.

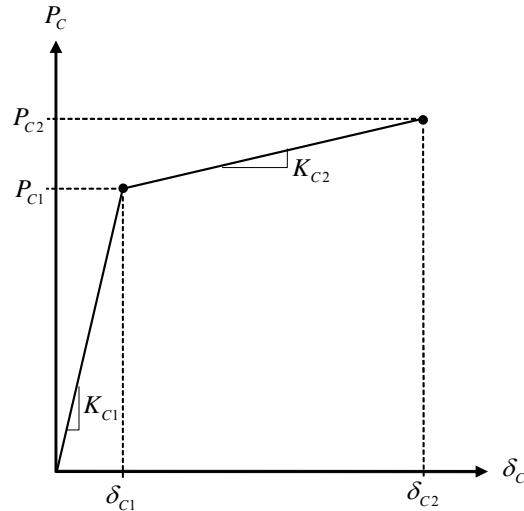


Figure 6.12 Double Angle Bolt Element Compression-Deformation Response.

The ultimate loading capacity of the bolt element in compression is defined through consideration of the following strength limit states;

- crushing in the angle legs denoted by the ultimate tension stress being reached in the angle legs parallel to the beam web (conservative);
- crushing in the beam web denoted by the ultimate tension stress in the beam web being reached (again, conservative);
- 20% increase above the ultimate bolt shear stress magnitude.

The initial stiffness, K_{C1} , is defined using the smaller of two axial stiffness magnitudes. If beam web yielding controls, the stiffness is defined as,

$$K_{T1} = \frac{A_{web}E}{L_c} \quad (6.9)$$

and if angle leg yielding controls, the stiffness is defined by,

$$K_{T1} = \frac{A_{angles}E}{L_c} \quad (6.10)$$

The areas are defined on the basis of the bolt element dimension, L_{be} . The compression length in the angle (or tension length over which strain accrues in the beam web) is defined as,

$$L_c = g_2 - \frac{d_h}{2} \quad (6.11)$$

The post-yield stiffness is defined rather arbitrarily using a 0.5% multiplier to account for moderate strain hardening in the material on the way to crushing.

It should be noted that the behavior of the supporting element (*e.g.* a column flange, a column web, and girder flange) is omitted. This may indeed be very important, but the complexity incurred through consideration of this behavior would render the analysis proposed intractable.

A MathCAD worksheet in Appendix 6.6 illustrates the computations needed to develop a nonlinear tension and compression response for a bolt element consisting of A325-N bolts in L4x3.5 angles. Expected yield and ultimate tensile stresses for the materials are used as recommended in the GSA guidelines (GSA 2003). The tension- and compression-deformation response parameters for bolt elements consisting of various angle leg thicknesses are given in Table 6.3. These parameters depend upon the limit states discussed previously and therefore, the beam web thickness will affect the parameter magnitudes. As a result, parameters for two beam wide-flange shapes are provided. These shapes are consistent with the beam and girder shapes used in the SAC buildings analyzed in chapters 3 and 4 of the report.

The tension and compression response for the bolt elements using the parameters outlined in Table 6.3 are shown in Figures 6.13 and 6.14 for the W18x35 and W21x68 wide flange shapes, respectively. The tension-deformation response varies considerably with beam shape and angle thickness. This is a byproduct of the varying limit states considered in the computations. For example, when thin angles are considered, the catenary tension action is allowed to form and rupture of the angle legs is the controlling limit state. However, as the angles get thicker, other limit states control the behavior. This is indicated by the “capping” of the tension forces in the 5/16, 3/8, and 1/2-inch angle thickness in the W18x35 beam shape and the 3/8 and 1/2-inch angle thickness with the W21x68 girder shape. The compression-deformation response is consistent indicating that the limit states controlling strength are consistent as well.

The bolt element ultimate strengths can be used to contribute to the determination of the tension capacity of the double angle connections through simple summation of the bolt element tension strengths in any given connection. However, two additional strength limit states must be considered beyond those considered in the bolt element strength determination. Therefore, the tensile capacity of the double-angle connection is determined through consideration of the following limit states;

- shear rupture of the bolts;

- tension fracture of the bolts including prying;
- block shear rupture in the angle legs parallel to the beam web;
- block shear rupture in the beam web;
- bearing tear-out failure in the angle legs parallel to the beam web;
- bearing tear-out failure in the beam web;
- catenary tension rupture in the angle legs perpendicular to the beam web.

Table 6.3 Bolt-Element Tension and Compression Response Parameters for Varying Angle Thickness
(all units in table are kips and inches).

Response Direction (1)	Parameter (2)	W18x35				W21x68			
		L4x3.5 Angles				L4x3.5 Angles			
		0.2500 (3)	0.3125 (4)	0.3750 (5)	0.5000 (6)	0.2500 (7)	0.3125 (8)	0.3750 (9)	0.5000 (10)
Tension	δ_{T1}	0.019	0.015	0.013	0.0095	0.019	0.015	0.013	0.0095
	δ_{T2}	0.105	0.088	0.077	0.064	0.105	0.088	0.077	0.064
	δ_{T3}	0.632	0.640	0.457	0.124	0.632	0.697	0.752	0.386
	P_{T1}	2.205	3.445	4.961	8.820	2.205	3.445	4.961	8.820
	P_{T2}	5.232	8.462	12.629	24.212	5.232	8.462	12.629	24.212
	P_{T3}	20.491	26.873	26.873	26.873	20.491	28.745	37.93	38.519
	K_{T1}	116.00	226.56	391.50	928.00	116.00	226.56	391.50	928.00
	K_{T2}	35.344	69.031	119.28	282.75	35.344	69.031	119.28	282.75
	K_{T3}	28.947	33.326	37.480	44.489	28.947	33.326	37.480	44.489
Compression	δ_{C1}	0.0030	0.0030	0.0030	0.0030	0.0022	0.0022	0.0022	0.0022
	δ_{C2}	0.1490	0.149	0.149	0.149	0.092	0.092	0.092	0.092
	P_{C1}	49.500	49.500	49.500	49.500	52.590	52.590	52.590	52.590
	P_{C2}	61.425	61.425	61.425	61.425	63.108	63.108	63.108	63.108
	K_{C1}	16,380	16,380	16,380	16,380	23,470	23,470	23,470	23,470
	K_{C2}	81.882	81.882	81.882	81.882	117.36	117.36	117.36	117.36

The MathCAD worksheet provided in Appendix 6.6 outlines the computations used to define the pure tension strength of the double web-angle connection.

The pure moment capacity of the double web-angle connection is determined using the bolt element tension- and compression-deformation response parameters described previously (Table 6.3). The pure moment condition is defined by the deformation and force states shown in Figure 6.15.

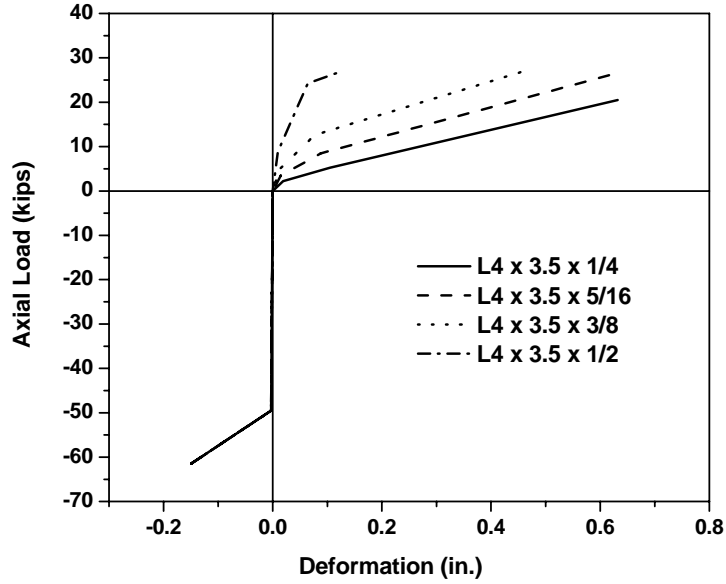


Figure 6.13 Bolt Element Tension and Compression Response for L4x3.5 Double Angles and W18x35.

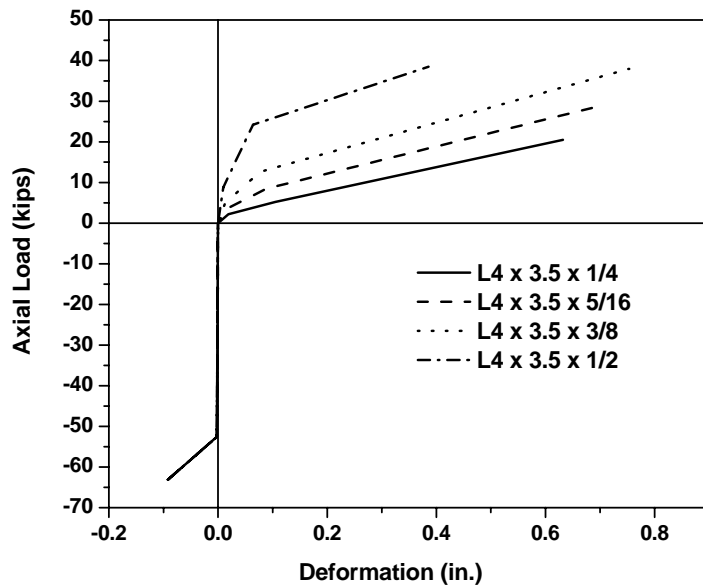


Figure 6.14 Bolt Element Tension and Compression Response for L4x3.5 Double Angles and W21x68.

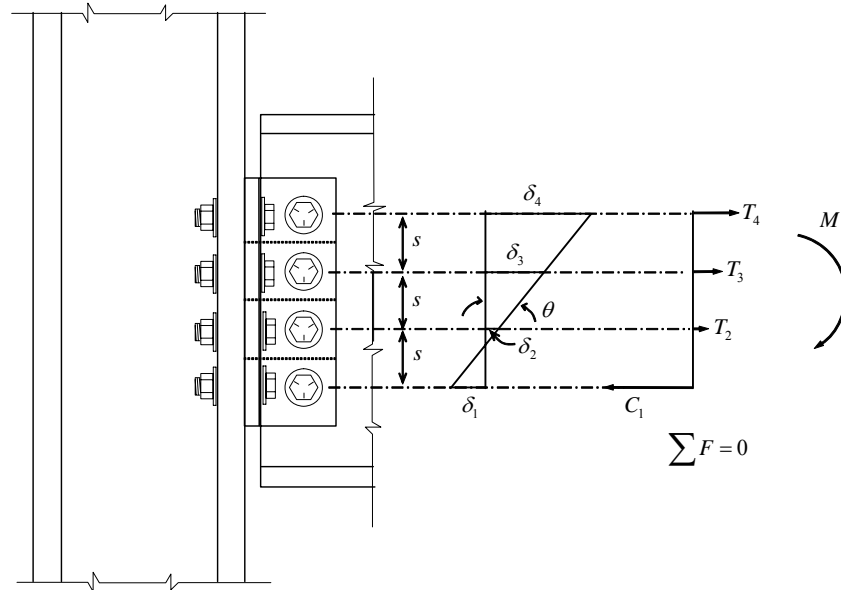


Figure 6.15 Double-Angle Pure-Moment Strength Condition.

The process for determining the pure moment capacity of the connection begins with defining the tension and compression response for each bolt element in the connection (see Figures 6.13 and 6.14). A controlling state of deformation in the extreme tension angle, δ_4 , or extreme compression angle, δ_1 , is assumed. These deformations are taken from the appropriate angle curves. The connection rotation angle, θ , is then varied until the summation of all forces determined using the bolt element response curves is zero. This corresponds to the pure moment capacity of the double angle connection. It should be noted that this process is iterative and the compression or tension deformation limit states may control the behavior.

The shear strength of the double angle connection given the beam shape chosen can be determined using the AISC Manual (AISC 2001b). It should be noted that unfactored strengths were utilized and therefore, all manual-obtained strengths were divided by 0.75. The shear strengths for the double angles and beam shapes considered assume: $L_{ev} = 1.5''$; $L_{eh} = 1.5''$; $\phi = 1.0$; and 3/4" A325N bolts in STD holes.

The beams in the grillage are assumed to be W18x35's and the girders are W21x68's. From the AISC-LRFDM (AISC 2001b), the W18 sections can support 3-5 rows of bolts, while the W21 sections can support 4-6 bolt rows with traditional spacing and end distances. Therefore, only these numbers of bolt rows were considered. Table 6.4 illustrates the pure tension, pure shear, and pure moment capacities of the double angle connections considered.

Table 6.4 Pure Tensile, Pure Shear and Pure Moment Capacities for Double Angle Connections (all forces are in kips and kip-feet).

L4 x 3.5 Thickness (1)	Bolt Rows (2)	W18x35			W21x68		
		Axial $\left(\frac{P}{P_y}\right)$ (3)	Shear $\left(\frac{V}{V_y}\right)$ (4)	Moment $\left(\frac{M}{M_p}\right)$ (5)	Axial $\left(\frac{P}{P_y}\right)$ (6)	Shear $\left(\frac{V}{V_y}\right)$ (7)	Moment $\left(\frac{M}{M_p}\right)$ (8)
1/4"	3	61.5 (0.12)	78.0 (0.31)	13.07 (0.05)	n.a.	n.a.	n.a.
	4	82.0 (0.16)	102.8 (0.41)	24.61 (0.09)	82.0 (0.08)	138.7 † (0.33)	24.61 (0.04)
	5	102.5 (0.20)	127.6 (0.50)	39.03 (0.14)	102.5 (0.10)	176.0 † (0.41)	39.54 (0.06)
	6	n.a.	n.a.	n.a.	123.0 (0.12)	213.3 † (0.50)	56.28 (0.08)
5/16"	3	80.6 (0.16)	78.0 (0.31)	17.47 (0.06)	n.a.	n.a.	n.a.
	4	107.5 (0.21)	102.8 (0.41)	32.21 (0.12)	115.0 (0.12)	147.3 (0.35)	34.60 (0.05)
	5	134.4 (0.26)	127.6 (0.50)	46.06 (0.17)	143.7 (0.14)	182.9 (0.43)	46.17 (0.07)
	6	n.a.	n.a.	n.a.	172.5 (0.17)	218.4 (0.51)	57.98 (0.09)
3/8"	3	80.6 (0.16)	78.0 (0.31)	18.00 (0.06)	n.a.	n.a.	n.a.
	4	107.5 (0.21)	102.8 (0.41)	33.07 (0.12)	151.7 (0.15)	147.3 (0.35)	35.28 (0.05)
	5	134.4 (0.26)	127.6 (0.50)	49.95 (0.18)	189.6 (0.19)	182.9 (0.43)	46.38 (0.07)
	6	n.a.	n.a.	n.a.	227.6 (0.23)	218.4 (0.51)	65.00 (0.10)
1/2"	3	80.6 (0.16)	78.0 (0.31)	19.15 (0.07)	n.a.	n.a.	n.a.
	4	107.5 (0.21)	102.8 (0.41)	32.95 (0.12)	154.1 (0.15)	147.3 (0.35)	37.68 (0.06)
	5	134.4 (0.26)	127.6 (0.50)	50.26 (0.18)	192.6 (0.19)	182.9 (0.43)	61.81 (0.09)
	6	n.a.	n.a.	n.a.	231.1 (0.23)	218.4 (0.51)	93.34 (0.14)

The yield and plastic capacities for the members are computed as follows;

$$P_y = F_y \cdot A$$

$$V_y = (0.6F_y) \cdot t_w \cdot (d - 2t_f)$$

$$M_p = F_y \cdot Z_x$$

using $F_y = 50 \text{ ksi}$. All shear strengths are controlled by the strength of the beam or girder web. A † symbol denotes exceptions where the shear strength is limited by the connection angle and/or bolt strength.

Table 6.4 indicates that the double-angle connection alone has a tensile capacity that ranges from 0.1-0.30 of the yield load of the cross-section. These are fairly significant tensile capacities (if taken as cumulative over all beam and girder members within the 3D system). The loading capacities are consistent with those found in testing by Owens and Moore (1992). The moment capacities are very low, however. The bending moment capacities range from 0.05 – 0.20 of the plastic moment capacity of the beam cross-section. This is consistent with the strength portion of the definition of flexible connections (AISC 2005a).

Bilinear moment-rotation response and axial load-extension response curves can be generated for the double angle connections using the bolt element parameters shown Figures 6.13 and 6.14. Compression response characteristics are only used for defining moment rotation response. The connections in the grillage are not expected to go into compression in the ineffective column scenarios considered. The tension secant stiffness for the bolt element can be defined as shown in Figure 6.16.

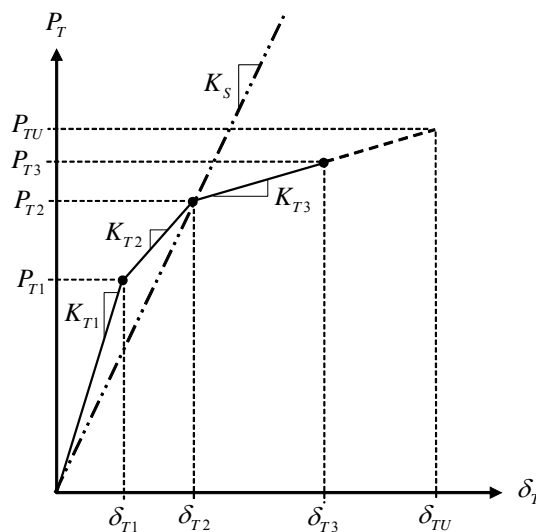


Figure 6.16 Bolt Element Tension Response with Secant Stiffness Representation.

This secant tension stiffness is defined as the initial linear stiffness of the bolt element. This stiffness is given by,

$$k_{BE} = K_s = \frac{P_{T2}}{\delta_{T2}} \quad (6.12)$$

The tensile capacity of the each bolt element in the double-angle connection then contributes to the tensile and moment capacity of the connection. The bilinear tension-deformation response of each bolt element is then characterized by the secant stiffness, k_{BE} , and the bolt element tensile capacity, P_{T3} .

The rotational and axial stiffness of the web-cleat connections are estimated using the magnitudes of the bolt element secant stiffness. In the case of axial tension, the axial stiffness of the double angle connection is simply the sum of the stiffness of each bolt element in the web cleat,

$$K_\delta = \sum_{i=1}^{n_b} k_{BE,i} \quad (6.13)$$

The rotational stiffness of the web-cleat connection varies with the number of bolts. A schematic illustration of the process is shown in Figure 6.17.

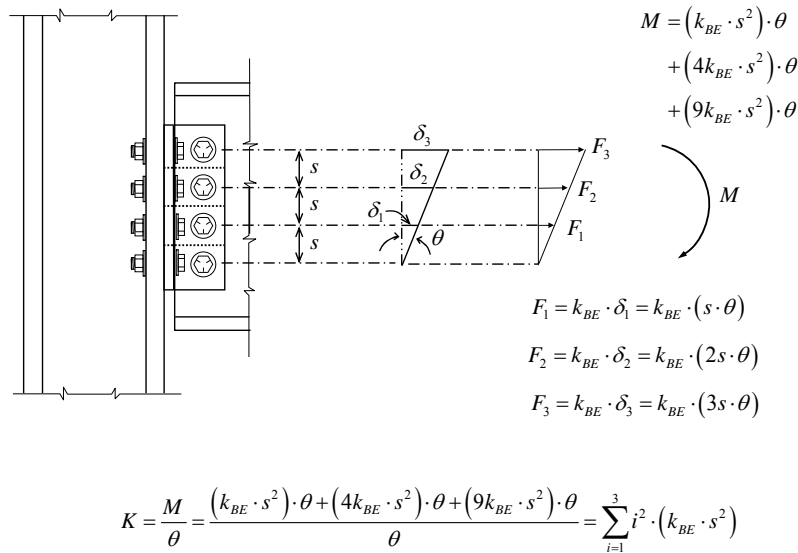


Figure 6.17 Schematic Illustrating Procedure Used to Compute Web-Cleat Connection Flexural Stiffness.

In general, if the bolt element stiffness, k_{BE} , is known and there is n_b bolt elements in the web cleat connection, the rotational stiffness can be computed as,

$$K_{\theta} = \sum_{i=1}^{n_b-1} i^2 \cdot (k_{BE} \cdot s^2) \quad (6.14)$$

where: s is the pitch of the bolt elements (taken as a constant value of 3 inches).

The axial stiffness and flexural stiffness of the web cleat connections can be defined as a function of the axial rigidity and flexural rigidity of the connected member. This process is shown below,

$$K_{\delta} = \alpha_{\delta} \cdot \frac{AE}{L} \quad (6.15)$$

$$K_{\theta} = \alpha_{\theta} \cdot \frac{EI}{L} \quad (6.16)$$

The stiffness characteristics of the steel grillage connections are summarized in Table 6.5.

Table 6.5 Stiffness Characteristics of Web Cleat Connections.

L4 x 3.5 Thickness and Secant Stiffness Parameters (1)	k_{BE} (k/in) (2)	Bolt Rows (3)	K_{δ} (k/in) (4)	K_{θ} (k-in/rad) (5)	W18x35 $AE/L = 829.7$ $EI/L = 41,083$		W21x68 $AE/L = 1,611$ $EI/L = 119,222$	
					α_{δ} (6)	α_{θ} (7)	α_{δ} (8)	α_{θ} (9)
1/4" $\delta_{T2} = 0.105''$ $P_{T2} = 5.23 k$	49.81	3	149.43	2,241.5	0.18	0.05	n.a.	n.a.
		4	199.24	6,276.1	0.24	0.15	0.12	0.05
		5	249.05	13,448.7	0.30	0.33	0.15	0.11
		6	298.86	24,656.0	n.a.	n.a.	0.19	0.21
5/16" $\delta_{T2} = 0.088''$ $P_{T2} = 8.46 k$	96.14	3	288.42	4,326.3	0.35	0.11	n.a.	n.a.
		4	384.56	12,113.6	0.46	0.29	0.24	0.10
		5	480.70	25,957.8	0.58	0.63	0.30	0.22
		6	576.84	47,589.3	n.a.	n.a.	0.36	0.40
3/8" $\delta_{T2} = 0.077''$ $P_{T2} = 12.63 k$	164.03	3	492.09	7,381.4	0.59	0.18	n.a.	n.a.
		4	656.12	20,667.8	0.79	0.50	0.41	0.17
		5	820.15	44,288.1	0.99	1.08	0.51	0.37
		6	984.18	81,194.9	n.a.	n.a.	0.61	0.68
1/2" $\delta_{T2} = 0.064''$ $P_{T2} = 24.21 k$	378.28	3	1,134.8	17,022.6	1.37	0.41	n.a.	n.a.
		4	1,513.1	47,663.3	1.82	1.16	0.94	0.40
		5	1,891.4	102,136	2.28	2.49	1.17	0.86
		6	2,269.7	187,249	n.a.	n.a.	1.41	1.57

The rotational stiffness of the web-cleat connections are well below the stiffness limit corresponding to flexible connections (AISC 2005a) given by, $\alpha_{\theta} = 2$. The majority of the rotational stiffness multipliers are in the range $0.05 \leq \alpha_{\theta} \leq 1.50$. One exception is the 5 bolt arrangement in the W18x35 beam member. The

axial stiffness multiplier for the majority of the connection arrangements lies in the range $0.10 \leq \alpha_\theta \leq 1.8$ with an exception being the 5-bolt connection in the W18x35 member with $\alpha_s = 2.3$.

The system analysis begins by computing the capacity of the concrete-steel composite slab system acting as a two-way membrane. The MathCAD worksheet contained in Appendix 6.5 illustrates these computations using theory previously discussed. The membrane capacity of the concrete slab-steel deck system is approximately 50-psf at 26.2 inches of vertical deflection at the center of the panel. This magnitude of vertical deflection corresponds to an approximate rotational demand of,

$$\theta = \tan^{-1} \frac{26.1''}{30'(12)} = 0.073 \text{ radians}$$

which is well below the limit of 0.21 radian rotation capacity (GSA 2003). It should also be noted that the rotation computed here is a total rotation (elastic plus plastic components). Therefore, the magnitude computed is conservative. The tension force in the steel deck running perpendicular to the in fill beams is approximately 566 lbs/in, which is consistent with all previous computations.

The capacity of the steel grillage can now be computed. A structural model for the steel floor framing system was developed for use in MASTAN2 (Ziemian and McGuire 2000). A schematic of the first analytical model considered is shown in Figure 6.18.

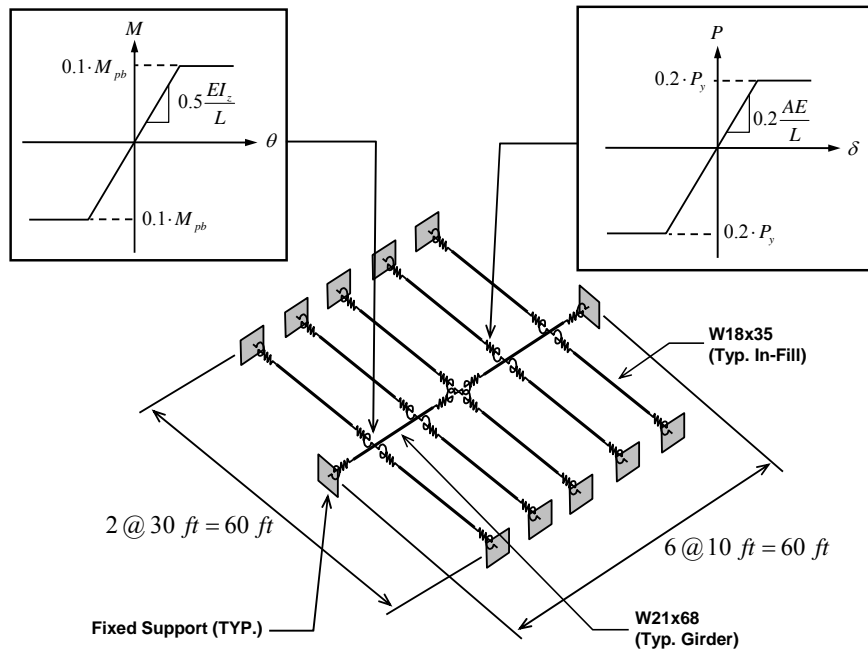


Figure 6.18 Steel Grillage Model Schematic (System 1) Illustrating Axial and Moment Connection Modeling for MASTAN2 Nonlinear Analysis.

The model contains structural steel beam-column elements, bilinear partially-restrained connections, and also axial-load-moment interaction diagrams that are used to define yielding at the ends of the beam column elements. The basis for the MASTAN2 analytical model is a structural steel grillage with fixed supports at all beams and columns located at the perimeter of the 60-ft by 60-ft panel. All members are modeled using multiple elements: in-fill beams are modeled using 10 elements and girders are modeled using 9 elements. The in-fill beams were modeled using 4 analytical segments. Two segments (*i.e.* 1/2 of the beam length) were centered on the beam mid-span. The end 1/4 lengths of beam were subdivided into 4 additional segments to facilitate connection modeling. Therefore, all in-fill beams contain end segments that are 1/16th of their span. The end segments in the girders (at column supports and interior column location) were broken down into 4 segments yielding end connection segments of 1/12th the girder span.

The connection characteristics typical of web-angle connections provided in Tables 6.4 and 6.5 were established in MASTAN2 in an indirect manner. Figure 6.18 illustrates the bilinear moment-rotation and load-extension behavior assumed in the connections. The axial tension and moment capacities chosen were consistent with those indicated in Table 6.4. Stiffness of the connections assumed were consistent with those found in Table 6.5. The bilinear connection characteristics are generated in MASTAN2 by using the built-in partial connection restraint capability for moment and then adjusting member cross-section properties to achieve moment capacities, axial stiffness characteristics, and axial capacity.

The end connections were modeled in the analytical segments of the beams and girders located immediately adjacent the fixed supports, the supporting girders, and the interior column. The connection rotational stiffness was input using the built-in capabilities with magnitude indicated in Figure 6.18. The connection moment capacity was input into the analysis by adjusting the beam or girder's plastic section modulus to $0.1 \cdot Z_x$. This resulted in a plastic moment capacity in the end regions of the in-fill beams at the levels indicated in Figure 6.18. The axial loading characteristics were included in a slightly different manner. MASTAN2 does not allow axial hinges to be directly modeled. The cross-sectional areas of the beam or girder in the end connection segments were defined to be 20% of the cross-sectional area of the members outside this hinge region. This reduction in cross-sectional area also created implied linear spring stiffness in this isolated region of the beam equal to 20% of the member's axial rigidity.

The method of modeling connections creates a "stub member" that has an axial capacity that is the same as the intended connection and a moment capacity that is the same as the connection intended. MASTAN2 then uses these pieces of information to create an interaction (yield) surface of the form shown in Figure 6.19. It should be noted that minor-axis bending is assumed to have a connection capacity that is equal to the minor axis moment capacity of the members and the connection stiffness in the minor-axis direction is infinite relative to the flexural rigidity of the connected beam (*i.e.* the connection is fully-restrained).

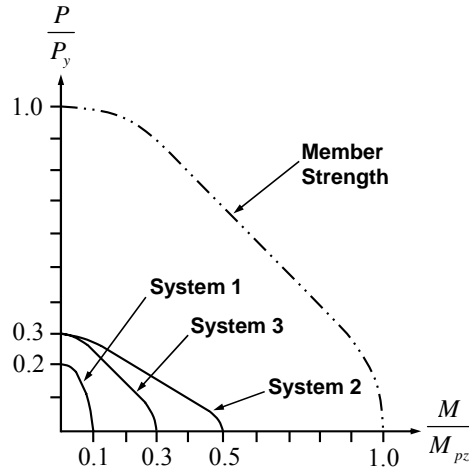


Figure 6.19 Member and Connection Interaction Surfaces for Connected Member and Three Grillage Systems (connection characteristics vary).

The beam members in the system were assumed to be composed of 50-ksi steel and the expected yield stress of the material (55-ksi) was used to define the yield stress in the analysis. This would result in a slight lowering of the strength ratios given in Table 6.4, but the connection moment and axial load strengths given in Figure 6.18 can be easily attained using the double angle web cleat connections considered.

Uniformly distributed loading was applied to the in-fill beams in the system and this, in turn, loads the interior girder. It should be noted that each floor system is evaluated independently under the assumption that each floor carries its own loading. The magnitude of the uniformly distributed loading applied to the girders was computed in the following manner. The total loading used previously in the study of the one- and two-way membrane and one-way catenary action in the floor slab was 93 psf. The MathCAD worksheet in Appendix 6.5 indicated that the floor slab system is capable of providing 50 psf toward this total with approximately 26 inches of deformation. The steel grillage will then be required to carry the following superimposed loading (with a deformation that is assumed to be compatible);

$$\begin{aligned} q_{grillage} &= \beta_{dynam} \cdot (1.0D + 0.25L) - 50 \\ &= \beta_{dynam} \cdot (93 \text{ psf}) - 50 \text{ psf} \end{aligned}$$

At pseudo-static loading levels ($\beta_{dynam} = 2.0$) prescribed in the GSA Guidelines (GSA 2003), the grillage will need to support a uniformly distributed loading of 136 psf. However, this assumes that the supporting column is “vaporized”. Furthermore, former studies (Marchand and Alfawakhiri 2004; Liu *et al.* 2005; Powell 2005) and the present research (see chapters 3-5) have shown that the multiplier commonly used

to simulate dynamic loading can vary considerably. If the supporting column is not “vaporized”, but simply compromised (*i.e.* it still has a fraction of its initial load capacity), then one might argue that the self-weight and mean point-in-time sustained live loading alone needs to be carried ($\beta_{\text{dynam}} = 1.0$) without dynamic multiplication. Therefore, in this case, the grillage must support 43-psf superimposed loading.

In order to evaluate the magnitude of the dynamic multiplier that may be expected for the SAC frames considered, the analytical model used for evaluating the ineffective column scenarios in the SAC 3-story frame was considered and the impact of column ineffectiveness rates was evaluated. Figure 6.20 illustrates the results of this evaluation.

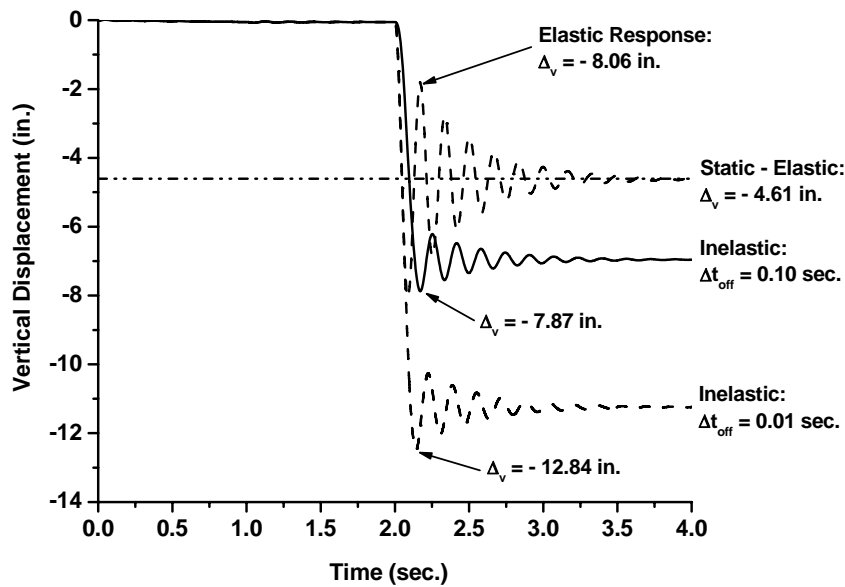


Figure 6.20 Peak Displacement Variation in SAC 3-Story Building for Various Analysis Types and Column Ineffectiveness Rates.

The peak inelastic displacement is very large when the column is rendered ineffective in $1/100^{\text{th}}$ of a second. This is essentially instantly vaporizing the column and the member goes from full capacity to absolutely no residual capacity. That is, the column is not severely damaged – it is gone. In this case, the dynamic multiplier for displacement should be taken as 2.8. However, previous analysis in chapters 3-5 indicate that forces are “capped” and the dynamic multipliers are not 2.0 and greater, but depend upon force redistribution within the system after the compromising event. In the case of an ineffectiveness rate of 0.10 seconds (perhaps a more reasonable scenario even though the column is still gone with no residual strength) the dynamic multiplier for displacement drops to 1.7 (a 40% reduction). The elastic rebound in the system for this ineffectiveness rate is also interesting and shown in Figure 6.20.

The previous side study indicates that perhaps a 1.70 dynamic multiplier is more appropriate for the building configuration considered. As a result, if $\beta_{dynam} = 1.7$ is adopted, the grillage must contribute 108 psf. Therefore, the uniformly distributed loading applied to the in-fill beams in the grillage was based upon 108 psf. Of course, the systems may not be able to carry this level of loading at levels of deformation that are compatible with the slab membrane action, but the 108-psf loading was used as the reference.

The MASTAN2 model shown in Figure 6.18 (referenced hereafter as System 1) was analyzed using 2nd order inelastic analysis. The load deformation response of the system is shown in Figure 6.21.

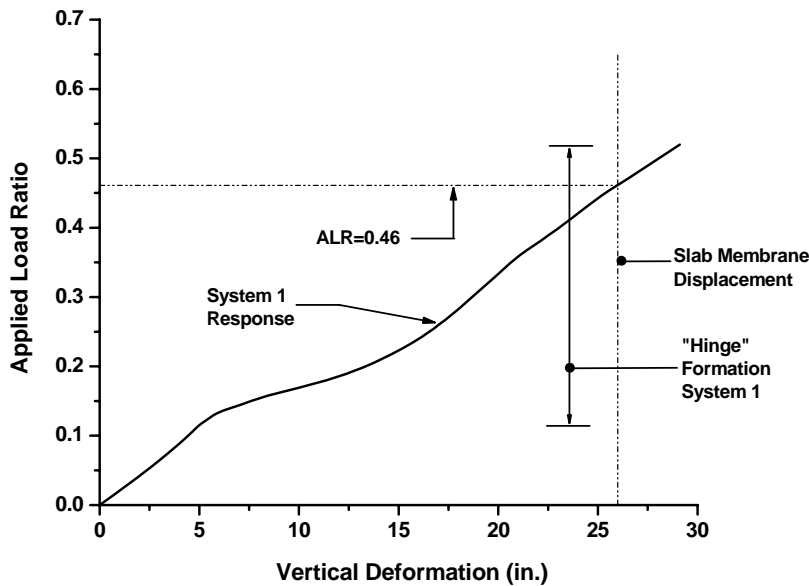


Figure 6.21 Load Deformation Response of System 1 (see Figure 6.18).

The load deformation response indicates that there is a very early transition from flexural behavior to catenary behavior in the grillage. The connection strengths and stiffness shown in Figure 6.18 reveal that the cross-sections at the ends of the members reach the yield surfaces (Figure 6.19) very early in the response and the large displacements result in catenary tension in the grillage forming. This transition is exhibited by the shallow yield plateau-like response and subsequent stiffening behavior.

The applied load ratio that results in deformations compatible with the membrane displacement computed earlier (26 inches) is 0.46. This indicates that the capacity of the system (both slab and grillage) is;

$$q_{cap} = 0.46(108) + 50 \approx 100 \text{ psf}$$

Therefore, the system can definitely support its self-weight and the mean point in time sustained live loading and there is some reserve for dynamic amplification: $\beta_{dynam} = 100/93 = 1.08$. If one were to assume that the

system could continue to deflect without membrane reinforcement in the slab rupturing, or the anchorage of this reinforcement being compromised (*e.g.* deflection to approximately 30 inches), the membrane capacity would increase and the catenary capacity of the grillage could increase. This increase is shown in Figure 6.21 at $ALR = 0.52$. This would result in the system capacity moving upward to,

$$q_{cap} = 0.52(108) + 50 \approx 106 \text{ psf}$$

and the dynamic multiplier would naturally increase as well ($\beta_{dynam} = 106/93 = 1.14$). One should note that shrinkage and temperature welded wire fabric reinforcement was assumed as well as 22-gauge steel deck with anchorage strength consistent with that of 5/8" arc-spot welds at 3 inches on center. Greater capacities may be attained if thicker deck is used, steel stud anchorage is assumed, or mild-steel reinforcement rather than welded wire mesh is implemented. It should be noted that the rupture strain and anchorage of the reinforcement should be considered if the membrane capacity and increased deformations are to be utilized.

At 26 inches of vertical displacement, the total rotation over the beam and girder span of 30 feet was computed previously as approximately 0.07 radians. This is very close to the plastic rotational limit of 0.06 radians recommended for web-angle connections (FEMA 2000c). However, the present rotational demand is "total" and the plastic demand will likely align itself close to this limit. Therefore, the rotational demands at the level of loading considered are not likely to cause rupture of the connections, but should be further evaluated.

It is doubtful that the system could support the GSA recommended dynamic multiplier of 2.0. However, one can say that the typical structural steel framing system can *resist* progressive collapse in the event an internal column is rendered ineffective and has significant inherent robustness. This statement is supported by the fact that the loading of $1.0D + 0.25L$ can be supported through catenary and flexural action in the structural steel framing and membrane action in the composite concrete-steel deck system. It should be noted that this behavior was estimated for the system without special modification and the connections should have strength and stiffness characteristics as indicated in the analytical model shown in Figure 6.18. Inspection of Tables 6.4 and 6.5 indicate the following connection configurations yield strength and stiffness characteristics consistent with the analytical assumptions;

W18x35 L4x3.5x5/16, x3/8, x1/2 with 4 or 5 bolt rows;

W21x68 L4x3.5x3/8, x1/2 with 5 or 6 bolt rows.

The angles above will yield axial stiffness magnitudes that are a little bit stiffer than the analytical model and bending stiffness magnitudes that are slightly larger as well.

The analysis results indicate that in order to attain adequate levels of inherent structural integrity in the steel system, one is better off choosing connection angles on the upper-end of those provided in the

Manual (AISC 2001b). It is also recommended to “fill up” the web of the beam and girder members with connecting bolts. In other words, use the maximum number of bolt rows that the beam or girder web can support. Furthermore, it is recommended that all flexible connections have the following characteristics;

$$P \approx 0.2P_y \text{ and } K_\delta \approx 0.2 \frac{AE}{L}$$

$$M \approx 0.1M_p \text{ and } K_\theta \approx 0.5 \frac{EI}{L}$$

These characteristics are consistent with the double angle connections that will result if the bolt row recommendations and angle thickness recommendations are followed. Finally, typical welded wire mesh can be used (*i.e.* that used for shrinkage and temperature reinforcement).

There are other connection types available for use in beam-to-girder and girder-to-column connections. For example, partially restrained beam-to-girder connections have been proposed (Rex and Easterling 2002) and there is long-standing use of partially restrained girder-to-column connections. A second model was analyzed and the connections chosen in this case were stronger and stiffer with respect to bending, but had only slightly more strength and stiffness with respect to axial deformations. This simulates the concrete slab contributing to increased flexural stiffness and strength. This system (now referred to as System 2 in Figure 6.18) is shown in Figure 6.22.

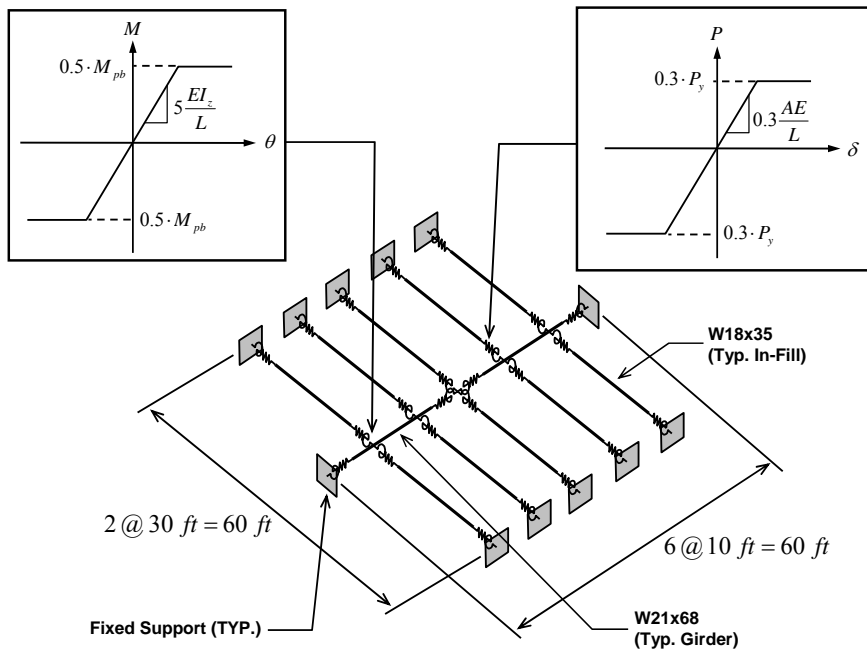


Figure 6.22 Steel Grillage Model Schematic (System 2) Illustrating Axial and Moment Connection Modeling for MASTAN2 Nonlinear Analysis.

The connection rotational stiffness and strength shown in Figure 6.22 are very close to those reported in (Rex and Easterling 2002) for partially restrained beam-to-girder connections. The axial strength and stiffness were increased slightly from that of System 1 to simulate the addition of a seat angle.

The same reference loading of 108 psf was applied to the steel grillage with the understanding that membrane action in the slab would support 50 psf. The load deformation response of the grillage system 2 (with system 1 included) is shown in Figure 6.23.

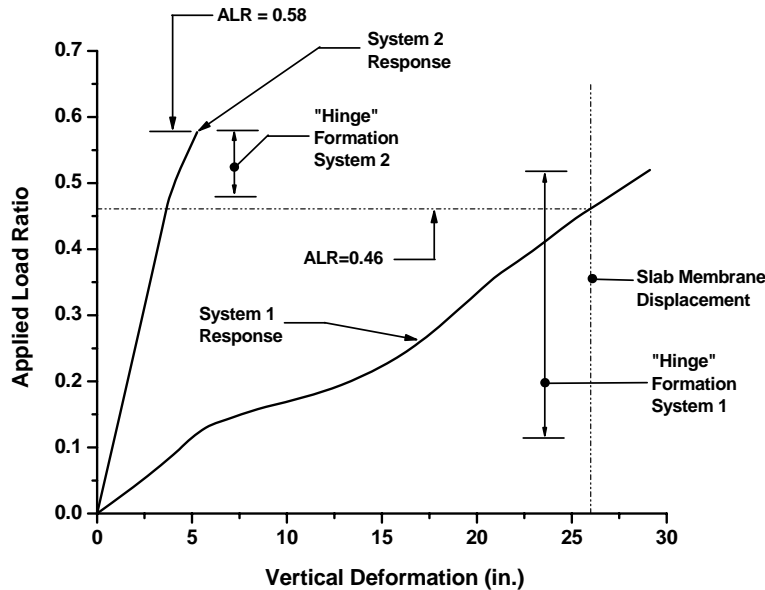


Figure 6.23 Load Deformation Response of Grillage Systems 1 and 2 (see Figures 6.18 and 6.22).

It is interesting to note that the catenary response is not present in System 2. The reason for this is that a plastic (flexural) mechanism forms at an applied load ratio of 0.58 with vertical deformation slightly less than 5 inches. This amount of vertical deformation is not sufficient to *activate* the contribution of geometric stiffness to the member stiffness matrices in the system. In other words, analytically, catenary action is not allowed to form and the system numerically “fails”. It is understood that there will be a *conversion* to catenary action once the flexural plastic hinge mechanism forms, but the structural analysis is not able to consider this transformation because analytically, the tangent stiffness matrix of the system is singular at the instant these beam mechanisms form.

System 2 exhibits significantly different behavior with regard to the ends of the members reaching the yield surface when compared to the original system. First of all, the number of hinges that form in System 2 is less than that of System 1. The span of load application over which hinges form is significantly larger in System 1 when compared to 2. One would like to have a system where there is a significant number of hinges

forming so that full advantage of the structural indeterminacy is exploited. When the hinges form over very short loading ranges, there is less redundancy and toughness in the *system*.

The significantly smaller deformation in System 2 at the formation of the collapse mechanism would indicate that the grillage will “fail” first with subsequent reliance on back-up capacity from the slab membrane action. In System 1, there appears to be a better synergy in response between the slab system and the structural steel grillage system. This suggests a better overall *system* response to the compromising event. The benefits of this type of response remain to be fully quantified and understood. The experimental rotations attained by (Rex and Easterling 2002) for the partially-restrained beam-to-girder connections were on the order of 0.05 radians. If one were to rely on catenary action after the flexural mechanisms occurs, the vertical deformations in the system would likely rapidly increase to those found in the first system (approximately 26 inches). As a result, even though the flexural mechanism forms early at 5 inches of deformation there will need to be an additional 21 inches of deformation in the grillage needed to activate catenary action in the secondary slab system. As a result, the rotational demands on these connections are likely to be on the order of 0.07 radians. It is unclear if the PR beam-to-girder connection can support his level of rotational demand without fracture. Therefore, additional study is recommended for PR connections.

A third system was evaluated. This system had a better balance between axial capacity and moment capacity than system 2. The system (System 3 in Figure 6.18) is shown in Figure 6.24.

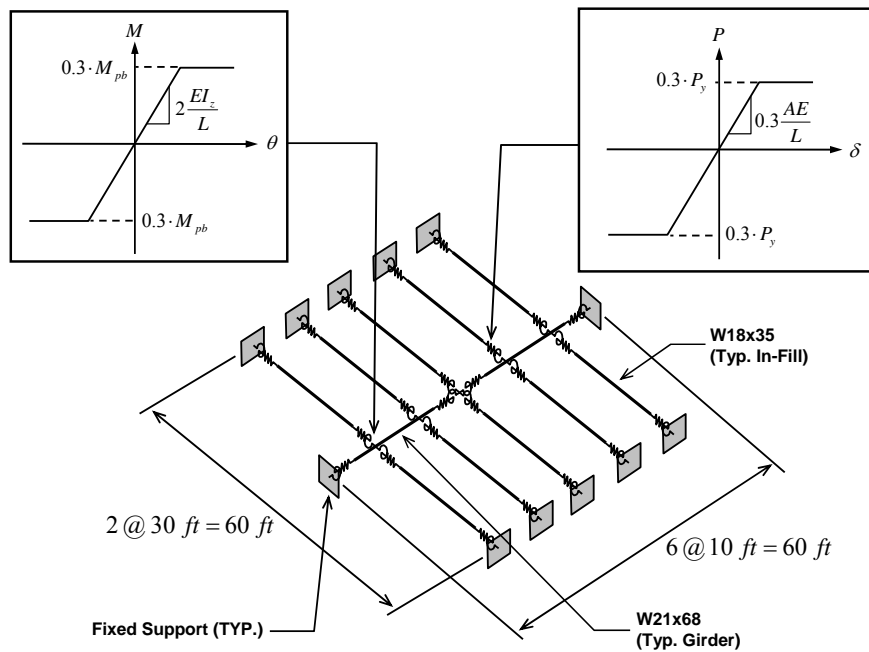


Figure 6.24 Steel Grillage Model Schematic (System 3) Illustrating Axial and Moment Connection Modeling for MASTAN2 Nonlinear Analysis.

The axial strength and stiffness for the connections in System 3 were left the same as those in System 2. The bending strength and stiffness of the connections were reduced to a level slightly above that in System 1 and below that in System 2.

The load deformation response of this system along with the response of Systems 1 and 2 are given in Figure 6.25. A smooth transition between flexural mechanism formation and catenary action in the steel grillage is clearly exhibited in the response.

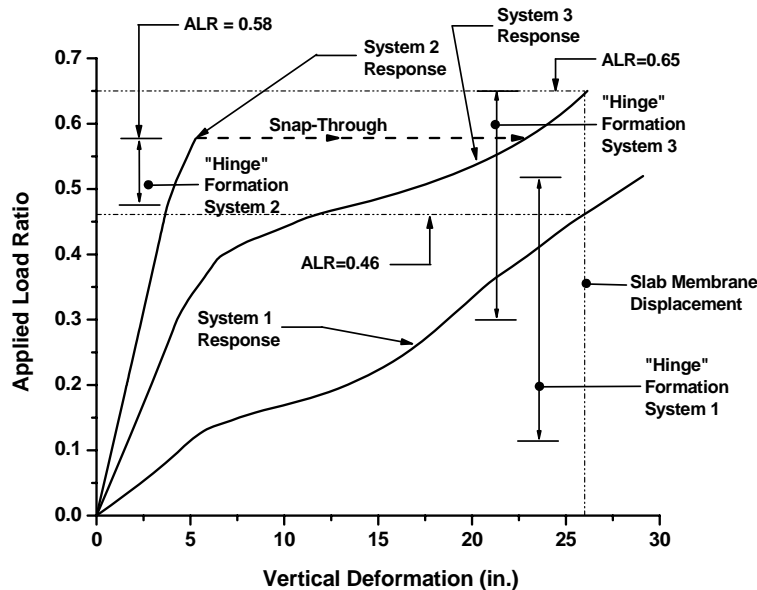


Figure 6.25 Load Deformation Response of Three Grillage Systems Considered.

As in System 1, there is a significant range of loading over which the interaction surface at the member ends is reached. This indicates a smooth transition between flexural and catenary action. The increased flexural stiffness in the connections in System 3 is the reason for the lessened vertical deformation prior to the formation of catenary tension behavior in the grillage.

The axial stiffness and strength of the connections in System 3 are consistent with those of System 2 and therefore, it is expected that the catenary behavior will be similar in the two systems once it is activated. As discussed previously, System 2 will likely incur an abrupt (perhaps dynamic) transition between the formation of a flexural collapse mechanism in the grillage and the formation of catenary tension in the grillage. This abrupt transition is analogous to snap-through behavior in arches. The snap-through deformations that are likely in System 2 are shown in Figure 6.25. As indicated, after the formation of the flexural collapse mechanism in the system, it is likely that the steel grillage will need to abruptly accumulate an additional 20 inches of deflection in order to reach the catenary tension stiffening that comes from the

contribution of geometric stiffness in the system. This magnitude of vertical deflection is likely to occur very quickly and the snap-through behavior is undesirable when compared to the smooth transition between these two primary load resistance mechanisms shown in Systems 1 and 3. It should be noted that the response of System 3 indicates it is not economically advantageous to provide additional bending moment capacity and stiffness when there is no enhancement in load carrying capacity. Furthermore, dynamic snap-through behavior may have adverse ramifications with regard to system integrity.

The analysis outlined indicates the axial capacities of the connections should be on the order of $0.2P_y - 0.3P_y$ and the bending moment capacities of the connections should be on the order of $0.1M_{pb} - 0.3M_{pb}$. When the moment capacity is low, there is a smooth transition between the formation of the flexural mechanism and the catenary tension behavior that is essentially secondary after the initial deformations associated with the flexural mechanism. If the moment capacity is too large, there may be snap-through-type behavior whereupon a significant magnitude of vertical displacement will rapidly take place prior to catenary formation. This appears undesirable and further study is warranted. It is interesting to note that the desired behavior can be easily achieved in the structural steel framing systems considered and therefore, this study suggests that limited special consideration of interior column ineffectiveness needs to be made other than the web angle bolt row recommendations previously described.

6.5 Concluding Remarks

This chapter in the report considered a variety of floor system scenarios by which interior in-fill beams, spandrel beams, and interior columns were rendered ineffective. A method to quantify the inherent structural integrity or robustness in a typical structural steel floor framing system was demonstrated. In general, the typical structural steel system may have the capability to resist the structure's self weight and mean point-in-time sustained live loading for a large variety of compromised component situations. One exception is the spandrel beam loss scenario whereby concentrated bands of mild-steel slab reinforcement at the perimeter appear to be sufficient to create significant structural integrity.

This section of the report simply summarizes the observations made during the analyses conducted for the floor framing systems. One major item of note, however, is that better information regarding anchoring strengths for steel deck to the structural steel members is needed and better information regarding the two-way reinforcement capabilities of fluted steel decking. These tests can serve as the basis for slab membrane strength computations and better estimates for the contribution of the composite steel-concrete floor deck system to the integrity of the building framing system can be obtained. Furthermore, the contribution of the steel studs employed to create composite action between the slab and beams should be assessed.

A typical structural steel framing arrangement with 30-ft by 30-ft framing bay was considered. The base system included: 2VLI22 steel deck and 6x6-W1.4xW1.4 welded wire mesh reinforcement. The system self-weight and mean point-in-time sustained live loading that needed to be supported in the event of ineffective components was 93 psf. Conclusions regarding behavior and strength of the typical slab system under a variety of compromising events follow.

One In-Fill Beam Rendered Ineffective:

The slab system typically present in a structural steel system is capable of carrying point-in-time loading in the event a single in-fill beam is rendered ineffective. This statement quantifies one measure of the inherent structural integrity or robustness in the system. The membrane action in the slab system is most effectively enhanced (*i.e.* one is able to approach GSA dynamic multipliers) by increasing the mild steel reinforcement in the system as shown below:

2VLI22 and 6x6-W1.4xW1.4	110 psf ($\beta_{dynam} \approx 1.2$)
2VLI22 and #3 at 12-inches on center	189 psf ($\beta_{dynam} \approx 2.0$)

Two In-Fill Beams Rendered Ineffective:

The typical panel found in structural steel floor systems is capable of supporting point-in-time loading likely at the time the two in-fill beams are rendered ineffective. Therefore, the typical steel structural system has a significant level of inherent robustness. GSA-level dynamic multipliers are able to be approached for this scenario when additional mild-steel reinforcement is provided as shown below:

#3 at 24 in. on center; 0.00458 in^2/in	119 psf at 12-in. defl. ($\beta_{dynam} \approx 1.3$)
#3 at 18 in. on center; 0.00611 in^2/in	140 psf at 12-in. defl. ($\beta_{dynam} \approx 1.5$)
#3 at 12 in. on center; 0.0092 in^2/in	178 psf at 12 in. defl. ($\beta_{dynam} \approx 1.9$)

Comparing the previous results for the single in-fill beam being lost, it can be said that the best balance in providing progressive collapse resistance for both one and two in-fill beams being lost would be to provide #3 mild-steel reinforcing bars at 12 inches on center throughout the system.

Ineffective Spandrel Beam and Adjacent In-Fill Beam(s):

The most effective method to create robustness in the event a spandrel beam is lost was determined to be providing a band of mild-steel reinforcement at the perimeter of the slab system. The loading capacity of the one-way catenary for this scenario was determined to be approximately 100 psf using a conservative estimate for tributary width. If the tributary width of slab carried by the catenary is rationally reduced, 4 – #4 bars are capable of supporting 168-psf loading, which allows for a dynamic multiplier of 1.8. As a result, providing a

one-way band of mild-steel reinforcement is likely to be sufficient to meet GSA-level loading and provide significant inherent robustness.

Distribution of slab reinforcement (in lieu of concentrated perimeter bands) was also studied. The distribution of mild-steel slab reinforcement throughout the exterior bays in the steel system was determined to be the most economical way to create inherent structural integrity and meet GSA-level dynamic loading magnitudes in the case of spandrel beam loss coupled with loss of adjacent in-fill beams. The analysis conducted indicated that #4 mild-steel reinforcing bars at 9 inches on center (laid in direction parallel to beams) was sufficient to inhibit progressive collapse in the event of lost supporting spandrel and in-fill beams.

Ineffective Spandrel Girder:

Another situation considered was the loss of a spandrel girder in the floor framing system. The typical slab arrangement considered is capable of providing progressive collapse resistance since the steel deck and welded wire mesh typically used is capable of creating membrane behavior with a capacity that exceeds the loading likely to be present. However, if the dynamic load multiplier of 2.0 is desired, additional reinforcement will likely be required. The steel deck contributes significantly to the membrane tension reinforcement and therefore, if GSA-level dynamic multipliers are desired, #4 at 14-inches on center was found to be acceptable. Coupled with the #4 at 9 inch arrangement described previously, the analysis conducted indicates that for the systems considered, GSA-level progressive collapse resistance can be provided simply by providing #4 at 9 inches on center parallel to the beams and #4 at 14 inches on center in the orthogonal direction.

Interior Column Rendered Ineffective:

A scenario whereby an interior column is rendered ineffective was also considered. This situation is intended to model floors in the steel structure where Veirendeel action in the framing system above a compromised column cannot be effectively created. As a result, each floor system is asked to support its own point-in-time loading or dynamically enhanced loading.

The typical slab and steel deck found in the steel structure considered was capable of contributing 50-psf at a vertical displacement of 26 inches. The total rotational demand at the perimeter of the slab panel corresponding to this deformation was found to be within the plastic rotational demand capacity for two-way and one-way concrete slab systems (GSA 2003).

A static nonlinear analysis of the typical 30-ft by 30-ft framing system that included nonlinear connection behavior consistent with that of web-cleat connections was conducted. The analysis indicated that the compromised system will likely be able to support the floor system's self-weight, partitions, and mean point-in-time sustained live loading of $1.0D + 0.25L$. It should be noted that dynamic response of the

system needs to be evaluated in order to fully appreciate the demands that will be placed on puddle welds, shear studs, and internal slab reinforcement.

The analysis results indicate that in order to improve the inherent structural integrity in the steel system, one should select connection angle thicknesses on the upper-end of those provided in the Manual (AISC 2001b). It is also recommended to “fill up” the web of the beam and girder members with connecting bolts. In other words, use the maximum number of bolt rows that the beam or girder web can support. Both of these rather simplistic measures will enhance the inherent robustness in the system.

The analysis conducted indicated that it is better to have smaller moment capacity and flexural stiffness for connections distributed throughout the floor framing system (as is typically found in structural steel interior framing arrangements). Furthermore, the axial capacities of the connections should be on the order of $0.2P_y - 0.3P_y$ and the bending moment capacities should be on the order of $0.1M_{pb} - 0.3M_{pb}$. When the moment capacity is low, there is the opportunity for smooth transition between the formation of the flexural mechanism and the catenary tension behavior that is secondary after the initial flexural mechanism formation. If the moment capacity is too large, there may be snap-through-type behavior whereupon a significant magnitude of vertical displacement will rapidly take place prior to catenary mechanism formation. This appears undesirable and further study with regard to the effect of snap-through is warranted.

In general, the analysis conducted indicates that balance between membrane action in the slab and catenary action in the steel grillage can be attained when the following axial and moment characteristics are met in regard to the connections at the ends of the beams and girders in the structural steel system;

$$M_{conn} \leq 0.30M_{pb} \text{ and } K_{\theta} \leq 2\frac{EI}{L}$$

$$P_{conn} \leq 0.3P_y \text{ and } K_{\delta} \leq 0.3\frac{AE}{L}$$

It is interesting to note that the desired behavior appears to be inherent in the typical structural steel framing systems considered. Therefore, this study suggests that there is opportunity to avoid special structural engineering consideration of interior column ineffectiveness scenarios if the web angle bolt row recommendations previously described are followed and larger connection angles thicknesses are implemented. Therefore, a typical structural steel framing system is likely to have significant inherent resistance to progressive collapse without special structural engineering.

It is recommended that the response of the entire 3D steel building with the connection characteristics outlined in this section be conducted. This will likely lead to some very interesting results with regard to the true robustness in steel building systems.

Appendix 6.1 – MathCAD Worksheet for Two-Way Membrane Capacity (20-ft by 30-ft panel).

Two-Way Membrane Strength Computations

Computations based upon procedure proposed by:

Hawkins, N.M. and Mitchell, D. (1979) "Progressive Collapse of Flat Plate Structures", *ACI Journal*, Title No. 76-34, July, American Concrete Institute, pp. 775-808.

Mitchell, D. and Cook, W.D. (1984) "Preventing Progressive Collapse of Slab Structures", *Journal of Structural Engineering*, Vol. 110, No. 7, ASCE, pp. 1513-1532.

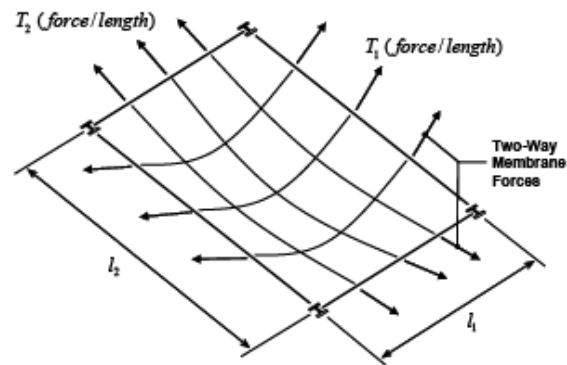
Membrane Schematic and Assumptions

Two-way membrane action in a slab panel is assumed after a supporting member is rendered ineffective. The short direction in the two way span is denoted with subscript 1 and the long direction is denoted with subscript 2.

The reinforcement in the short direction is assumed to consist of steel deck (composite or form-deck) and welded wire mesh. The reinforcement in the long direction is assumed to consist of welded wire mesh. It should be noted that if the panel is square, the user should simply choose the long and short direction.

The reinforcing steel in the membrane is assumed to be elastic-perfectly-plastic. The capacity of the membrane is assumed to be reached when the long direction reinforcement is at yield. The short direction strain follows from compatibility of deformations at the center of the concave shape. The membrane is assumed to form a circular pattern, when a catenary parabola is most appropriate.

An illustration of the scenario assumed is shown below.



Panel Dimensions

$$l_1 := 240 \quad (\text{in.}) \quad \text{Short direction} \quad l_2 := 360 \quad (\text{in.}) \quad \text{Long direction}$$

Slab Reinforcement

$$A_{sm1} := 0.00233 \quad (\text{sq. in.}) \quad \text{Area of WWM per inch parallel to short dimension: 6x6-W1.4xW1.4.}$$

$$A_{d1} := 0.01416 \quad (\text{sq. in.}) \quad \text{Area of steel deck per inch parallel to short dimension: 40\% of 2VLI22.}$$

$$A_{sm2} := 0.00233 \quad (\text{sq. in.}) \quad \text{Area of WWM per inch parallel to long dimension: 6x6-W1.4xW1.4..}$$

$$f_{ys1} := 65000.0 \quad (\text{psi}) \quad \text{Yield stress of WWM parallel to short dimension.}$$

$$f_{yd1} := 40000.0 \quad (\text{psi}) \quad \text{Yield stress of steel deck parallel to short dimension.}$$

$$f_{ys2} := 65000.0 \quad (\text{psi}) \quad \text{Yield stress of WWM parallel to long dimension.}$$

Assumed Strains and Resulting Stresses

$$\varepsilon_2 := 0.001 \quad (\text{in./in.}) \text{ User MUST input this value.}$$

$$\varepsilon_1 := \varepsilon_2 \cdot \left(\frac{l_2}{l_1}\right)^2 \quad \text{float,6} \rightarrow .225000\text{e-}2 \quad (\text{in./in.}) \text{ User should compare to rupture strain.}$$

$$f_{s1} := \begin{cases} 29000000.0 \cdot \varepsilon_1 & \text{if } \varepsilon_1 \leq \frac{f_{ys1}}{29000000.0} \\ f_{ys1} & \text{otherwise} \end{cases} \quad \text{float,6} \rightarrow 65000.0$$

$$f_{d1} := \begin{cases} 29000000.0 \cdot \varepsilon_1 & \text{if } \varepsilon_1 \leq \frac{f_{yd1}}{29000000.0} \\ f_{yd1} & \text{otherwise} \end{cases} \quad \text{float,6} \rightarrow 40000.0$$

$$f_{s2} := \begin{cases} 29000000.0 \cdot \varepsilon_2 & \text{if } \varepsilon_2 \leq \frac{f_{ys2}}{29000000.0} \\ f_{ys2} & \text{otherwise} \end{cases} \quad \text{float,6} \rightarrow 65000.0$$

Compute Uniform Load Capacity of Membrane

Compute edge tensions per unit length

$$T_{1m} := A_{sm1} \cdot f_{s1} \quad \text{float,4} \rightarrow 151.5 \quad T_{2m} := A_{sm2} \cdot f_{s2} \quad \text{float,4} \rightarrow 151.5$$

$$T_{1d} := A_{dl} \cdot f_{d1} \quad \text{float,6} \rightarrow 566.400$$

Membrane Capacity Based Upon Tension Capacity at Edge of Panel (Hawkins and Mitchell 1979; Mitchell and Cook 1984):

$$w_{\text{edge}} := \frac{2 \cdot (T_{1m} + T_{1d}) \cdot \sin(\sqrt{6 \cdot \varepsilon_1})}{l_1} + \frac{2 \cdot (T_{2m}) \cdot \sin\left(\frac{l_1}{l_2} \cdot \sqrt{6 \cdot \varepsilon_1}\right)}{l_2}$$

$$w_{\text{edge}} \quad \text{float,4} \rightarrow .7587 \quad (\text{psi})$$

Membrane Capacity Based Upon Tension Capacity at the Interior of the Panel (Hawkins and Mitchell 1979);

$$w_{\text{pos}} := 2 \cdot \sqrt{6 \cdot \varepsilon_1} \cdot \left[\frac{T_{1m} + T_{1d}}{l_1} + (T_{2m}) \cdot \frac{l_1}{l_2^2} \right]$$

$$w_{\text{pos}} \quad \text{float,4} \rightarrow .7603 \quad (\text{psi})$$

Ultimate Strength of Membrane

$$w_u := \begin{cases} w_{\text{edge}} & \text{if } w_{\text{edge}} \leq w_{\text{pos}} \\ w_{\text{pos}} & \text{otherwise} \end{cases}$$

$$q_u := w_u \cdot 144 \text{ float, 5} \rightarrow 109.25 \quad (\text{psf})$$

Vertical Deflection in Membrane:

$$\delta := \frac{3 \cdot l_1 \cdot \varepsilon_1}{2 \cdot \sin(\sqrt{\delta \cdot \varepsilon_1})}$$

$$\delta \text{ float, 4} \rightarrow 6.987 \quad (\text{in.}) \text{ downward}$$

Appendix 6.2 – MathCAD Worksheet for Two-Way Membrane Capacity (30-ft by 30-ft panel).

Two-Way Membrane Strength Computations

Computations based upon procedure proposed by;

Hawkins, N.M. and Mitchell, D. (1979) "Progressive Collapse of Flat Plate Structures", *ACI Journal*, Title No. 76-34, July, American Concrete Institute, pp. 775-808.
 Mitchell, D. and Cook, W.D. (1984) "Preventing Progressive Collapse of Slab Structures", *Journal of Structural Engineering*, Vol. 110, No. 7, ASCE, pp. 1513-1532.

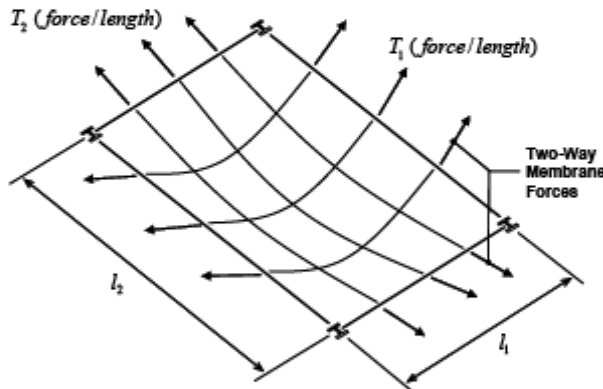
Membrane Schematic and Assumptions

Two-way membrane action in a slab panel is assumed after a supporting member is rendered ineffective. The short direction in the two way span is denoted with subscript 1 and the long direction is denoted with subscript 2.

The reinforcement in the short direction is assumed to consist of steel deck (composite or form-deck) and welded wire mesh. The reinforcement in the long direction is assumed to consist of welded wire mesh. It should be noted that if the panel is square, the user should simply choose the long and short direction.

The reinforcing steel in the membrane is assumed to be elastic-perfectly-plastic. The capacity of the membrane is assumed to be reached when the long direction reinforcement is at yield. The short direction strain follows from compatibility of deformations at the center of the concave shape. The membrane is assumed to form a circular pattern, when a catenary parabola is most appropriate.

An illustration of the scenario assumed is shown below.



Panel Dimensions

$l_1 := 360$ (in.) Short direction $l_2 := 360$ (in.) Long direction

Slab Reinforcement

- $A_{sm1} := 0.00233$ (sq. in.) Area of WWM per inch parallel to short dimension: 6x6-W1.4xW1.4.
- $A_{d1} := 0.01416$ (sq. in.) Area of steel deck per inch parallel to short dimension: 40% of 2VLI22.
- $A_{sm2} := 0.00233$ (sq. in.) Area of WWM per inch parallel to long dimension: 6x6-W1.4xW1.4.
- $f_{ys1} := 65000.0$ (psi) Yield stress of WWM parallel to short dimension.
- $f_{yd1} := 40000.0$ (psi) Yield stress of steel deck parallel to short dimension.
- $f_{ys2} := 65000.0$ (psi) Yield stress of WWM parallel to long dimension.

Assumed Strains and Resulting Stresses

$$\varepsilon_2 := 0.003 \quad (\text{in./in.}) \text{ User MUST input this value.}$$

$$\varepsilon_1 := \varepsilon_2 \left(\frac{l_2}{l_1} \right)^2 \quad \text{float, 6} \rightarrow .3\text{e-}2 \quad (\text{in./in.}) \text{ User should compare to rupture strain.}$$

$$f_{s1} := \begin{cases} 29000000.0 \cdot \varepsilon_1 & \text{if } \varepsilon_1 \leq \frac{f_{ys1}}{29000000.0} \\ f_{ys1} & \text{otherwise} \end{cases} \quad \text{float, 6} \rightarrow 65000.0$$

$$f_{d1} := \begin{cases} 29000000.0 \cdot \varepsilon_1 & \text{if } \varepsilon_1 \leq \frac{f_{yd1}}{29000000.0} \\ f_{yd1} & \text{otherwise} \end{cases} \quad \text{float, 6} \rightarrow 40000.0$$

$$f_{s2} := \begin{cases} 29000000.0 \cdot \varepsilon_2 & \text{if } \varepsilon_2 \leq \frac{f_{ys2}}{29000000.0} \\ f_{ys2} & \text{otherwise} \end{cases} \quad \text{float, 6} \rightarrow 65000.0$$

Compute Uniform Load Capacity of Membrane

Compute edge tensions per unit length

$$T_{1m} := A_{sm1} \cdot f_{s1} \quad \text{float, 4} \rightarrow 151.5 \quad T_{2m} := A_{sm2} \cdot f_{s2} \quad \text{float, 4} \rightarrow 151.5$$

$$T_{1d} := A_{d1} \cdot f_{d1} \quad \text{float, 6} \rightarrow 566.400$$

Membrane Capacity Based Upon Tension Capacity at Edge of Panel (Hawkins and Mitchell 1979; Mitchell and Cook 1984):

$$w_{\text{edge}} := \frac{2 \cdot (T_{1m} + T_{1d}) \cdot \sin(\sqrt{6} \cdot \varepsilon_1)}{l_1} + \frac{2 \cdot (T_{2m}) \cdot \sin\left(\frac{l_1}{l_2} \cdot \sqrt{6} \cdot \varepsilon_1\right)}{l_2}$$

$$w_{\text{edge}} \quad \text{float, 4} \rightarrow .6461 \quad (\text{psi})$$

Membrane Capacity Based Upon Tension Capacity at the Interior of the Panel (Hawkins and Mitchell 1979):

$$w_{\text{pos}} := 2 \cdot \sqrt{6} \cdot \varepsilon_1 \cdot \left[\frac{T_{1m} + T_{1d}}{l_1} + (T_{2m}) \cdot \frac{l_1}{l_2^2} \right]$$

$$w_{\text{pos}} \quad \text{float, 4} \rightarrow .6480 \quad (\text{psi})$$

Ultimate Strength of Membrane

$$w_u := \begin{cases} w_{\text{edge}} & \text{if } w_{\text{edge}} \leq w_{\text{pos}} \\ w_{\text{pos}} & \text{otherwise} \end{cases}$$

$$q_u := w_u \cdot 144 \text{ float}, 5 \rightarrow 93.034 \quad (\text{psf})$$

Vertical Deflection in Membrane:

$$\delta := \frac{3 \cdot l_1 \cdot \varepsilon_1}{2 \cdot \sin(\sqrt{\delta \cdot \varepsilon_1})}$$

$$\delta \text{ float}, 4 \rightarrow 12.11 \quad (\text{in.}) \text{ downward}$$

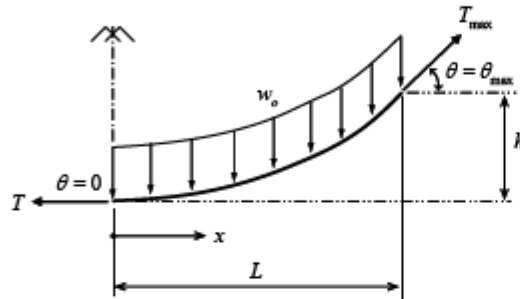
Appendix 6.3 MathCAD Worksheet for One-Way Membrane Capacity; Spandrel Beam Ineffective.

One-Way Catenary Action of Slab System

Computational procedure based upon simple catenary parabola structural mechanics theory. A discussion of the procedure can be found in:

Hibbeler, R.C. (2008) *Structural Analysis, 6th Edition*, Pearson Prentice-Hall, Upper Saddle River, NJ.

The fundamental parameters for the one-way catenary is shown in the schematic below:



Two regions of behavior are possible. The strength limit state of the catenary may be limited by the maximum tensile force or the horizontal tensile force at the centerline of the catenary span.

Slab Material and Thickness Parameters

$A_s := 0.800$ (sq. in.) Area of reinforcement in catenary span direction: 4 - #4 bars.

$A_d := 0.0$ (sq. in.) Area of steel deck in catenary span direction.

$f_{sy} := 60000.00$ (psi) Yield stress of slab reinforcement.

$f_{dy} := 40000.00$ (psi) Yield stress of steel deck material.

$L_1 := 5$ (ft.) Width of slab tributary to catenary.

Catenary Span Information

$L := 180$ (in.) One-half the span of the catenary.

$\beta := 0.08$ (unitless) The "sag" parameter defining tolerable sag in catenary.

$h := \beta \cdot L \text{ float}, 5 \rightarrow 14.40$ Tolerable "sag" in catenary

Strain in Catenary Reinforcement:

$$L_{\text{new}}(h, L) := \int_0^L \sqrt{1 + \frac{4h^2}{L^4} \cdot x^2} dx$$

$$s := \frac{L_{\text{new}}(h, L) - L}{L} \text{ float, 6} \rightarrow .425043\text{e-}2$$

$$\mu_{\text{demand}} := \frac{29000000.0}{f_{sy}} s \text{ float, 3} \rightarrow 2.05$$

Catenary Distributed Load Capacities*Based Upon Mid-Span Tension Capacity*

$$w_{\text{ou1}} := \frac{2 \cdot [(A_s \cdot f_{sy} + A_d \cdot f_{dy}) \cdot h]}{L^2}$$

$$w_{\text{ou1}} \text{ float, 5} \rightarrow 42.667 \quad (\text{lbs./in.}) \quad \text{Uniformly distributed load capacity.}$$

Based Upon Support Tension Capacity

$$w_{\text{ou2}} := \frac{A_s \cdot f_{sy} + A_d \cdot f_{dy}}{L} \left[1 + \left(\frac{L}{2 \cdot h} \right)^2 \right]^{-0.50}$$

$$w_{\text{ou2}} \text{ float, 5} \rightarrow 42.131 \quad (\text{lbs./in.}) \quad \text{Uniformly distributed load capacity.}$$

Capacity of Catenary

$$w_{\text{ou}} := \begin{cases} w_{\text{ou1}} & \text{if } w_{\text{ou1}} \leq w_{\text{ou2}} \\ w_{\text{ou2}} & \end{cases}$$

$$q_u := \frac{w_{\text{ou}} \cdot 12}{L_1} \text{ float, 4} \rightarrow 101.1 \quad (\text{psf})$$

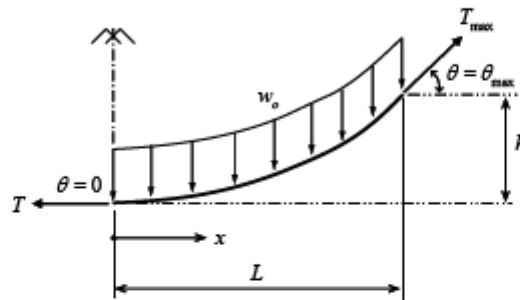
Appendix 6.4 MathCAD Worksheet for One-Way Membrane Capacity; Spandrel Girder Rendered Ineffective.

One-Way Catenary Action of Slab System

Computational procedure based upon simple catenary parabola structural mechanics theory. A discussion of the procedure can be found in:

Hibbeler, R.C. (2008) *Structural Analysis, 6th Edition*, Pearson Prentice-Hall, Upper Saddle River, NJ.

The fundamental parameters for the one-way catenary is shown in the schematic below:



Two regions of behavior are possible. The strength limit state of the catenary may be limited by the maximum tensile force or the horizontal tensile force at the centerline of the catenary span.

Slab Material and Thickness Parameters

$A_s := 0.028$	(sq. in.)	Area of reinforcement in catenary span direction.
$A_d := 0.2125$	(sq. in.)	Area of steel deck in catenary span direction (50% of 2VLI 22 effective).
$f_{sy} := 65000.00$	(psi)	Yield stress of slab reinforcement.
$f_{dy} := 40000.00$	(psi)	Yield stress of steel deck material.
$L_1 := 1.0$	(ft.)	Width of slab tributary to catenary.

Catenary Span Information

$L := 180$	(in.)	One-half the span of the catenary.
$\beta := 0.075$	(unitless)	The "sag" parameter defining tolerable sag in catenary.
$h := \beta \cdot L \text{ float}, 5 \rightarrow 13.500$		Tolerable "sag" in catenary

Strain in Catenary Reinforcement:

$$L_{\text{new}}(h, L) := \int_0^L \sqrt{1 + \frac{4h^2}{L^4} \cdot x^2} dx$$

$$\epsilon_s := \frac{L_{\text{new}}(h, L) - L}{L} \text{ float, 6} \rightarrow .373744\text{e-}2$$

$$\epsilon_d := \frac{L_{\text{new}}(h, L) - L}{L} \text{ float, 6} \rightarrow .373744\text{e-}2$$

$$\mu_s := \frac{29000000.0}{f_{sy}} \cdot \epsilon_s \text{ float, 3} \rightarrow 1.67$$

$$\mu_d := \frac{29000000.0}{f_{dy}} \cdot \epsilon_d \text{ float, 3} \rightarrow 2.71$$

Catenary Distributed Load Capacities*Based Upon Mid-Span Tension Capacity*

$$w_{\text{ou1}} := \frac{2 \cdot [(A_s \cdot f_{sy} + A_d \cdot f_{dy}) \cdot h]}{L^2}$$

$$w_{\text{ou1}} \text{ float, 5} \rightarrow 8.6000 \quad (\text{lbs./in.}) \quad \text{Uniformly distributed load capacity.}$$

Based Upon Support Tension Capacity

$$w_{\text{ou2}} := \frac{A_s \cdot f_{sy} + A_d \cdot f_{dy}}{L} \cdot \left[1 + \left(\frac{L}{2 \cdot h} \right)^2 \right]^{-0.50}$$

$$w_{\text{ou2}} \text{ float, 5} \rightarrow 8.5049 \quad (\text{lbs./in.}) \quad \text{Uniformly distributed load capacity.}$$

Capacity of Catenary

$$w_{\text{ou}} := \begin{cases} w_{\text{ou1}} & \text{if } w_{\text{ou1}} \leq w_{\text{ou2}} \\ w_{\text{ou2}} & \end{cases}$$

$$q_u := \frac{w_{\text{ou}} \cdot 12}{L_1} \text{ float, 4} \rightarrow 102.1 \quad (\text{psf})$$

Appendix 6.5 MathCAD Worksheet for Two-Way Membrane of Steel-Concrete Composite Slab System with Ineffective Interior Column.

Two-Way Membrane Strength Computations

Computations based upon procedure proposed by;

Hawkins, N.M. and Mitchell, D. (1979) "Progressive Collapse of Flat Plate Structures", *ACI Journal*, Title No. 76-34, July, American Concrete Institute, pp. 775-808.

Mitchell, D. and Cook, W.D. (1984) "Preventing Progressive Collapse of Slab Structures", *Journal of Structural Engineering*, Vol. 110, No. 7, ASCE, pp. 1513-1532.

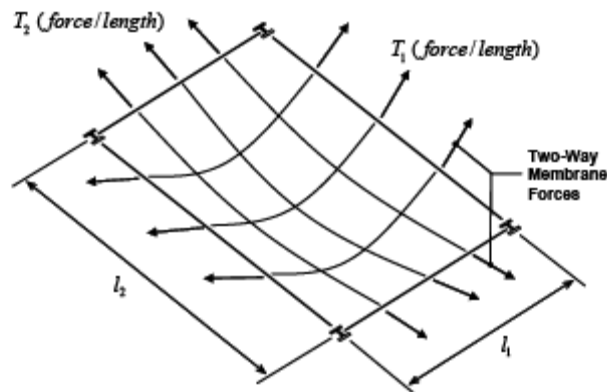
Membrane Schematic and Assumptions

Two-way membrane action in a slab panel is assumed after a supporting member is rendered ineffective. The short direction in the two way span is denoted with subscript 1 and the long direction is denoted with subscript 2.

The reinforcement in the short direction is assumed to consist of steel deck (composite or form-deck) and welded wire mesh. The reinforcement in the long direction is assumed to consist of welded wire mesh. It should be noted that if the panel is square, the user should simply choose the long and short direction.

The reinforcing steel in the membrane is assumed to be elastic-perfectly-plastic. The capacity of the membrane is assumed to be reached when the long direction reinforcement is at yield. The short direction strain follows from compatibility of deformations at the center of the concave shape. The membrane is assumed to form a circular pattern, when a catenary parabola is most appropriate.

An illustration of the scenario assumed is shown below.



Panel Dimensions

$l_1 := 720$ (in.) Short direction $l_2 := 720$ (in.) Long direction

Slab Reinforcement

$A_{sm1} := 0.00233$ (sq. in.) Area of WWM per inch parallel to short dimension: 6x6-W1.4xW1.4.

$A_{d1} := 0.01416$ (sq. in.) Area of steel deck per inch parallel to short dimension: 40% of 2VLI22.

$A_{sm2} := 0.00233$ (sq. in.) Area of WWM per inch parallel to long dimension: 6x6-W1.4xW1.4.

$f_{ys1} := 65000.0$ (psi) Yield stress of WWM parallel to short dimension.

$f_{yd1} := 40000.0$ (psi) Yield stress of steel deck parallel to short dimension.

$f_{ys2} := 65000.0$ (psi) Yield stress of WWM parallel to long dimension.

Assumed Strains and Resulting Stresses

$$\varepsilon_2 := 0.0035 \quad (\text{in./in.}) \quad \text{User MUST input this value.}$$

$$\varepsilon_1 := \varepsilon_2 \cdot \left(\frac{l_2}{l_1} \right)^2 \quad \text{float, 6} \rightarrow .35\text{e-}2 \quad (\text{in./in.}) \quad \text{User should compare to rupture strain.}$$

$$f_{s1} := \begin{cases} 29000000.0 \cdot \varepsilon_1 & \text{if } \varepsilon_1 \leq \frac{f_{ys1}}{29000000.0} \\ f_{ys1} & \text{otherwise} \end{cases} \quad \text{float, 6} \rightarrow 65000.0$$

$$f_{d1} := \begin{cases} 29000000.0 \cdot \varepsilon_1 & \text{if } \varepsilon_1 \leq \frac{f_{yd1}}{29000000.0} \\ f_{yd1} & \text{otherwise} \end{cases} \quad \text{float, 6} \rightarrow 40000.0$$

$$f_{s2} := \begin{cases} 29000000.0 \cdot \varepsilon_2 & \text{if } \varepsilon_2 \leq \frac{f_{ys2}}{29000000.0} \\ f_{ys2} & \text{otherwise} \end{cases} \quad \text{float, 6} \rightarrow 65000.0$$

Compute Uniform Load Capacity of Membrane

Compute edge tensions per unit length

$$T_{1m} := A_{sm1} \cdot f_{s1} \quad \text{float, 4} \rightarrow 151.5 \quad T_{2m} := A_{sm2} \cdot f_{s2} \quad \text{float, 4} \rightarrow 151.5$$

$$T_{1d} := A_{d1} \cdot f_{d1} \quad \text{float, 6} \rightarrow 566.400$$

Membrane Capacity Based Upon Tension Capacity at Edge of Panel (Hawkins and Mitchell 1979; Mitchell and Cook 1984):

$$w_{\text{edge}} := \frac{2 \cdot (T_{1m} + T_{1d}) \cdot \sin(\sqrt{6 \cdot \varepsilon_1})}{l_1} + \frac{2 \cdot (T_{2m}) \cdot \sin\left(\frac{l_1}{l_2} \cdot \sqrt{6 \cdot \varepsilon_1}\right)}{l_2}$$

$$w_{\text{edge}} \quad \text{float, 4} \rightarrow .3487 \quad (\text{psi})$$

Membrane Capacity Based Upon Tension Capacity at the Interior of the Panel (Hawkins and Mitchell 1979):

$$w_{\text{pos}} := 2 \cdot \sqrt{6 \cdot \varepsilon_1} \cdot \left[\frac{T_{1m} + T_{1d}}{l_1} + (T_{2m}) \cdot \frac{l_1}{l_2^2} \right]$$

$$w_{\text{pos}} \quad \text{float, 4} \rightarrow .3500 \quad (\text{psi})$$

Ultimate Strength of Membrane

$$w_u := \begin{cases} w_{\text{edge}} & \text{if } w_{\text{edge}} \leq w_{\text{pos}} \\ w_{\text{pos}} & \text{otherwise} \end{cases}$$

$$q_u := w_u \cdot 144 \text{ float}, 5 \rightarrow 50.219 \quad (\text{psf})$$

Vertical Deflection in Membrane:

$$\delta := \frac{3 \cdot l_1 \cdot \varepsilon_1}{2 \cdot \sin(\sqrt{\delta \cdot \varepsilon_1})}$$

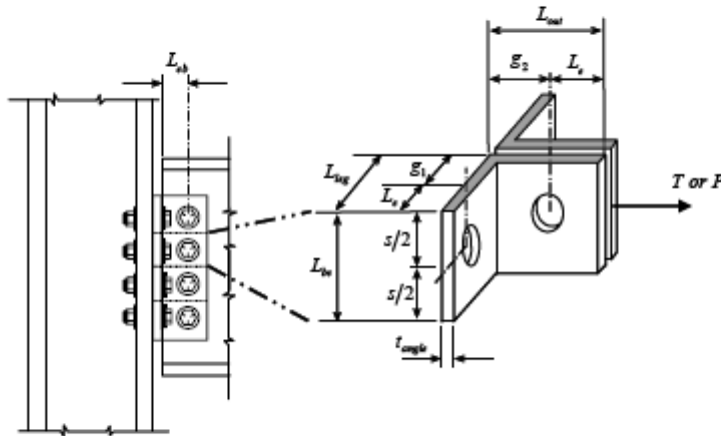
$$\delta \text{ float}, 4 \rightarrow 26.18 \quad (\text{in.}) \text{ downward}$$

Appendix 6.6 MathCAD Worksheet for Angle-Bolt-Element Nonlinear Tension and Compression Response and Pure Tension Capacity.

Pure Tension Capacity of Double Web Angle Connected Member and Bolt Element Load-Deformation Response Computations

The pure tension capacity of the member/connection is computed using procedures found in the AISC Manual (AISC 2001) and those recommended by Thornton (1985). The load-deformation response of the double-angle "bolt elements" are generated using procedures recommended by Shen and Astanah-Asl (2000) and Liu and Astanah-Asl (2000) with input from the prying computations of Thornton (1985).

The connection considered and general terminology is shown below.



Angle Properties and Connection Dimensional Data (A36 Material: L4x3.5x0.25; 3.5" on beam/girder)

$F_{y\text{angle}} := 49.0 \cdot 1.05$	expected yield stress (ksi)
$F_{u\text{angle}} := 66.0 \cdot 1.05$	expected ultimate tensile stress (ksi)
$E := 29000.00$	elastic modulus (ksi)
$g_1 := 2.500$	bolt gage distance in supported leg (in.)
$g_2 := 2.000$	bolt gage distance in outstanding leg (in.)
$L_{\text{leg}} := 4.000$	length of angle leg in contact with supporting element (in.)
$L_{\text{out}} := 3.500$	length of outstanding angle leg (in.)
$L_{\text{be}} := 3.00$	pitch (spacing) of bolts within angle and/or length of bolt element (in.)
$L_e := L_{\text{leg}} - g_1$	edge distance at leg in contact with supporting member (in.)
$t_{\text{angle}} := 0.25$	thickness of the angle (in.)
$k := 0.25$	fillet dimension (in.)

Beam/Girder Material and Web Thickness (W18x35 Beam and ASTM A572 Material)

$F_{tbeam} := 1.05 \cdot 65.0$	Expected ultimate tensile stress for beam/girder web material.
$F_{ybeam} := 1.10 \cdot 50.0$	Expected yield stress for beam/girder web material.
$L_{eb} := 1.500$	End distance for bolt in the beam/girder web
$t_{wbeam} := 0.300$	Beam/girder web thickness

Bolt-Related Properties and Parameters (3/4" A325 Bolts)

$d_b := 0.75$	diameter of the bolt
$d_h := d_b + \frac{1}{16}$	diameter of bolt hole (std. holes)
$F_{ub} := 120.0$	ultimate tensile stress of the bolt
$n_t := 10$	number of threads per inch on bolt
$N_s := 2$	number of shear planes
$n_b := 3$	number of bolts in outstanding leg of angle in connection

Net Tension and Shear Areas for Bolt (N-type bolts assumed)

$$A_{bt} := 0.7854 \left(d_b - \frac{0.9743}{n_t} \right)^2 \quad A_{bv} := 0.8 \left(\frac{\pi \cdot d_b^2}{4} \right)$$

$$A_{bt} = 0.334 \quad A_{bv} = 0.353$$

BOLT ELEMENT LOAD-DEFORMATION RESPONSE**Second Moment of Area**

$$I_a := \frac{1}{12} \cdot L_{be} \cdot t_{angle}^3$$

$$I_a = 3.906 \times 10^{-3}$$

Ultimate Tensile Strain for Angle Material

$$\epsilon_u := 100 \cdot \frac{F_{yangle}}{E}$$

$$\epsilon_u = 0.177$$

Yield Moment Capacity

$$M_y := \frac{L_{be} \cdot t_{angle}^2}{6} \cdot F_{yangle}$$

$$M_y = 1.608$$

Plastic Moment Capacity

$$M_p := \frac{L_{be} \cdot t_{angle}^2}{4} \cdot F_{yangle}$$

$$M_p = 2.412$$

Shear Failure of the Bolts (N-type bolts assumed and no joint length factor)

$$P_v := (0.62 \cdot F_{ub}) \cdot (A_{bv}) \cdot N_s$$

$$T_v := n_b \cdot P_v$$

$$T_v = 157.771$$

$$P_v = 52.59$$

Tensile Failure of Bolts (twice as many bolts in tension as shear)

$$P_t := 2(A_{br} F_{ub})$$

$$T_t := n_b \cdot P_t$$

$$T_t = 240.812$$

$$P_t = 80.271$$

Prying Action in the Bolts

$$b := \varepsilon_1 - \frac{t_{\text{angle}}}{2}$$

$$b_{\text{prime}} := \varepsilon_1 - \frac{t_{\text{angle}}}{2} - \frac{d_h}{2}$$

$$a_{\text{prime}} := \min\left(L_{\text{leg}} - \varepsilon_1 + \frac{d_h}{2}, 1.25 \cdot b + \frac{d_h}{2}\right)$$

$$\delta_1 := 1 - \frac{d_h}{L_{be}}$$

$$\rho := \frac{b_{\text{prime}}}{a_{\text{prime}}}$$

$$\alpha := \frac{1}{\delta_1 \cdot (1 + \rho)} \left[\frac{8(A_{br} F_{ub}) \cdot b_{\text{prime}}}{L_{be} \cdot t_{\text{angle}}^2 \cdot F_{y\text{angle}}} - 1 \right]$$

$$P_{\text{prying}} := \begin{cases} 2.0 \left[\frac{(A_{br} F_{ub}) \cdot (1 + \delta_1 \cdot \alpha)}{1 + \delta_1 \cdot \alpha \cdot (1 + \rho)} \right] & \text{if } \alpha < 0 \\ 2.0 \left[\frac{L_{be} \cdot t_{\text{angle}}^2 \cdot F_{y\text{angle}} \cdot (1 + \delta_1 \cdot \alpha)}{8 \cdot b_{\text{prime}}} \right] & \text{if } \alpha > 1 \\ 2.0 \left[\frac{(A_{br} F_{ub}) \cdot (1 + \delta_1 \cdot \alpha)}{1 + \delta_1 \cdot \alpha \cdot (1 + \rho)} \right] & \text{otherwise} \end{cases}$$

$$T_{\text{prying}} := n_b \cdot (P_{\text{prying}})$$

$$T_{\text{prying}} = 120.331$$

$$P_{\text{prying}} = 40.11$$

Beam Web Bearing Failure (tear out limit state)

$$P_{\text{btoweb}} := 1.2 \cdot F_{u\text{beam}} \cdot (L_{eb} - 0.5 \cdot d_h) \cdot t_{w\text{beam}}$$

$$T_{\text{btoweb}} := n_b \cdot P_{\text{btoweb}}$$

$$T_{\text{btoweb}} = 80.62$$

$$P_{\text{btoweb}} = 26.873$$

Angle Bearing Failure (tear out limit state - 2 angles)

$$P_{\text{broangle}} := 2.0 \left[1.2 \cdot F_{\text{uangle}} \cdot (L_{\text{out}} - \xi_2 - 0.5 \cdot d_h) \cdot t_{\text{angle}} \right]$$

$$T_{\text{broangle}} := n_b \cdot P_{\text{broangle}}$$

$$T_{\text{broangle}} = 136.434$$

$$P_{\text{broangle}} = 45.478$$

Tension Deformation Response Curve**Initial (elastic) Stiffness**

$$K_{T1} := 2 \cdot \left[\frac{12 \cdot E \cdot I_a}{\xi_1^3} \cdot \left[1 - \frac{3 \cdot \xi_2}{4 \cdot (\xi_1 + \xi_2)} \right] \right]$$

$$K_{T1} = 116$$

Force at Initial Yield

$$P_{T1} := 2 \cdot \left[\frac{4 \cdot \xi_1 + \xi_2}{\xi_1 \cdot (2 \cdot \xi_1 + \xi_2)} \cdot M_y \right]$$

$$P_{T1} = 2.205$$

Force at Mechanism Formation

$$P_{T2} := 2 \cdot \left(\frac{2 \cdot M_p}{\xi_1 - k - \frac{d_h}{2}} \right)$$

$$P_{T2} = 5.232$$

Displacement at Ultimate Load

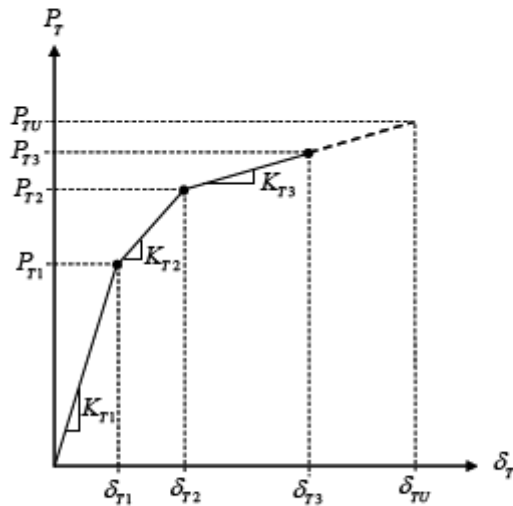
$$\delta_{TU} := 2 \cdot (\xi_1 - k) \cdot s_u \cdot \sqrt{\frac{t_{\text{angle}}}{(\xi_1 - k) \cdot s_u}}$$

$$\delta_{TU} = 0.632$$

Yield Displacement

$$\delta_{T1} := \frac{P_{T1}}{K_{T1}}$$

$$\delta_{T1} = 0.019$$

**Tangent (post-yield) Stiffness**

$$K_{T2} := 2 \cdot \left[\frac{3 \cdot E \cdot I_a}{\xi_1^3} \cdot \left(1 - \frac{3 \cdot \xi_2}{8 \cdot \xi_1 + 6 \cdot \xi_2} \right) \right]$$

$$K_{T2} = 35.344$$

Tensile Capacity of an Angle Leg

$$N_p := (L_{be} - d_h) \cdot t_{\text{angle}} \cdot F_{\text{uangle}}$$

$$N_p = 37.898$$

Tensile Force at Ultimate Catenary Load

$$P_{cat} := 2.0 \left(N_p \cdot \sin \left(\arctan \left(\frac{\delta_{TU}}{\xi_1 - k} \right) \right) \right)$$

$P_{cat} = 20.491$

$$T_{cat} := n_b \cdot P_{cat}$$

$T_{cat} = 61.474$

Tensile Force at Strength Limit

$$P_{T3} := \min(P_{cat}, P_{btoweb}, P_{btoangle}, P_{prying}, P_t, P_v)$$

$P_{T3} = 20.491$

Displacement at Tensile Strength Limit State

$$\delta_{T3} := \delta_{T2} + \frac{P_{T3} - P_{T2}}{K_{T3}}$$

$\delta_{T3} = 0.632$

Displacement at Mechanism Formation

$$\delta_{T2} := \delta_{T1} + \frac{P_{T2} - P_{T1}}{K_{T2}}$$

$\delta_{T2} = 0.105$

Geometric Stiffness for Final Branch

$$K_{T3} := \frac{P_{cat} - P_{T2}}{\delta_{TU} - \delta_{T2}}$$

$K_{T3} = 28.947$

Compression Deformation Response Curve

Compression Length of Angle

$$L_c := \xi_2 - \frac{d_h}{2}$$

$L_c = 1.594$

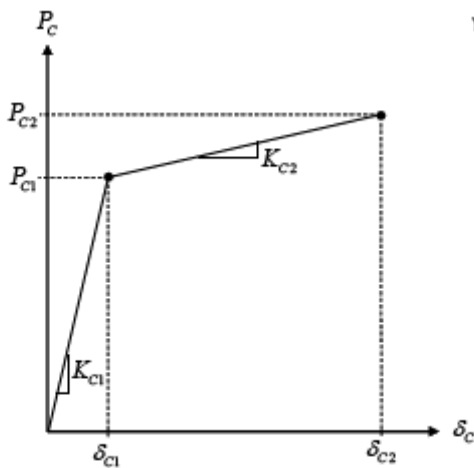
Angle Cross-Sectional Area

$$A_a := L_{be} \cdot 2t_{angle}$$

$A_a = 1.5$

Strain Hardening Ratio

$$\alpha_{harden} := 0.005$$



Yield Force

$$P_{yangle} := F_{yangle} \cdot A_a \quad P_{ybeam} := F_{ybeam} \cdot L_{be} \cdot t_{wbeam}$$

$$P_{C1} := \min(P_{yangle}, P_{ybeam}, P_v)$$

$P_{C1} = 49.5$

Ultimate Force

$$P_{uangle} := F_{uangle} \cdot A_a \quad P_{ubeam} := F_{ubeam} \cdot L_{be} \cdot t_{wbeam}$$

$$P_{C2} := \min(P_{uangle}, P_{ubeam}, 1.20 \cdot P_v)$$

$P_{C2} = 61.425$

Initial Stiffness

$$K_{C1} := \begin{cases} \frac{L_{be} \cdot t_{wbeam} \cdot E}{L_c} & \text{if } P_{ybeam} \leq P_{yangle} \\ \frac{A_a \cdot E}{L_c} & \text{otherwise} \end{cases}$$

$$K_{C1} = 1.638 \times 10^4$$

Tangent Stiffness

$$K_{C2} := \alpha_{harden} \cdot K_{C1}$$

$$K_{C2} = 81.882$$

Yield Displacement

$$\delta_{C1} := \frac{P_{C1}}{K_{C1}}$$

$$\delta_{C1} = 3.023 \times 10^{-3}$$

Ultimate Displacement

$$\delta_{C2} := \delta_{C1} + \frac{P_{C2} - P_{C1}}{K_{C2}}$$

$$\delta_{C2} = 0.149$$

PURE TENSION CAPACITY OF DOUBLE ANGLE**Block Shear Rupture in Outstanding Angle Leg (2 angles contribute to strength)**

$$A_{gt} := (n_b - 1) \cdot L_{be} \cdot t_{angle}$$

$$A_{gv} := 2(L_{out} - g_2) \cdot t_{angle}$$

$$A_{nt} := A_{gt} - [(n_b - 1) \cdot d_h] \cdot t_{angle}$$

$$A_{nv} := A_{gv} - 2 \left(\frac{d_h}{2} \right) \cdot t_{angle}$$

$$T_{ygt} := F_{yangle} \cdot A_{gt}$$

$$T_{fnt} := F_{uangle} \cdot A_{nt}$$

$$T_{ygv} := 0.60 \cdot F_{yangle} \cdot A_{gv}$$

$$T_{fvv} := 0.60 \cdot F_{uangle} \cdot A_{nv}$$

$$T_{bsangle} := \begin{cases} 2 \cdot (T_{fnt} + \min(T_{ygv}, T_{fvv})) & \text{if } T_{fnt} \geq T_{fvv} \\ 2 \cdot (T_{fvv} + \min(T_{ygt}, T_{fnt})) & \text{otherwise} \end{cases}$$

$$T_{bsangle} = 197.072$$

Block Shear Rupture in the Beam Web

$$A_{gt1} := (n_b - 1) \cdot L_{be} \cdot t_{wbeam} \quad A_{gv1} := 2(L_{eb} \cdot t_{wbeam})$$

$$A_{nt1} := A_{gt1} - [(n_b - 1) \cdot d_h] \cdot t_{wbeam} \quad A_{nv1} := A_{gv1} - 2\left(\frac{d_h}{2}\right) \cdot t_{wbeam}$$

$$T_{ygt1} := F_{ybeam} \cdot A_{gt1} \quad T_{fnt1} := F_{ubeam} \cdot A_{nt1} \quad T_{ygv1} := 0.60 \cdot F_{ybeam} \cdot A_{gv1} \quad T_{fnv1} := 0.60 \cdot F_{ubeam} \cdot A_{nv1}$$

$$T_{bsweb} := \begin{cases} T_{fnt1} + \min(T_{ygv1}, T_{fnv1}) & \text{if } T_{fnt1} \geq T_{fnv1} \\ T_{fnv1} + \min(T_{ygt1}, T_{fnt1}) & \text{otherwise} \end{cases}$$

$$T_{bsweb} = 116.452$$

Strength of Double-Angle Connection in Pure Tension

$$T_{cap} := \min(T_v, T_t, T_{bsangle}, T_{bsweb}, T_{prying}, T_{btoangle}, T_{btoweb}, T_{cat})$$

$$T_{cap} = 61.474$$

References

Shen, J. and Astaneh-Asl, A. (2000) "Hysteresis Model of Bolted Angle Connections" *Journal of Constructional Steel Research*, Vol 54, 317-343.

Liu, J. and Astaneh-Asl, A. (2000) "Cyclic Tests on Simple Connections, Including Effects of the Slab", Report No. SAC/BD-00/03, SAC Joint Venture, June 2000.

AISC (2001) *Manual of Steel Construction*, American Institute of Steel Construction, Chicago, IL.

Thornton, W.A. (1985) "Prying Action - A General Treatment", *Engineering Journal*, Second Quarter, American Institute of Steel Construction, Chicago, IL, 67-75.

Chapter 7

Summary, Conclusions and Recommendations

7.1 Summary

The present analytical effort sought to identify and quantify sources of inherent robustness in structural steel framing systems. It was readily apparent that there was very limited understanding of the force and ductility demands placed on connections within steel structural systems when subjected to abnormal loading events and an overall understanding of the loading transfer mechanisms present in the typical structural steel system during these events. Therefore, the research effort took one step backward in a more fundamental direction and sought not only to evaluate demand placed on connections within the steel system, but to also generate estimates for the inherent robustness in structural steel systems and the force and displacement/rotation demands that would likely be placed on the connections within structural steel systems. This information is tailor made for the next step in evaluating connections for robustness and resiliency using experimental and further detailed analytical work.

A literature survey was conducted to gain insights from past experience in both the United States and the United Kingdom. This literature survey resulted in a sound research direction for the present effort that extends the current body of knowledge. Three structural steel building systems were analyzed for GSA-type compromised-system scenarios in which columns within the perimeter of the framework were rendered ineffective. Three-, ten-, and twenty-story SAC pre-Northridge Boston buildings were analyzed using elastic time history analysis and inelastic time history analysis (when appropriate). Membrane and catenary action within the structural steel system (with 30-ft by 30-ft regular framing grid) and concrete-steel composite floor slab were also evaluated.

Observations regarding the analysis results were synthesized and conclusions were drawn with respect to the demands placed on the connections within perimeter moment-resisting frame systems, the likelihood of catenary action in multistory framing systems, and the demands placed on column splices and moment resisting connections during abnormal loading events of the type considered. The membrane and catenary study yielded recommendations for connection characteristics, slab reinforcement scenarios, and anchorage forces that lead to enhanced robustness in the steel system.

7.2 Conclusions

A significant analytical effort was undertaken to quantify the robustness (*i.e.* the inherent structural integrity) present in structural steel building systems. As a result, the conclusions are best highlighted via sub-sections in this section of the report. Conclusions and observations resulting from the analysis of the 3-story, 10-story,

and 20-story SAC buildings analyzed as well as the membrane and catenary action study is summarized in the section.

7.2.1 Three-Story SAC Frame Analysis

There are quite a few general conclusions and observations regarding structural steel framing systems that can be drawn from the analysis conducted on the 3-story Boston SAC frame. First of all, there is significant inherent robustness present in structural steel buildings with perimeter moment-resisting frames. However, the robustness and inherent structural integrity will be lessened if unidirectional moment connections are utilized. All moment-resisting connections within a steel framework should be designed assuming complete moment reversal. End plate connections with bolt arrangements that are unsymmetrical about the beams axis of bending should not be allowed.

A comparison of elastic and inelastic analysis results for the framework demonstrated that elastic time history analysis can lead to moment, shear, and axial load demands that differ considerably from inelastic analysis. The demand-to-capacity ratios as defined for the present study are significantly different when these two approaches are utilized. Inelastic time history analysis is the best analytical approach to use for progressive collapse mitigative analysis.

The plastic rotation demands computed for this framework indicate that moment resisting connections detailed to the latest guidelines will likely meet the deformations demands required to maintain a stable structural system during the compromised column event considered. As a result, connection ductility does not appear to be the governing factor in limiting robustness or inherent structural integrity in the framing system analyzed. Furthermore, Vierendeel action in the framework are important sources of inherent robustness and this phenomena can lead to significant reductions in connection demands and tie forces.

The strain rates that arose in the members of the framework considered with column ineffectiveness rate of 0.01 seconds with 5% inherent structural damping indicated that intermediate strain rates are being seen at the connections within the system and a reduction in fracture toughness of the steel material need not be considered when evaluating inherent structural integrity and robustness. However, it is important to note that connection detail (geometric) effects were not considered in the analysis conducted.

Of the frameworks considered, the three story framework has the least amount of Vierendeel action activated when lower-story columns are rendered ineffective. In this framework, there is simply fewer moment resisting framing bays above a compromised level. As a result, the three-story frame can be used to assess minimum likely tying forces needed for horizontal framing elements in typical moment-resisting framing systems needed to ensure a minimal level of general structural integrity.

The inelastic analysis conducted indicated that beam-to-column connections would likely be subjected to axial force demands that were less than 5% of the axial tension or axial compression capacity of the beam members. Therefore, a conservative recommendation would be to design the connections for axial demands equal to 5% of the beam cross-section's tensile yield capacity (gross cross-section) and assume that this tension force acts simultaneously with the beam's plastic moment capacity. Designing for this additional *tying force* (in the case of tension) would enhance the robustness of the steel framing system. The ability of common moment-resisting connections to support the connected beam's plastic moment capacity simultaneously with 5% of the gross-area tension yield force for the member would be a prudent future experimental endeavor.

The peak tension force (or tying force) in the girders of the 3-story framework seen in the inelastic analysis can also be phrased in terms of the gravity loading applied to the beam or girder. The peak tying forces seen for this frame and event considered was 33% of the total gravity loading applied to the girder immediately adjacent to the compromised column. A tie force expression analogous to those in the UFC was generated,

$$F_t = 0.33 \cdot [GRAV]$$

The inelastic time history analysis also indicated that tensile force demands in column splices (if there are any splices in a 39-foot column member) would likely be minimal. If a beam collapse mechanism in the framing above a compromised column does not form, the column stack directly above the compromised member will likely have compression force in the columns at each story.

If one defines a minimum level of general structural integrity, as being the ability to carry structure self-weight along with mean sustained point-in-time live loading, then it can be said that the 3-story SAC framework considered has built-in general structural integrity. The study conducted demonstrated that a steel framework designed without special progressive-collapse mitigation procedures has a minimum level of general structural integrity after the occurrence of a compromised column scenario commonly used in progressive collapse-mitigative design methodologies.

7.2.2 Ten-Story SAC Frame Analysis

While many of the conclusions for the 10-story building considered can be drawn directly from the 3-story analysis results, it is prudent to review some of the results seen for this analysis and draw conclusions that are directly applicable to mid-rise steel systems.

In general, the analysis indicated that there was a lack of appreciable interstory drift of the column member ends relative to one another and small vertical deformations of the beam ends relative to one another.

This resulted in the conclusion that geometric nonlinear effects are not significant in this framework for the ineffective column scenarios considered. The maximum vertical deflection of the floor system immediately above a column rendered ineffective was approximately 3 inches. This is extremely small given the span of 60 feet and therefore, catenary action will not develop. The load carrying mechanism at work in this frame (as in the 3-story framework) is Vierendeel action of the stories above the compromised column.

Tensile force demands in the column splices were not seen and therefore, similar conclusions regarding column splices can be brought to this framework as well. The connection demands at the ends of the beam members in the framework suggested that plastic demands were not present under the compromising events considered. The bending moment and shear demands appear to be well within the limits of modern ductile moment-resisting connections that are designed to support the plastic moment capacity of the beam member. The axial load demands in the beam members are negligible as a result of the 8-9 stories of moment resisting framing creating Vierendeel action. Tying forces for lower-floor compromising events need not be considered. However, the minimum tying force recommended for the 3-story frame is valid for this frame.

Strain rates in members in the immediate vicinity of the ineffective column were found to be in the intermediate rate category and therefore, a reduced fracture toughness and elevated yield of the material could be ignored. As with the 3-story frame, however, it should be emphasized that connection geometry and stress-raiser effects were not considered and further evaluation in this regard is warranted.

Demand-to-capacity ratios for all members in the frame configuration analyzed did not lead to yielding in members near the compromised column. Beams and columns are expected to respond to ineffective columns at the ground floor level in an elastic manner. This conclusion must be tempered with the knowledge that Vierendeel action plays a large role. The three-story SAC building analysis indicates that when there are three-stories above the compromised or ineffective column, inelastic behavior should be expected. As a result, the upper-stories of multi-story frames may be more susceptible to initiating progressive collapse mechanisms in the stories below.

7.2.3 Twenty-Story SAC Frame Analysis

It is apparent that the twenty-story model frame contained a significant degree of redundancy. Admittedly, this was expected going into the analysis. When a compromising event occurs in the exterior perimeter frame (*e.g.* a single column becomes ineffective), the model engages a large number of adjacent members in the vicinity of the event to distribute the loading to other members within the framework. As the twenty-story building has a large number of members relative to the three- and ten-story model buildings, the frame is able to sustain a similar column removal event without difficulty. In fact, the members can respond to the event in an elastic manner. Of course, rendering multiple columns within any given story may change the conclusions

drawn here, but as outlined in the literature synthesis and review, the objectives of the present study were to attempt to quantify robustness and recommend general structural integrity provisions for steel systems. Removal of multiple columns in story would imply threat-specific knowledge and that is best handled with threat-specific design provisions.

A number of connections within the frame experienced a loading reversal (e.g. connection immediately above compromised column; and connections immediately below due to rebound) indicating that rigid connections be designed for full moment reversals. This should be true of all building types.

It is also apparent that significant dynamic load increases were not present after the compromising events considered for this frame. The dynamic response of the structure indicates only an 11% increase in deflection due to the ineffectiveness of a column. This suggests that the 2.0 multiplier to simulate the dynamic effects of loading during the compromising event may be appropriate only for a limited number of frame configurations and types (e.g. the three-story framework considered in this study). Again, the significant redundancy of the frame can be attributed to limiting the dynamic effect. Through the previous two model buildings studied, it can be concluded that less redundant frames exhibit greater dynamic effects.

Strain rates resulting from column ineffectiveness rates of 0.01 seconds were found to be very close to those strain rates classified as intermediate or below. The 5% damping magnitude (felt to be conservatively low) was also seen to be sufficient in reducing these strain rates very rapidly with time after the “event”. The same caution related to connection geometric effects should be applied.

This analysis of the twenty-story frame was limited to independent removal of two ground level columns. While preliminary analyses ruled out the study of more columns in the ground level of the structure, other compromising events may have more significance. For instance, had members been compromised at higher levels within the structure, greater dynamic effects, strain rates and increased dynamic loading effect would be expected. The effects seen with this alternate event would be expected to be similar to those found in the three story frame, but the framing system was significantly different than the former frames considered. While upper level columns of the structure support a lesser magnitude of load, fewer members are available to distribute loading in the event. Additionally, the events leading to ineffective members at the interior of the frame were not studied. The presence of flexible connections between interior columns and beams/girders presents an inherent analytical instability in the event that a column becomes ineffective (i.e. if pinned connections are assumed, a mechanism is created a-priori once an interior column is rendered ineffective).

7.2.4 Membrane and Catenary Response

The benefit of Vierendeel action in the floors above the level containing the compromised column diminishes as one rises in the framework. In general, one would expect similar behavior to that of the 3-story framework when columns at the upper-levels of buildings with 4 and more stories are rendered ineffective. This led to the idea that robustness in the steel system cannot be fully understood unless a measure of the inherent contribution of the composite floor system through two-way membrane and catenary action is considered.

This recognition led to a variety of scenarios in which interior in-fill beams, spandrel beams, and interior columns within the typical regular 30-ft by 30-ft framing system with in-fill beams spaced at 10 feet on center. The steel deck considered in this study was 2VLI22 and 6x6-W1.4xW1.4 welded wire mesh. The progressive collapse resistance (*i.e.* inherent structural integrity or robustness) in this structural steel system was demonstrated. In general, it appears that the typical structural steel system has sufficient inherent robustness to resist self-weight and mean point-in-time sustained live loading for a large variety of compromised component situations. One exception is the spandrel beam loss scenario whereby concentrated bands of mild-steel slab reinforcement at the perimeter appear to be sufficient to create significant structural integrity.

The typical structural steel floor slab system is capable of carrying non-amplified self-weight and mean point-in-time sustained live loading in the event a single in-fill beam is rendered ineffective through membrane action. The membrane action in the slab system is most effectively enhanced (*i.e.* one is able to approach GSA dynamic loading multipliers) by increasing the mild steel reinforcement in the system. The typical floor system is also capable of supporting non-amplified point-in-time loading likely at the time the two in-fill beams are rendered ineffective. Therefore, the typical steel structural system has a significant level of inherent robustness. GSA-level dynamic multipliers are likely to be approached for this scenario when additional mild-steel reinforcement is provided in the concrete floor slab. The membrane analysis indicated that the best balance in providing progressive collapse resistance for both one and two in-fill beams being lost would be to provide #3 mild-steel reinforcing bars at 12 inches on center throughout the concrete floor slab rather than typical welded wire mesh reinforcement.

The most effective method to create robustness in the event a spandrel beam is lost or rendered ineffective is to provide a band of mild-steel reinforcement at the perimeter of the slab system. For the 30-foot framing bay considered, a band of 4 continuous #4 bars are likely to be sufficient to meet GSA-level pseudo-dynamic loading and provide significant progressive collapse resistance in the structural steel system given this compromising event.

Distribution of slab reinforcement (in lieu of concentrated perimeter bands) was also studied. The distribution of mild-steel slab reinforcement throughout the exterior bays in the steel system was determined to be the most economical way to create enhanced structural integrity and meet GSA-level dynamic loading magnitudes in the case of spandrel beam loss coupled with loss of adjacent in-fill beams. The analysis conducted indicated that #4 mild-steel reinforcing bars at 9 inches on center (laid in direction parallel to beams) acting in combination with the orthogonally-fluted steel deck was sufficient to significantly inhibit progressive collapse in the event of lost supporting spandrel and in-fill beams.

Investigation of system response to loss of a spandrel girder in the floor framing system indicated that the typical slab arrangement considered has significant inherent robustness since the steel deck and welded wire mesh typically used is capable of creating membrane behavior with a capacity that exceeds the point-in-time live loading magnitude. However, if the dynamic load multiplier of 2.0 is desired, additional reinforcement will likely be required. The steel deck contributes significantly to the membrane tension reinforcement and therefore if GSA-level dynamic multipliers are desired, #4 at 14-inches on center was found to be acceptable. Coupled with the #4 at 9 inch arrangement described previously, the analysis conducted indicates that for the systems considered, GSA-level progressive collapse prevention can be provided simply by including #4 mild-steel reinforcing bars at 9 inches on center parallel to the beams and #4 bars at 14 inches on center in the orthogonal direction.

A scenario whereby an interior column is rendered ineffective was also considered. This situation is intended to model the upper floors in the steel structure where Vierendeel action in the framing system above a compromised column is not effectively activated. As a result, each floor system is asked to support its own self-weight and mean point-in-time sustained live loading. The concrete slab reinforcement and steel deck assumed in the steel structure considered was capable of contributing 50-psf at a vertical displacement of 26 inches. The total rotational demand at the perimeter of the slab panel corresponding to this deformation was found to be within the plastic rotational demand capacity for two-way and one-way concrete slab systems (GSA 2003).

A 3D static nonlinear analysis of a typical 30-ft by 30-ft framing system that included nonlinear connection behavior consistent with that of web-cleat connections was conducted. The analysis indicated that while it is doubtful that the typical structural steel framing system could support the GSA-level dynamic loading estimates thereby having inherent progressive collapse prevention capability in the event of a lost interior column, one can say that the typical structural steel framing system can *resist* progressive collapse in the event an internal column is rendered ineffective. This statement is supported by the fact that the system self-weight and mean point-in-time live loading can be supported through catenary and flexural action in the

structural steel framing and membrane action in the composite concrete-steel deck system with traditional clip angle (web cleat) connections.

The analysis results indicate that in order to improve the inherent structural integrity in the steel system, one should select connection angles with thickness on the upper-end of those provided in the steel manual (AISC 2001b). Enhanced robustness can also be achieved if the web of the beam and girder members contains the maximum number of bolt rows that the beam or girder web can support.

The analysis conducted indicated that better response to compromising events may result when lower connection moment capacity and flexural stiffness is present within the connections in the system. When the moment capacity is low, there appears to be a smooth transition between the formation of the flexural mechanism and the catenary tension behavior that is essentially secondary after the initial compromising event. If the moment capacity is too large, there may be snap-through-type behavior whereupon a significant magnitude of vertical displacement will rapidly take place prior to catenary formation. This appears undesirable and further study with regard to the effect of snap-through is warranted.

In general, the analysis conducted indicated that balance between membrane action in the slab and catenary action in the steel grillage can be attained when the following axial and moment characteristics are met in regard to the connections at the ends of the beams and girders in the structural steel system;

$$M_{conn} \leq 0.30M_{pb} \text{ and } K_{\theta} \leq 2 \frac{EI}{L}$$

$$P_{conn} \leq 0.3P_y \text{ and } K_{\delta} \leq 0.3 \frac{AE}{L}$$

It is interesting to note that the desired behavior described appears to be inherent in typical structural steel framing systems. Therefore, the study suggests that no special consideration of interior column ineffectiveness needs to be required at design time to create robustness in the typical steel framing system. The typical structural steel framing system appears to have significant inherent resistance to progressive collapse.

In general, a fairly simple approach to enhance structural integrity would be to use washers beneath the bolt heads and the nuts. The combined effects of tension and bending in steel connections (especially clip angles) may result in the bolt heads or nuts “tearing” through the bolt holes in the connecting components (Owens and Moore 1992). The use of washers at both locations in steel systems will add a measure of additional robustness to the connections.

7.3 Recommendations for Further Research

The present research effort does not close the book on inherent robustness in structural steel framing systems. It has merely opened the book and began the reading the early chapters. There is much left to do, but the present effort can be used to set the course for future efforts to demonstrate that special design loading conditions and procedures may not be needed to preserve or create inherent robustness and resistance to progressive collapse in structural steel building systems. This section provides insights and recommendations for future research work in this regard.

Corner column ineffectiveness needs to be evaluated. This would be most important in the case of the 3-story framework since moment resisting connections were not located at the perimeter in the corners of the system. In the case of buildings 4-stories and taller with moment resisting connections continued around the perimeter, it is possible that a corner column could be “lost” and the framework could remain stable. In instances where the steel building is three-stories in height or less, the engineer (and society) may consider a sacrificial corner of the structure. This may be done by not using washers between the bolt heads and nuts to facilitate ease in these components from tearing through the connecting angles (Owens and Moore 1992). Discontinuous steel deck, saw-cuts in the concrete slab, planned locations of discontinuous slab reinforcement, and larger-spacing for puddle welds for connecting the deck to the structural steel shapes can also facilitate sacrificial portions at the corners of the structural system. It should be emphasized that study of corner column removal scenarios should not be done without consideration of orthogonal framing and 3D inelastic structural analysis considering connection realistic response characteristics.

The framing system used in the 20-story SAC building framework should be studied further. The relatively irregular column arrangement (relative to the 3- and 10-story frame) likely will result in significantly different behavior when membrane and catenary response is considered.

The capacities of composite concrete-steel deck floor systems in membrane tension require additional study. The membrane and catenary analysis conducted assumed that approximately 550 lb/in deck anchorage forces was present. The equated to 5/8” puddle welds at 3 inches on center. Experimental studies on two-way composite steel-concrete floor systems should be conducted. The formation of compression rings at the supported edges should be validated via this testing. The anchorage forces present in the system will also be elucidated through this testing. The contribution and effectiveness of shear studs present to generate composite behavior between the steel beams and concrete slab components also should be evaluated. Perhaps guidelines could be generated to give a structural engineer a roadmap to ensure that this anchorage is present in the floor systems.

It is recommended that the 3D analysis of the steel buildings considered in this study be conducted with connection characteristics outlined in the report. This will lead to some very interesting insights in relation to the true robustness in these systems. Furthermore, the ability to consider composite behavior between the floor deck and the wide-flange framing members needs to be conducted to evaluate demands placed on all components of the steel system as recently done for fire in the U.K.

The impact of snap-through-type behavior in the steel framing system as flexural capacity is exceeded and loading resistance is continued through to catenary mechanisms requires further evaluation. The analysis conducted in this effort indicates that some connection configurations may result in a significant amount of vertical displacement rapidly taking place as the transition from flexural action to catenary action occurs. This rapid accumulation of deformation may result in additional dynamic effects that need consideration. Furthermore, the ability to balance moment capacity and axial capacity in the connections throughout the system given typical connection types needs further evaluation. True axial-shear-moment interaction surfaces for structural steel connections will eventually be needed if 3D behavior of the structural system is to be simulated.

It is well known that the concrete slab present in typical steel framing systems will increase the negative moment capacity of the typical beam-to-column connection and it is likely that this increased negative moment capacity will extend to beam-to-girder connections. SAC research has illustrated that the negative moment capacity of flexible connections can be affected by the presence of the concrete slab. The increased strength and stiffness of the connection, however, is short lived. Once significant cracking takes place in the slab, the connection strength migrates downward toward the strength of the connection alone if the slab reinforcement is not intended to contribute to the negative moment capacity. This transition and the subsequent force redistribution that would take place were not considered in the present study. It would be prudent to generate a series of analysis and/or experiments that would help to understand this relatively complex behavior. The importance of this stems from concerns that the lower moment capacity needed to ensure smooth transition between flexural mechanism and catenary behavior is seen in real systems.

A distinction between *resistance* to progressive collapse and *prevention* of progressive collapse needs to be made by the structural engineering profession. The structural steel system has inherent resistance to disproportionate collapse as demonstrated by the analyses undertaken in this research effort. Therefore, if one seeks resistance to progressive collapse then the present study has demonstrated that typical steel framing systems already have measurable levels of this resistance without specialized engineering intervention. However, if one desires progressive collapse prevention, then the present study's recommendations of enhanced slab reinforcement, thicker connection angles, and greater numbers of bolt rows (at a minimum) should be implemented. The question for specification writers is: "Should all steel structures have a minimal

level of general structural integrity and what is this minimum level?” If this means the steel structural system should be able to carry its self-weight and mean point-in-time sustained live loading present when a compromising event occurs, then typical steel structural systems appear to have this minimal level of general structural integrity without special design considerations (for some compromising scenarios). The analyses conducted in this study can contribute to this effort, but more work needs to be done.

This page is intentionally left blank.

Cited References

- ACI. (1997). *ACI Design Handbook; SP-17(97)*, American Concrete Institute, Farmington Hills, MI,
- ACI. (2005). *Building Code Requirements for Structural Concrete (ACI 318-05) and Commentary (ACI 318R-05)*, American Concrete Institute, Farmington Hills, MI,
- AISC. (2001a). *Load and Resistance Factor Design Specifications for Structural Steel Buildings*, American Institute of Steel Construction, Chicago, IL,
- AISC. (2001b). *Manual of Steel Construction*, American Institute of Steel Construction, Chicago, IL,
- AISC. (2005a). *Load and Resistance Factor Design Specifications for Structural Steel Buildings (ANSI/AISC 360-05)*, American Institute of Steel Construction, Chicago, IL,
- AISC. (2005b). *Seismic Provisions for Structural Steel Buildings (ANSI/AISC 341-05)*, American Institute of Steel Construction, Chicago, IL,
- AISI. (2001). *North American Specification for the Design of Cold-Form Steel Structural Members (AISI/COS/NASPEC 2001)*, American Iron and Steel Institute, Washington, D.C.,
- Allam, A., Burgess, I., and Plank, R.(2000) "Simple Investigations of Tensile Membrane Action in Composite Slabs in Fire." *International Conference on Steel Structures of the 2000's*, Istanbul, Turkey, 327-332 (www.shef.ac.uk/fire-research/publications.html),
- ASCE. (2002). *SEI/ASCE 7-02: Minimum Design Loads for Buildings and Other Structures*, American Society of Civil Engineers, Reston, VA,
- ASCE. (2006). *ASCE/SEI 7-05: Minimum Design Loads for Buildings and Other Structures*, American Society of Civil Engineers, Reston, VA,
- Astaneh-Asl, A., Call, S. M., and McMullin, K. M. (1989a). "Design of Single Plate Shear Connections." *Engineering Journal*, First Quarter, American Institute of Steel Construction, Chicago, IL, 21-31.
- Astaneh-Asl, A., Liu, J., and McMullin, K. M. (2002). "Behavior and Design of Single Plate Shear Connections." *Journal of Constructional Steel Research*, 58, 1121-1141.
- Astaneh-Asl, A., Nader, M. N., and Malik, L. (1989b). "Cyclic Behavior of Double Angle Connections." *Journal of Structural Engineering*, 115(5), American Society of Civil Engineers, Reston, VA, 1101-1118.
- ASTM. (1997). *E 399 - Standard Test Method for Plane-Strain Fracture Toughness of Metallic Materials*, ASTM, West Conshohocken, PA,
- Bailey, C. G., White, D. S., and Moore, D. B. (2000). "The Tensile Membrane Action of Unrestrained Composite Slabs Simulated Under Fire Conditions." *Engineering Structures*, 22, 1583-1595.
- Barsom, J. M., and Rolfe, S. T. (1999). *Fracture and Fatigue Control in Structures: Applications of Fracture Mechanics*, ASTM, West Conshohocken, PA,

- BRE. (2005a). *DTLR - Guidance on Robustness and Provision Against Accidental Actions - The Current Applications of Requirement A3 of the Building Regulations 1991*. Office of the Deputy Prime Minister, London, ENG, <http://www.odpm.gov.uk/>.
- BRE. (2005b). *DTLR Framework Report: Proposed Revised Guidance on Meeting Compliance with the Requirements of Building Regulation A3: Revision of Babbie, Allott and Lomax Proposal*. Project Report Number 205966, Office of the Deputy Prime Minister, London, ENG, <http://www.odpm.gov.uk/>.
- Breen, J. E., and Siess, C. P. (1979). "Progressive Collapse - Symposium Summary." *ACI Journal*, 76(9), American Concrete Institute, Detroit, MI, 997-1004.
- BSI. (2003). *BS 5950 - Structural use of Steelwork in Building. Part 1: Code of Practice for Design in Simple and Continuous Construction*, British Standards Institution, London, U.K.,
- Buettner, D. R. (1979). "Discussion of 'Structural Integrity of Large Panel Buildings' by M. Fintel and D.M. Schultz." *ACI Journal*, 76(11), American Concrete Institute, Detroit, MI, 1232-1233.
- Burgess, I. W., Huang, Z., and Plank, R. J. (2001) "Non-Linear Modelling of Steel and Composite Structures in Fire." *International Seminar on Steel Structures in Fire*, Shanghai, China, 1-15 (www.shef.ac.uk/fire-research/publications.html),
- Cai, J., Burgess, I. W., and Plank, R. J. (2002). *A Generalized Steel/Reinforced Concrete Beam-Column Element Model for Fire Conditions*. University of Sheffield - Department of Civil and Structural Engineering, Sheffield, U.K., www.shef.ac.uk/fire-research/publications.html.
- Christiansson, P. (1982). *Steel Structures Subjected to Dynamic Loads in Connection with Progressive Collapse - Dynamic Buckling*. Report Number D7:1982 (ISBN 91-540-3681-X), Swedish Council for Building Research, Stockholm, Sweden,
- CISC. (2004). *Handbook of Steel Construction - Eighth Edition*, Canadian Institute of Steel Construction, Willowdale, ONT,
- Corley, W. G. (2002) "Applicability of Seismic Design in Mitigating Progressive Collapse." *NIBS Workshop on Prevention of Progressive Collapse*, Rosemont, IL, National Institute of Building Sciences, www.nibs.org.
- CSI (2004) *SAP2000*, Computers & Structures, Inc., Berkeley, CA.
- Culver, C. G. (1976). "Live Load Survey Results for Office Buildings." *Journal of the Structural Division*, 102(ST12), American Society of Civil Engineers, Reston, VA, 2269-2284.
- DeStefano, M., and Astaneh-Asl, A. (1991). "Axial Force-Displacement Behavior of Steel Double Angles." *Journal of Constructional Steel Research*, 20, Elsevier Science, Ltd., 161-181.
- DeStefano, M., Astaneh-Asl, A., DeLuca, A., and Ho, I. (1991) "Behavior and Modeling of Double Angle Connections Subjected to Axial Loads." *1991 Annual Technical Session - Inelastic Behavior and Design of Frames*, Chicago, IL, Structural Stability Research Council, 323-334,

- DeStefano, M., DeLuca, A., and Astaneh-Asl, A. (1994). "Modeling of Cyclic Moment-Rotation Response of Double-Angle Connections." *Journal of Structural Engineering*, 120(1), American Society of Civil Engineers, Reston, VA, 212-229.
- DOD (2002). *Unified Facilities Criteria (UFC) - DoD Minimum Antiterrorism Standards for Buildings (UFC 4-010-01)*. http://www.wbdg.org/ccb/browse_cat.php?o=29&c=4.
- DOD (2005). *Unified Facilities Criteria (UFC) - Design of Buildings to Resist Progressive Collapse (UFC 4-023-03)*. http://www.wbdg.org/ccb/browse_cat.php?o=29&c=4.
- Dusenberry, D. O., and Hamburger, R. O. (2005) "An Energy-Based Pushdown Analysis Procedure for Evaluating Progressive Collapse Resistance." *Proceedings of the North American Steel Construction Conference*, Montreal, Quebec, Canada, CD-ROM,
- Ellingwood, B., and Leyendecker, E. V. (1978). "Approaches for Design Against Progressive Collapse." *Journal of the Structural Division*, 104(ST3), 413-423.
- Ellingwood, B. R. (2002) "Load and Resistance Factor Criteria for Progressive Collapse Design." *National Workshop on Prevention of Progressive Collapse*, Rosemont, IL, Multihazard Mitigation Council, National Institute of Standards and Technology,
- Ellingwood, B. R., and Culver, C. (1977). "Analysis of Live Loads in Office Buildings." *Journal of the Structural Division*, 103(ST8), American Society of Civil Engineers, Reston, VA, 1551-1560.
- FEMA. (2000a). *FEMA-355A: State of the Art Report on Base Metals and Fracture*, SAC Joint Venture and Federal Emergency Management Agency, Washington, D.C.,
- FEMA. (2000b). *FEMA 356 - Prestandard and Commentary for the Seismic Rehabilitation of Buildings*, American Society of Civil Engineers and the Federal Emergency Management Agency, Washington, D.C.,
- FEMA. (2000c). *State of the Art Report on Connection Performance (FEMA-355D)*, SAC Joint Venture and Federal Emergency Management Agency, Washington, D.C.,
- FEMA. (2000d). *State of the Art Report on Systems Performance of Steel Moment Frames Subject to Earthquake Ground Shaking (FEMA-355C)*, SAC Joint Venture and Federal Emergency Management Agency, Washington, D.C.,
- Fintel, M., and Schultz, D. M. (1979). "Structural Integrity of Large Panel Buildings." *ACI Journal*, 76(5), American Concrete Institute, Detroit, MI, 583-620.
- Girhammar, U. A. (1980a). *Behavior of Bolted Beam-Column Connections Under Catenary Action in Damaged Steel Structures*. Report Number D12:1980 (ISBN 91-540-3213-X), Swedish Council for Building Research, Stockholm, Sweden,
- Girhammar, U. A. (1980b). *Dynamic Fall-Safe Behavior of Steel Skeleton Structures Having Bolted Connections*. Report Number D13:1980 (ISBN 91-540-3215-6), Swedish Council for Building Research, Stockholm, Sweden,

- Girhammar, U. A. (1980c). *Dynamic Response of Two-Span Steel Beams Subject to Removal of Interior Support*. Report Number D11:1980 (ISBN 91-540-3211-3), Swedish Council for Building Research, Stockholm, Sweden,
- Grierson, D. E., Safi, M., Xu, L., and Liu, Y. (2005a) "Simplified Methods for Progressive-Collapse Analysis of Buildings." *Proceedings of the 2005 Structures Congress and the 2005 Forensic Engineering Symposium*, New York, NY, American Society of Civil Engineers, CD-ROM,
- Grierson, D. E., Xu, L., and Liu, Y. (2005b). "Progressive-Failure Analysis of Buildings Subjected to Abnormal Loading." *Computer-Aided Civil and Infrastructure Engineering*, 20, Blackwell Publishing, Malden, MA, 155-171.
- Griffiths, H., Pugsley, A., and Saunders, O. (1968). *Report of the Inquiry into the Collapse of Flats at Ronan Point, Canning Town*. Her Majesty's Stationary Office, London, U.K.,
- GSA (2003). *Progressive Collapse Analysis and Design Guidelines for New Federal Office Buildings and Major Modernization Projects*. www.oca.gsa.gov.
- Hamburger, R., and Whittaker, A. (2004) "Design of Steel Structures for Blast-Related Progressive Collapse Resistance." *North American Steel Construction Conference (NASCC)*, Long Beach, CA, American Institute of Steel Construction, (CD-ROM),
- Hawkins, N. M., and Mitchell, D. (1979). "Progressive Collapse of Flat Plate Structures." *ACI Journal*, 76(8), American Concrete Institute, Detroit, MI, 775-808.
- Hibbeler, R. C. (2006). *Structural Analysis, Sixth Edition*, Pearson Prentice-Hall, Upper-Saddle River, NJ,
- Huang, Z., Burgess, I. W., and Plank, R. J. (2000a). "Effective Stiffness Modelling of Composite Concrete Slabs in Fire." *Engineering Structures*, 22, 1133-1144.
- Huang, Z., Burgess, I. W., and Plank, R. J. (2000b). "Three-Dimensional Analysis of Composite Steel-Framed Buildings in Fire." *Journal of Structural Engineering*, 126(3), 389-397.
- Huang, Z., Burgess, I. W., and Plank, R. J. (2003a). "Modeling Membrane Action of Concrete Slabs in Composite Buildings in Fire. I: Theoretical Development." *Journal of Structural Engineering*, 129(8), 1093-1102.
- Huang, Z., Burgess, I. W., and Plank, R. J. (2003b). "Modeling Membrane Action of Concrete Slabs in Composite Buildings in Fire. II: Validations." *Journal of Structural Engineering*, 129(8), 1103-1112.
- ISE. (1969). "The Implications of the Report of the Inquiry into the Collapse of Flats at Ronan Point, Canning Town." *The Structural Engineer*, 47(7), The Institution of Structural Engineers, London, ENG, U.K., 255-284.
- ISE. (1971). "The Resistance of Buildings to Accidental Damage." *The Structural Engineer*, 49(2), The Institution of Structural Engineers, London, ENG, U.K., 102.
- ISE. (1972a). "Discussion - Stability of Modern Buildings." *The Structural Engineer*, 50(7), The Institution of Structural Engineers, London, ENG, U.K., 275-288.

- ISE. (1972b). "Stability of Modern Buildings." *The Structural Engineer*, 50(1), The Institution of Structural Engineers, London, ENG, U.K., 3-6.
- Iwankiw, N., and Griffis, L. G. (2004). *Comparison of Structural Performance of Multi-Story Buildings Under Extreme Events*, American Institute of Steel Construction, Chicago, IL,
- Khabbazan, M. M. (2005). "Progressive Collapse." *The Structural Engineer*, 83(12), The Institution of Structural Engineers, London, U.K., 28-32.
- Khandelwal, K., and El-Tawil, S.(2005) "Progressive Collapse of Moment Resisting Steel Frame Buildings." *Proceedings of the 2005 Structures Congress and the 2005 Forensic Engineering Symposium*, New York, NY, American Society of Civil Engineers, CD-ROM,
- Leyendecker, E. V., Breen, J. E., Somes, N. F., and Swatta, M. (1976). *Abnormal Loading on Buildings and Progressive Collapse: An Annotated Bibliography, Building Science Series 67*. U.S. Department of Commerce, National Bureau of Standards, Washington, DC,
- Leyendecker, E. V., and Ellingwood, B. R. (1977). *Design Methods for Reducing the Risk of Progressive Collapse in Buildings*. NBS Building Science Series 98, Center for Building Technology, Institute for Applied Technology, National Bureau of Standards, U.S. Department of Commerce, Washington, DC,
- Liu, J. (2003). "" University of California - Berkeley, Berkeley, CA.
- Liu, J., and Astanah-Asl, A. (2000a). "Cyclic Testing of Simple Connections Including Effects of Slab." *Journal of Structural Engineering*, 126(1), 32-39.
- Liu, J., and Astanah-Asl, A. (2000b). *Cyclic Tests on Simple Connections Including the Effects of the Slab*. Report No. SAC/BD-00/03, SAC Joint Venture,
- Liu, R., Davison, B., and Tyas, A.(2005) "A Study of Progressive Collapse in Multi-Storey Steel Frames." *Proceedings of the 2005 Structures Congress and the 2005 Forensic Engineering Symposium*, New York, NY, American Society of Civil Engineers, CD-ROM,
- Magnusson, J.(2004) "Learning From Structures Subjected to Loads Extremely Beyond Design." *North American Steel Construction Conference (NASCC)*, Long Beach, CA, American Institute of Steel Construction, (CD-ROM),
- Mahendran, M., and Moor, C. (1999). "Three-Dimensional Modeling of Steel Portal Frame Buildings." *Journal of Structural Engineering*, 125(8), American Society of Civil Engineers, Reston, VA, 870-878.
- Marchand, K. A., and Alfawakhiri, F. (2004). *Blast and Progressive Collapse. Facts for Steel Buildings Number 2*, American Institute of Steel Construction, Chicago, IL,
- MathSoft (2005) *MathCAD*, MathSoft, Boston, MA.
- McGuire, R. K., and Cornell, C. A. (1974). "Live Load Effects in Office Buildings." *Journal of the Structural Division*, 100(ST7), American Society of Civil Engineers, Reston, VA, 1351-1378.

- McNamara, R. J.(2003) "Conventionally Designed Buildings: Blast and Progressive Collapse." *AISC and Steel Institute of New York Symposium: Blast and Progressive Collapse*, New York, NY, American Institute of Steel Construction, Chicago, IL,
- Milner, M. W., Edwards, S., Turnbull, D. B., and Enjily, V. (1998). "Verification of the Robustness of a Six-Storey Timber-Frame Building." *The Structural Engineer*, 76(16), Institution of Structural Engineers, London, ENG, 307-312.
- Mitchell, D., and Cook, W. D. (1984). "Preventing Progressive Collapse of Slab Structures." *Journal of Structural Engineering*, 110(7), 1513-1532.
- Munoz-Garcia, E., Davison, B., and Tyas, A.(2005) "Structural Integrity of Steel Connections Subjected to Rapid Rates of Loading." *Proceedings of the 2005 Structures Congress and the 2005 Forensic Engineering Symposium*, New York, NY, American Society of Civil Engineers, CD-ROM,
- Nair, R. S.(2004) "Progressive Collapse Basics." *North American Steel Construction Conference (NASCC)*, Long Beach, CA, American Institute of Steel Construction, (CD-ROM),
- NIST. (2005). *Final Report on the Collapse of the World Trade Center Towers*. NIST NCSTAR 1 - Federal Building and Fire Safety Investigation of the World Trade Center, National Institute of Standards and Technology, Technology Administration, U.S. Department of Commerce, Washington D.C., <http://wtc.nist.gov/>.
- ODPM. (2005). *The Building Regulations 2000 - Structure; Approved Document A*, Office of the Deputy Prime Minister, London, ENG, <http://www.odpm.gov.uk/>.
- Owens, G. W., and Moore, D. B. (1992). "The Robustness of Simple Connections." *The Structural Engineer*, 70(3), Institution of Structural Engineers, London, U.K., 37-46.
- Park, R. (1964). "Tensile Membrane Behaviour of Uniformly Loaded Rectangular Reinforced Concrete Slabs with Fully Restrained Edges." *Magazine of Concrete Research*, 16(46), London, ENG, 39-44.
- Park, R., and Gamble, W. R. (1980). "Chapter 12 - Membrane Action in Slabs." *Reinforced Concrete Slabs*, R. Park, ed. eds., John Wiley & Sons, Inc., New York, NY, pp. 562-612.
- Popoff, J., A. (1975). "Design Against Progressive Collapse." *PCI Journal*, March-April, Prestressed Precast Concrete Institute, Chicago, IL, 44-57.
- Powell, G. P.(2005) "Progressive Collapse: Case Studies Using Nonlinear Analysis." *Proceedings of the 2005 Structures Congress and the 2005 Forensic Engineering Symposium*, New York, NY, American Society of Civil Engineers, CD-ROM,
- Rahamian, A., and Moazami, K.(2003) "Non-Linear Structural Integrity Analysis." *AISC and Steel Institute of New York Symposium: Blast and Progressive Collapse*, New York, NY, American Institute of Steel Construction, Chicago, IL, www.aisc.org.

- Regan, P. E. (1975). "Catenary Action in Damaged Concrete Structures." *ACI Publication SP-48: Industrialization in Concrete Building Construction*, American Concrete Institute, ed. eds., American Concrete Institute, Detroit, MI, pp. 191-224.
- Rex, C. O., and Easterling, W. S. (2002). "Partially Restrained Composite Beam-Girder Connections." *Journal of Constructional Steel Research*, 58, 1033-1060.
- Shen, J., and Astanteh-Asl, A. (1999). "Hysteretic Behavior of Bolted-Angle Connections." *Journal of Constructional Steel Research*, 51, Elsevier Science Ltd., 201-218.
- Shen, J., and Astanteh-Asl, A. (2000). "Hysteresis Model of Bolted Angle Connections." *Journal of Constructional Steel Research*, 54, Elsevier, 317-343.
- Shipe, J. A., and Carter, C. J.(2004) "Defensive Design: Blast and Progressive Collapse Resistance in Steel Buildings." *2004 AISC/SEI Structures Congress*, Nashville, TN, American Society of Civil Engineers, (CD-ROM),
- Speyer, I. J. (1976). "Considerations for the Design of Precast Concrete Bearing Wall Buildings to Withstand Abnormal Loads." *PCI Journal*, March-April, Prestressed Precast Concrete Institute, Chicago, IL, 18-51.
- Thornton, W. A. (1985). "Prying Action - A General Treatment." *Engineering Journal*, Second Quarter, American Institute of Steel Construction, Chicago, IL, 67-75.
- Vulcraft. (2005). *Vulcraft Steel Roof and Floor Deck Catalog*, Vulcraft - A Division of Nucor Corporation, www.vulcraft.com.
- Wales, M. W., and Rossow, E. C. (1983). "Coupled Moment-Axial Force Behavior in Bolted Joints." *Journal of the Structural Division*, 109(5), American Society of Civil Engineers, Reston, VA, 1250-1266.
- Ziemian, R. D., and McGuire, W. (2000) *MASTAN2 Ver. 1.1*, John Wiley & Sons, New York, NY.